Evaluation of a Dentine Hybrid Self-Adhesive Restorative Material Interface

Abuljadayel, Roaa Abdulsalam

Awarding institution:
King's College London

Evaluation of a Dentine Hybrid Self-adhesive Restorative Material Interface

Roaa Abdulsalam Abuljadayel

A thesis submitted for the degree of

Doctor of Philosophy

King's College London

2019

Abstract

Self-adhesive resin cements have become an integral part of luting of indirect restorations. Recently, a new formula as a derivative of this cement has been introduced as a self-adhesive, dual-cure, hybrid resin/glass ionomer (DC-HRI), bulk-fill coronal restorative material that could replace large amalgam restorations. These materials could be self-adhesive due to the acidic nature of their phosphorylated methacrylate monomers along with improved mechanical properties due to high silanated filler content. This thesis was constructed around three specific aims; Firstly, optical, mechanical and chemical characterisation of natural caries, partially demineralised dentine models against control sound dentine. Secondly, to investigate potential interfacial dentine remineralisation of the experimental material compared to a commercial highly viscous GIC (EQUIA Fill, GC, Tokyo, Japan) and a Bulk Fill resin composite (Filtek Bulk Fill, 3M, USA) bonded with a self-etch “Universal” adhesive. Thirdly, to examine the sealing and the adhesive properties of the new material compared to the control materials, when bonded to these different dentine substrates. The *in-vitro* demineralised dentine model, natural infected and affected carious dentine and sound controls were initially characterised using various advanced optical imaging techniques. These techniques included two-photon fluorescence microscopy, fluorescence lifetime imaging and second harmonic generation imaging (used as a stable correlative substrate reference), to assess optical changes before and after aging the samples. In addition, Raman spectroscopy was used to detect the mineral peak intensity changes. These non-invasive techniques allowed differentiation between the carious zones and other dental substrates without labelling, assisted by their Knoop microhardness readings. Tissue interactions with GIC and the experimental material resulted in significant changes in the optical properties of infected, affected and demineralised dentine. A significant increase in Raman mineral peak intensity was noticed with the demineralised dentine and caries-affected dentine due to the possible mineral precipitation and ionic exchange. In addition, carefully calibrated fluorescent dye micro-permeability experiments (a direct indicator of water uptake within materials and interfaces), in conjunction with specific material labelling through the dentine interface, revealed inadequate

sealing with all the material groups. However, better adhesion was observed with the *in-vitro* demineralised dentine group. This thesis demonstrates the successful use of non-invasive multimodal evaluation techniques in determining the changes in dentine properties and in investigating potential remineralisation benefits from the use of an experimental self-adhesive bulk-fill hybrid restorative material.

Table of contents

Abstract 2
Table of contents 4
Table of Figures 8
List of Tables 18
List of abbreviations 18
Acknowledgement 20
Introduction 22
Research aims and objectives 24
Chapter 1. Literature Review 25
Thesis structure 26
1.1 Dentine structure 28
1.1.1 Introduction 28
1.1.2 Organic matrix 29
1.1.3 Mineral content 35
1.2 Caries process 36
1.2.1 Introduction 36
1.2.2 Zones of a carious lesion 38
- **Caries-infected dentine (CID)** 38
- **Caries-affected dentine (CAD)** 39
- **Dental caries detection and differentiation** 40

1.2.3 Bonding to carious dentine 45
1.3 *In-vitro* demineralised dentine 46
1.3.1 Effect of acid-etching on dentine 48
1.3.2 Dentine remineralisation 49
1.4 Dental biomaterials 54
1.4.1 Glass-ionomer cement 56
1.4.2 Resin-modified glass-ionomer cements (RMGICs) 58
1.4.3 Self-adhesive resin cement 59
1.4.4 Hybrid resin/glass ionomer self-adhesive restoration 60
1.4.5 Bulk-fill resin composites 61

1.4.6 Scotchbond Universal adhesive 62
1.5 Evaluation of dental restorations 64
1.5.1 Bond strength tests 65
1.5.2 Failure mode analysis 69
1.5.3 Interface morphology and sealing efficiency 70
1.6 Optics and biophotonics in dental research 73
1.6.1 General optical properties 73
1.6.2 Biophotonics in Dentistry 78
- **Fluorescence in dental tissues** 78
- **Two-photon microscopy (2p)** 81
- **Second harmonic generation** 82
- **Fluorescence lifetime imaging (FLIM)** 83
- **Raman spectroscopy** 85

Chapter 2. *In-vitro* optical, chemical and mechanical characterisation of different dentine substrates 90
2.1. Introduction 90
2.2. Materials and methods 95
2.2.1. Demineralised dentine sample preparation 95
2.2.2. Measurement of dentine demineralisation depth 96
2.2.3. Characterisation of sound and demineralised dentine 97
- **Optical assessment; (SHG, AF and FLIM) and spectroscopy** 97
- **Mechanical assessment; Knoop hardness number (KHN)** 98
- **Chemical assessment; Raman spectroscopy** 98

2.2.4. Carious dentine tissue characterisation 99
Specimen preparations 99
Two photon microscopy and spectroscopy (AF, SHG intensity and spectrum and FLIM imaging) and analysis 100
Microhardness measurement 102
2.2.5 Statistical analysis 102
2.3. Results 104
2.3.1. Depth of dentine demineralisation 104
2.3.2. Characterisation of sound, demineralised and carious (infected and affected) dentine before storage 106
- **Chemical assessment using Raman phosphate intensity analysis before storage** 109
- **Spectra analysis** 110

2.3.3. Characterisation of sound, demineralised and carious (infected and affected) dentine after storage 112

2.4. Discussion 116

2.4.1 Characterisation of sound, demineralised and carious (infected and affected) dentine before storage 118

2.4.2 Characterisation of sound, demineralised and carious (infected and affected) dentine after storage 120

Chapter 3. *In-vitro* Demineralised Dentine Interactions with the Novel Dual-cure Hybrid Resin Ionomer (DC-HRI) 123

3.1 Introduction 123

3.2 Materials and methods 126

3.2.1 Assessment of dentine changes after storage with materials 128

3.2.2 Statistical analysis 129

3.3 Results: 134

3.3.1 Characterisation after material storage 134

3.4 Discussion: 142

3.4.1 Sample preparation 142

3.4.2 Effect of tested materials on the dentine substrates 145

3.5 Conclusions: 149

Chapter 4. Stain-free optical evaluation of carious dentine interaction with the novel DC-HRI restoration 150

4.1 Introduction 150

4.2 Materials and methods 154

4.2.1 Sample preparation 154

4.2.2 Characterisation of carious dentine after 4 weeks storage with materials 156

4.2.3 Statistical Analysis 160

4.3. Results 160

4.3.1 Carious zones characterisation using the two-photon microscopy 160

A. Autofluorescence intensity AF (AU): 162

B. Fluorescence life time imaging FLIM (ns): 164

C. Second harmonic generation SHG (AU): 165

4.3.2 Microhardness measurements 166

4.3.3 Raman Spectroscopy 170

4.4. Discussion 171

Chapter 5. The physical and morphological characteristics of the dentine interface with a novel dual cure hybrid resin ionomer (DC-HRI) 180

5.1 Introduction 180

5.2 Materials and Methods 184

5.2.1 Micro-shear bond strength test (μSBS) ... 184
- Sample selection and preparation ... 184
- Simple partial demineralised dentine model (phosphoric-acid etched dentine) 186
- Bonding procedures and micro-shear bond test ... 186
- De-bonded failure mode evaluation ... 186

5.2.2. Sample preparation for two-photon microscopic interfacial evaluation 187
- **Morphological interface group (n=6)** ... 187
- **Micro-permeability group (n=9)** ... 187

5.2.2.1 Two-photon imaging ... 189

5.2.3 Statistical analyses ... 189

5.3 Results ... 190

5.3.1 Micro-shear bond strength test ... 190

5.3.1.1 De-bond failure mode evaluation ... 192

5.3.2 Two-photon interface evaluation ... 195

5.3.2.1 Morphological interface group of single-labelled materials ... 195

5.3.2.2 Double-labelled micro-permeability ... 195

5.3.2.3 Pilot study ... 200

5.4. Discussion ... 201

5.4.1 Micro-shear bond strength test: ... 203

5.4.2 Micro-permeability and two-photon imaging ... 210

5.4.3 Pilot study ... 213

Chapter 6. General discussion and future work ... 215

6.1 General discussion ... 215

6.5 Suggestions for future work ... 228

Appendix ... 231

Appendix A - List of Documents ... 234

Appendix B - Summary of HRA Assessment ... 234

References ... 242

Table of Figures

Figure 1-1. Organisational flow chart of the experiments accomplished in this study with the analytical methods employed……28

Figure 1-2. Flowchart of the literature review discussion points……...28

Figure 1-3. SEM image of dentinal tubules Image copyright: Edward Messelt, ARR... 30

Figure 1-4. SEM image representing the dentinal tubules surrounded by peritubular dentine and inter-connected by the inter-tubular dentine. (studyblue.com)..... 32

Figure 1-5. The structure of collagen is represented by a collagen triple helical structure. Collagen molecules contain non-triple helical areas at both N, and C terminal ends. The repeated cross-linked collagen fibrils showing the periodic banding patterns and demonstrating the D-periodic unit with a single overlap (Molecular biology of Collagen, a major structural protein. Figure ©2000 by Griffiths et al)..... 33

Figure 1-6. Modified Keyes-Jordan diagram shows the interaction of bacterial oral flora and dietary carbohydrates on the tooth surface over time. Dental caries onset and activity are more complicated and affected by many modifying risk and protective factors. (Modified from Keyes PH, Jordan HV: Factors influencing initiation, transmission and inhibition of dental caries. In Harris RJ, editor: Mechanisms of hard tissue destruction, New York, 1963, Academic Press.)..... 37

Figure 1-7. A photomicrograph of a carious tooth section displaying the different dentine caries layers as labelled; the caries infected dentine (dark brown zone), caries-affected dentine (brighter colour), and sound dentine..... 38

Figure 1-8. Flowchart describing caries detection techniques. 40

Figure 1-9. Mechanistic studies on demineralization-remineralization for cariology research (published in Web of Science 2014–2016)..... 47

Figure 1-10. RelyX Unicem chemical composition..... 59

Figure 1-11. Flowchart showing the variables that influence the bond strength testing (Sirisha et al., 2014)..... 66

Figure 1-12. Graphical representation of electromagnetic wave propagating in free space..... 74

Table of figures

Figure 1-13. The electromagnetic spectrum Wavelengths of interest in this paper are the visible light spectrum from 400 nm to 700 nm and the range of near-infrared light from 750 nm to 1500 nm..... 75

Figure 1-14. Jablonski diagram illustrating important optical transitions occur in a scattering/absorbing/fluorescent molecule. http://www.bodyyouknow.org/raman-spectroscopy (a) In single-photon fluorescence, the photon energy is fully absorbed by the fluorophore and re-emitted with different energy and wavelength. (b) Multiphoton excitation requires two-photon with half energy of excitation wavelength to induce fluorescence. (c) Rayleigh (elastic) scattering happens when an incident photon scattered with the same energy but in different direction. (d) Raman (inelastic scattering); it can be either stoke shift in which the incident photon is scattered with reduced energy and longer wavelength, while the other type of inelastic scattering is called anti-stokes shift where the energy of the scattered photon is increased while the wavelength is decreased..... 75

Figure 1-15. Raman spectra of sound dentine between 100-3100 cm-1 wavenumbers showing the featured peaks and the allocated bands for these peaks are summarised in Table 1-8. 87

Figure 2-1. Characterisation before materials application; (1) 10 extracted sound teeth divided into two halves with a right-angle reference point. (2) Right portion of dentine (S; sound) was covered using yellow vinyl tape leaving the other half window (4mm) for dentine demineralisation (D; demineralised). Demineralisation was carried out using an acid etching protocol with 37% phosphoric acid for 60 seconds. (3) Then, evaluation of the demineralisation protocol was made by assessing changes in SHG and AF intensity and spectra, and changes in the fluorescence life time using two-photon microscope. It was followed by Knoop hardness number (KHN) evaluation and by using Raman spectroscopy to assess changes in mineral peak..... 96

Figure 2-2. Schematic diagram of the cross-sectional view of the demineralised dentine model (red surface), (top surface is the blue region), previously etched with 37% phosphoric acid etchant gel for 60 seconds. The diagram shows the direction of the Raman scan from the top surface (including the air) towards the deeper dentine of the same sample. Average of six points were selected on the grey scale image obtained after Raman imaging, depth profile was plotted to measure the depth of the

demineralisation from the top surface reaching the sound dentine within the same sample. 97

Figure 2-3. Schematic diagram of the tested model and a representative grey-scale image of Raman phosphate peak intensity at 959 cm^{-1} of sound and demineralised with the marked reference point (RP, red arrow). The scan directed from the sound dentine surface towards the demineralised surface with the demarcated line (previously marked by the surgical blade), to separate the two dentine areas. 99

Figure 2-4. Scaled calibrated scanned macro-photograph of the carious lesion representing the applied techniques for measurement including 2p characterisation (AF, SHG, FLIM and spectrum) and tissue hardness measurement..... 101

Figure 2-5. Representative depth-profile plots were obtained from the grey scale image of the demineralised lesion and the internal sound controls within the same sample, using Image J software analysis (ImageJ, Wayne Rasband, NIH, USA). It showed the gradual increase in the phosphate peak intensity from the demineralised area towards the sound dentine (ranging from 3000-5000 a.u.). Average demineralisation depth was calculated from six points on the sample which extended in the range between 500-600 µm..... 105

Figure 2-6. Representative 2-photon images of Autofluorescence (AF), Second harmonic generation (SHG), and fluorescence life time imaging (FLIM) were shown for each dentine substrate (infected, affected, demineralised and sound) used in this study. AF image was the brightest with the highest intensity value in the infected dentine. SHG image in the demineralised group was the brightest and with the highest intensity among other groups. FLIM images are gradually changing in colour from tissue to another; as the blue colour represent the infected dentine that have the shortest lifetime, with more greenish colour in the affected and demineralised dentine and getting gradually more reddish in the sound dentine with the longest life time values. 107

Figure 2-7. Representative histograms presenting the difference between dentine substrates in each measured parameter separately. Error bars depict standard errors of means (SE). (*) indicates significant difference between dentine substrates. AF of the infected tissues recorded the highest intensity mean and reduced towards the sound dentine. In SHG histogram, the highest intensity belongs to the demineralised tissues and the least in the infected tissues. Hardness was the least in infected tissues followed by the demineralised then affected dentine. FLIM showed gradual increase in lifetime from infected towards sound tissues. 108

Figure 2-8. Representative histogram showed the significant difference (*) in Raman phosphate peak intensity (p=0.004), between sound (blue) and demineralised (orange) dentine before storage. Error bars represent the standard errors of mean (SE). 109

Figure 2-9. Representative spectra were plotted and showing; (A) The recorded points across the carious dentine zones have recorded the highest AF signal intensity and lowest SHG intensity were observed in the infected dentine (red line). The next line showed reduction in AF, and slight increase in SHG, which indicates caries-affected dentine (green line). Sound dentine showed the least AF and highest SHG spectral peaks (blue line). (B) the recorded points across sound/demineralised model, showed an increase in SHG signals (orange line) compared to sound (blue), while no AF signal was detected in both sound and demineralised dentine groups. 111

Figure 2-10. (A, B) Representative grey-scale images are showing the direction of the Raman scan on the cross-section surface of both carious model and the demineralised model after PBS storage. (C) Histogram is showing the difference in the calculated average Raman phosphate peak intensity of different dentine substrates after storage. Error bars represent the standard error of means. Results reported the least phosphate peak intensity was related to infected tissues compared to all other groups (p=0.001) and marked by (*) in the graph. No difference was noticed in the phosphate peak between the demineralised sample and sound dentine after storage (p=0.39), and with the affected dentine (p=0.81). 113

Figure 2-11. Percentage changes of mean intensity values of each optical characterisation technique with different substrates were calculated and plotted in bar graphs for effective comparison following dentine storage. Infected and affected values were reduced in all measured techniques, but they were not significant from the sound dentine control group. A significant decrease in SHG intensity of the demineralised group compared to the sound dentine (0.01), associated with a significant increase in the demineralised tissue hardness compared to the infected and affected tissues (p=0.005, 0.003 respectively). 114

Figure 2-12. Representative images of autofluorescence (AF), Second harmonic generation (SHG), and fluorescence life time imaging (FLIM) were shown for each dentine substrate after storage. Infected and affected dentine intensity images were brighter than other groups, which was associated with the blue-green FLIM images indicating short life time for these tissues. SHG intensity image was brighter than AF in the demineralised group with more greenish lifetime image indicating no change in the lifetime after storage. Sound dentine is showing the green-red lifetime image as before the storage image. 115

Figure 3-1. Schematic diagram showing the model used in the study (A) Sample before storage with the marked reference point and top surface characterisation using two-photon, Raman spectroscopy and Knoop hardness number (KHN) as described in

chapter 2 (section 2.2.3). (B) cross-section view through the dentine/restoration interface, showed the position of the corresponding recorded points of the AF and SHG intensities, FLIM and Raman phosphate peaks intensities (black squares) and Knoop hardness points (red diamonds) based on a previously recorded reference point (yellow). Marked line using a sharp blade is well delineated between sound and demineralised dentine. 131

Figure 3-2. Diagram showing the setup and sample distribution for four interfacial dentine group evaluation. Letters (S, D) represents sound and demineralised dentine respectively. (A) Five random demineralised models were selected as tested samples for each group before restorations were applied and characterisation undertaken. (B) Samples were then restored with the three tested materials and one negative control group without restoration. Samples were incubated at 37°C temperature in phosphate buffer solution (PBS) solution. (C) After storage, samples were sectioned based on the previously marked reference point and re-evaluation of auto-fluorescence (AF) and second harmonic generation (SHG) intensity, fluorescence life time (FLIM), Raman mineral peaks intensity and Knoop hardness number (KHN) was done to calculate the percentage change. Further statistical analysis of the obtained percentage changes was performed. 133

Figure 3-3. Representative two-photon and FLIM images are showing sound and demineralised dentine groups. (A) Set of sound and (B) demineralised dentine images at the baseline (before material application), and after storage with different materials were presented. Qualitative 136

Cont. (Fig. 3-3) evaluation of autofluorescence and second harmonic generation images showed minimal changes between groups, especially in sound EQUIA Fill group, while measuring their intensity quantitatively showed some significant variations. However, FLIM images evaluation showed the difference between the experimental groups compared to the baseline and to the control group as well. It is well noticed that FLIM images remained red in EQUIA and DC-HRI in the sound groups but not with the Filtek Bulk Fill group. In addition, FLIM images became redder in the demineralised group after storage with EQUIA and DC-HRI groups. The reddish colour may indicate longer lifetime which may represent similar properties to the sound dentine. However, bluish-green colour indicated shorter lifetime and may indicates dentine degradation..... 137

Figure 3-4. Percentage change (%) of autofluorescence (AF) intensity in sound and demineralised dentine showed a significant decrease in Filtek Bulk Fill group intensity (B+, B-). There were no significant changes in intensities of the other groups with the sound dentine. However, the demineralised group showed a significant increase in intensity of the DC-HRI (D-) and EQUIA (E-) groups with no change in the control group

(C-). Abbreviations used stands for different materials groups; (D+) DC-HRI sound dentine, (E+) EQUIA sound dentine, (B+) Bulk Fill sound dentine, (C+) control sound dentine, (-) referred for the demineralised dentine groups of the corresponding materials. Error bars represent the standard errors of means. 138

Second harmonic generation intensity (SHG) 138

Figure 3-5. Percentage change of SHG intensity showed an increase in Bulk Fill group with both sound and demineralised dentine (B+, B-) and sound EQUIA (E+). Decrease in intensity of both sound and demineralised experimental group (D+, D-) but was comparable to the control group (C+, C-). No change was noticed in demineralised EQUIA group (E-). Error bars represent standard errors of means. 139

Figure 3-6. Percentage change of sound dentine FLIM showed no significant changes in lifetime between the materials but significant decrease was noticed in the control group. Demineralised dentine showed significant increase in EQUIA group only. Error bars represent standard errors of means. 140

Figure 3-7. Percentage change of KHN showed no changes in sound dentine groups, with significant increase in demineralised experimental and EQUIA groups. Error bars represent standard errors of means. 141

Figure 3-8. Percentage change of Raman intensity showed significant increase in demineralised EQUIA and DC-HRI groups compared to the control group, while no change was observed in any of the sound groups. 142

Figure 4-1. Experimental design for the sample preparation (A) previously recorded points including the carious zones and the sound controls points before storage. (B) Sectioning of the sample through the dentine/ restoration interface that was positioned at the carious line. An additional cut was applied through the sound internal control dentine/ materials interface points that was selected away from the caries line and based on the reference angle. 157

Figure 4-2. Representative AF image showing how to select the dentine for intensity measurement using Image J software excluding the restoration from the analysis. ... 158

Figure 4-3. Sample preparation for Raman imaging showing (A) Representative clinical macrograph that show the selected area for Raman imaging including the different carious zones (infected, affected and sound dentine). (B) Montage image after Raman mineral peaks analysis. 160

Figure 4-4. Representative AF, FLIM images of different caries tissue zones before materials application are showing the increase in redness from infected layer toward the sound dentine which become redder in colour. The AF image was brighter in the infected tissue than the other zones. 161

Figure 4-5. Graphs are showing the changes in AF intensity in the different carious zones (infected, affected and sound dentine). Significant increase in AF intensity was noticed in both infected and affected zones when bonded with DC-HRI and EQUIA against the control group as indicated using (*), with a decrease in Bulk Fill and control groups. However, a non-significant change was noticed with the sound dentine in all materials groups. 163

Figure 4-6. Graphs are showing the changes in FLIM in different carious zones (caries infected, affected and sound dentine). A non-significant increase in the lifetime was noticed among all dentine tissues when bonded to all materials group. 164

Figure 4-7. Graphs showing that there was no significant effect from different materials groups on the SHG intensity in all carious dentine layers. 165

Figure 4-8. Representative graphs showed the percentage changes in the hardness of carious zones after storage with different restorative materials. The significant increase in hardness was only noticed in the caries infected dentine when bonded to DC-HRI and EQUIA. No significant changes were observed with the caries affected dentine substrate. However, decrease in hardness was noticed among all materials groups when bonded to the sound dentine. (*) denotes significant difference from control group. Error bars in al graphs represent standard error of means. 166

Figure 4-9. Representative Two-photon imaging of the interface between caries-infected dentine/ DC-HRI, GIC and Bulk Fill composite. The figure compares baseline auto-fluorescence, second harmonic generation intensities and lifetime images for the caries-infected dentine before materials application with the after-storage images for each group (control, no material), (After storage group)……..164

Figure 4-10. Representative Two-photon imaging of the interface between caries-affected dentine/ DC-HRI, GIC and Bulk Fill composite. The figure compares baseline auto-fluorescence, second harmonic generation intensities and lifetime images for the caries-affected dentine before materials application with the after-storage images for each group (Control (no material), (after storage group). 168

Figure 4-11. Representative Two-photon imaging of the interface between sound dentine/ DC-HRI, EQUIA and Bulk Fill composite. The figure compares baseline auto-fluorescence, second harmonic generation intensities and lifetime images for the sound dentine before materials application with the after-storage images for each group (Control (no material), (after storage group). 169

Figure 4-12. Graphs showed Raman intensity values of different dentine carious zones. DC-HRI and EQUIA recorded the highest intensity among all substrates, while Bulk Fill

showed comparable intensity values to the control groups (*) denotes significance from control group. 171

Figure 5-1. Representative sample for caries-affected dentine used in this study that previously was characterised by Knoop hardness test. 185

Figure 5-2. Steps of micro-shear samples preparation and examination: **(a)** adjust the polyvinyl tubes on the flat dentine surface. **(b)** fill the tube with the tested materials as per manufacturer's instructions, then gentle removal of the tube following storage and directly before the test was performed. **(c)** fix the dentine sample on the metal jig and run the micro-shear test until failure occurs. 187

Figure 5-3. Micro-permeability sample preparation; following cavity restoration with fluorescein labelled restorations for 24hrs before imaging. (A) injection of an aqueous solution of rhodamine B into a cleaned pulp chamber of up-side down mounted restored teeth, it was left for 3 hours before sectioning. (B) Bucco-lingual sectioning through the dentine material interface and polished with serial SiC papers (1200, 2000, and 2500) and ultra-sonicate for 3 mins in between and 5mins after final polishing. 188

Figure 5-4. Mean micro-shear bond strength values before and after aging the materials (DC-HRI, EQUIA Fill, Filtek Bulk Fill) with different dentinal substrates. Error bars depict standard errors, * Indicates a statistically significant difference ($p<0.0001$) from DC-HRI in identical testing conditions. ^ Indicates a statistically significant effect of storage time within each substrate. Similar letters indicate no significant difference between sound and caries storage groups. % represents percentage of pre-test failures (PTFs) in parentheses. A. Graph showing the difference between DC-HRI and Bulk Fill composite with different substrates in different storage time. B. Graph compared the mean bond strength of DC-HRI and EQUIA Fill with different dentine substrates in different storage times. 190

Figure 5-5. Graphs showing the mode of failures of tested materials with different dentine substrates in different storage timing. The majority of failures were adhesive in nature, followed by mixed and cohesive that were minimal. A similar pattern of failure was noticed between DC-HRI and EQUIA within the demineralised group. In both sound and carious groups, DC-HRI materials showed a similar figure of failure. 193

Figure 5-6. Representative SEM micrographs showed different patterns of DC-HRI failure with different substrates. Mixed failure of the demineralised dentine storage group showed a combination of empty (A) and blocked tubules (C) (A1, 2). Cohesive failure of demineralised dentine within the material with dentinal tubules blocked with the material (B1, 2). Adhesive failure of 24hrs sound dentine showed the empty opening of the dentine tubules (C 1, 2). 194

Figure 5-7. Representative two-photon fluorescence images of fluorescein labelled DC-HRI material bonded to sound and demineralised/etched dentine. (a) thin interfacial layer (6-8 μm), with a lateral diffusion of fluorescein dye into the lateral tubules, labelled by red arrows, which indicates the initial acidity of the material, and may reflect changes in the peritubular and inter-tubular dentine. (b) Thicker interfacial layer (21 μm) due to the pre-etching of the dentine surface using 37% phosphoric acid gel for 60 seconds to create the simple artificial caries affected dentine (CAD) model. Both sound and demineralised dentine hybrid interfacial layers are indicated by the yellow dashed lines. 195

Figure 5-8. Representative 2-Photon micrographs of DC-HRI/ dentine interface with both sound and etched dentine. Column a, e (green) shows the fluorescein-labelled material and intrinsic dentine autofluorescence, column b, f (red) represent the rhodamine-B dyed pulpal fluid, column c, g (blue) show intrinsic fluorescence images of dentinal collagen as a reference called second harmonic generation (SHG). Column d, h (combined) show a composite image of the three channels. These channels showed fluorescein diffused below the dentine/material interface and into the lateral dentine tubules (a1, e1), together with the permeation of rhodamine-B through the interface into the restoration above the interface (b1, f1), with the minimal mixing of the dyes at the sound dentine interface (d1), and a diffuse mixing of the dyes was noticed in the demineralised dentine below the interface (black arrow h1).This mixing may indicate that the acidity of the material affected the inter-tubular and peri-tubular dentine structure. However, a clear hollow space just above the interface was also noticed in both sound and etched groups (a1, e1), which has been filled by the rhodamine dye as labelled by the yellow arrow in (b1, f1, e1, h1). No mixing of rhodamine and fluorescein at this space was found as presented in (d1, h1), this band was only characteristic to the DC-HRI group only. SHG channels showed an intact collagen in the sound group (c1), with a minimal change in the superficial dentine layer (labelled by white arrows in g1) duo to etching of dentine in this group. 196

Figure 5-9. The EQUIA group didn't show the fluorescein diffusion into the sound dentine group (a3), with minimal penetration of the dye in the demineralised group (e3). Gap was noticed in the sound dentine group at the interface as labelled by yellow arrows (a3, d3). Rhodamine-B labelled multiple cement projections were clearly noticed in both groups (d3, h3), with a partial seepage into the cement matrix (d3, h3). Both dyes were clearly mixed at and below the interface in the demineralised dentine group (white arrows, h3). 198

Figure 5-10. Filtek Bulk Fill group displayed a fluorescent labelled adhesive layer in sound dentine with short resin tags obtained in the sound dentine (a3). Spherical voids were also noticed at the junction between the fluorescein labelled adhesive and rhodamine-B dye diffused from the pulp at the interface (d3, white arrows). However, in the demineralised/etched dentine, the scalloped appearance of well-defined resin tags was presented with mixing of dyes at the interface but no diffusion into the composite structure (h3). SHG images of both groups reflect alteration in the superficial layer of the collagen image due to etching with variable thickness of this layer (c3, g3, yellow arrows). 200

Figure 5- 11. Representative 2-photon micro-permeability micrographs of (A) Fuji II LC RMGI which showed complete absorption of rhodamine-B dye through the material bulk with thin hybrid layer formation. (B) DC-HRI showed the absorption layer confined to the area of thematerial adjacentto the interface with a thin interfacial zone and lateral infilteration of fluorescein dye released from the labelled material…….200

List of Tables

Table 1-1. Clinical diagnosis techniques for caries differentiation. 41
Table 1-2. Laboratory techniques used for caries differentiation. 42
Table 1-3. Summary of the advance clinical caries detection techniques. 43
Table 1-4. In-vitro dentine artificial caries models. 47
Table 4-1. Table shows the experimental groups according to restorative material used…….. 154
Table 5-1. Number of samples tested for micro-shear bond strength in each group…….184

List of abbreviations

Minimal invasive dentistry (MID)

Tooth-restoration complex (TRC)

Resin-based composites (RCs)

Extracellular matrix (ECM)

Matrix metalloproteinase enzyme (MMPs)

Enamel-dentine junction (EDJ)

Non-collagenous proteins (NCPs)

Dentine sialophosphoprotein (DSPP)

Small Integrin Binding Ligand, N-linked Glycoprotein (SIBLING)

Dentine SialoProtein (DSP)

Dentine matrix protein 1 (DMP-1)

Dentine Glycoprotein (DGP)

Dentine Phosphoproteins (DPP)

Osteopontin (OPN)

Arbitrary Unit (A.U.)

Membrane-type MMPs (MT-MMPs)

List of tables and abbreviations

Amorphous calcium phosphate (ACP)

Modified sealed restorations (MSR)

Glycosaminoglycan (GAG)

Electron probe microanalysis (EPMA)

Transverse microradiography (TMR)

Caries-affected dentine (CAD)

Caries-infected dentine (CID)

Autofluorescence (AF)

Second harmonic generations (SHG)

Fluorescence lifetime imaging (FLIM)

Knoop hardness number (KHN)

Two-photon microscopy (2p)

Glass-ionomer cements (GICs)

Dual-cure hybrid resin/ionomer cement (DC-HRI)

Resin-modified glass-ionomer cements (RMGICs)

Scotch bond Universal adhesive (SBU)

Hydroxyapatite (HA)

Transverse Microradiography (TMR)

Acknowledgement

This thesis is dedicated to my lovely son Mahmoud

In the name of Allah most gracious most merciful, to whom all the praises and thanks for the gifts I have been blessed with, for the patience, for the strength, for the endurance of being able to complete this PhD journey.

I would like to acknowledge the Dental Biomaterials Department at King Abdulaziz University, College of Dentistry Jeddah, Saudi Arabia and to the Royal Embassy of Saudi Arabia, Cultural Bureau in London for their generous financial grant and continuous support throughout my study and for awarding me this opportunity.

The completion of this PhD degree would not have been possible without the support of all members of the Tissue Engineering and Biophotonics Department, Dental Institute, King's College London. I would like to express my deepest appreciation to all those involved.

I would like to express my sincere gratitude to:

Professor Timothy Watson, my first supervisor for his continuous support throughout my PhD study, for his patience, encouragement, cooperation, understanding and immense knowledge. His guidance and great experience helped me in all the time of research. I could not have imagined having a better advisor and mentor for my PhD study.

Professor Avijit Banerjee, my second supervisor for his patience, advice and valuable comments throughout formulating and correcting my dissertation.

Dr. Frederic Festy, for offering his support and expertise in explaining the physical backgrounds behind all the techniques we used in this thesis, as well as maintaining the two-photon microscopy throughout my PhD studies as well as helping in the analytical part of my experiments.

Acknowledgement

Dr. Sasha Scambler, my postgraduate coordinator for her advice and continuous evaluation of my progression during my studies.

Dr. Victoria Boyes, post-doctoral researcher, for her help and support during the designing of the experiments and performing pilot studies.

Mr. Peter Pilecki, for his continuous assistance in the lab and proof reading my thesis and requesting materials.

Mr. Andiappan Manoharan, for his invaluable advice on statistics.

To all my friends and colleagues for their help and encouragement in my difficult times.

I owe special appreciation and deepest gratitude for my beloved parents Eman Jaber and Abdulsalam Abuljadayel for their indefinite support, prayers and endless love.

My warmest love goes to my one and only, my lovely son, Mahmoud for his patience to be with a busy studying mom and sharing me all the difficult and pleasant times to complete my studying journey.

Introduction

One of the major challenges in dentistry has been to find an ideal restorative material that is biocompatible, mimics the physical and mechanical properties of the tooth structure, while maintaining a good adhesion to dentine and enamel and resist degradation in the oral cavity. In attempt to accomplish these characteristics together with the increase in the aesthetic demands by patients, glass-ionomer cement restorations (GICs) were initially introduced as a tooth-coloured material. Wide ranges of improvements in materials technology have led to the current development of resin-modified glass ionomer cements (RMGICs) and resin composites (RCs).

In line with these advances, it is also challenging for dentists and patients to choose which ideal line of treatment is suitable, especially when dealing with deep carious lesions. Bulk-fill resin composites are becoming increasingly popular due to the clinical appeal of reducing the application time into the cavity preparation. However, a material with a high viscosity and an anti-cariogenic property is preferred when treating such lesions. None of the GICs, RMGICs or Bulk-fill composites have fulfilled these requirements. However, one manufacturer (3M) has introduced a new experimental high viscosity, bulk-fill, self-adhesive coronal restorative material has named DC-HRI to restore deep carious cavities and replace amalgam restorations. This material combines the advantages of fluoride release of GICs and improved mechanical properties of resin composites. It might have potential for caries inhibition or remineralisation when restoring deeper carious lesions.

Nowadays, carious lesions can be treated conservatively and effectively using a minimally invasive approach especially if the pulp inflammatory changes are considered to be reversible. This caries excavation approach may result in mixed dentine substrates left in the cavity including: infected, affected, sound dentine. Studying the new experimental materials' interaction with dental tissues and their therapeutic potential is essential to assess their efficacy and thus clinical applications. Several techniques and devices have been used for these assessments.

Multimodal non-invasive microscopic evaluations were used to provide valuable information about chemical composition, microstructure and the fluorescence

behaviour of tissues. Dentine has a unique organic and inorganic structure that generates unique optical properties when interacting with light. The obtained optical and chemical properties are beneficial in dental research, for studying and understanding the interaction behaviour and morphology between dentine and dental materials. This understanding may influence dental practice and even the quality of dental care provided.

This work aimed to study the adhesive and sealing ability and the interfacial interaction between the new experimental self-adhesive restoration with the complex structure of carious and sound dentine. It also aimed to evaluate its potential for tissue healing or remineralisation when compared with conventional equivalent materials used to restore deep carious lesions. To facilitate this aim, advanced optical imaging techniques have been used to explore optical and chemical changes within dentine substrates.

Research aims and objectives

The studies carried out and presented in this thesis aimed to evaluate the effect of the recently introduced dual-cured hybrid resin/ionomer (DC-HRI), self-adhesive restorative material, on the optical properties and mineral content of sound and carious dentine substrates. In addition, testing the adhesive and sealing ability with these substrates was carried out. These evaluations were based on the validation of non-invasive *in-vitro* methods, using two-photon fluorescence microscopy, fluorescence lifetime imaging and Raman spectroscopy. They were used for the characterisation of dentine caries and monitoring changes in optical and chemical properties within dentinal tissues as an effect of the materials' application.

The objectives of this study were:

1- To study, characterise and validate the use of multi-modal non-invasive optical techniques in differentiating between several dentinal substrates including: sound, caries-infected, caries-affected and demineralised dentine before materials' applications based on their fluorescence properties.
2- To assess the effect of DC-HRI (3M, USA) coronal restorative materials on the optical and chemical properties of *in-vitro* demineralised dentine model against sound control dentine and to compare it with equivalent materials such as glass ionomer cement and resin composite bonded with a self-etch "Universal" adhesive.
3- To evaluate the changes in dentine optical properties using two-photon fluorescence and fluorescence lifetime imaging as a result of the materials' interaction with carious dentine zones and sound dentine,
4- To monitor any changes in the mineral contents of carious zones or the *in-vitro* demineralised dentine following interaction with restorative materials using Raman spectroscopy, to validate any remineralisation potential of the new material.
5- To evaluate the morphology of the interface with the potential sealing ability of the applied materials as well as testing their adhesive ability with

a variety of dentine substrates in different storage times using the micro-shear bond strength test and micro-permeability.

Thesis structure

In this thesis, the first chapter is dedicated to a critical review of the literature. It includes four main subjects discussing the sound, carious and *in-vitro* demineralised dentine substrates, the dental materials used in this study, the various techniques applied to conduct this research and bond strength and interfacial permeability. The subsequent chapters include the experiments of this project which are divided into four main studies. In chapter 2, the first experiment characterises the different dentine substrates used through this project. These results were used as baseline data for future comparison when interacting with restorative materials. In chapter 3, multimodal evaluations of changes in the optical and chemical properties of the *in-vitro* demineralised dentine were measured following interaction with DC-HRI and other comparative materials using two-photon microscopy and Raman spectroscopy. In chapter 4, evaluation of any potential remineralisation effect of DC-HRI and control materials on different carious zones were compared to the sound dentine control. In chapter 5, measurement of the micro-shear bond strength with qualitative assessment of the sealing ability of different materials was undertaken with different dentine substrates using the two-photon micro-permeability study. The experiments accomplished in this study were summarised in the following flow chart (Fig. 1-1)

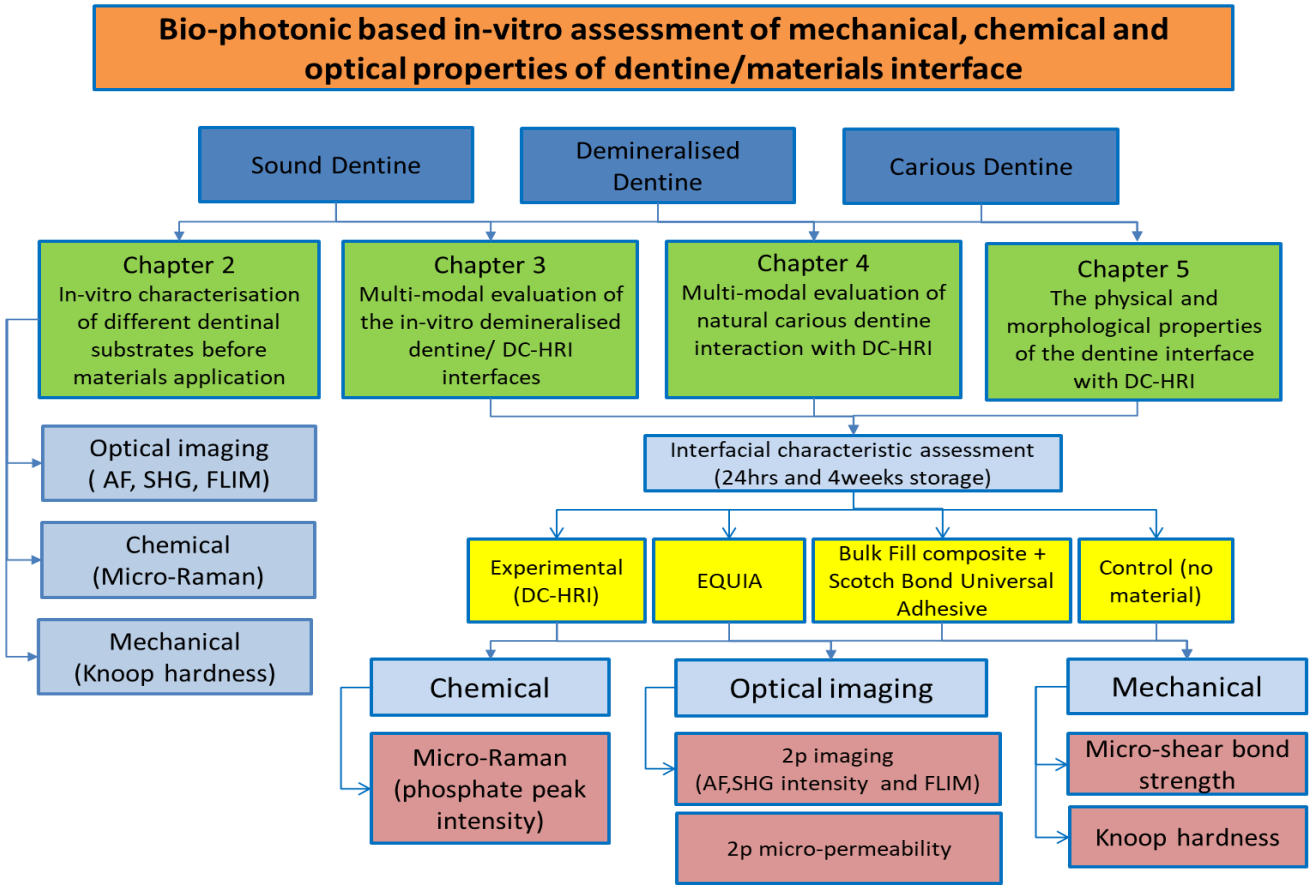

Figure 1-1. Organisational flow chart of the experiments accomplished in this study with the analytical methods employed.

Chapter 1. Literature Review

The following flow chart summarises the topics that will be discussed in the literature review (Fig. 1-2).

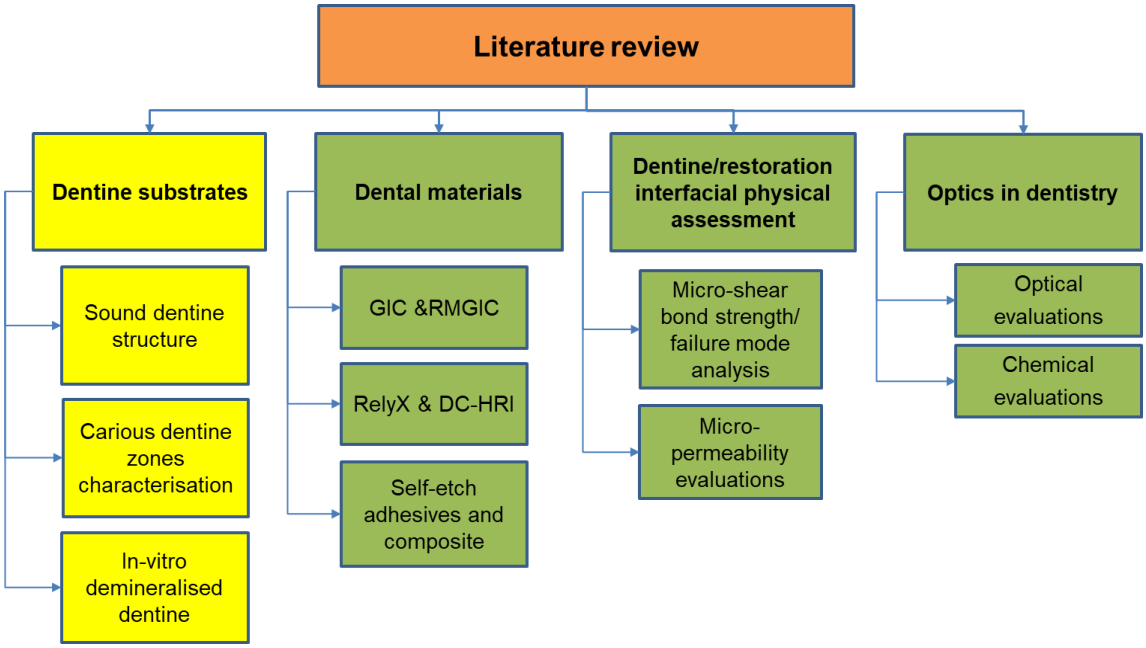

Figure 1-2. Flowchart of the literature review discussion points

1.1 Dentine structure

1.1.1 Introduction

Dentine is an anisotropic composite material, which is a thick mineralized tissue that lies between the enamel and pulp tissues in the crown and is surrounded by cementum in the root. It forms the bulk of the tooth and gives the tooth its elastic properties and shape under the brittle enamel structure to withstand occlusal forces without fracturing (Pashley, 1991).

As for connective tissues in general, the components of the extracellular space primarily give the tissue its functional characteristics. Dentine is considered as a modified connective tissue that is derived from the highly specialised ectomesenchymal cells, the odontoblasts, found in the dental papilla (Linde and Goldberg, 1993), which are responsible for the synthesis of an organic dentine

matrix. According to the formation process, dentine can be classified to three different types: (1) primary dentine, (2) secondary dentine, and (3) tertiary dentine. Primary and secondary dentine are parts of physiological dentine formation. During tooth development, primary dentine initially forms and slowly progresses into secondary dentine throughout the vital life of the tooth. However, tertiary dentine is formed to protect the pulp against noxious stimuli, such as the caries process (Summitt et al., 2006).

Dentine is a porous biological tissue composed of a mineral phase (70% in weight), organic material (20% in weight) and (10% in weight) water. On a volume basis, which may provide a more relevant picture, the mineral and the organic phases account for about 50 and 30%, respectively (Linde and Goldberg, 1993, Marshall Jr et al., 1997b). Dentinogenesis occurs simultaneously by two processes generated by odontoblasts: (a) deposition of the collagen matrix network; followed by (b) mineral precipitation of the inorganic phase (Goldberg et al., 2011).

1.1.2 Organic matrix

All collagen types found within the dentine extracellular matrix (ECM) are fibrillar structural macromolecules. Type I collagen is the predominant type found in the organic dentine structure (90% by weight) with a minimal amount of type III and V. These structural macromolecules act as scaffolds for mineralisation. Other non-collagenous proteins also exist in ECM include proteoglycans, phospholipids and enzymes. They can promote hydroxyapatite crystal nucleation and regulate the mineralisation. Matrix metalloproteinases (MMPs) have a role in the physiological and pathological processes in dentine and dentine adhesive interface degradation (Chaussain-Miller et al., 2006).

Structure and Physiology of Dentine

- Dentine tubules:

The major morphologic characteristic of dentine is fluid-filled dentine tubules radiating outward from the pulp to the exterior cementum or enamel border. The tubules are lined by an organic sheath called the lamina limitans, and the tubules themselves consist of the odontoblast process and dentine fluid. These tubules join the dentine to the pulp and neural plexus, hence providing dentine its sensitive nature (Fig.1-3, arrows). A rich collagen fibre network is found in peritubular and inter-tubular dentine (Pashley and Carvalho, 1997).

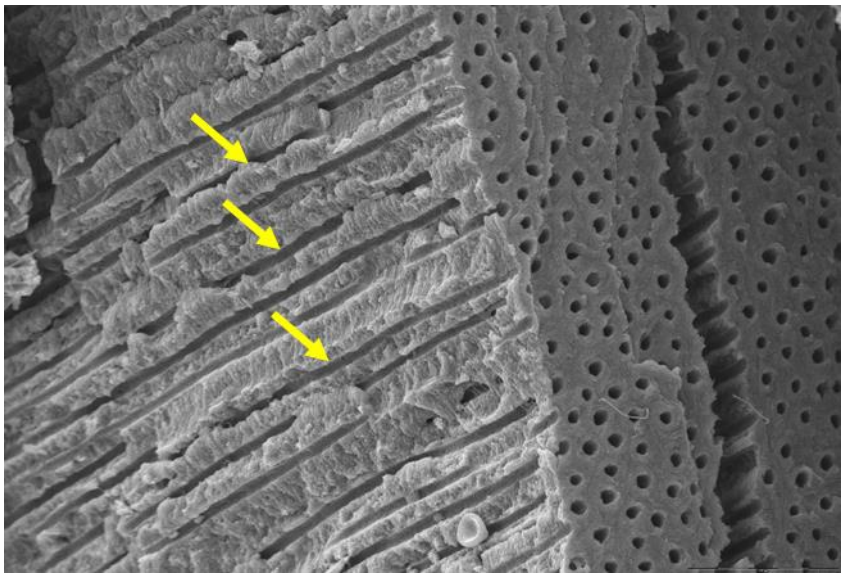

Figure 1-1. SEM image of dentinal tubules Image copyright: Edward Messelt, ARR.

Dentine tubule size, thickness and quantity are dependent on their location within dentine, age and the degree of mineralization that all affect the permeability. Their density and diameter decrease from the pulp towards the enamel-dentine junction (EDJ). Furthermore, dentine permeability is also influenced by the number of tubules and their branching (Mjör, 2002). According to the hydrodynamic theory, when the dentine gets exposed, the dentine fluid moves across the dentine. This movement has been called “transdentinal permeability” that stimulates the nervous stimuli and causes dentinal pain and sensitivity. It is also responsible for the moistness of exposed dentine by the outward movement of the dentine fluid from the pulp. Another type of dentine permeability is noted when adhesive resin monomers penetrate from the surface into tubule lamina

that is called intratubular permeability. The aim of this type of permeability is to allow permeation of resin to seal the exposed tubules and contribute to resin retention. Dental tubules have an inner diameter about 0.8-2.5μm, their lumens are enclosed by a highly mineralised peritubular dentine with only 10% of its volume consisting of collagen fibrils.

- Intertubular/Peritubular dentine:

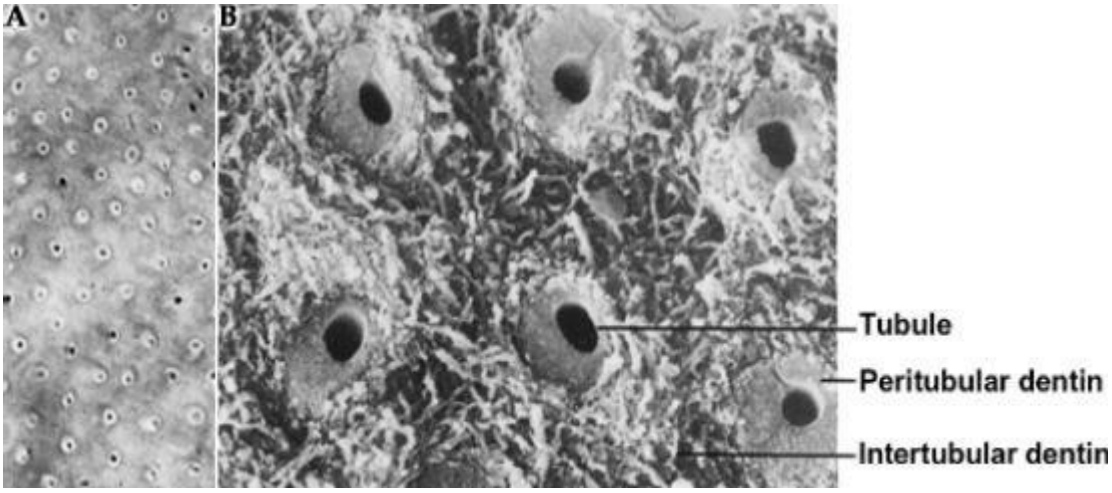

Figure 1-2. SEM image representing the dentinal tubules surrounded by peritubular dentine and inter-connected by the inter-tubular dentine. (studyblue.com).

Intertubular dentine (the matrix in between the tubules) contains around 30% mineralised collagen that is wrapped around the tubules perpendicular to their long axis. It consists of a tightly interwoven network of collagen fibrils in which apatite crystals are deposited. Transverse dentine sections show a hyper-mineralised ring around the tubule known as peritubular dentine (Fig.1-4). Understanding dentine architecture contributes to the appropriate management of different dentine conditions such as caries or cracked tooth syndrome (Elbaum et al., 2007). As a result, the bonding to dentine substrate will vary according to its location and is enhanced in the shallower dentine compared to the deep dentine (Marshall Jr et al., 1997a, Yang et al., 2006).

.

- Collagen

From a microstructural perspective, the collagen fibrils in dentine reinforce the matrix by serving as a scaffold for mineral crystallites. In the intertubular dentine, collagen fibrils are distributed randomly but circumferentially around tubules. The fibrils are randomly arranged perpendicular to the tubules and the orientation of the long axes of the apatite crystals are parallel to the collagen fibrils.

The ECM contains different collagen types with fibrillar structural macromolecules that have a characteristic triple helical conformation. Type I consists of three α helical chains; two identical α1 chains and one distinct α2 chain intertwined to form a 280 nm molecule (Goldberg et al., 2011) (Fig.1-5).

Additionally, each helical chain has non-triple helical regions at both the NH_2-terminal and COOH-terminal ends (Butler et al., 1984). This helical formation is characterised by the intertwining of three helical polypeptides forming a fibrous "coiled coil" structure with a three-dimensional network called "tropocollagen" (Van Der Rest and Garrone, 1991). Each of these chains contains a characteristic left-handed amino acid sequence of polyproline, often termed as a polyproline type II helix. Then, glycine residue is required to be present in every third position in the polypeptide chain and many of the remaining amino acids X and Y are proline or hydroxyproline. About 35% of the non-glycine positions in the repeating unit Gly-X-Y are occupied by proline, found almost exclusively in the X-position, and 4-hydroxyproline, predominantly in the Y-position (Van der Rest and Garrone, 1990).

The dentine collagen has more cross-linking fibrils than the bone collagen. Type I collagen fibrils represent the pillar of collagen structure, positioned perpendicular to the non-collagen protein. Cross-linking causes a period where the collagen molecules overlap, followed by a gap before the next collagen molecule. This is called the D-periodic gap/overlap spacing or "D-spacing" as shown in Fig. 1-5 (Orgel et al., 2006).

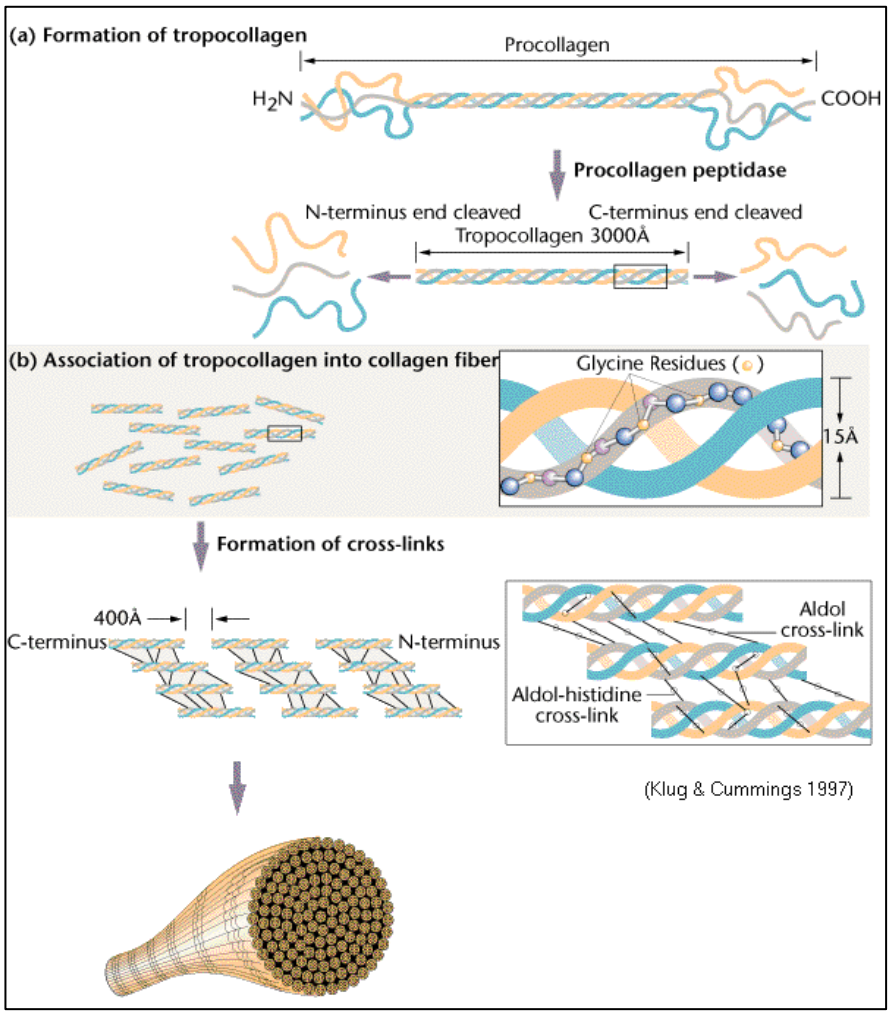

Figure 1-3. The structure of collagen is represented by a collagen triple helical structure. Collagen molecules contain non-triple helical areas at both N, and C terminal ends. The repeated cross-linked collagen fibrils showing the periodic banding patterns and demonstrating the D-periodic unit with a single overlap (Molecular biology of Collagen, a major structural protein. Figure ©2000 by Griffiths et al).

Non-collagenous proteins (NCPs)

Many investigations performed before 1980 have reported several non-collagenous components in pre-dentine and dentine (Leaver et al., 1976). In addition to collagen, ECM of the dentine encompasses multiple NCPs (including different Proteoglycans, PGs), enzymes and phospholipids (Goldberg and Boskey, 1996). It has been suggested that there is a separate family of calcium-binding phosphoproteins, termed the SIBLING proteins (small integrin binding ligand, N-linked glycoprotein) (Fisher and Fedarko, 2003). They comprise dentine

sialophosphoprotein (DSPP) and dentine matrix protein 1 (DMP-1) (Bellahcène et al., 2008).

NCPs are found with variable extents covering the collagen, playing structural, metabolic, and functional roles in soft and calcified tissues. They are associated strongly with the mineralisation of dentine matrix and promote HA crystal nucleation (Qin et al., 2004). NCPs can bind selectively to the forming HA crystals, to guide their growth in specific directions with different crystal shape formations. At the same time, they provide the rest of the molecular domains available for protein attachment or cell adhesion.

ECM also includes γ-carboxyglutamate containing proteins such osteocalcin and matrix Gla protein. The former “Osteocalcin” regulates the hydroxyapatite crystals growth. It has been also found participating in the blood coagulation cascade. In contrast, matrix Gla protein such as Osteopontin (OPN) and phosphoglycoprotein (MEPE) were found to inhibit dentine mineralisation and are found in both mineralised and non-mineralised but they still have the potential to bridge between cells and HA. On the other hand, some additional glycophosphoproteins are also expressed during the mineralisation phase of bone and dentine such as dentine matrix protein 1 (DMP1), dentine sialophosphoprotein (DSPP) and its subdomains; dentine phosphoproteins or phosphophoryn (DPP) and dentine sialoproteins (DSP). When these proteins found in high concentrations, they bind to CaP nanoparticles to inhibit further mineral nuclei formation which could prevent further pathologic calcification (George and Veis, 2008).

- Enzymes

There are many enzymes found in the dentine ECM including alkaline phosphatase which provides inorganic phosphate for mineralisation. However, there is also the MMP family, composed of 23 members that, based on substrate specificity and homology, are divided into the following six groups: collagenases, gelatinases, stromelysins, matrilysins, membrane-type MMPs (MT-MMPs), and other MMPs which are contributing in extracellular matrix degradation. In the dentine–pulp complex, MMPs play a crucial role in regulating and controlling both physiological (the organization of enamel and dentine organic matrix, or they may

regulate mineralization by controlling the proteoglycan turnover) and pathological processes (inflammation and tumour invasion) (Palosaari et al., 2003).

Dentine caries is a pathological process represented by demineralization and followed by degradation of the exposed organic matrix that consists mainly of type I collagen. This degradation of the dentine collagenous matrix has been attributed to MMP activity (Tjäderhane et al., 1998). In dentine, MMP-8 “human interstitial collagenases” can play a role in collagen degradation. Additionally, the gelatinases MMP-2 and MMP-9 can further deteriorate the triple helical confirmation of collagen. They may be involved in the release of dentinal growth factors (Hannas et al., 2007).

1.1.3 Mineral content

The dentine mineral phase consists of calcium-deficient and carbonate-rich hydroxyapatite $Ca_5(PO_4)_3(OH)$ crystals. There are two mineral components of dentine: magnesium and carbonate-substituted calcium hydroxyapatite crystals, which are arranged in a crystalline lattice structure to give the dentine its hardness (Banerjee et al., 1999). Carbonate substitution in biological apatite increases apatite solubility (Legeros and Tung, 1983).

HA crystals are needle-shaped with a thickness of approximately 5 nm and a length of 20 nm (Mjör, 1984). Their low calcium content makes their structure more prone to acid dissolution and more vulnerable to caries attack than stoichiometric apatite (Legeros and Tung, 1983). The initiation of mineralisation during dentinogenesis is explained by three mechanisms:

- Spontaneous precipitation of calcium phosphate when the supersaturation level is exceeded.
- Nucleation of the crystals containing phosphoprotein and glycoprotein in the form of spherical structures, which grow and fuse with neighbouring spheres.
- Deactivation of bone mineral inhibitors.

Type I collagen and NCPs control the growth and direction of forming crystals (Jones et al., 1984). When calcium and phosphate ions are highly saturated, an intermediate precursor polymorph such as amorphous calcium phosphate (ACP), octa-calcium phosphate and di-calcium phosphate dihydrate, are created and apparently transformed to hydroxyapatites. Therefore, type I collagen allows crystal deposition by providing the ideal framework for mineralisation. On the

other hand, the NCPs control the nucleation and apatite growth. This has been mediated by providing the carboxylic acid and phosphate to function as nucleation sites of Ca/P ions and regulate subsequently crystallised apatite form, size and direction. In addition, dentine mineralisation occurs in an incremental linear pattern which can reflect the rhythmicity and disturbance in mineralisation (Niu et al., 2014).

1.2 Caries process

1.2.1 Introduction

Dental caries is the most prevalent non-communicable chronic disease to have spread rapidly throughout the world with a significant social impact. It is considered an important cause of pain and dental loss. It is a multi-factorial, lifestyle-related disease (Paula et al., 2012). The mechanism of the caries process starts at the enamel surface when the bacteria present in the oral biofilm ferment dietary carbohydrates to form organic acid by-products. The drop in the pH below the critical value (pH 5.5), with the increased density of the biofilm and the amount of the cariogenic bacteria may facilitate caries initiation and progression (Dawes, 2003). Traditionally, the tooth-biofilm-carbohydrate interaction has been illustrated by the classical Keyes-Jordan diagram (Fig.1-6). Several modifying risk and protective factors can influence the dental caries process and progression.

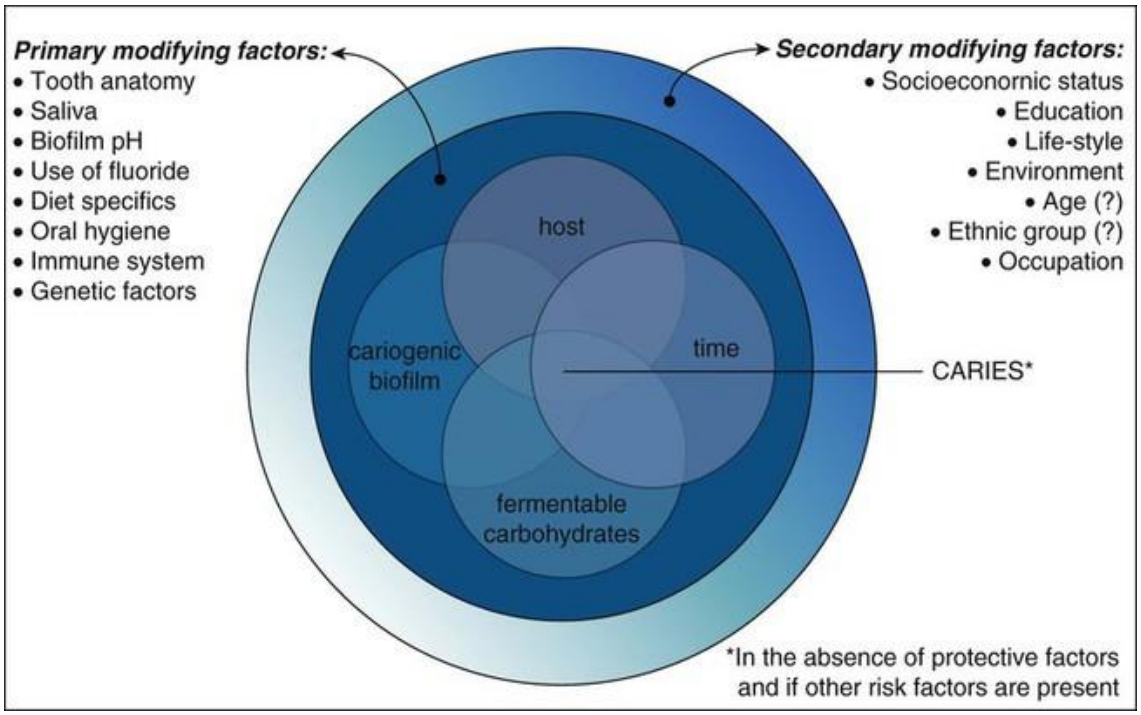

Figure 1-4. Modified Keyes-Jordan diagram shows the interaction of bacterial oral flora and dietary carbohydrates on the tooth surface over time. Dental caries onset and activity are more complicated and affected by many modifying risk and protective factors. *(*Modified from Keyes PH, Jordan HV: Factors influencing initiation, transmission and inhibition of dental caries. In Harris RJ, editor: *Mechanisms of hard tissue destruction*, New York, 1963, Academic Press.).

- **Mineral dissolution:**

As mentioned in section 1.1.3, the dentine mineral matrix is primarily constituted of $Ca_5(PO_4)_3(OH)$ crystals. HAP starts to dissolve when immersed in an unsaturated solution until equilibrium is achieved. Fermentation of dietary carbohydrates by acidogenic bacteria present in the plaque results in the production of different acids such as lactic, acetic and propionic acids that demineralize enamel and dentine. Calcium, phosphate, and hydroxyl ions accumulate until saturation of the saliva is reached. Following this, ion accumulation, pH increase, and re-deposition of these minerals occurs and may re-mineralise the surface (Yu et al., 2017). Buffering components and fluoride application can also arrest the carious lesion along with the regular physical disruption of the dental biofilm (Selwitz et al., 2007).

Carious dentine histologically has been divided into two main altered layers (Fig.1-7), an outer heavily contaminated (infected) zone with irreversible

structural degeneration and an inner layer of caries-affected partially demineralised dentine (Fusayama and Terashima, 1972, Banerjee and Watson, 2015).

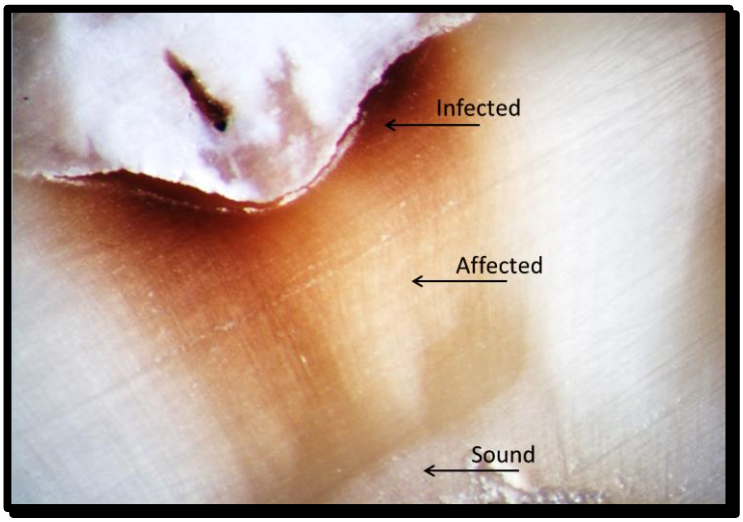

Figure 1-5. A photomicrograph of a carious tooth section displaying the different dentine caries layers as labelled; the caries infected dentine (dark brown zone), caries-affected dentine (brighter colour), and sound dentine.

1.2.2 Zones of a carious lesion

Minimally invasive dentistry (MID) advocates dental tissue preservation by the selective removal of the heavily infected / contaminated carious dentine. The success of early detection of the carious lesion plays a key role for better management of the disease. This initial management can then promote preventive therapeutic measures and encourage the remineralisation of non-cavitated lesions (Pretty, 2006). Caries lesion differentiation and assessment requires a combination of understanding of the caries histology with clinical experience in order to avoid the unnecessary cutting of the repairable caries-affected dentine (Banerjee and Watson, 2015).

- **Caries-infected dentine (CID)**

This is characterised as heavily bacterially contaminated, highly demineralised, physiologically non-remineralisable, necrotic dentine showing non-reversible denatured collagen fibrils with loss of cross-linkage appearance. Clinically, it appears as a dark brown, soft and wet layer (Fusayama et al., 1966, Kidd and Fejerskov, 2004). These structural changes in collagen are permenant and irreversible. Microbial invasion of carious lesions may induce the progressive

demineralization of the dentine surface. In consequence, an adaptive response of the odontoblasts may follow, in the form of a reactionary dentine matrix to limit bacterial invasion in dentinal tubules. Some clinical studies have shown a reorganization of the dentine following the soft carious removal (Massara et al., 2002, Maltz et al., 2013). However, other studies have reported the same phenomena in both permanent and primary teeth when the soft dentine hasn't been excavated (Mertz-Fairhurst et al., 1998b, Gruythuysen, 2010, Chibinski et al., 2013).

- **Caries-affected dentine (CAD)**

CAD is the inner layer of carious dentine that is partially demineralized with more intact collagen fibres. Clinically, it is described as a paler brown, harder, sticky and scratchy dentine (Banerjee, 1999). The mineral phase of CAD is composed of carbonate-rich hydroxyapatite. A study, using Fourier-transform infrared imaging (FTIR), has shown a reduced crystalline structure of CAD with lower mineral content compared to the normal dentine (Spencer et al., 2005). A micro-Raman spectroscopy investigation has suggested that the mineral carbonate peak intensity at 1070 cm^{-1} was lower in CAD compared to sound dentine. In addition, a lower magnesium content was noted when caries infected and affected dentine were examined by the electron probe microanalysis (EPMA) compared with intact dentine, although the densities of calcium (Ca) and phosphorus (P) in CAD were relatively similar to intact dentine (Doi et al., 2004).

Histologically, CAD can be subdivided into three zones: the turbid zone, the transparent zone, and the subtransparent zone (Fusayama, 1979, Yamada et al., 1983, Marshall et al., 1997, Marshall et al., 2001). The turbid zone contains no peritubular dentine with a demineralized intertubular dentine (Marshall et al., 1997a). However, this layer is able to remineralise due to the presence of the cross-linked intact collagen (Marshall et al., 1997a, Perdigão, 2010). It also contains a living odontoblastic process that helps in remineralization.

In the transparent zone, an intact peritubular and intertubular dentine was observed. It can be hypomineralised or hypermineralised, with limited bacterial invasion. The dentine tubules in the transparent zone may be partially or completely occluded by minerals. These β-tricalcium phosphate (Daculsi et al., 1987) crystals are acid-resistant and have a rhomboid-shape, termed

"Whitlockite" in an attempt to isolate the carious lesion and indirectly protect the pulp from the penetration of substances (Frank et al., 1966). The Whitlockite crystals have a weaker crystalline structure than hydroxyapatite. Therefore, it is relatively softer than the sound dentine (Ogawa et al., 1983, Banerjee, 1999, Marshall et al., 2001). In the rapidly progressing lesion, no tubular occlusion was noticed (Kidd, 2004). Sound dentine collagen in this layer enables the remineralisation process (Fusayama, 1991).

The subtransparent area represents the transitional area from the transparent zone towards the normal dentine. In this zone, a normal tubular structure with very fine intratubular crystals was observed (Marshall et al., 2001). These crystals have a plate-like structure or granular shape attached to the collagen fibrils.

- **Dental caries detection and differentiation**

Caries detection refers to the determination of the presence and the extent of carious lesion with the judgement of its activity. The most commonly used caries detection techniques are summarised in Fig. 1-8.

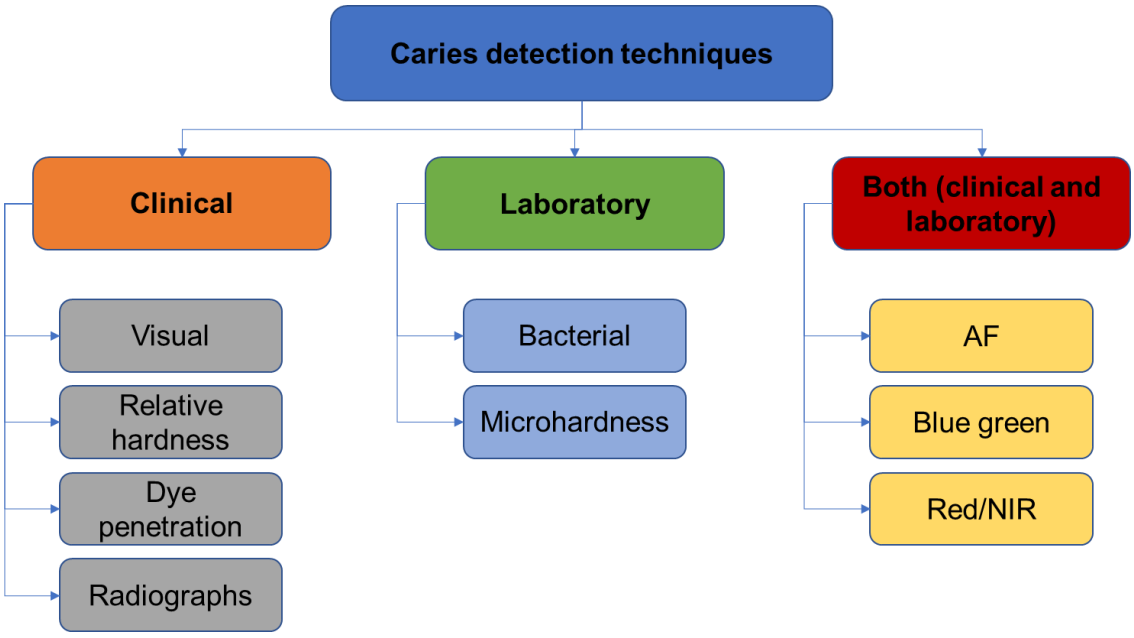

Figure 1-6. Flowchart describing caries detection techniques.

A definitive clinical caries diagnosis can be achieved using a combination of the following traditional aids presented in Table 1-1.

Table 1-1. Clinical diagnosis techniques for caries differentiation.

Clinical caries diagnostic techniques	Methods	Reliability	Limitations	References
Visual inspection	Colour change is caused by Maillard reaction; pale brown for infected dentine and darker brown for affected dentine	Subjective	Low sensitivity to the lesion. Colour and hardness are influenced by lesion age, severity, light and hydration of the tooth	(Bader et al., 2001, Banerjee et al., 2000)
Tactile sensation	Rounded end dental explorer to examine the moisture and consistency of the lesion	Subjective	Operator skills dependent, low sensitivity and high specificity to caries	(Kidd, 2004)
Caries detector Dyes	Application of acid red stain; classified to dark pink (infected), light pink (affected), whitish (sound).	Subjective	Low tissue types specificity leads to unnecessary tissue removal	(Pugach et al., 2009)
Radiography	Bitewing, panorama, digital radiographs	Subjective	Superimposition of caries, Patient x-ray exposure	(Haak, et al., 2001, Moreira et al., 2011)

Hardness (Cariotester)	Portable micro-hardness tester, assessing the progress of the lesion during caries removal in the clinic	Objective	It requires flat surface for accurate measurement.	(Shimizu et al., 2013)

Many laboratory studies attempted to differentiate between the caries-infected dentine and caries affected-dentine based on the difference in their causative pathogens and hardness number. These methods are summarised in Table 1-2.

Table 1-2. Laboratory techniques used for caries differentiation.

Laboratory caries detection techniques	**Bacterial analysis**			**Microhardness**
General comments	• a gold standard to which all other tissue differentiation techniques are compared. • Streptococcus mutans, is the chief pathogen associated with caries, followed by Lactobacillus casei and most prominent in caries infected dentine (Kidd et al. 1996).			• used as a reference for dentine's inherent physical properties • CID, KHN < 25 • CAD range from 25 to 40 • Sound KHN<40 • (Ogawa et al., 1983; Banerjee et al., 2010a)
	1- Culturing: specified known pathogens are cultured (Hoshino, 1985).	**2-PCR:** DNA sequence analysis (Iwami et al., 2008). Long incubation time (Lussi et al., 2004).	**3- FISH:** using fluorescent probe to detect rRNA sequences (Banerjee et al., 2002)	

In recent years, the possibilities for accurate caries detection have progressed considerably. The focus has returned to the use of light in the infrared or near-infrared (NIR) region. Advanced clinical diagnostic methods in Table 1-3 can be used as complementary methods to the conventional methods mentioned in Table 1-1.

Table 1-3. Summary of the advance clinical caries detection techniques.

Caries detection device	**Definition**	**Light/laser used**	**Limitations**	**Suggestion**	**References**
Fibre-optic transilluminat ion (FOTI)	Based on light scattering from demineralised areas which appear darker than the sound areas	Hand piece /white light	Low specificity leads to over excavation, subjective	Increasing the wavelength to NIR transillumin ation, allows deeper tissue penetration (DIFOTI)	(Pretty 2006b, Fried 2010, Limeback 2012, Abogazala h N et al., 2017)
Quantitative light induced fluorescence (QLIF)	Real time auto-fluorescen ce of the lesion mineral content, depth, size and severity	Violet-blue light excitation (290-450nm), emission 540 green filter.	Not reliable, limited depth, outcome affected by calculus, dryness and surrounding lights	Should be combined with conventiona l methods	(Karlsson 2010)

Laser-induced fluorescence (DIAGNOdent)	Quantitative fluorescence intensity (0-99) in caries, while (0-12) in sound	Emit 655 red light diode lasers	Low specificity to the sound, false positive reading. Caries endpoint is doubtful	Dry, clean, non-stained surface is indicated, complementary to the conventional methods.	(Lussi 2004, Thais Gimenez et al., 2016, Gokhan Ozkan et al., 2017)
NIR transillumination	Penetrate deeper with less scattering, better contrast	Infrared laser (780-1550nm)	Not quantitative	Images are better visualised when are taken from multiple angles	(Karlsson 2010, (Gokhan Ozkan et al., 2017)
Fluorescence-aided caries excavation (FACE)	Visualizing the metabolic products of oral microorganisms known as porphyrins, objective method	Violet light, dentine auto-fluoresce (wavelength, 405 nm), Sound tissues fluoresce green, while carious tissue fluoresces orange-red	The cavity should be fully opened and accessible, more reliable to the cavity floor than the walls, limited field of view	Can be used in a fully wide opened cavity with no undermined enamel	(Lai G 2014, Koç Vural U 2017)

1.2.3 Bonding to carious dentine

The traditional complete “non-selective” carious tissue removal is no longer recommended during the operative management of deep lesions. Instead, a partial, “selective” elimination of caries leaving the soft infected tissue over the pulp is thought to maintain the pulp vitality and thus retain teeth for a longer time (Schwendicke *et al.*, 2016).

Intact collagen fibrils are believed to play the key role in remineralisation (Zhao et al., 2017), as they provide a scaffold for apatite crystal attachment (Perdigao et al., 2010). Clinically, the dentine substrate following selective carious tissue removal may exhibit “mixed” chemical and mechanical characteristics and it includes a combination of CID, CAD and sound dentine. When this cavity is restored, theoretically, the restoration placed impedes the supply of dietary carbohydrate to the sealed bacteria, which leads to bacterial inactivation and lesion arrest (Marggraf et al., 2018). However, the collapsed collagen fibres reduce penetration and infiltration of the monomers within the dentine layer. This has clinical relevance where the sealing quality may be impaired and microleakage can take place. Microleakage presents as microscopic voids between the collagen fibrils which were left by the incomplete diffusion of the adhesive monomers.

Despite this, a recent study has reported that there were no significant differences between the bond strength to the CAD or CID. This can be explained by the fact that the demineralization in CAD and the partially denatured collagen acts in a similar way to totally degenerated CID, especially in long-term storage (Costa et al., 2017). Despite the ability of CAD to interact with adhesive systems, the intrinsic characteristic of CAD results in a lower bonding performance compared with the sound dentine, regardless of the adhesive systems used (Pinna *et al.*, 2015). The use of Fourier-transform infrared (FTIR) imaging has shown a loss of crystallinity in the CAD mineral phase, besides the reduced mineral content and spectral changes in the secondary structure of collagen (Spencer *et al.*, 2005). In addition, the tubular occlusion by the mineral intratubular deposits of *Beta*-tricalcium phosphate or “whitlockite” deposits make this tissue impermeable to dentine fluids. However, the wetness of CAD may originate from the inter-tubular

mineral replacement by the water which hampers proper adhesion of the hydrophobic resin and therefore porosities will result within the hybrid layer (Pinna *et al.*, 2015). Furthermore, a decrease in the bond strength and the durability of this substrate has been reported in the literature regardless of the bonding technique and the restorative material used (Nakajima et al., 1995, Yoshiyama et al., 2002, Shibata et al., 2016). The hydrolysis of the interfacial layer in the CAD may be due to nano-leakage and degradation by MMPs (Erhardt et al., 2008).

1.3 *In-vitro* demineralised dentine

Artificial carious lesions in dentine allow investigations of different strategies for caries prevention, excavation techniques or treatment of dentine carious lesions. *In-vitro* models are required in such experiments whose objectives involve testing an isolated single process, as more complex variables may confound the results (Moron *et al.*, 2013).

Despite significant advances in preventive and restorative dentistry, replacement of tooth fillings is still problematic due to the limited durability of resin-based restorative materials when bonded to the demineralised dentine. Based on the diversity of structures and morphology of the bonded substrate, laboratory methods used to mimic such a scenario should be carefully chosen. Different types of studies have been proposed for the induction of artificial caries in human dentine (Amaechi et al., 1998). Consequently, various studies play a key role in cariology research by investigating caries pathogenesis, prevention and treatment.

A mechanistic study can be defined as an experiment that can test and analyse the biological or the chemical events associated with an effect. In demineralisation/remineralisation studies, the molecular and physiological mechanisms by which substances exert their effect on teeth are explored (Yu et al., 2017). Dentine models with caries-like lesions have been produced to resemble the CAD, and to overcome standardisation issues when using natural caries samples. These methodologies are summarised by a recent review (Yu et al., 2017) in the literature and they are categorised into in-situ, *in-vitro* or *in-vivo* studies as shown in Fig.1-8. An *in-vitro* study is the type most commonly used in the literature and can be subdivided into acidic chemical models or microbiological caries induction which are summarised in Table 1-4.

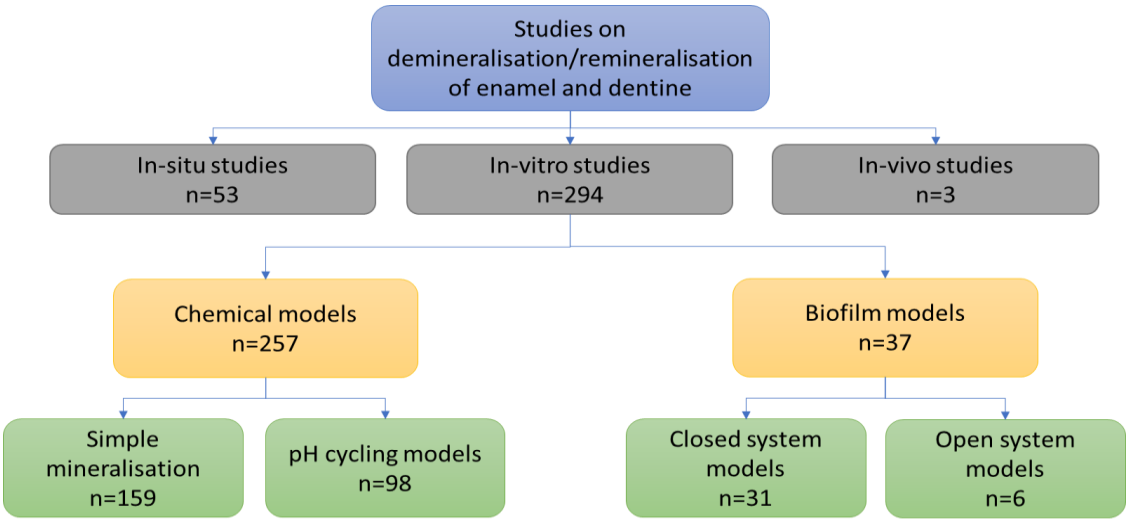

Figure 1-7. Mechanistic studies on demineralization-remineralization for cariology research (published in Web of Science 2014–2016).

Some studies have attempted to use chemical and bacterial methods for *in-vitro* creation of caries-like lesions as substrates for bonding or testing new materials as summarised in Table1-4.

Table 1-4. *In-vitro* dentine artificial caries models.

Type of *in-vitro* dentine carious models	**Biofilm carious induction**		**Chemical models**	
	Open system	Closed system	Simple demineralisation	pH-cycling method
Advantages	Produce models similar to natural dentine caries in terms of colour, hardness and the presence of two distinct layers (Clarkson et al., 1984, (Marquezan et al., 2009).		Mild organic acids such as lactic acid and acetate acids have created lesion closer to the natural caries	Does not require large sample size, together with the lower variability in the produced lesion (Damato et al., 1990).
Disadvantages	• Microbial culture models in the open system are more complex and time consuming compared to the chemical approach (Yu et al., 2017).		• The acidified gel has impurities that is responsible for the development of subsurface lesions (Featherstone et al., 1978). • The produced artificial lesions are different in their	pH-cycling produces greater demineralisation compared to acid gelation.

	• They result in an excessive softness of dentine.	physical and mechanical properties. Hence the obtained results are not comparable, and conclusions could be different (Moron et al., 2013).	

1.3.1 Effect of acid-etching on dentine

Acid-etching is the key step in preparing the tooth for the adhesive restorative treatment, especially when applying the total-etch approach. This concept was first proposed by Buonocore for enamel etching, to increase the bond strength of acrylic fillings to the etched porous enamel surface (Buonocore, 1955). Since then, controversies concerning the etchant type, concentration, length of etch, and rinsing time have developed. The success obtained with enamel etching inspired its use on dentine surfaces. However, acid treatment of the dentine surface failed to provide bond strength similar to that obtained with enamel. At that time, Fusayama et al. demonstrated that the bond strength improved when they applied a bonding system with 40% phosphoric acid for 60 secs on enamel and dentine simultaneously (Fusayama et al., 1979). Furthermore, Gwinnett and Kanca (1992) reported that application of a hydrophilic bonding agent following conditioning of the dentine with 37% phosphoric acid for 15 secs resulted in a gap-free interface between resin and tissue both in *in-vivo* and *in-vitro* studies. The application of 37% phosphoric acid was then reduced to 15-30 secs, followed by copious rinsing with water for 30 secs to simplify the bonding procedure. A study by Barkmeier et al., (1992) has shown that conditioning the dentine surface with 35% and 10% phosphoric acid gel and 10% maleic acid for 15 and 60 secs provided similar micromorphological effect on the dentine surface.

The application of conditioning agents to dentine surfaces leaves a surface with partial or total removal of the smear layer and exposed collagen (Ceballos et al., 2002). In addition, they result in the demineralisation of the peritubular and intertubular dentine and opening of the dentine tubules (Van Meerbeek et al., 1992). Nevertheless, many factors have influenced the degree of surface etching

and demineralisation of enamel and dentine. Furthermore, acid-etching dentine and loss of the hydroxyapatite crystals that support collagen may create voids in between the collagen fibres. It is difficult for adhesive monomers to penetrate the collapsed or the denatured collagen (Pashley, 1992).

Acid-etching exposes dense collagen fibres, leaving residual HA crystals at the base of the demineralised zone (Van Meerbeek et al., 1993). It increases the water wettability of the dentine surface regardless of the etchant used (Aguilar-Mendoza et al., 2008). Dentine etching proceeded in two stages; rapid rate demineralisation of 70-75% of the mineral components, while the remaining minerals were then removed slowly (Kinney et al., 1995). Balooch et al. (2008) confirmed that the intrafibrillar minerals were dissolved at a slower rate compared with extrafibrillar using Raman microscopy and small angel X-ray scattering.

Mineral content and hardness profiles can be used as indicators for the depth-related properties of artificial carious lesions. Therefore, a quantitative measure of the mineral content such as transverse microradiography (TMR) has been used for this purpose and to assess transverse mineral distribution of caries lesion in dentine (Moron et al., 2013). It is considered as the gold standard for mineral quantification of caries lesions *in-vitro*. On the other hand, cross-sectional hardness (CSH) or surface hardness (SH) may reflect the mechanical resilience of the dental hard tissue. However, it is still debated whether CSH or SH analysis might reflect depth mineral alterations of carious dental tissues.

1.3.2 Dentine remineralisation

Repair of the defective tooth restoration and remineralisation of the hypo-mineralised carious dentine are considered the major challenges for operative and preventive dentistry. Biomimetic mineralisation simulates the natural process of mineral crystal formation without using special equipment or strict conditions. For an effective remineralisation to occur, reformation of the inorganic mineral-like structure is highly indicated (Cao et al., 2015). Thus, to improve the durability of dental restorations, and to control caries progression, biomimetic dentine remineralisation has been highlighted. Dentine remineralisation is more complex than enamel remineralisation. The aim of dentine remineralisation is to reform a dentine microstructure of the demineralised collagen matrix. This can be

expressed by intrafibrillar HA formation to occlude the open dentine tubules. The enamel surface contains residual seed mineral crystals which are absent in dentine lesions. In agreement with this statement, under the same remineralising conditions, remineralisation occurs on the surface of acid-etched enamel but not with acid-etched dentine (Bertassoni et al., 2009). Such a result may be attributed to the limited amount of the residual mineral crystal and exposure of collagen type I in the acid-etched dentine. From a biological point of view, different mechanisms of apatite growth and crystallisation have been proposed for dentine remineralisation. They are classified into classical and non-classical approaches.

- **Classical top-down remineralisation approach**

It is also known as the ion-based crystallisation approach. This approach involves epitaxial growth over existing seeds crystallites. Thus, this concept may not be applicable for remineralising the completely demineralised dentine or CID as their surface lacks seed crystals which are required for apatite growth. The dentine surface has been demineralised artificially before the biomimetic mineralisation using different methods including: phosphoric acid etching (PA) with concentrations 32% to 37%, as a demineralising agent (Reyes-Carmona et al., 2009, Cao et al., 2013) or (EDTA) at 17% or 0.5 M concentrations (Alves et al., 2013). In addition, pH cycling was also reported for this purpose (Leiendecker et al., 2012).

Remineralisation can be induced using fluoride releasing restorations and bioactive containing adhesives and is mainly based on the deposition of calcium and phosphate ions over the pre-existing apatite crystals. These crystals act as nucleation sites allowing further precipitation of ions from the surrounding media. This process initiates from primary building blocks like atoms, ions or molecules, providing clusters. Eventually, some clusters reach the size of a so-called critical crystal nucleus which grow further via ion-by-ion attachment and unit cell replication (Niu et al., 2014). The top-down mineralization approach occurs by epitaxial growth over seed crystallites rather than spontaneous nucleation of minerals on the organic matrix (Koutsoukos and Nancollas, 1981). In addition, matrix proteins play a pivotal role in the regulation of mineral nucleation and growth. This approach results in extrafibrillar mineralisation of the collagen matrix but not the intrafibrillar compartments. This may refer to the uncontrolled size and

orientations of these developed minerals during the classical mineralisation process.

Previous findings from an earlier study confirmed that the mineral distribution of the demineralised surface layer had an effect on the characteristics of subsequent mineralisation, including the location and density of mineral deposition (Kawasaki et al., 2000). Recent studies on this type of classical remineralisation have considered it non-functional or incomplete remineralisation (Tay and Pashley, 2008, Liu et al., 2011b).

- **Non-classical remineralisation approach**

An alternative *in-vitro* biomimetic remineralisation approach refers to the “bottom up” remineralisation that does not depend on the existence of seed crystallites and may be considered as a feasible method for remineralisation of partially or totally demineralised dentine. It relies on the backfill of the demineralised dentine using a synthetic substitute for certain dentine NCP that plays a specific role in biomineralisation. Interfibrillar and intrafibrillar dentine remineralisation have been demonstrated using this biomimetic scheme. Intrafibrillar remineralisation being crucial for maintenance of the mechanical properties of the mineralised dentine matrix (Kinney et al., 2005). There are two suggested analogues; the first is polyanionic molecules such as polyacrylic acid which promotes the formation of liquid like amorphous calcium phosphate (ACP) (Niu et al., 2014). This will aid in intrafibrillar mineralisation of the fibrillar collagen through a flowable nano-precursor which infiltrates the water filled gap zones in the dentinal collagen fibrils, where they precipitate as polyelectrolyte-stabilised apatite nanocrystal aggregates (Tay and Pashley, 2008, Liu et al., 2011a, Leiendecker et al., 2012). These crystals support the collagen fibres and protect its molecules from further degradation. In addition, intrafibrillar remineralisation significantly increases collagen mechanical properties to mimic those of mineralised tissues (Ryou et al., 2012) and resists the external challenges, such as temperature, endogenous enzymes, bacterial acids and other chemical factors. Crystal precipitation is guided by the second analogue, which is a dentine matrix phosphoprotein substitute (Dai et al., 2011). This analogue is usually a polyphosphate molecule, such as sodium metaphosphate, that helps in the crystalline alignment in the gap zones (Leiendecker et al., 2012), then to a hierarchical dentine remineralisation.

In the bottom-up approach, type I collagen molecules undergo self-assembling at the nanoscopic scale to provide highly-ordered macromolecular structures. It is well-documented that type I collagen acts as a template for ACP attraction in the biomineralisation process. Using this approach, hybrid layers formed by etch-and-rinse adhesives (Sauro et al., 2009) and moderately aggressive self-etch adhesives (Liu et al., 2011b), as well as completely demineralised dentine lesions (250–300 μm thick) can be remineralised (Leiendecker et al., 2012). Dentine ultrastructure was preserved in a phosphate containing fluid with a calcium release system, in which polyacrylic acid (PAA) and polyvinyl-phosphonic acid (PVPA) were used as analogues of NCPs (Niu et al., 2014, Jin et al., 2018).

Recently, this approach has been applied in dentine remineralisation experiments. It was found by Cao et al. that the presence of casein phosphopeptide-stabilized ACP induced a higher remineralisation degree of dentine surfaces (Cao et al., 2013). Another study has demonstrated the dentine remineralisation in the existence of the additive PAA, during which ACP is initially formed in the collagen matrix and further transformed into hydroxyapatite and proceeds towards the surface (Wang et al., 2013). Compared to the classical approach, the non-classical remineralisation approach is considered more advantageous as it provides continuous replacement of intrafibrillar water by apatite crystals. It also helps in fibrillar self-assembly without the existence of nucleation sites (Liu et al., 2011b).

In the bottom up approach, calcium-silicate based cements such as MTA, act as a calcium source (Tay and Pashley, 2008, Leiendecker et al., 2012). When these cements hydrated, they release calcium in the form of calcium hydroxide (Camilleri, 2011) and silicon ions in the underlying dentine (Han and Okiji, 2011). Compared to fluoride, silica was found to induce more effective dentine remineralisation (Saito et al., 2004). It has been suggested in earlier studies that calcium silicate cements provide a potential caustic effect due to their high alkalinity, which favours apatite formation and dentine matrix phosphorylation in phosphate-rich fluids (Tay et al., 2007)

Apatite formation was also reported when the hydrated calcium silicate cement was stored in phosphate-rich media and characterised as calcium-deficient apatite (Chen et al., 2009). Likewise, an earlier study on Biodentine cement (a

calcium silicate-based restorative material) confirmed the cement's bioactivity and potential remineralisation effects on sound and completely demineralised dentine (Atmeh et al., 2015). On the other hand, GICs did not show the same remineralisation effect in the completely demineralised dentine samples. However, it showed better remineralisation action in *in-vitro* partially demineralised dentine and natural caries-affected dentine samples (Sajini S. 2016) which would be valuable regarding the cements' clinical applications in deep carious lesions.

In the literature, several dental materials have been used in attempts to remineralise the demineralised dentine both *in-vivo* and *in-vitro*. The materials used in this study will be discussed in the following section.

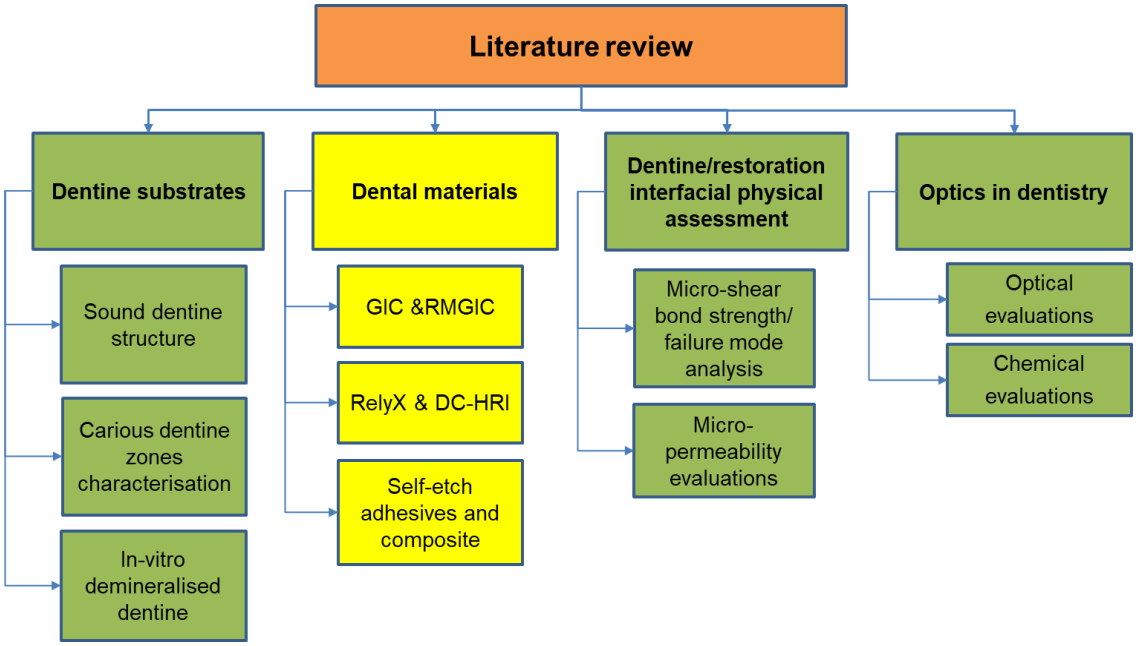

1.4 Dental biomaterials

Dental biomaterials have been used for the replacement, repair, support and regeneration of the lost or defective dental hard tissues (Hench and Ethridge, 1975). Initially, it was thought that the ideal restorative materials used in the oral cavity should be stable, biologically inert, biocompatible and passive without any interactions with the body tissues or fluids and with acceptable mechanical properties. Dental amalgam, resin composites and dental cements are the materials of choice with such properties. Many of the present generation of materials are still based upon this concept. However, in the past two decades, bio-interactive materials have been introduced to demonstrate an interaction between restorative materials and tooth tissue. This evolution has helped in tissue healing and prevents disease progression. Biomineralisation is believed to induce biological responses through biochemical and biophysical reactions that lead to the formation of an apatite layer. The deposited apatite-like compounds transform into HA crystals improving the tissue's mineral content and thus its mechanical properties.

As the research evolves, significant development of new materials or improvement in the performance of the existing materials has been noticed. This evolution has been mainly directed towards the conservative methodologies of minimally invasive dentistry. Therefore, the non-operative application of materials

with a remineralisation potential has been recommended when restoring dental caries conservatively. This may help to reverse the demineralisation process caused by the dental caries.

Several classes of restorative materials have been claimed as bioactive materials, which have additional clinical applications for bioactivity outside the scope of this review, including endodontic sealers, root end fillers, and root perforation repair materials. These remineralising materials include fluoride- and/or calcium-containing pulp capping materials, bonding agents, resin composites, resin cements, glass-ionomer cements, hybrid resin/glass materials and sealants (Vallittu et al., 2018). They are summarised in Table 1-5.

Table 1-5. Summary of the development of most bioactive pulp capping/restorative materials

Authors	Materials	General comments
(Gandolfi et al., 2015)	Calcium hydroxide	Since 1930, calcium hydroxide liners have become the gold standard material for pulp capping. An antimicrobial action by raising the pH, and the ability to induce reparative dentine by growth factors release stimulations in dentinal collagen were characteristic properties for these materials. However, their solubility, inability to bond to tooth and inadequate sealing properties have limited their modern use.
(Torabinejad et al., 1995).	MTA	In 1993, a mix of Portland cement (tricalcium silicate, dicalcium silicate and tricalcium aluminate) and a radiopaque agent (bismuth oxide) was launched as mineral trioxide aggregate (MTA). This material has the same mechanism of action as calcium hydroxide, but it seals to tooth structure. Additionally, it can lay down calcium phosphate layer in the presence of phosphate containing solution. Unfortunately, it requires 2 hours and 45 minutes final setting time and it is difficult to manipulate
(Kaur et al., 2017) (Simila et al., 2018)	Biodentine (Septodont)	In 2009, it was presented with a tricalcium silicate powder added to calcium chloride liquid instead of water. This has improved the material setting to only 12 minutes. It has excellent sealing ability through formulation of mineral tags within the dentinal tubules. There is a lack of long term observational clinical evidence about Biodentine.
(Berg and Croll, 2015).	(Activa BioActive	In 2014, it was brought to the market as an “RMGI with a bioactive resin matrix and bioactive glass fillers.” This material is able to release calcium, fluoride and

	Restorative, Pulpdent)	phosphate ions. The exact classification of this material is unclear, as it combines methacrylate resins with polyacrylic acid copolymers, suggesting it may be a compomer.
(Croll et al., 2015)	(Cention N, Ivoclar Vivadent)	In 2017, another restorative material that provides ion-release of calcium fluorosilicate glass in a methacrylate resin was introduced. These materials have provided a relatively acceptable performance in clinical trials without using an adhesive. There is still lack of clinical evidence for long-term use of these materials without an adhesive.

Another group of restorative materials claimed their bioactivity by the release of calcium, phosphate and fluoride ions. Some authors have recommended this ability is more accurately termed “biointeractivity”(Gandolfi et al., 2012).

In the current project, different bio-interactive or inert materials (conventional high-viscosity glass-ionomer cements, experimental hybrid resin/glass-ionomer cement and resin composite Bulk-fill material) are investigated for their potential in demineralised dentine repair or caries inhibition compared to that of sound dentine controls.

1.4.1 Glass-ionomer cement

In the late 1960s, Glass-ionomer cements (GICs) were introduced by Alan Wilson and Brian Kent at the Laboratory of the Government Chemist, London, for commercial use as a decomposable glass and water-soluble acid (Wilson and Kent, 1971). Since that time, they have been subjected to extensive researches and developments. Ever since their first introduction, their chemical adhesion makes these cements act as an essential part of the armamentarium of restorative dentistry as well as aesthetic properties and fluoride release (Sidhu, 2011).

Glass-ionomers set by an acid-base reaction within 2–3 min from mixing. This reaction takes place between the polyalkenoic acid and the ion-leachable glass particles. Therefore, this interaction results in the movement of ions Na^{+}, $Ca^{2+,}$ or Sr^{2+} from the glass into the polyacid solution, followed by Al^{3+} ions when the acid attacks the glass surface. This initial phase is known as a dissolution phase. Following ion release, the polyacids molecules become ionised and follow a more

linear form. An interactive ion-exchange between the freshly mixed glass ionomer and wet dentine takes place, leads to chemo-mechanical interaction between the two substrates (Wilson et al., 1983, Watson, 1999, Sennou et al., 1999, Yiu et al., 2004). This ionisation will facilitate the crosslinking of the carboxylic acid group in the later stage of gelation (Walls, 1986). The crosslinking leads to the formation of the final set matrix including insoluble rigid polysalt, unreacted glass particles embedded in that matrix. Water plays a critical role in the setting process and it is essential in the maturation process (Billington et al., 2006, Lohbauer, 2009). It is distributed in two forms; loose water that can be lost through desiccation or bounded chemically to the matrix (Nicholson, 1998).

This ionic exchange provides the GIC the capability to remineralise the carious dentine and tip the balance in favour of apatite formation and promotes their adhesion to the tooth substrate.

The next breakthrough in the development of GIC was the introduction of highly viscous compositions, aiming to be used in conjunction with the Atraumatic Restorative Treatment (ART) technique, in which hand caries excavation is applied (Frencken et al., 1996). In the current study, a high-viscosity glass-ionomer restoration was selected as a control restorative material to be compared with the new experimental material. This selection was based on that all materials are highly viscous with self-adhesive properties to replace amalgam restorations in the deep posterior cavities.

Clinically, GICs are highly recommended as anti-cariogenic materials that can induce the remineralisation of the carious dentine due to fluoride release which is one of the major advantages of GICs. In the acidic media, an increase in fluoride release from the GICs was anticipated to buffer this medium (Nicholson et al., 1999), hence, it can be easily taken up by hydroxyapatite of the tooth (Lewis et al., 2013) to form fluorapatite in the adjacent tooth structure thereby making it more resistant to demineralisation. The second advantage is their self-adhesion properties to the tooth structure which takes place in a number of stages. First, fresh cement paste is placed allowing proper wetting of the tooth surface due to the hydrophilic nature of both cement and dentine. Second, hydrogen bond formation between the free carboxyl groups of the cements and water on the tooth surface (Wilson, 1974). Third, true ionic bonds replace these hydrogen bonds

and result in slow formation of ion-exchange layers between the tooth and the cement (Ngo et al., 2006).

1.4.2 Resin-modified glass-ionomer cements (RMGICs)

Several modifications have been implemented to the conventional GICs in an attempt to overcome their downsides of the sluggish nature of the setting reaction, limited working time along with prolonged moisture sensitivity and poor mechanical properties (Moshaverinia et al., 2011). The key modifications involve incorporation of auto-cured or photo-cured resin systems into GICs to produce resin modified glass ionomer cements (RMGICs) (Wilson, 1990). In addition, there have been several modification attempts to improve GICs' mechanical properties by incorporation of polyvinyl phosphonic acid (Khouw-Liu et al., 1999), fibre-reinforcement (Lohbauer et al., 2003), silica particles (Tjandrawinata et al., 2004) and bioactive apatite (Moshaverinia et al., 2011).

RMGICs were introduced in the late 1980s to overcome the initial high solubility of GICs. They contain the same essential components as conventional glass-ionomers (basic glass powder, water, polyacid), but the acid-base reaction neutralisation was supplemented by additional polymerisation reaction through the incorporation of water soluble monomers and a photo initiator to stimulate the setting reaction (Berzins et al., 2010). The monomer is typically 2-hydroxyethyl methacrylate (HEMA) and the initiator is camphorquinone (Mitra, 1991). These hybrid materials have developed to combine the anti-carious potential of GICs and the favourable mechanical properties of a resin composite. The superior properties offered by RMGICs include increased working time, reduced setting time, less moisture sensitivity and improved mechanical properties (Nicholson, 2010).

Compared to the GICs, biocompatibility of RMGICs are compromised due to the release of the cytotoxic HEMA monomer in the first 24 hrs and its ability to diffuse through the dentine to the pulp cells (Kan et al., 1997, Palmer et al., 1999). However, clinical studies have shown a high success rate when used as an indirect pulp capping material (Marchi et al., 2007, de Souza Costa et al., 2007). On the other hand, RMGICs have a superior caries preventive effect when compared to the conventional resin composite restoration (Yengopal and Mickenautsch, 2011). Another study has reported the significant decrease of

bacterial counts in the sealed partially excavated caries lesions by RMGICs compared to amalgam restoration (Kreulen et al., 1997).

1.4.3 Self-adhesive resin cement

RelyX™ Unicem cement is a dual-curing, self-adhesive universal resin cement for adhesive cementation of indirect ceramic, composite or metal restorations. No bonding or conditioning of the tooth is required before its application. Compared to the multi-step composite cements, RelyX™ Unicem is characterised by a higher moisture tolerance and fluoride release. It is essentially characterised by high dimensional stability, excellent adhesion to the tooth structure and good aesthetics among other cements (Zidan et al., 2015). It is available in two formulations: as powder/liquid Aplicap and paste/paste Maxicap capsules (3M, St.Paul, USA). The cement chemical composition is summarised in Fig. 1-10.

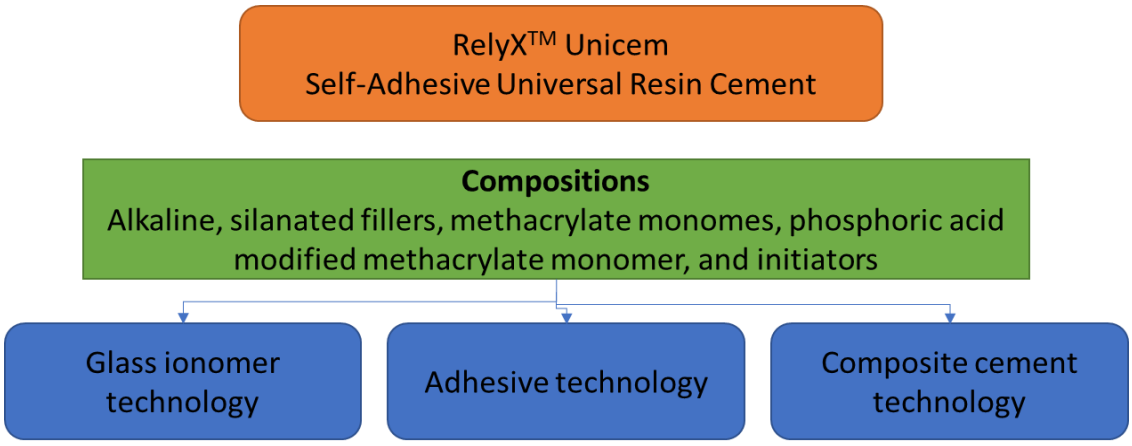

Figure 1-8. RelyX™ Unicem chemical composition

It has a combination of acidic methacrylate monomers that contain several phosphoric acid groups and carbon double bonds. Phosphoric acid groups contribute to self-adhesion, while double carbon bonds are responsible for the high reactivity of the methacrylate monomers. Thus, the cement shows a high degree of cross-linking following setting and high mechanical properties can be achieved which may contribute in the long-term stability of the cement. It includes two types of filler: silanated (chemically embedded into the matrix), and alkaline (basic) that can react with the phosphoric acid groups of the methacrylate monomers during the neutralisation reaction. These fillers are responsible for buffering or increasing the initial acidity following the mixing of the cement (Zorzin et al., 2012). A simultaneous neutralisation reaction takes place to overcome the

initial acidity of the cement by fluoride release. During setting, cement transforms from hydrophilic to hydrophobic nature.

1.4.4 Hybrid resin/glass ionomer self-adhesive restoration

Recently, a new formula as a derivative of RelyX™ cement was introduced as a bulk-fill, highly viscous, dual-cure hybrid resin/ionomer (DC-HRI, 3M, USA), coronal restorative material that could replace large amalgam restorations in deep cavities. The new experimental material combines the self-adhesiveness, the anti-cariogenic properties of GICs and the high mechanical strength of the resin composite bulk-fill restorations. Therefore, they are anticipated to induce similar effects to these materials, when they interact with the dentine substrates. The objective of developing this kind of restoration was to reduce technique sensitivity and for simple handling without sacrificing good adhesion to tooth structure in deep cavities.

They contain mainly surface modified glass powder, oxide glass chemicals, and calcium hydroxide in their powder. The liquid involves mono, di, and tri-glycerin-dimethacrylate phosphoric acid ester, tri-ethylene glycol dimethacrylate, substituted dimethacrylate. These chemical compositions are the same as those mentioned in the Rely X™ composition, but with an increased powder/liquid ratio in order to increase their mechanical properties.

However, it has been reported previously that self-adhesive resin cements provide a relatively low shear bond strength to dentine as they don't dissolve the smear layer (Goracci et al., 2006) and they interact superficially with the tooth surface. Since self-adhesive cements are applied without pre-treatment for luting, penetration of and interaction with the underlying dentine are questioned. Results showed that self- adhesive cements were not able to dissolve/penetrate the smear layer completely (Monticelli et al., 2008). Likewise, it is suggested that the experimental material provides a similar low bond strength to dentine, as it has higher viscosity than the luting cements.

The manufacturer claims that DC-HRI has shown promising physical properties data. However, there is still lack of any clinical evidence data.

1.4.5 Bulk-fill resin composites

Compared to dental amalgam, resin composites (RCs) have improved aesthetics, with a conservative cavity preparation (Hickel and Manhart, 2001) and micromechanical adhesion to the tooth structure using special bonding adhesives. However, they have several shortcomings regarding their mechanical properties, polymerisation shrinkage, abrasion and wear resistance, marginal leakage, thermal expansion and toxicity (Anseth et al., 1995, Lovell et al., 2001, Ferracane, 2005). In addition, layering techniques can incorporate voids and are time-consuming. Current changes in the composite are more towards developing systems with a reduced polymerisation shrinkage, as well as providing self-adhesive properties to the tooth structure (Ferracane, 2011). Modern RCs have higher bond strengths to dentine compared with RMGICs and GICs (Nujella et al., 2012). This is in agreement with the results provided in this thesis.

In order to simplify and speed-up the placement of large posterior RC restorations, manufacturers have provided a range of materials which can be placed in single or deeper increments, known as bulk-fill RCs. Bulk-fill restoratives include either lower amount of nanofillers or increasing the filler size to decrease light scattering. They have been marketed to restore around 4-5 mm cavity depth. This high depth of curing is referred to the presence of different photo-initiators that are more translucent which facilitate the passage of light to much deeper layers (Jang et al., 2015). This eventually will minimise the time needed for posterior restorations and decrease their technique sensitivity. Bulk-fill materials exhibit less shrinkage stress than conventional RCs (El-Damanhoury and Platt, 2014).

Bulk-fill composites can be provided in either low (flowable) or high- viscosity form according to their indications. High-viscosity bulk-fill composites comprise greater amounts of filler particles compared to low-viscosity bulk fill composites. Therefore, better adaptation but greater polymerisation shrinkage may result when flowable composite is used. Due to their lower mechanical properties, it is advocated be finished with a 2-mm capping layer of a high-viscosity bulk-fill composite resin, especially when restoring high-stress bearing areas (Bucuta et al., 2014). In the current study, bulk-fill composites

were used in a high-viscosity form as a comparative material to both GICs and DC-HRI.

1.4.6 Scotchbond Universal adhesive

Self-etch adhesives do not require a separate acid etch step, as demineralisation and priming occur simultaneously. Compared to etch and rinse systems, self-etch systems have shown reduced technique sensitivity, shorter application time and less post-operative sensitivity (Van Meerbeek et al., 2003, Van Meerbeek et al., 2005). These factors allowed for better standardisation and a large increase in self-etch adhesives usage among clinicians (Perdigao, 2007). They do not remove but incorporate the smear layer in the hybridised complexes. Some studies reported incomplete resin infiltration for some self-etch adhesives (Tay et al., 2002). However, they showed a reduction in post-operative sensitivity following placement of posterior composite restorations (Unemori et al., 2004).

Self-etch adhesive materials have been suggested for indirect pulp capping as they are utilised to improve retention, minimise microleakage, and reduce post-operative sensitivity of resin composite restorations. When managing deep cavities or even pulp exposure, the hypothesis of pulp healing can be guaranteed if adequate sealing of the pulp against bacteria or controlled haemorrhage is achieved, together with placement of acidic restorative materials (Pereira et al., 2000, Modena et al., 2009).

Scotchbond™ Universal adhesive is known as a “multi-mode” or “multi-purpose” adhesive according to the mode of its application, as self-etch (SE) adhesives, etch-and-rinse (ER) adhesives, or as SE adhesives on dentine and ER adhesives on enamel (a technique commonly referred to as “selective enamel etching”) (Perdigão et al., 2012). It differs from the current self-adhesive systems by the incorporation of monomers allowing chemical adhesion to the dental substrates, hence the durability of the bond may be prolonged (Haefer et al., 2013). It utilises phosphorylated monomers in an aqueous solution. It contains an etchant: 34% phosphoric acid, water, glycol and amorphous silica, and an adhesive: MDP phosphate monomer, dimethacrylate resins, HEMA, fillers, water, initiator and silane.

The bonding mechanism of self-etch adhesive systems is two-fold, micro-mechanical interaction and chemical bonding; providing improved restoration durability (Giannini et al., 2015). The micro-mechanical bonding contributes in resistance to the mechanical stress, while the chemical bond with hydroxyapatite reduces the hydrolytic degradation and maintains the marginal seal for a longer period (Van Meerbeek et al., 2011). The functional acidic monomers are composed of specific carboxylic, phosphonic or phosphate groups, such as Phenyl-P, 10-methacryloyloxydecyl dihydrogenphosphate (10-MDP), acrylic ether phosphonic acid and other phosphoric acid esters. 10-MDP monomer has a dihydrogenphosphate group from is responsible for etching and chemical bonding, while its long carbonyl chain provides the hydrophobic properties and hydrolytic stability to this acidic monomer.

Yoshiyama et al. examined the interfacial morphology of two bonding systems (Single Bond, 3M and Fluoro Bond, Shofu) to caries-infected dentine, coupled with the measurement of μTBS, and reported lower bond strength to carious dentine compared to that of sound dentine regardless the type of adhesive used (Yoshiyama et al., 2004). It has been also reported in a recent study that SU adhesive has provided higher bond strength values in self-etch mode in sound dentine compared to artificially induced CAD (Follak et al., 2018a). On the other hand, a previous study showed that the performance of this adhesive was the same for both sound and artificial CAD (Lenzi et al., 2015).

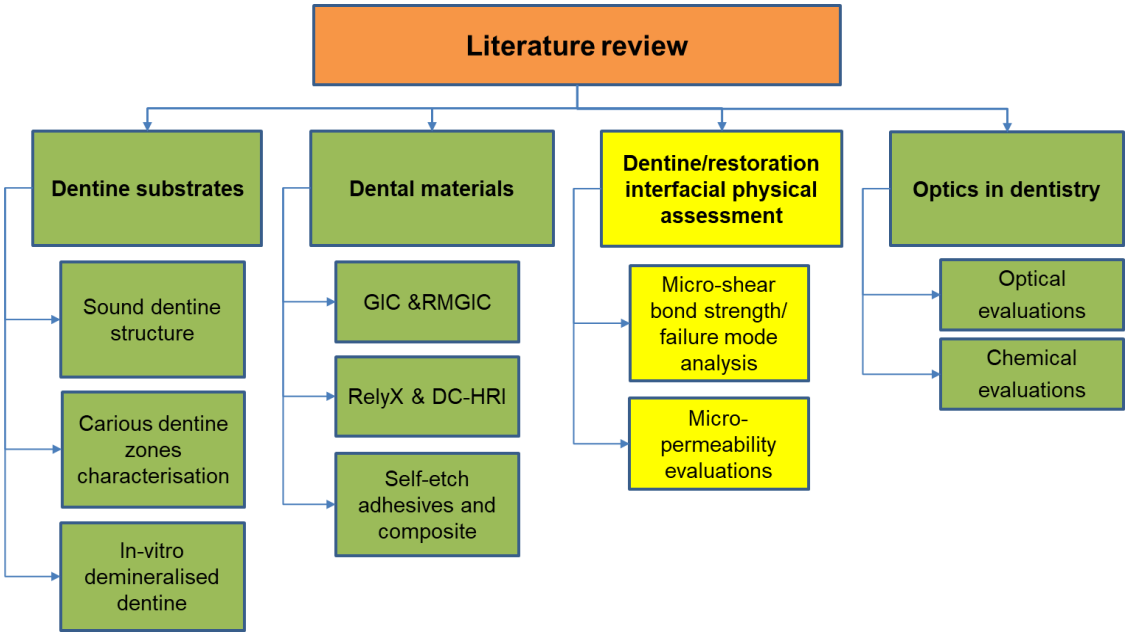

1.5 Evaluation of dental restorations

Despite the laboratory studies can effectively predict restoration performance, correlating their data with clinical performance is challenging, and there are no truly predictive tests of long term clinical performance (Bayne, 2007, Green and Banerjee, 2011). Thus, the ultimate objective of a laboratory test should be data collection to predict the eventual clinical outcome. Nevertheless, it is without doubt that these tests afford valuable information on the preclinical performance of dental restorative materials which can provide, to some extent, an estimate on the predictability of their clinical performance (Braga et al., 2010). According to Van Meerbeek et al. (2010), the advantages of laboratory investigations over clinical trials are:

- Speed in data gathering
- Relative ease of test methodology
- Ability to specify and isolate one parameter while keeping other variables constant
- Direct comparison of new and/or experimental material or techniques with the current gold standard
- Use one setup to compare many experimental groups

- Relatively inexpensive test protocols/instruments

In the oral environment, dental restorations are exposed to stresses from mastication forces. These forces may cause failure or deformation of the restoration/tooth interface and thus affect the durability of the restoration. The most commonly used *in-vitro* method for assessment of dental restorative materials is the bond strength test (De Munck et al., 2012). Additionally, interface morphology, microleakage, nanoleakage and micro-permeability are also used for the dentine sealing ability assessment of the bonding agent and dental restorations. Bond strength testing is one of the key aspects used to screen new products and to study the influence of experimental variables. Van Noort & others (1989), however, demonstrated that bond strength cannot be regarded as a material property. In contrast, they may largely depend on the actual test set-ups; therefore, it is not surprising that recorded bond strengths differ from one lab to another due to test variables such as sample geometry, type of material and substrate, and size of the bonding surface area examined (Van Noort et al., 1989).

1.5.1 Bond strength tests

The adhesive ability of dental restorations can predict, to some extent, the longevity of a restoration. Based on the size of the bond area, bond strength can be measured statically using macro- or micro- test setups. Static tests are categorised into macro-tests where the bonded area larger than 3 mm^2, whilst micro-tests have a bond area less than 3 mm^2. Both can be measured in a shear, tensile or push-out protocol. During mastication, mechanical stress by chewing forces, thermal and chemical stress along with changes in temperature and pH will have an effect on the bond integrity unlike dynamic tests where the specimen is in a dynamic state.

- **Macro-shear bond test/push-out**

In a shear bond test, two materials are connected via an adhesive agent and loaded in shear until failure. It has been the most highly used test, as no further specimen processing was required after the bonding procedure. Although this test is fast and easy to apply, the generated stress distribution is heterogenous. It has been reported earlier that several factors can influence various parameters

in bond strength testing. These factors may be related to the tooth substrate, study design, materials used, storage time, different configurations used for shear test such as wire loops or knife edges (Leloup et al., 1998, De Munck et al., 2012). Another type of shear test is called the push-out test, which can be used to test the retentive ability of endodontic posts. It has never been adopted as a universal bond-strength test method, due to the more laborious specimen preparation involved as well as the more time-consuming methodology (Goracci et al., 2004)

- **Macro-tensile test**

In a tensile bond test, the test sample undergoes stresses on both side. It can be actively held to the gripping device using special glue or clamps or passively without glue. The stresses associated with the tensile test are far more homogenous across the interface than in a shear test. It is suitable for hard materials such as cements bonded to ceramics and metal alloys (Armstrong et al., 2010, Van Meerbeek et al., 2010).

There are lots of variables that can affect the Macro-test results which are summarised in Fig. 1-11.

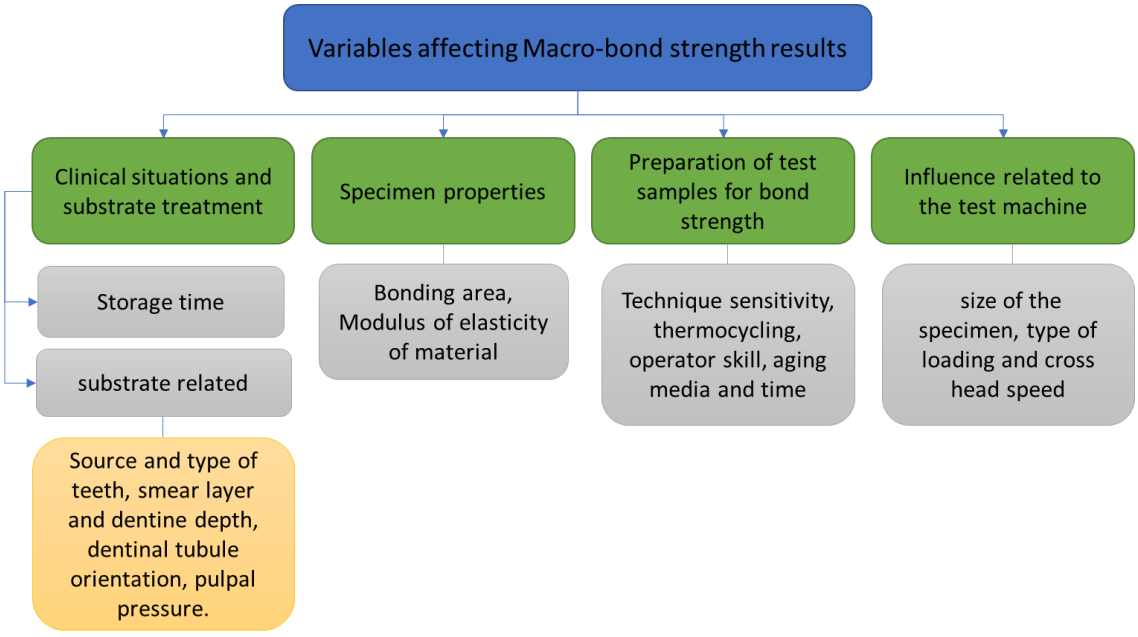

Figure 1-9. Flowchart showing the variables that influence the bond strength testing (Sirisha et al., 2014).

- **Micro-tensile test**

A micro-tensile bond strength (μTBS) methodology has been promoted since the mid-1990s by Sano and others to overcome the limitations of macro-tests, in which the material is adhered to dentine, then sectioned into individual composite/dentine sticks with a rectangular cross-sectional area of (0.8–1 mm^2) and pulled apart (Sano et al., 1994, Pashley et al., 1999, Armstrong et al., 2017). These authors demonstrated that micro-tensile bond strength was inversely related to the bonded surface area (Sano et al., 1994). Although much higher bond strengths than by other techniques were measured, most adhesive failures still occurred at the interface between tooth substrate and adhesive.

The advantages of this technique include faster sample collection and better economic use of teeth (multiple micro-specimens from one tooth), better control of regional differences (centre or peripheral sides of teeth), obtaining higher interfacial bond strengths and more uniform loading stress distribution over a smaller bonded area (less cohesive failure is expected) (Neves et al., 2008). This provides reliable bond strength data as the adhesive failure represents the “true” adhesive bond strength value while the cohesive failure can result from technical errors within the test setup (Scherrer et al., 2010). Additionally, this test enables the use of high-magnification imaging techniques after de-bonding for the evaluation of the failure mode in comparison with macro-tensile bond strength testing (Armstrong et al., 2010, El Zohairy et al., 2010).

However, the major disadvantage of μTBS-testing is that it’s considered a technically demanding test and a relatively fragile sample preparation technique. Thus, special care should be taken to minimise/limit the production of microfractures at the interface during specimen preparation; brittle materials in particular cannot stand such forces. Other important factors such as specimen–jig configuration, attachment, and specimen-loading alignment, greatly affect the final result and so must be consistent within the test set-up to provide meaningful data interpretation (Van Meerbeek et al., 2010).

Micro-shear test

More recently, some authors have advocated a new test method as a substitute for the conventional shear test: the so-called "micro-shear" bond strength (μSBS) test, using specimens with smaller dimensions (ranges between 0.7-1.5mm^2), for better stress distributions (Shimada et al., 2002). This test combines the ease of manipulation, regional and depth profiling of a variety of substrates, together with the ability to test several specimens from one tooth. It causes fewer voids and less stress-raising factors in smaller bonded areas than those that possibly occur in larger areas. The μSBS test allows testing of small areas, and it has the same advantages as the μTBS, with no sectioning procedures required to obtain specimens, as these laboratory procedures themselves may induce early micro-cracking within the specimen (Ferrari et al., 2002). Therefore, it is recommended to be used with brittle materials. However, this protocol has a shortcoming in the difficulty in confining the bonding agent to the area tested, which is required by ISO-standard No. 11405 (2003) (ISO, 2003), and may result in a thick adhesive layer and non-uniform loading condition (Yildirim et al., 2008). In addition, the variability in test configurations including wire loops, points and knife edge made the comparison of the results between studies more challenging (McDonough et al., 2002).

Moreover, the majority of studies have used polyethylene tubes as a mould to be filled with the examined material before storage; they are then removed by the operator using a scalpel blade before testing (Shimada et al., 2002, Andrade et al., 2010). The pressure exerted on the blade by the operator to cut through and remove the polyethylene tubes may be transferred to the material cylinder and consequently form cracks along the specimen. Additionally, this pressure may lead to stresses at the adhesive interface and cause premature failures. Some authors keep the tube in position while testing to avoid such pressure, claiming that there is no difference in bond strength if Tygon tubes were either kept or removed for load application (Foong et al., 2006, Sirisha et al., 2014).

However, a closer look at the number of pre-test failures (PTF) indicated that even gentle removal of the Tygon tubes induces some level of stress at the interface, since the tube removal procedure yields a high number of PTFs. The controversy around the usage of the Tygon tubes has led to testing a new

methodology. A study by Scherrer et al. (2010) has tested the effect of keeping the Tygon tube before the composite rod was placed on the dentine surface on the results obtained. Higher resin-dentine bond strength values and no PTFs were reported, which indicated that this factor affects the bond strength values (Scherrer et al., 2010).

On the other hand, due to the small bonded area, PTFs can occur in many specimens immediately after construction, depending on the adhesive system and method of specimen manufacture. Nevertheless, these PTFs must be correctly included in the statistical analysis, something which is often neglected (Scherrer et al. 2010).

1.5.2 Failure mode analysis

Following bond strength evaluation, the de-bonded surfaces were reassessed to determine the mode of failure within the specimen. It is considered as an important parameter for interpreting bond strength results. It was reported that there is no clear consensus in the literature regarding failure mode classification as they were assessed using different analytical microscopy technologies (Scherrer et al., 2010).

Although the physical bonding is always present, it is considered very weak. On the other hand, the chemical bonding may provide covalent, ionic, metallic, and chelation bonding. The most common adhesion mechanism for dental materials remains mechanical interlocking.

Failure mode has been divided into three main types: adhesive, cohesive or mixed failure. Cohesive failure happens within the test material or tooth substrate itself. Adhesive failures occur at the adhesive interface between the material and the tooth and mixed failure represents a mixture of adhesive and cohesive failure within the same fractured surface (Armstrong et al., 2010, Scherrer et al., 2010).

In fact, it has been reported that there is a direct positive correlation between the bond strength and cohesive failure. Low magnification of stereomicroscopes has been used to evaluate cohesive failures. Proper assessment of the mode of failure for the adhesive interface or mixed failures can be made using a Tandem Scanning Microscope (TSM) or a Scanning Electron Microscope (SEM) (Scherrer et al., 2010).

A meta-analytical study by Leloup et al. found that there is a linear correlation between the failure mode and the mean bond strength; the higher the bond strength, the higher the incidence of cohesive failure due to errors in the alignment of the specimen along the long axis of the testing machine whereas, adhesive failure happens at the weak interface (Leloup et al., 2001). Conversely, other studies reported that the micro-shear bond strength tests usually show the predominance of adhesive/mixed failures, with few cohesive failures reported (Shida et al., 2009). This may be attributed to the fact that the load was correctly applied in the micro-shear test; therefore, giving more consistent results than those found for the μTBS test.

1.5.3 Interface morphology and sealing efficiency

Clinical problems such as micro-leakage and the influx of fluid can be prevented by effective adequate sealing and intimate bonding at the tooth-restoration interface (Carvalho et al., 2012, Gupta et al., 2017). Microleakage is the movement of bacteria, fluids, molecules, and/or ions at the tooth/restoration interface/margins. It can lead to several adverse effects, such as recurrent caries, higher sensitivity of the restored tooth, and interfacial staining (Hashemikamangar et al., 2016, Gupta et al., 2017). Another type of leakage, termed as nanoleakage, has also been described as a movement of fluid through the bonded dentine interface. It is mainly caused by dentine acid-etching which induces oral and dentinal fluid penetration into the hybrid layer (Yang et al., 2015). Many factors can influence the fluid interfacial infiltration such as hydrophilicity and type of bonding agent as well as its application technique. Nanoleakage is the key indicator of a material's sealing ability and the quality of the hybrid layer or dentine/restoration interface, which in turn affects the durability of the restoration (Ayar et al., 2016).

There are several techniques used for the assessment of the adhesive joint between the dentine and the restorative materials, including scanning electron microscopy (SEM), transmission electron microscopy (TEM), Raman spectroscopy, fluorescence confocal microscopy and two-photon microscopy (Griffiths et al., 1999, Watson et al., 2014). Specimen dehydration and special preparations are required for SEM evaluation. This makes the use of SEM difficult for interfacial dynamic relationship assessment. In dental research, confocal laser

scanning microscopy (CLSM) has been utilized widely to acquire high-resolution optical sections of the dentin/adhesive interface (Watson and Boyde, 1991, Watson, 1997, Paulo et al., 2006, Toledano et al., 2014, Toledano et al., 2015b). Moreover, confocal microscopy has the advantage of visualization of the subsurface interface up to 100 μm with minimal and less destructive sample preparation (Jardine et al., 2016).

Dentine/material sealing ability can be evaluated by different laboratory methods including nanoleakage, micro-leakage and micro-permeability. Microleakage studies use organic dyes to simulate the passage of fluids between a cavity wall and the restorative material applied to it (De Munck et al., 2005). However, this method provides a gross assessment of the interface quality and lacks the detection of small differences between various materials. To overcome this problem, Suppa et al. have examined the nanoleakage through the porosities in the hybrid layer using SEM and TEM (Suppa et al., 2005). Silver nitrate is the most commonly used staining material for nanoleakage assessment due to its extremely small diameter (0.059 nm) which allows easy infiltration of the interfacial zone. It is mainly used to verify the discrepancy between the depth of the demineralized zone and monomer diffusion, which occurs as a result of the presence of water around collagen fibrils. Porosities may result from incomplete infiltration of the primer and resin into the demineralised dentine, and/or from shrinkage during polymerization.

For three decades, labelling dental adhesives with the traditional fluorescent dyes like rhodamine and fluorescein has been used *in-vitro* for ultra-morphological assessment of the tooth-adhesive interface (Watson et al., 2000, Toledano et al., 2013). This can be done by simple mixing of fluorescein or rhodamine with the fluid resin with no covalent bond formed between them or they may also be added during the manufacturing process (Watson and Boyde, 1991). When the polymerisation of the adhesive occurs, the dye molecules become entrapped in the polymer network and label it.

Another type of interfacial study technique for assessing the diffusion of the fluorophore from the pulp chamber into adhesive the interface is called micro-permeability. Using this method, the permeation of a fluorescent dye towards the bonded interface reflects the intimacy of the hybrid layer to the bonded interface.

In addition, the tubule-sealing abilities of the bonding systems can be evaluated by the diffusion of fluorescent molecules into microporosities from the pulpal direction. Using conventional light microscopy, these dyes have been also used to assess the cavosurface margin integrity of a restoration (microleakage) to external fluids (Paulo et al., 2006).

Fluorescent labelling of the restorative materials or bonding agents allows the study of the relation between these materials and dentine. It is essential for understanding the nature and dynamics of this interface. However, the introduction of the fluorophore within these chemical systems may adversely affect the polymerization process by reducing the monomer conversion or by inhibiting the light from reaching the photo-initiators (Paulo et al., 2006). In a previous study, using confocal/two-photon microscopy, combination of fluorescent dyes was initially tested then applied providing enough separation between the excitation and emission wavelength of the two used dyes. Fluorescein powder was mixed with the material in combination with a 0.25% rhodamine-B solution for micro-permeability assessments (Paulo et al., 2006, Watson et al., 2014).

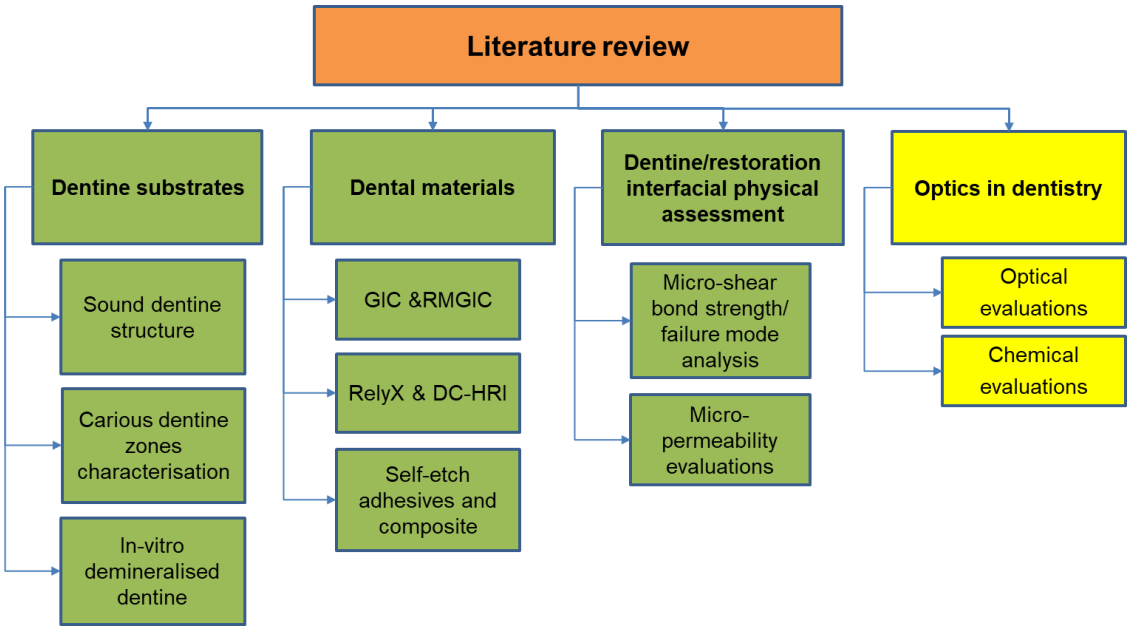

1.6 Optics and biophotonics in dental research

1.6.1 General optical properties

Currently a great interest is being directed towards the application of optical techniques for medical imaging, diagnosis, therapy and surgery (Baldwin, 2012). It was inspired by the introduction of novel lasers, growing improvement of fibre-optic techniques and other associated technologies. Ongoing investigations in the medical field have led to progression and expansion of studying the optical properties of different biological tissues.

Medical optics are mainly based on the mechanism of light interaction with biological tissues and spatial distribution of light in the target tissue (Lutskaya et al., 2012). These interactions can be classified into two levels: the “geometrical optics” which deals with the light interaction when directed to the surface or larger objects such as reflection and refraction. On the other hand, “physical optics” is the second type that deals with the matter at the molecular level interaction that will be discussed in this section.

In physics, electromagnetic wave represents electric and magnetic fields that simultaneously oscillate in planes mutually perpendicular to each other and to the direction of propagation through space as shown in Fig.1-12. It is characterised by its frequency, wavelength, amplitude and speed.

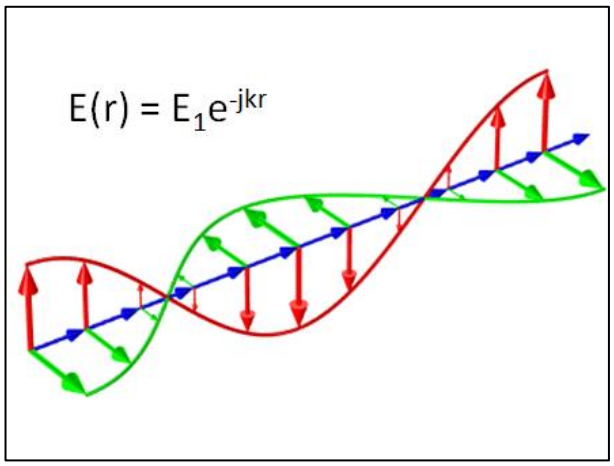

Figure 1-10. Graphical representation of electromagnetic wave propagating in free space

Frequency is the number of complete cycles of oscillation per second, expressed in s–1 = Hz (hertz), while the wavelength (λ) is the distance between two consecutive peaks or troughs in a wave. The relation between the wavelength and the frequency can determine the speed of electromagnetic wave. Electromagnetic radiation is viewed as a stream of particles called photons (i.e. quantaⅡ). Each photon has the energy proportional to the frequency of the electromagnetic wave.

The term light represents part of the electromagnetic spectrum with wavelengths ranged from 1 mm to 80 nm (optical wavelength region). The electromagnetic spectrum reflects the distribution of electromagnetic radiation according to wavelengths and photon energies including the infrared (>700 nm), the visible (blue, yellow and red from 400-700), and the ultraviolet radiation (<400) as shown in Fig.1-13. Light can interact with matter in three ways: absorption, transmission, and reflection.

- **Scattering of light**

Light scattering, along with the reflection and absorption, is one of the most important physical processes that determine the visual perception of most objects. Scattering is the deflection of a light beam from a straight path in different directions that highly affects the light propagation in biological tissues. When the scattered light has the same wavelength as the incident light, this type of

scattering is called elastic scattering or “Rayleigh scattering” (Sathyanarayana 2005). Non-elastic scattering or “Raman scattering” happens when a small proportion of the incident photons are scattered with an increase or decrease in their energy as shown in Fig. 1-14.

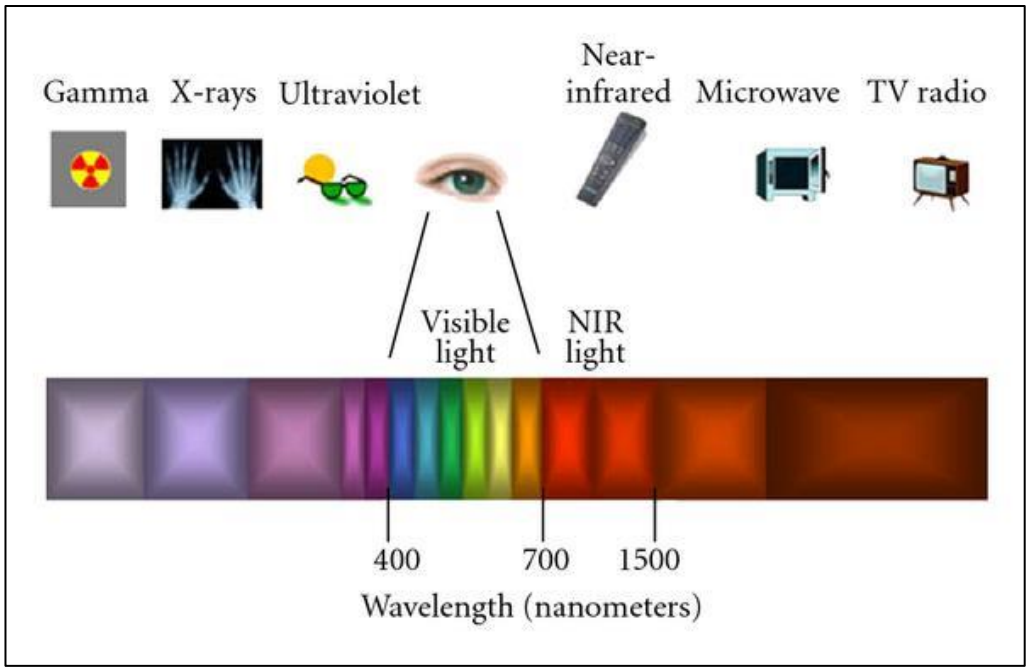

Figure 1-11. The electromagnetic spectrum Wavelengths of interest in this paper are the visible light spectrum from 400 nm to 700 nm and the range of near-infrared light from 750 nm to 1500 nm.

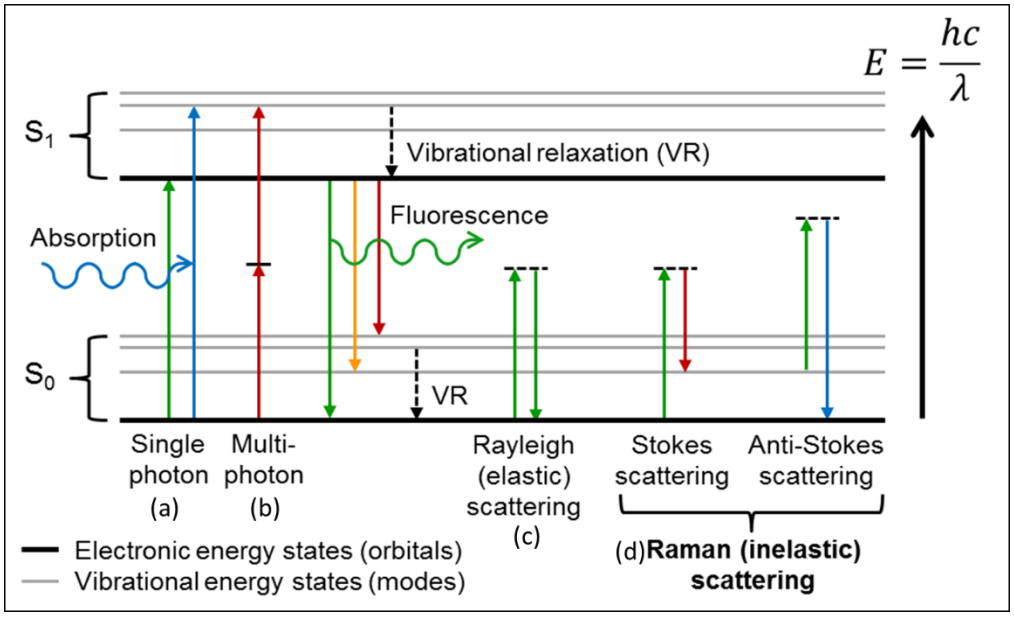

Figure 1-12. Jablonski diagram illustrating important optical transitions occur in a scattering/absorbing/fluorescent molecule. http://www.bodyyouknow.org/raman-

spectroscopy (a) In single-photon fluorescence, the photon energy is fully absorbed by the fluorophore and re-emitted with different energy and wavelength. (b) Multiphoton excitation requires two-photon with half energy of excitation wavelength to induce fluorescence. (c) Rayleigh (elastic) scattering happens when an incident photon scattered with the same energy but in different direction. (d) Raman (inelastic scattering); it can be either stoke shift in which the incident photon is scattered with reduced energy and longer wavelength, while the other type of inelastic scattering is called anti-stokes shift where the energy of the scattered photon is increased while the wavelength is decreased.

- **Fluorescence**

Fluorescence is the absorption of light with a specific wavelength by a substance and its emission at the same time with a longer wavelength. Such a substance emits more visible light than it receives, making it appear brighter than a non-fluorescent substance. The physical principle behind the fluorescence can be explained when an electron absorbs some type of energy and got excited to a higher quantum level then it loses its energy as photons and the electron relaxed back to a lower quantum level “ground state”(Goldys, 2009), re-emitting the absorbed energy into the surrounding medium through radiative (fluorescence and phosphorescence) and non-radiative (heat) forms of decay. Therefore, the emitted photons have lower energy than incident light energy but with longer wavelength (Masters and So, 2008).

- **Fluorophores**

Fluorescent molecules are called “fluorophores”, which have specific excitation and emission wavelengths or spectra. When fluorophores get excited, the ratio of emitted photons is characteristics for each fluorophore which is described as quantum yield. In addition, fluorescence lifetime is also characteristic for each fluorophore which allowed differentiation between fluorophores. Each fluorophore exhibits distinct optical characteristics as described in Table 1-6:

Table 1-6. Optical characteristic features of fluorophores (Learmonth et al., 2009, Karlsson, 2010):

Fluorophore characteristic features	Definition
Excitation and emission spectra	Specific energy required by the molecule to be able to fluoresce.
Quantum yield energy	Ratio of the emitted/ absorbed photons, measures quantitively the emission efficiency
Fluorescence life-time	The time required by excited fluorescent molecules prior to their return to the ground state.

Fluorophores can be intrinsic or extrinsic in nature. Some organic molecules are capable to fluoresce under certain excitation wavelengths, they are called intrinsic fluorophores. This process is described as autofluorescence (AF) or natural fluorescence which originates from a range of molecules that could be either metabolites within the cell or extra-cellular structural components. The most common sources of auto-fluorescence are listed in Table 1-7 (Knight and Billinton, 2001). However, the nature of auto-fluorescence in human dentine is still not clear (Matsumoto et al., 2000).

Table 1-7. Common sources of Auto-fluorescence (Knight and Billinton, 2001).

Auto-fluorescence source	Typical Excitation Wavelength (nm)	Typical Emission Wavelength (nm)
Flavin	380-490	520-560
Nicotinamide adenine dinucleotide (NADH and NADPH)	360-390	440-470
Lipofuscin	360-490	430-670
Advanced glycation end products (AGEs)	320-370	385-450
Elastin and collagen	440-480	470-520
Lignin	488	530
Chlorophyll	488	685

Although the auto-fluorescence behaviour of the molecule is beneficial when coupled with other stain-free imaging techniques such as fluorescence lifetime imaging (FLIM) and second harmonic generation (SHG), it can be considered as a source of background noise when examined specimens are labelled with extrinsic fluorophore. However, stain-free imaging allows studying of living tissues with minimal intervention, depending on the characteristic behaviour of their intrinsic components under optical excitation.

1.6.2 Biophotonics in Dentistry

- **Fluorescence in dental tissues**

As to the fluorescence of human teeth, two phenomena should be individually considered. Firstly, the fluorescent emission by ambient UV light is helpful for a satisfactory aesthetic restoration of teeth. Second, the fluorescent emission by a specific wavelength artificial light, such as a laser that varies by the excitation wavelength (Hermanson et al., 2008, Zhang et al., 2011). The latter phenomenon is used for the detection of dental caries and the identification of dental/ restorative materials interface which will be discussed in the following paragraphs.

Regarding dental tissues, AF detection has been an area of research in the past decades aimed to understand the fluorescence behaviour of sound and carious tooth tissues and to identify the origin of this natural fluorescence. Benedict et al. reported that enamel and dentine can fluoresce when they excited with UV light. Since then, many researchers have studied fluorescence (Benedict, 1928). Hoerman and Mancewicz et al. (1964) indicated that the phosphorescence of calcified tissues is originated mainly from organic content and the relative fluorescence intensity of enamel is 1/3 of that observed in dentine. However, a study by Armstrong, reported that the fluorescence of dentine is likely derived from inorganic complexes with some organic compounds or molecules attached to the inorganic compounds (Armstrong, 1963).

If it were purely inorganic, one would expect to see healthy dentine and hyper-mineralised dentine fluorescing brighter and stronger than carious demineralised dentine (Banerjee and Boyde, 1998). Therefore, assuming that the fluorophore is organic in nature, the source of AF in carious dentine might be due to exogenous

fluorescent molecules which has been supported by the progressive enhancement of AF with the lesion progress and further destruction of dentine (Banerjee and Boyde, 1998). The ECMs of living tissues contribute to auto-fluorescence emissions due to the highly intrinsic quantum yield of collagen and elastin (Georgakoudi et al., 2002).

van der Veen and ten Bosch were the first to report AF induced by dentine demineralisation using the confocal laser scanning microscopy (CLSM) imaging of sound and *in-vitro* demineralized, non-carious human root dentine (Veen and Bosch, 1995). They indicated that dentine intrafibrillar and/or extrafibrillar apatite exhibits fluorescence quenching capability through inhibiting the electronic excitability of collagen in its excited state. Thereby, removal of the apatite from the mineralized collagen may result in amplified auto-fluorescence of the demineralized collagen matrix (Veen and Bosch, 1995, Zhou et al., 2016).

In the *in-vitro* demineralised dentine studies, it was noticed that AF intensity have shown two opposite observations. Banerjee and colleagues have further extended the use of AF generated by demineralized dentine as an adjunctive marker for carious tissues detection and monitoring their progression with CLSM. They found an enhanced AF signal intensity within the demineralised dentine, supporting the claim that chromophores responsible for the AF signal should be organic in nature. When carious dentine was excited at 488 nm, emission intensity was found to be 2.44 times greater than that of sound dentine, while the intensity of emission peak spectrum was red-shifted from 545–556 nm (Banerjee et al., 2010a).

With the demineralisation process, the unavoidable shrinkage of dentine tissue will enhance the genuine AF. However, this shrinkage can be reduced when carious dentine is embedded in polymethylmethacrylates (PMMA), thereby, strong AF is generated (Banerjee and Boyde, 1998). In addition, dequenching or concentrated chromophores may result with the dentine demineralisation. The nature of AF in carious dentine is dependent on the excitation wavelength used. If blue light is employed, green fluorescence will result which is attributed to the breakdown of the structural protein. Non-dental studies also indicated that the increase in AF intensity may be related to modification/reductions in collagen crosslinks (Chai et al., 2011, Lutz et al., 2012).

A recent study reported an increase in AF of the demineralized dentine without adhesive infiltration compared to mineralized dentine (Zhou et al., 2016), confirming the conclusions from previous work (Banerjee et al., 2010a, Almahdy et al., 2012).

Dentine fluoresces more brilliantly than enamel and this is assumed to be due to tryptophan and hydroxypyridimium which have emission peaks at 350 and 400 nm, respectively (Hoerman and Mancewicz, 1964b, Foreman, 1980b). Another study showed an emission peak of the human dentine at 450 nm rather than 350–400 nm (Fukushima et al., 1987). Regardless of the controversy of the AF origin in dental tissues, all these studies confirmed that it is an intrinsic fluorophore which is influenced by the health and integrity of the dental tissues. To explain these controversy, some authors suggested that AF of human dentine originates from multiple fluorophores such as collagen cross-liking and hydroxyapatite–pyridinoline complex and can be used as a reliable indicator for the health and integrity of the dental tissues (Fukushima et al., 1987, Fujimoto and Adachi-Usami, 1988).

As has been investigated, the loss of mineral from the enamel and dentine is likely to modify most of the optical properties of teeth, such as scattering, reflection, absorption, and fluorescence. Therefore, when dental tissues are affected by caries, one can expect changes in both the organic and inorganic components of dentine. Hence, the fluorescence behaviour of dental tissues will be affected. Higher fluorescence intensity was observed with blue-green excitation in carious dentine which reduced towards sound dentine and was referred to the structural protein degradation by bacteria or certain proteases (Terrer et al., 2016). It has been also reported a shift of the carious dentine spectrum towards longer wavelengths due to accumulation of different fluorophores. These molecules might be the advance glycation end products known to be produced by the Maillard reaction or porphyrins (Slimani et al., 2018). Other studies suggested that excitation of carious tissue in the red region allowed emission of AF signal due to Protoporphyrin IX (bacterial decomposition by product), and other oral bacterial (König et al., 1999). These data agree well with the AF results of the two-photon studies presented in this thesis.

- **Two-photon microscopy (2p)**

Optical microscopy has evolved rapidly to become one of the most important biomedical research techniques today. Non-linear optical imaging refers to the "non-conventional" interaction between light and matter. This interaction happens when the material system responds in a nonlinear manner following the excitation with extremely high photon flux, such as a pulsating laser (Boyd and Masters, 2008). In the non-linear 2p microscopy, the fluorophores are excited only when simultaneous absorption of the two consequent photons which promote the transition of their energy to an excited state. In this technique, an intense laser with a double excitation wavelength is required for the fluorophore emission resulting in a non-linear fluorescence (Fig. 1-14b). As the non-linear excitation requires an intense high energy, hence, the probability of tow-photon absorption under day light or arc lamb is virtually zero (Goppert-Mayer, 1931). This only can happen when a high enough number of photons is localised in a small volume at the focal plane of the objective lens, hence, photobleaching decreased. Two-photon microscopy uses near-infrared femtosecond lasers that generate nonlinear optical signals in the visible spectral range such as the second-harmonic generation (SHG) and the two-photon excitation fluorescence (2PEF) (Loew et al., 2002, Yeh et al., 2002, Zipfel et al., 2003, Brockbank et al., 2008, He et al., 2017). In confocal microscopy, an aperture positioned in the conjugate focal plane of the objective lens is used to minimise the out of focus light beams directed to the sample or reflected by it, which further improves the image quality (Watson, 1997). However, two-photon microscopy doesn't require a pinhole, and it provides superior three-dimensional optical sectioning as the microscopic field is confined to the area irradiated by two consequent photons. Thereby, a deeper penetration up to 500 µm can be obtained with lower photo-toxicity to the specimen. Additionally, a wider separation between the excitation and emission spectra was noticed which reduces the background scattering (Denk et al., 1990).

In dental research, 2p was used to observe molecular structure modifications of enamel, collagen and dentine degradation during natural or artificial caries process (Hall and Girkin, 2004, Kao, 2004a, Lin et al., 2011, Terrer et al., 2016, Slimani et al., 2018). They claimed that combining the nonlinear optical signals with other stain-free microscopy techniques such as fluorescence lifetime (FLIM)

and second harmonic generation (SHG) (Lin et al., 2011) provides promising novel techniques for caries detection and in studying the tooth tissues with minimal interventions.

- **Second harmonic generation**

Second harmonic generation (SHG) is a non-linear process between the light and matter. The main organic matrix in dentine is the fibrous collagen, which is known to generate an intense second harmonic and AF signal. SHG requires highly ordered molecular structures and is allowed only for non-centrosymmetric molecules such as collagen type I. It also requires a high intensity laser source to generate SHG signals by additional frequency component with double the frequency (2ω), half the wavelength, of the excitation light, which is the SHG signal. This signal is accompanied with the usual linear component that results in Rayleigh scattering (Boyd, 2003). SHG was first used to explore the normal structure of dental tissues by Altshuler et al. (1984) who observed the SHG signal in sound dentine mainly, and to lesser extent in sound enamel. This led to assumption that the origin of these signals in dentine from the collagen fibrils and not from the mineral content. Further studies confirmed the role of collagens in SHG signals emission (Kim et al., 1999, Kao, 2004b, Chen et al., 2007, Elbaum et al., 2007, Cloitre et al., 2013).

A study by Lutz et al. (2012) reported that when changes occur in the interspace of the collagen molecules within a collagen fibril, a variable intensity of the SHG might result. Consequently, if the collagen cross-linking reduced, theses interspaces increase and enhancement of the SHG signals may follow (Lutz et al., 2012). It cannot be excluded that reduced crosslinking might advocate a parallel orientation or influence the bipolarity and therefore higher SHG intensity generated.

In a recent study, it has been proven that the SHG/2PEF ratio is a sensitive parameter to study the molecular changes of dentine during the caries process (Terrer et al., 2016). They noticed that when there was an increase in the fluorescence intensity in the infected dentine, the corresponding SHG signals of the same infected tissue decreased, which may indicate the destruction of the collagen matrix throughout the caries progression. However, this reduction in the SHG intensity was varied from one infected tissue to another. The encountered

slight variations in the SHG signal for the different stages of the infected dentine may attributed to the fact that SHG is collected in transmission; hence, the recovered intensity might depend on the samples thickness (Slimani et al., 2018). Moreover, the structure of collagen protein may change as a result of exposure to heat or enzymatic cleavage. Thus, the SHG signals were found to be affected as a consequence to these changes (Kim et al., 2000, Lin et al., 2006). Therefore, SHG was suggested to study the changes in dentine structure during the caries attack or when dentine in contact with applied materials (Lin et al., 2011, Atmeh et al., 2012, Terrer et al., 2016, Slimani et al., 2018).

- **Fluorescence lifetime imaging (FLIM)**

Fluorescence lifetime is the time required by electronic excited-state fluorophores (nanoseconds) to exponentially (e) decrease their energy (to a more favourable ground state) via loss of energy through fluorescence (Berezin and Achilefu, 2010). It is characterised by fluorescence lifetime τ and is mapped spatially using a microscope equipped with a detector capable of high-frequency modulation (Lakowicz et al., 1992). It has become widely used for various biological and medical diagnoses and a characteristic feature for each specific molecule. Fluorescence lifetime helps delineate between two or more compounds having similar wavelengths emission. FLIM measurements seek to obtain the characteristic lifetime from the fluorescence decay profile.

AF spectra from dental tissues have been used for caries diagnosis (Thomas et al., 2011). However, a precise characterisation of dental tissues can be limited when relying on intensity-based measurement techniques. These techniques may suffer from fluctuation in laser intensity, concentration of fluorophores, and scattering of light. Moreover, dentine and enamel exhibit similar auto-fluorescence spectral profiles, so they are difficult to be differentiated spectrally. In contrast, fluorescence lifetime can distinguish between their spectra and is not affected by the laser intensity or fluorophore concentration. It offers also critical information on molecular dynamics such as molecular conformation and the changes resulted from interaction with other molecules (Lakowicz, 2004). FLIM has been widely used in recording different cellular parameters such as ion concentration (Hille et al., 2009), pH of the environment (Hanson et al., 2002), and oxygen saturation (Gerritsen et al., 1997) and it is directly dependent upon

excited-state reactions. These unique independent characteristics allowed FLIM to be used as an additional distinct microscopic marker and support its integration into the family of molecular imaging tools.

It has been previously reported in AF section that the natural fluorescence originated from multiple intrinsic chromophores. This has been confirmed by different studies investigated the FLIM in dental tissues (Alfano & Yao 1981, König et al. 1993, Matsumoto et al. 1999, (McConnell et al., 2007), Lin et al. 2011). In these studies, multi-component exponential decay curves could be representing a different intrinsic fluorophore (Matsumoto et al., 1999). Although most of the results of these studies were consistent; however, they also showed some discrepancy regarding the effect of dental caries on FLIM. It has been reported that FLIM of carious dentine is longer than that of sound dentine tissues (Koenig et al., 1993), while in McConnell et al. (2007) they detected opposite results (McConnell et al., 2007). FLIM or (Time-Resolved Fluorescence) may be achieved by several methods, depending on the required sensitivity and time regions; including steady state (Cominelli et al., 2017) and time-gated (time resolved) (Sytsma et al., 2003). A steady-state measurement of the fluorescence emission (intensity vs wavelength) gives an a verage and relative representation. In this method, lifetime imaging is directly performed by measuring the fluorescence intensity and averaging its value over time to generate a lifetime map of the sample. Using steady state method is performed for monitoring the sample's functional changes as a result of environmental factors along with gathering information about its morphology and status (Becker et al., 2006). The time-gated method uses a pulsating laser source to record a fluorescence decay curve with a high-speed fluorescence detection system either using many time gates with equal width or by time gate scanning. When several time gates used, lifetimes shorter than hundreds of picoseconds are typically difficult to resolve, while the time gate scanning method achieves higher temporal resolution at the expense of photon collection efficiency, as the narrow gate excludes the majority of the detected photons. This technique provides an absolute real time recorded lifetime value for each excited fluorophore. Therefore, the intensity of each pixel in the obtained image indicates the fluorescence lifetime of the fluorophore instead of its fluorescence intensity (Grauw, 1998).

In contrast to the steady-state method, image contrast was enhanced with the time-resolved imaging due to elimination of the background fluorescence. This method is able to differentiate between the fluorophores that have similar excitation and emission spectra, depending on the difference in their fluorescence lifetime. Based on FLIM imaging advantages, it is considered a very useful technique for monitoring treatment responses and to delineate healthy from pathologic tissues.

- **Raman spectroscopy**

Over the past 20 years, microRaman spectroscopy has introduced an important analytical technique, providing effective chemical specificity and spatial resolution for analyzing natural and synthetic materials. This spectroscopic technique is non-destructive and used to detect the chemical content of tissues, and to examine the materials depending on the vibrational energy signatures (Fingerprints) and rotational modes of the chemical bonds, which made their molecular structure. Diseased tissues are known to cause modifications in cellular orientation and biochemical changes in the tissue, these changes cause alteration in the vibrational spectra. Hence, the spectrum obtained from diseased tissue can be compared to and distinguished from the baseline spectrum of normal tissue (Wachsmann-Hogiu et al., 2009, Ramakrishnaiah et al., 2015).

In this technique, a monochromatic laser beam source used to illuminate the material through an objective lens. When the excitation photons of the illuminating beam strike the sample, they get scattered in different direction with the same or different energy. Despite most of the interactions between the incident photons and the scattering light beam produce Rayleigh spectra, a small proportion of the incident photons showed inelastic scattering to produce the Raman spectra as shown in Fig. 1-14-d. Raman scattering can be subdivided into Stokes and Anti Stokes Raman scattering. Rayleigh scattering occurs when there is no change in the amount of energy between the incident photons and the sample molecules, in which the scattered photon has the same wavelength as the incident photon. In Stokes Raman scattering, the resulting energy of the scattered photon is smaller while the wavelength is longer. On the other hand, anti-Stokes Raman scattering provided photon with higher energy but with shorter wavelength. These changes in the wavelength and energy of the photons is termed “Raman shift”.

Raman spectroscopy requires no or minimal sample preparation and a rapid, non-destructive optical spectrum is easily obtained (Williams and Everall, 1995).

Spectral charts were then extracted from the generated Raman spectra with the use of a charge-coupled device (CCD). These charts contain multiple characteristic peaks which they allocated to their wave-number. Each peak in these charts indicates a unique vibrational mode in the molecule. These peaks represent an intrinsic “molecular fingerprint” of the sample which is known as the Raman spectrum. In addition, quantitative information about the structure of the examined sample can be drawn from each peak intensity within the volume of the scanned area (Penel et al., 1998). As an example, Fig. 1-15 shows sound dentine Raman spectra with their characteristic peaks. The allocated bands for these peaks are summarised in Table 6. In the dentine spectrum, four main bands were observed, representing the fundamental frequency modes v1, v2, v3, v4. The sharpest and most prominent band, v1, corresponds to the symmetrical stretching of the tetrahedron of oxygen atoms surrounding the phosphorous atom. These indicate the presence of crystalline phosphate-based minerals in dentine (Ramakrishnaiah et al., 2015).

Conventionally, micro-Raman intensity map is generated through point-by-point serial scanning. This mapping takes a very long acquisition time. A faster StreamLine™ scanning technique has recently been introduced (Renishaw Plc, Wotton-under-Edge, UK) with an integrated distinctive hardware and software. It provides less acquisition times for large, artefact-free images. It is a dynamic Raman mapping coupled with line-laser illumination of the sample and CCD scanning technologies (Hédoux et al., 2011). Samples can move in a vertical and horizontal direction thought he use of motorized synchronised stage. This combination makes Raman mapping performance to be 200 times faster than the conventional point by point mapping (www.renishaw.com). To date, the use of the StreamLine™ scanning technologies have not been reported in the dental literature. After Streamline Raman scanning, the imaged area is represented as a series of points producing a chemical Raman image. Each point has its own Raman spectrum to determine the chemical structure of the sample at that point.

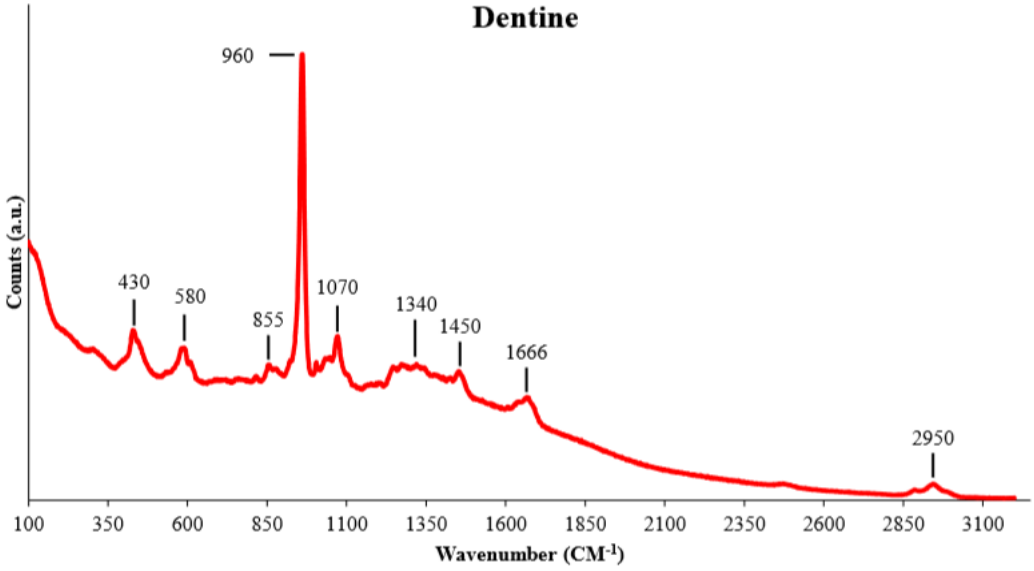

Figure 1-13. Raman spectra of sound dentine between 100-3100 cm^{-1} wavenumbers showing the featured peaks and the allocated bands for these peaks are summarised in Table 1-8.

Table 1-8. The common Raman peaks and their correlated band assignments found in the Raman spectrum of dentine the histological component of each tentative band assignment is included; v: vibration mode (Spencer et al., 2000)

Peaks wavenumber (cm^{-1})	**Allocated band and correlated histological component**
430	(v2) of PO_4^{-3} (O−P−O bond), Hydroxyapatite
580	(v4) of PO_4^{-3} (O−P−O bond), Hydroxyapatite
855	C-C, organic material
960	(v1) of PO_4^{-3} (P−O bond), Hydroxyapatite
1070	(v1) of CO_3, Hydroxyapatite
1340 **1666**	Amide III, Protein Amide I, Protein
2950	C-H banding, Organic material

As stated earlier, dental caries is presented by demineralisation of inorganic substance (mineral hydroxyapatite crystals) and destruction of the organic substance such as collagen. Direct representation of chemical content and relatively simple and reliable application of Raman scanning encouraged their use in dental research. Several studies used Raman spectroscopy for diagnosing and characterising enamel and dentine caries through monitoring the phosphate peaks (959 cm^{-1} v1) which represents the mineral phase of the tooth structure (Hewko and Sowa, 2010, Almahdy et al., 2012, Mohanty et al., 2013, Alkheraif, 2014, Parker et al., 2014, Akkus et al., 2017). It has been also employed to detect remineralisation of the dental tissue by assessing the changes in its intensity which reflects quantitatively the dynamic mineral changes (Sauer et al., 1994, Parker et al., 2014, Milly et al., 2014, Coello et al., 2015).

Moreover, Raman analysis has widely contributed to chemical composition analysis of dental materials to assess chemical changes associated with the materials' setting and maturation, such as calcium silicate cements and GIC and the nature of their interaction of the underlying tissues (Martinez-Ramirez et al., 2006, Atmeh et al., 2012). Micro-characterization of biomaterials not only helps researchers to better understand the interaction of biomaterials with tissues but also helps to improve their properties to match the intraoral condition (Seah et al., 2009). Hence, knowing the exact composition of the dental materials helps to alter and modify their properties. Although Energy-dispersive X-ray spectroscopy (EDS) is the most popular technique for elemental analysis or chemical characterization of dental materials; EDS requires a long time for specimen preparation. Therefore, Raman spectroscopy is the method of choice for accurate identification of chemical compounds, and their functional group when examining enamel or dentine.

Based on the review of literature, laboratory tests are useful for studying new operative techniques and materials prior clinical implementations. However, they have to be reproducible, with known parameters, and low variability between operators and institutions to provide internationally valid and acceptable results. Non-invasive multimodal imaging protocol used in the current study are useful for knowing the details of ultramorphological features of the dentin-resin interface which may influence the material selection decision in clinical practice. Studying

the chemical, mechanical and optical properties of the interface between dentine and new material is crucially important for anticipating the materials clinical suitability. In addition, testing the adhesive and the sealing ability of the new material may predict the longevity of a restoration to some extent.

Nevertheless, there are still clinical trials are needed to provide a conclusive clinical decision about the material.

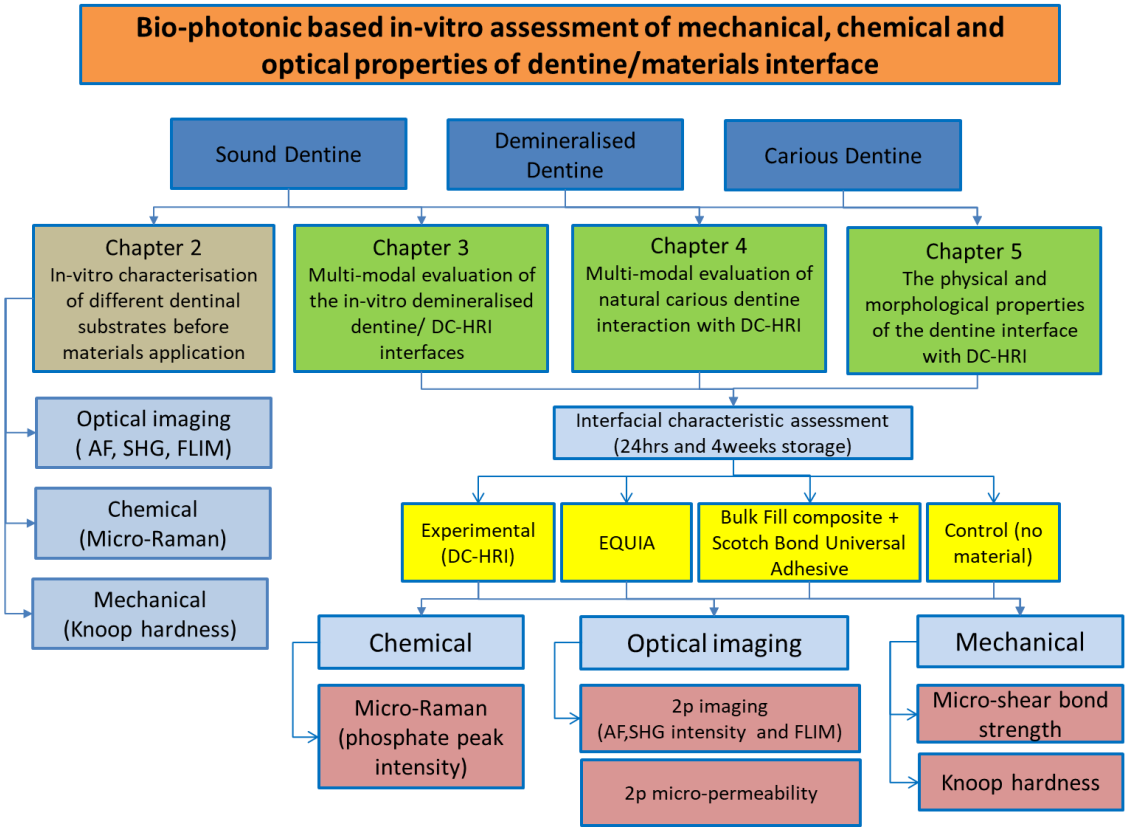

Chapter 2. *In-vitro* optical, chemical and mechanical characterisation of different dentine substrates

2.1. Introduction

Handling deep carious lesions in close proximity to a vital pulp can be a significant challenge to dental practitioners. Traditional management of the carious lesion dictated a complete removal of both bacterially contaminated “infected” and primarily demineralised “affected” carious dentine, to “restrict” further caries progression and to retain a well-mineralised sound dentine surface to receive the dental restoration (Thompson et al., 2008). The evolving understanding of the dental caries process and the carious lesion histopathology have led to a paradigm shift in their clinical management (Ismail et al., 2013). Therefore, based on the minimally invasive approach, a complete debridement of the soft caries-infected layer is recommended when closely overlying the pulp, whilst retaining the relatively harder, biologically repairable caries-affected dentine (CAD) to which a dental restoration may be bonded (Fusayama, 1972, Ogawa et al., 1983, Maltz et al., 2017). This approach aims to repair or restore damaged or defective tooth structure to maintain pulp sensibility (vitality), function and aesthetics (Banerjee and Watson, 2015). It has been questioned how to determine

accurately the extent of the carious lesion excavation endpoint when managing deep carious lesions. The delineation between these layers is essential, both clinically and in laboratory investigations, to minimise the unnecessary removal of the restorable part of tooth tissue and to enhance its reparative potential (Pugach et al., 2009). Such conservative management will additionally save patients money and time, by avoiding pulp exposure and further endodontic treatment, and will indirectly influence their behaviour towards further dental treatment (Schwendicke et al. 2013). In clinical practice, dentists and therapists must deal with the caries-affected dentine (CAD) substrate, which may not provide the necessary clinical longevity of the tooth-restoration complex (TRC) for clinical function (Wang et al., 2007). However, promising long-term outcomes have been found following the removal of heavily infected tissues while leaving the deepest layer of undisturbed carious dentine (Maltz et al., 2012).

In the literature, several techniques have been implemented in an attempt to delineate the carious zones histology as mentioned in the literature review (1.2.2). Caries-infected and affected dentine are substrates which exhibit different chemical compositions and morphology. Likewise, artificial carious lesion models exhibited a different structure and histology compared to the natural carious lesion. Natural carious tissues exhibit more complicated micro-structural damage, due to different rates, stages and locations of the caries process (Yang et al., 2011). To provide more clinically relevant data, it is necessary to investigate certain optical and mechanical properties of natural lesions, which can improve the understanding of the basic structure of CAD substrates compared to the partially demineralised dentine.

In the present study, a simple demineralisation protocol using 37% phosphoric acid gel etching for 60 seconds was used, as it is the commonly used acid-etching agent in clinical dentistry. This protocol has provided a partially demineralised dentine model (Cao. et al., 2013). Thus, modified optical features could be expected as a result of mineral loss and collagen exposure by the acid demineralisation, compared to the natural lesion.

Minimally invasive caries management dictates quantitative techniques which can detect the carious lesion at an early stage and to differentiate between the carious dentine histology. Therefore, caries diagnosis may improve when

traditional methods are combined with more sensitive methods, which also help the clinician to monitor non-operative care. The use of light has been reported in the literature for the clinical caries detection (Alfano et al., 1984, Stookey et al., 1999, Karlsson, 2010, Rechmann et al., 2012). There are several optical techniques that have been used for the clinical carious tissue detection such as:

- Optical coherence tomography (OCT) (Shimada et al., 2015).
- Laser-induced fluorescence (LF) (F Shakibaie et.al, 2011, L Liu - 2014)
- Fibre-optic trans-illumination (FOTI) (ML Laitala et. al, 2017)
- Quantitative light-induced fluorescence (QLF) (Pontes LRA et. al, 2017).

Moreover, laboratory evaluation methods have been used to characterise and monitor changes during the caries process using different techniques such as:

- Atomic force microscopy (AFM) (Marshall et al., 2004)
- X-ray diffraction (XRD) (Kinney et al., 2001)
- Fourier transform infrared spectroscopy (FTIR) (Almhöjd et al., 2014)
- Raman spectroscopy (Almahdy et al., 2012, Toledano et al., 2017).
- Two-photon microscopy (2-photon) (Lin et al., 2011, Almahdy et al., 2012) that was selected for dentine assessment in this study.

Two-photon microscopy, with a non-linear illumination source at near-infrared (NIR) wavelengths, can provide deep sample imaging with high resolution, less scattering and optically thin sample sectioning (Abraham et al., 2010, Terrer et al., 2016). It can also provide useful information about a specimen's structure and its optical properties by creating a simultaneous image based on their natural fluorescence signatures (two-photon autofluorescence, 2p AF) and the coherent non-linear phenomenon of second harmonic generation (SHG). Many authors have used it to study and characterise the dentine and their interactions with different restorative materials (D Alpino et al., 2006, Sauro et al., 2009, Atmeh et al., 2012, Crosignani et al., 2012, Atmeh et al., 2015) or caries characterisation (Kao, 2004, Hall and Girkin, 2004, Lin et al. 2010, Terrer et al., 2016).

Despite multiple possible origins of AF, it has been proposed as a microscopic marker in caries studies, although the nature of the AF is still unknown (Banerjee and Boyde, 1998, Matsumoto et al., 2000, Almahdy et al., 2012). Several studies confirmed that collagen is the source of SHG signals in dental tissues (Kim et al., 2000, Chen et al., 2007, Lin et al., 2011). When collagen destruction or modification by acids takes place, it is expected that a change in these signals such as a decrease in their intensity in caries samples would be observed (Kao, 2004). Intensity might be influenced by many factors including laser fluctuation, scattering and fluorophore concentrations (Lin et al., 2011). Therefore, more reliable measures should accompany these measurements to confirm the results, such as fluorescence lifetime imaging (FLIM) and spectroscopy imaging. As reported earlier in the review section (1.6.2), FLIM can be affected by pH and oxygen ion concentrations. It can detect structural changes in dental tissues such as caries or mineralisation (Webb et al., 2002; Lin et al., 2011).

Moreover, a spectrometer was connected to the two-photon microscope to analyse and compare spectral signals obtained from representative samples at the same time as their intensity recording. This technique acquires point by point measurements with accessibility to all examined tissues, using simple analysis. Additionally, for chemical characterisation, Micro-Raman spectroscopy was used, a quantitative chemical assessment methodology to detect the chemical content of tissues through their characteristic molecular vibrational energy signatures of the Raman phosphate peak at 959cm^{-1} was used to assess the degree of demineralisation in carious/demineralised dentine compared to sound tissues (Wachsmann-Hogiu et al., 2009, Almahdy et al., 2012, Ramakrishnaiah et al., 2015). These measurements were further correlated with the “gold standard” Knoop hardness measurements (KHN), as an indirect indicator of mineral and physical property changes.

Aims:

1- To compare the difference in optical, mechanical and chemical properties of sound dentine vs. partially demineralised dentine and natural caries before and after storage in phosphate buffered saline solution (PBS).

2- The results obtained were used as a control data for future comparison of the same properties, after storage with various restorative materials in the following chapters.

Objectives:

The following analytical techniques were applied in this study: two-photon AF, SHG, FLIM and spectroscopy, correlated with tissue hardness measurement (KHN) of the same points within the samples. These measurements were followed by Raman spectroscopic imaging and mineral peak intensity measurements.

Null hypotheses were that:

1- The measured optical and mechanical properties would be similar between the examined dentine substrates and against the sound control group before storage.

2- No difference in the measured properties between substrates after PBS storage.

2.2. Materials and methods

2.2.1. Demineralised dentine sample preparation

Ten extracted sound molar teeth were collected under an ethics protocol (Reference 16/SW/0220, see appendix), stored in a refrigerated distilled water within four weeks post-extraction. Roots were sectioned using a water-cooled diamond wafering blade (Benetec Limited, London, UK) at a slow speed (330 RPM) using a hard tissue microtome (Isomet 1000, Buehler, Lake Bluff, IL, USA), just below the cemento-enamel junction to create a horizontal reference. Each tooth was mesio-distally sectioned into two 2mm thick flat dentine slices. Samples were then polished using 600-grit carborundum paper under running water. A reference point was prepared using diamond bur (Diaswiss Diamond Bur FG #008 Super Fine Grit Cylinder Shape PK/6) to facilitate marking a starting point of imaging as elucidated in Fig. 2-1. Another longitudinal reference line was made using a surgical blade in the middle of dentine surface yielding two dentine segments. The right half including the reference point (around 4 mm-widths) was used as an internal sound control with no treatment of the dentine surface and then covered using yellow vinyl tape (1231-8767, Fisher scientific, Laboratory equipment supplier in Loughborough, England). The other half (4mm-width) was partially demineralised using 37% phosphoric acid etchant gel for 60 seconds (Cao et al., 2013).

After demineralisation, all samples were rinsed with deionised water and ultrasonicated for 5 minutes.

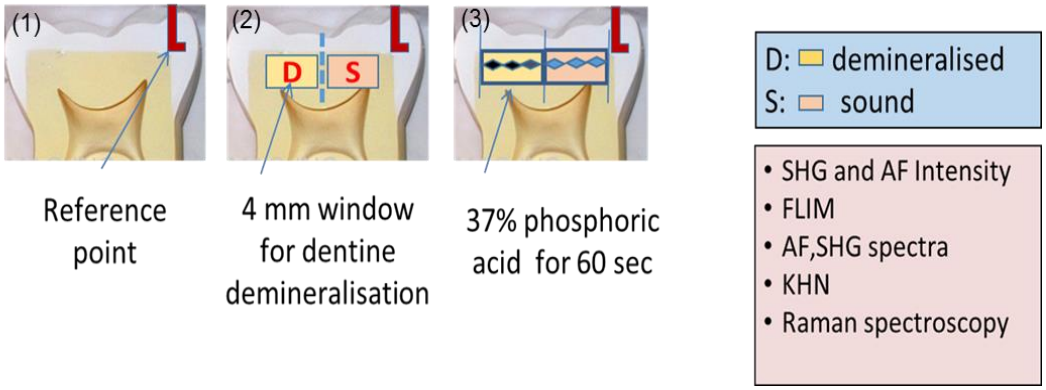

Figure 2-1. Characterisation before materials application; (1) 10 extracted sound teeth divided into two halves with a right-angle reference point. (2) Right portion of dentine (S; sound) was covered using yellow vinyl tape leaving the other half window (4mm) for dentine demineralisation (D; demineralised). Demineralisation was carried out using an acid etching protocol with 37% phosphoric acid for 60 seconds. (3) Then, evaluation of the demineralisation protocol was made by assessing changes in SHG and AF intensity and spectra, and changes in the fluorescence life time using two-photon microscope. It was followed by Knoop hardness number (KHN) evaluation and by using Raman spectroscopy to assess changes in mineral peak.

2.2.2. Measurement of dentine demineralisation depth

Acid etching with 37% phosphoric acid gel for 60 seconds was used in this study to partially remove the minerals from the superficial dentine surface, to create a dentine demineralisation model (Cao et al., 2013). A selected scanning area (2500x2284 µm) was focused with 250 µm inter-spectrum distance, along the axis parallel to enamel-dentine junction (EDJ), and 2.7 µm along the axis perpendicular to EDJ. The demineralisation depth of the created lesions was measured on the cross-sectioned surface of dentine samples. Grey-scale image was obtained, and a depth profile was extracted from this image using Image J software analysis (ImageJ, Wayne Rasband, NIH, USA), to measure the changes in the Raman phosphate peak intensity (960 cm^{-1}) from the top surface of the created lesion compared to the deeper sound dentine (internal control) of the same sample (Fig.2-5) (Milly et al., 2014). A schematic diagram showing the direction of the scan and depth measurement is shown in Fig 2-2.

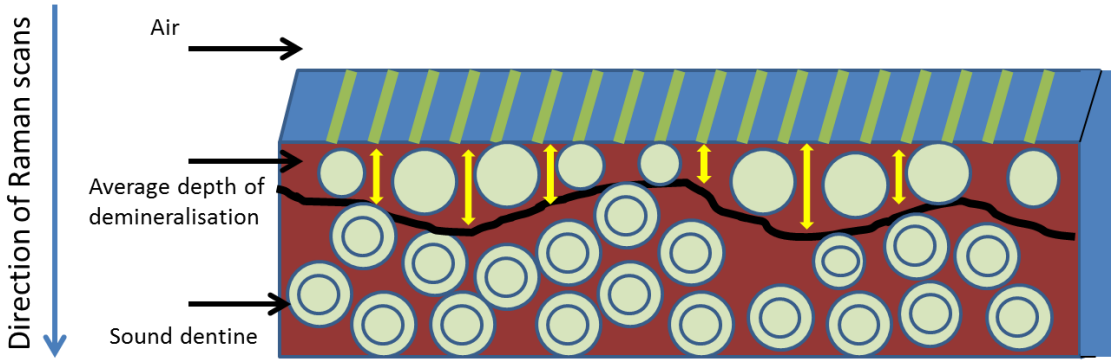

Figure 2-2. Schematic diagram of the cross-sectional view of the demineralised dentine model (red surface), (top surface is the blue region), previously etched with 37% phosphoric acid etchant gel for 60 seconds. The diagram shows the direction of the Raman scan from the top surface (including the air) towards the deeper dentine of the same sample. Average of six points were selected on the grey scale image obtained after Raman imaging, depth profile was plotted to measure the depth of the demineralisation from the top surface reaching the sound dentine within the same sample.

2.2.3. Characterisation of sound and demineralised dentine

- **Optical assessment; (SHG, AF and FLIM) and spectroscopy**

Following sample preparation and sonication, immediate imaging of the samples commenced by recording six points in both sound and demineralised area of dentine with 500µm inter-points distances, using an in-house built two-photon microscope for quantitative imaging of natural AF, SHG intensity (256 x 256 pixels) with FLIM and spectrum recording at the same time. Before imaging, the laser power was measured to standardise the setting throughout the whole experiment using an automated power meter connected to the microscope (PM30, Thorlabs GmbH, Germany). This measured the power at the sample surface to eliminate any effect of laser intensity fluctuation. The sample was then placed on a cover slip and the reference point was located. The lower edge of the dentine slice was aligned parallel to the edge of the cover slip as a horizontal reference. A 20x 0.75 NA air objective lens was used with 854 nm excitation wavelength, a 550 ± 20 nm emission filter for AF and 427±10 nm for SHG and 16 mW laser power. A fibre-optic spectrometer (AvaSpec-ULS2048L, Avantes Ltd, Netherlands) was installed within the same microscope apparatus and used to

obtain spectra for both AF and SHG from each point on the imaging line ranging from (400-700 nm).

- **Mechanical assessment; Knoop hardness number (KHN)**

Following imaging, the tissue hardness of the previously imaged points was measured directly using a Struers Duramin (Struers Ltd., Denmark) microhardness tester. A 10-g load was used for 15 s to produce a diamond-shaped indentation that was assessed using a 40× 0.65 NA objective. Manufacturer's software was used to calculate the KHN for each point in both the sound and demineralised surfaces.

- **Chemical assessment; Raman spectroscopy**

To evaluate differences in phosphate mineral peaks between sound and demineralised dentine, a Renishaw in Via Raman microscope (Renishaw Plc, Wotton-under-Edge, UK) running in Streamline^{TM} scanning mode was used. A 20x 0.40 NA air objective was used to focus samples and to create a live video montage image. This facilitated selection of the scanning area (800x7800 µm) including sound and demineralised dentine, starting from the marked reference point. A demarcated line in between was drawn using a sharp scalpel, with 50 µm distance in width (x-axis) and a 2.7 µm (y-axis) resolution across the interface. A 785 nm diode laser (100% laser power) was used and Raman signal was acquired using a 600-diffraction grating cantered at 960 cm^{-1}, and a 2 seconds CCD exposure time. After scanning was completed, images were uploaded into an in-house program designed for curve fitting and then generate grey-scale images together with depth profiles of phosphate peak intensity at 959 cm^{-1} (PO_4^{-3}(v1)) across sound and demineralised areas as shown in Fig. 2-3. Image J software (ImageJ, Maryland, USA) was used to process the obtained image which represented the peak height. Peak height intensity was calculated, and a ratio was then averaged for both sound and demineralised dentine separately.

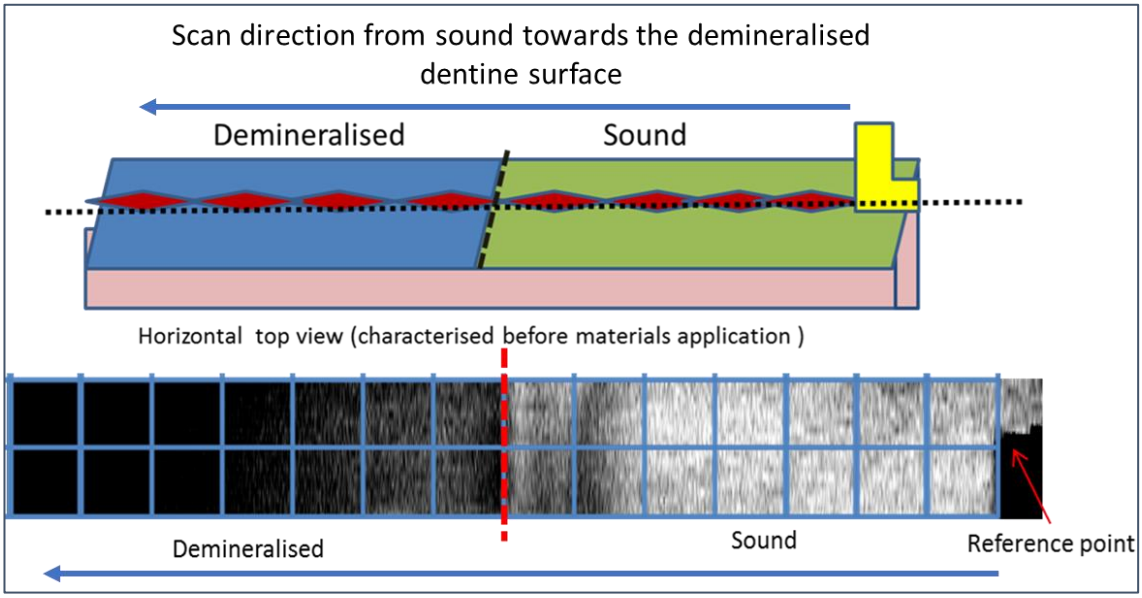

Figure 2-3. Schematic diagram of the tested model and a representative grey-scale image of Raman phosphate peak intensity at 959 cm^{-1} of sound and demineralised with the marked reference point (RP, red arrow). The scan directed from the sound dentine surface towards the demineralised surface with the demarcated line (previously marked by the surgical blade), to separate the two dentine areas.

2.2.4. Carious dentine tissue characterisation

Specimen preparations

Fifteen extracted human teeth with deep carious lesions (extending halfway through the dentine) that were selected after hemi-sectioning through the centre of the lesion, with no pulp exposure, were collected using an ethics approved by NHS Health Research Authority (Reference 16/SW/0220), stored in a refrigerated distilled water within four weeks post-extraction. Roots of all the teeth were sectioned just below the cemento-enamel junction to be used later as a horizontal reference for imaging. Each tooth was then hemi-sectioned longitudinally through a carious lesion into two halves using a slow-speed (300 rpm) water-cooled diamond wafering blade XL 12205, (Benetec Ltd, London, UK). Buccal and palatal surfaces were also sectioned to obtain a flat dentine surface. Teeth were selected based on caries criteria of a suitable carious dentine surrounded by a healthy sound tissue, not extending to the pulp. A reference point was prepared perpendicular to the dentine edge on both halves, using a flat diamond bur (Diaswiss Diamond Bur FG #008 Super Fine Grit Cylinder Shape PK/6) for accurate interval measurements and data

recording starting from this reference point. Scaled scanned clinical photographs of each tooth half were used for these measurements (Fig. 2-4). All samples were labelled and stored in separate glass vials containing distilled water before material application.

Two photon microscopy and spectroscopy (AF, SHG intensity and spectrum and FLIM imaging) and analysis

An in-house two-photon microscope with similar operating parameters and sample positioning as used in the previous section was utilised for recording AF, SHG, FLIM and spectrum. Following sectioning, samples were rinsed and ultra-sonicated for 3 mins with deionised water. Based on a previously printed scaled photograph of the lesion, X and Y position from the reference angle were located and saved. Then, regular intervals about 500 µm in distance at Y position toward the pulp were recorded in sound dentine. Another line across the carious dentine zones with a measured distance from the reference angle was also imaged. This gave a data of approximately 11-14 points across both sound and carious dentine zones from each dentine half as presented in Fig.2-4. Samples were evaluated using a two-photon microscope with a 20x 0.75 NA air objective lens, 854 nm excitation wavelength and 550 ± 20 nm emission filter. From each point measurement, a fluorescence and SHG intensity image with 256 x 256 pixels image format was recorded using a photomultiplier tube and a TCSPC counting card (HPM-100-40 hybrid detector and SPC-150 card, Becker & Hickl GmbH, Germany). AF and SHG intensity of each image were calculated for each point and allocated to different tissue types (caries infected, affected, and sound) based on the current reference KHN of these tissues. This calculation was assisted by using Image J analysis software (ImageJ, Wayne Rasband, NIH, USA). The intensity values were averaged for each tissue type in each group and these values were then calculated and plotted. Using FLIM, images of the same points, 256 x 256 pixels each, were obtained for each sample at the same time as intensity was recorded. Using TRI2 FLIM analysis software (courtesy of Paul Barber, Grey Cancer Institute, Oxford), the fluorescence decay curves were fitted using a bi-exponential model and the average lifetime was calculated for each image and averaged for each tissue layer in each experimental group and further were displayed as a bar graph. Representative AF and SHG signals spectra were

also recorded and transmitted to a fibre-optic spectrometer (AvaSpec-ULS2048L, Avantes Ltd, Netherlands) installed within the microscope apparatus. They were displayed as a spectrum shown in Fig. 2-9. The range of wavelengths used was from 400-700 nm and SHG was detected at 427 nm and AF at 550 nm.

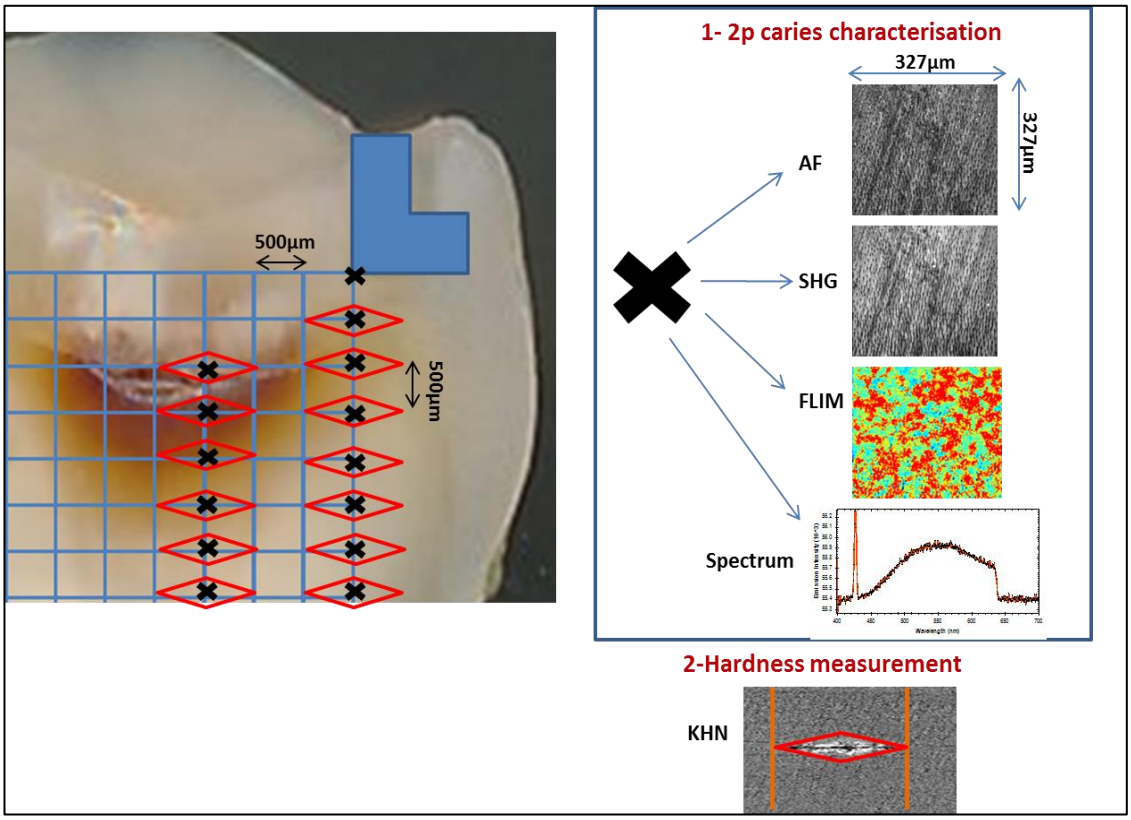

Figure 2-4. Scaled calibrated scanned macro-photograph of the carious lesion representing the applied techniques for measurement including 2p characterisation (AF, SHG, FLIM and spectrum) and tissue hardness measurement.

Microhardness measurement

The KHN of previously imaged points was measured through a 40x 0.65 NA objective and recorded using Struers Duramin microhardness tester (Struers Ltd., Denmark) which was calculated using the manufacturer's software. A force of 10 g for 15 seconds was used to produce diamond shaped indentations in previously located positions. After that, the collected data from two-photon imaging were allocated to the hardness number of each recorded point which represents different tissue zones. When Knoop hardness number (KHN) was <25, the tissue was considered caries-infected dentine (CID), while caries-affected dentine had KHN ranging from 25 to 40 and the sound dentine KHN >40 (Ogawa et al., 1983, Banerjee et al., 2010). After all measurements were made, the samples were cleaned with deionised water and then stored in PBS solution (Oxoid Limited, Hampshire, UK) at 37˚C for four weeks. A cross-sectional cut was then made through the imaged surface based on the recorded reference point and re-imaging of the same points were performed to compare changes of these properties after storage. The following formula was used to calculate the percentage changes between before and after storage data:

$$(Xa - Xb) / Xb) \times 100\%,$$

Where Xa is the value after storage, Xb is the initial value before storage.

2.2.5 Statistical analysis

Descriptive statistics were used to summarise the outcome measure for each technique separately. The normality of the outcome was checked using Kolmogorov-Smirnov and Shapiro Wilk's test. Since the outcome was not normal, the values were log transformed and the transformed data were used for the analyses as presented in the appendix C. A one-way ANOVA test was used to compare significant differences between dentine substrates for each method before and after samples storage performed using IBM SPSS Statics Viewer 21 Software (IBM United Kingdom limited, UK). Then, post-hoc Tukey's test was used to differentiate between any two tissue types. An independent t-test was also performed to compare Raman peak intensity before storage between sound and demineralised dentine surfaces only. No statistical analysis was performed on the two-photon spectroscopy results, as the spectrometer was changed many

times during the experiment, resulting in non-comparable values between the set of samples. Only representative samples of both caries and demineralised model were used to present a spectra plot showing the difference between the caries zones, demineralised and sound dentine.

2.3. Results

2.3.1. Depth of dentine demineralisation

Analysis of the Raman scan images showed a lower mineral peak intensity in demineralised lesions. It was represented by a gradual increase in intensity (ranging from 3000-5000 a.u.) from the demineralised lesion towards the sound dentine within the same samples, when interpreting the depth profile plot of phosphate peak intensity. The average depth of the six points measured on the cross-section sample (Fig. 2-3) is extended approximately between 500-600μm (Fig. 2-5).

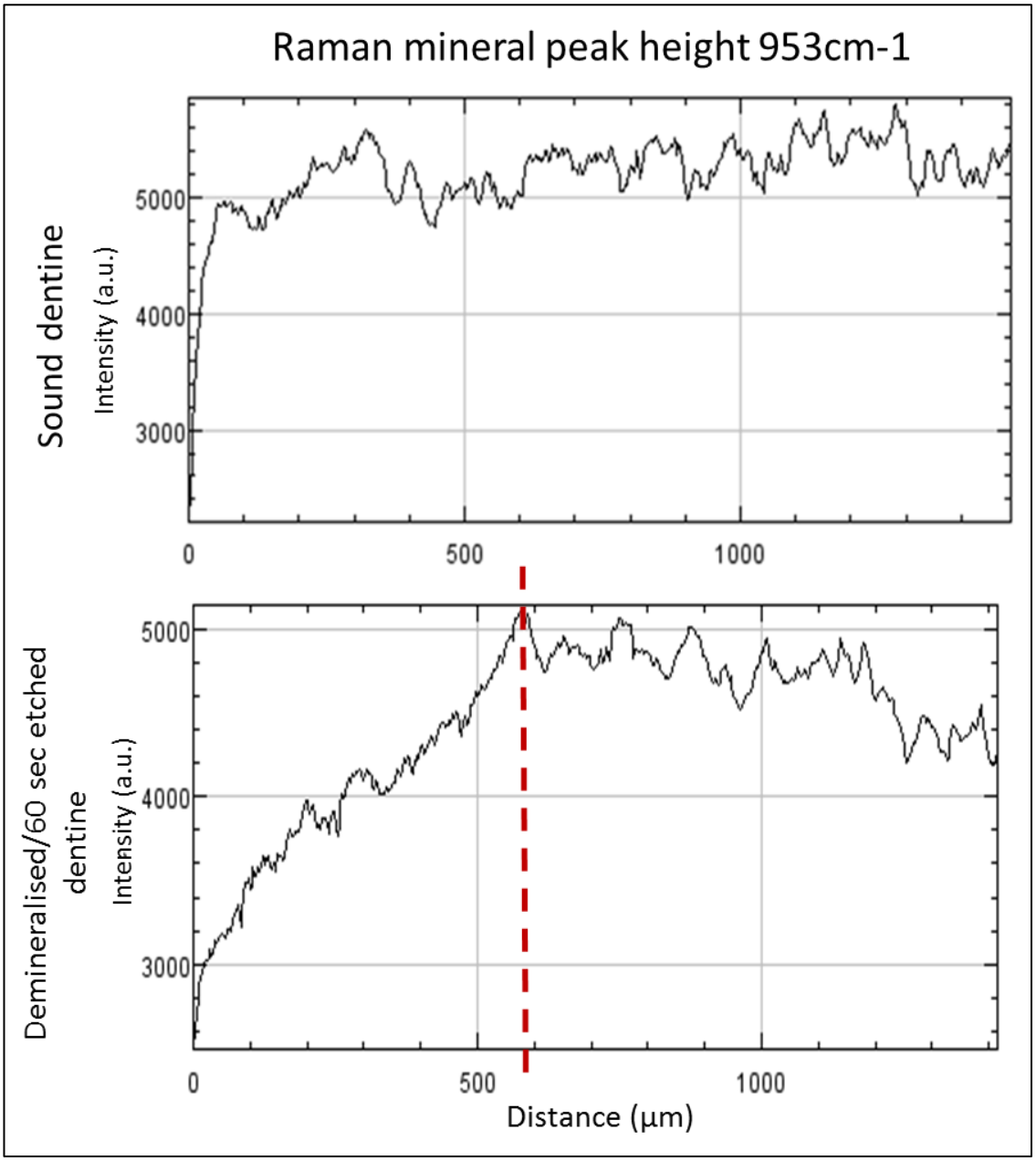

Figure 2-5. Representative depth-profile plots were obtained from the grey scale image of the demineralised lesion and the internal sound controls within the same sample, using Image J software analysis (ImageJ, Wayne Rasband, NIH, USA). It showed the gradual increase in the phosphate peak intensity from the demineralised area towards the sound dentine (ranging from 3000-5000 a.u.). Average demineralisation depth was calculated from six points on the sample which extended in the range between 500-600 µm.

2.3.2. Characterisation of sound, demineralised and carious (infected and affected) dentine before storage

Representative images of the various optical parameters in different dentine substrates are shown in Fig. 2-6. The differentiation between the intensity of different carious dentine zones were verified based on the reference KHN of each tissue. The infected tissues showed the highest AF intensity which was observed as the brightest image compared to other groups, whilst SHG image was the brightest with the demineralised substrate. FLIM images change in colour from blue to red; as the blue colour represents the short lifetime, while the red colour indicated the longer lifetime. Therefore, the infected tissues were blue in colour and it changes gradually into reddish colour with the sound tissues (see Fig. 2-6).

AF of the infected tissues was the highest in intensity (50 a.u.± 4.6 (standard error)), compared to other substrates and reduced significantly (p=0.001) towards sound tissues (18.4 a.u. ± 0.7) as shown in Fig. 2-7. AF of the demineralised dentine was lower significantly (17.7a.u. ± 1.3) than the affected dentine (31.3 a.u. ± 3.2) (p= 0.008), but not significantly lower than the sound dentine (18.4a.u. ±0.7) (p=0.87). SHG of demineralised tissue (92 a.u. ± 4) was the highest among all groups (p=0.001). FLIM images showed a gradual increase in lifetime from infected (1.2 ns ± 0.05) towards sound dentine (1.7 ns ± 0.01) with no significant difference between affected and demineralised group (1.5 ns ± 0.03, 1.55 ns ±0.02 respectively).

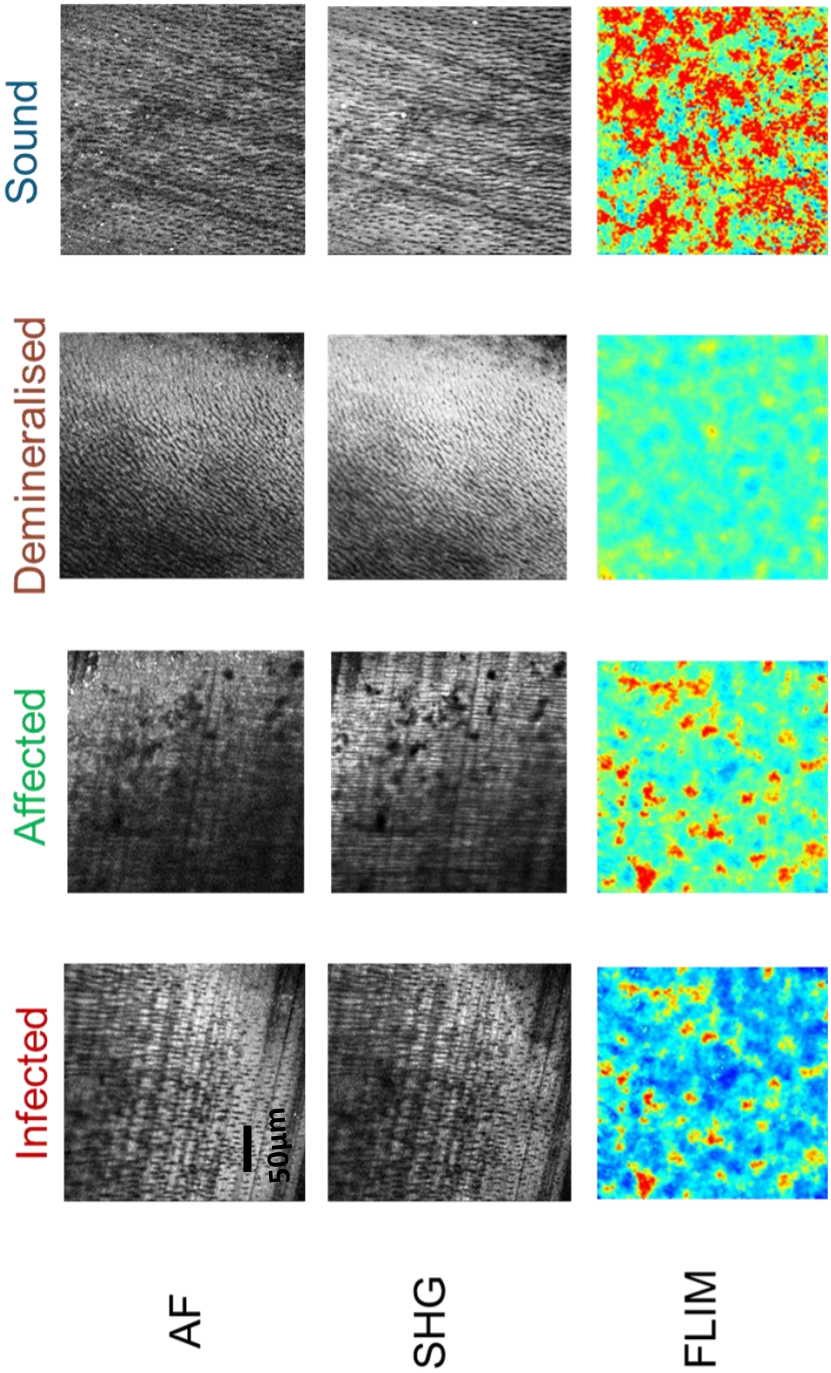

Figure 2-6. Representative 2-photon images of Autofluorescence (AF), Second harmonic 0generation (SHG), and fluorescence life time imaging (FLIM) were shown for each dentine substrate (infected, affected, demineralised and sound) used in this study. AF image was the brightest with the highest intensity value in the infected dentine. SHG image in the demineralised group was the brightest and with the highest intensity among other groups. FLIM images are gradually changing in colour from tissue to another; as the blue colour represent the infected dentine that have the shortest lifetime, with more

greenish colour in the affected and demineralised dentine and getting gradually more reddish in the sound dentine with the longest life time values.

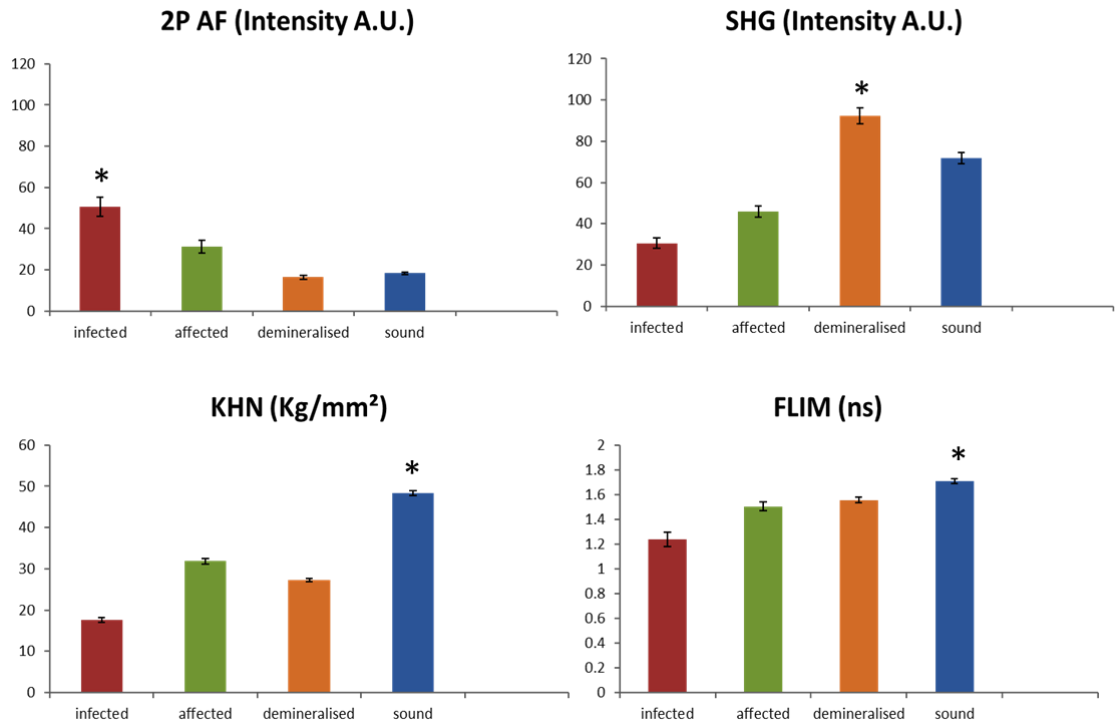

Figure 2-7. Representative histograms presenting the difference between dentine substrates in each measured parameter separately. Error bars depict standard errors of means (SE). (*) indicates significant difference between dentine substrates. AF of the infected tissues recorded the highest intensity mean and reduced towards the sound dentine. In SHG histogram, the highest intensity belongs to the demineralised tissues and the least in the infected tissues. Hardness was the least in infected tissues followed by the demineralised then affected dentine. FLIM showed gradual increase in lifetime from infected towards sound tissues.

- **Chemical assessment using Raman phosphate intensity analysis before storage**

As mentioned earlier, no Raman scans were performed on the carious samples before storage as most of the pilot samples were burned, but it was recorded for sound and demineralised samples only. However, after four weeks' storage in phosphate buffered saline, a reduced laser power (50%) was used to image only six points across the carious dentine zones, to minimise carious tissue laser exposure time and burning of the samples. It was noticed that the dark-coloured samples absorbed most wavelengths of light and were more likely to get burned. Results of Raman intensity in sound and demineralised surface before storage are reported in Fig. 2-8. A t-test showed a significant difference between the two substrates, as sound recorded (201 a.u. ± 5), and demineralised (163 a.u. ± 4 (SE)), (p=0.004).

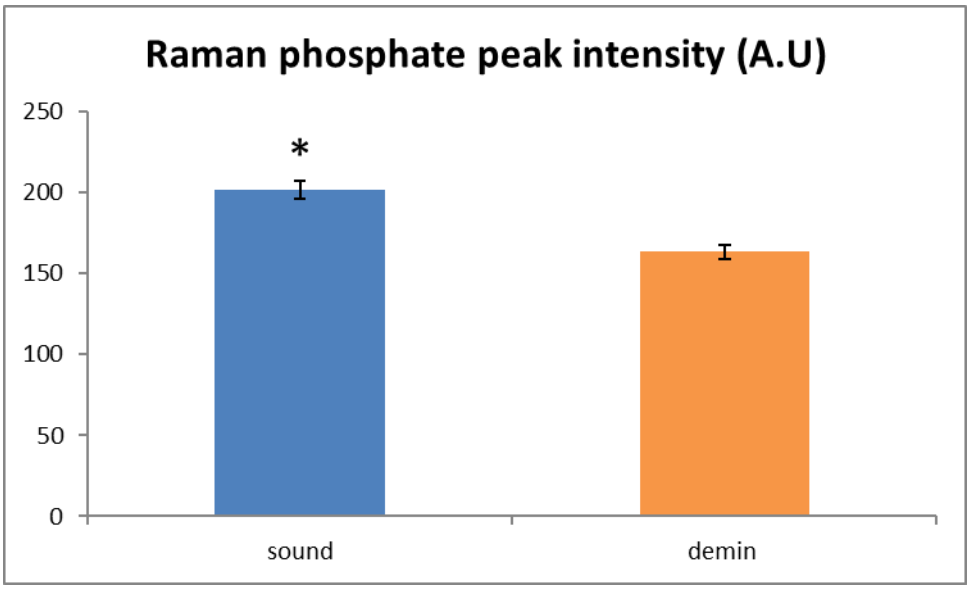

Figure 2-8. Representative histogram showed the significant difference (*) in Raman phosphate peak intensity (p=0.004), between sound (blue) and demineralised (orange) dentine before storage. Error bars represent the standard errors of mean (SE).

- **Spectra analysis**

Representative spectra were plotted for the carious samples and the *in-vitro* demineralised samples separately (Fig. 2-9 A, B). With regards the carious spectra, the infected tissues (red line) generated the highest AF signal intensity and it reduced gradually toward the sound dentine (blue line) (Fig. 2-9 A). In contrast, SHG signals recorded the reverse, as it increased significantly towards the sound tissues as shown (Fig. 2-9 A). Regarding the *in-vitro* demineralised samples, no AF signal was detected in both sound and demineralised dentine. However, SHG signals were prominent (orange line) in the demineralised tissues compared to the sound dentine (blue line) as shown in Fig. 2-9 B.

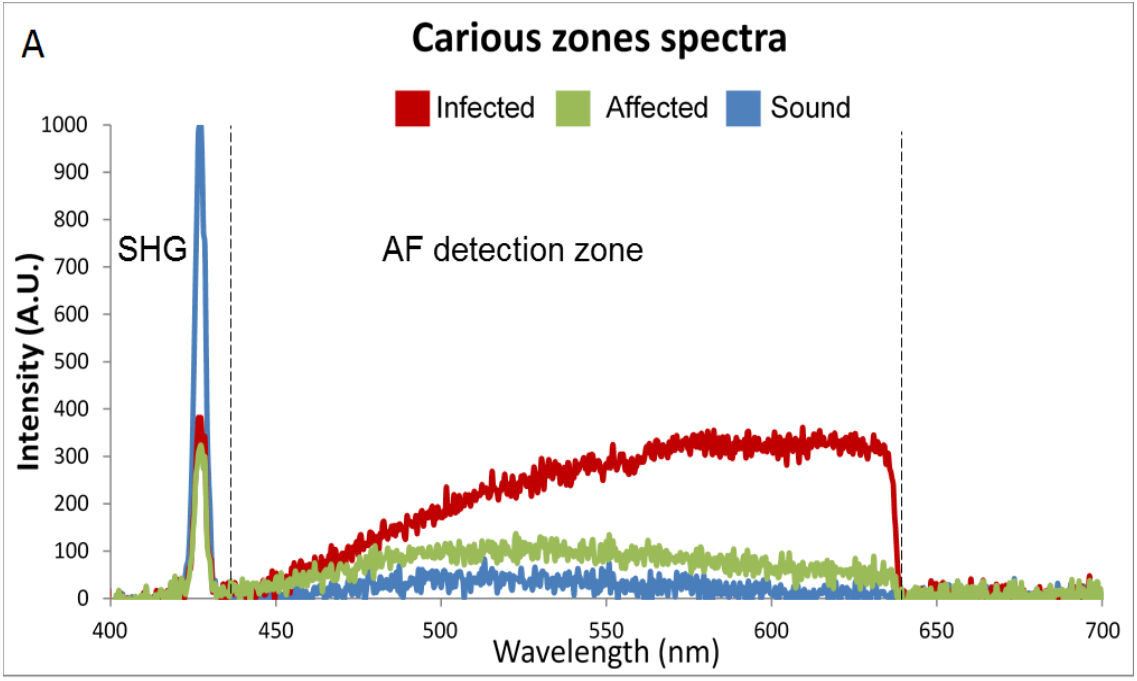

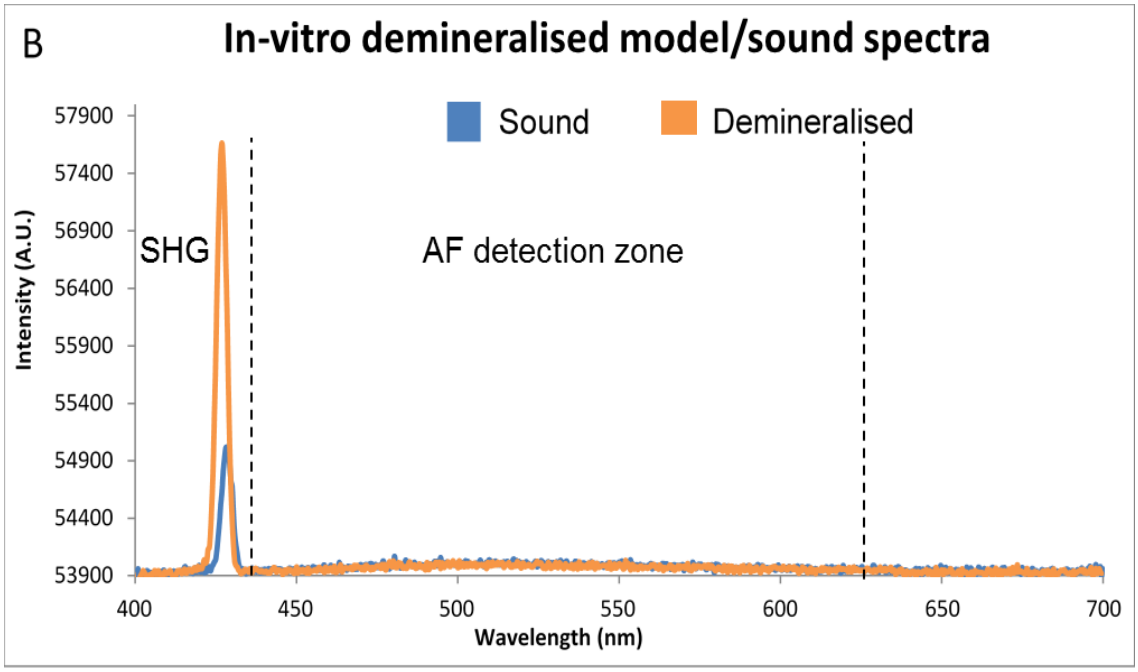

Figure 2-9. Representative spectra were plotted and showing; (A) The recorded points across the carious dentine zones have recorded the highest AF signal intensity and lowest SHG intensity were observed in the infected dentine (red line). The next line showed reduction in AF, and slight increase in SHG, which indicates caries-affected dentine (green line). Sound dentine showed the least AF and highest SHG spectral peaks (blue line). (B) the recorded points across sound/demineralised model, showed an increase in SHG signals (orange line) compared to sound (blue), while no AF signal was detected in both sound and demineralised dentine groups.

2.3.3. Characterisation of sound, demineralised and carious (infected and affected) dentine after storage

The Raman phosphate peak intensities of all substrates were recorded on the dentine cross-section after PBS storage and their mean were calculated as shown in Fig. 2-10 A, B, C. The least phosphate peak intensity was related to infected tissue (105 a.u. ±14), which was significantly different from all other groups (p=001). The demineralised dentine was comparable and insignificantly different from sound dentine (p=0.39), after storage (180 a.u. ± 2, 170.6 a.u. ± 5.2 respectively; Fig. 2-10.C). In addition, it wasn't significantly different from the natural caries-affected dentine (155a.u ±11.9), (p=0.81). Results of other applied techniques were presented as a percentage change based on the calculation of the difference between mean values before and after storage in PBS solution (Fig. 2-11). Infected dentine tissues showed a significant reduction in most of their examined properties following the storage in PBS, reduction in AF (-22% ±9) with a bright intensity image, reduction in SHG intensity (-14% ± 11), together with a shorter lifetime (-16% ± 8.5), (Fig.2-12). In addition, tissue hardness was also reduced by (-8% ±3.4). Affected dentine and sound controls showed insignificant changes in their properties following storage. However, the demineralised dentine substrate showed a statistically significant reduction in SHG intensity only (-29.2% ±8), with an increase in tissue hardness (11% ± 4).

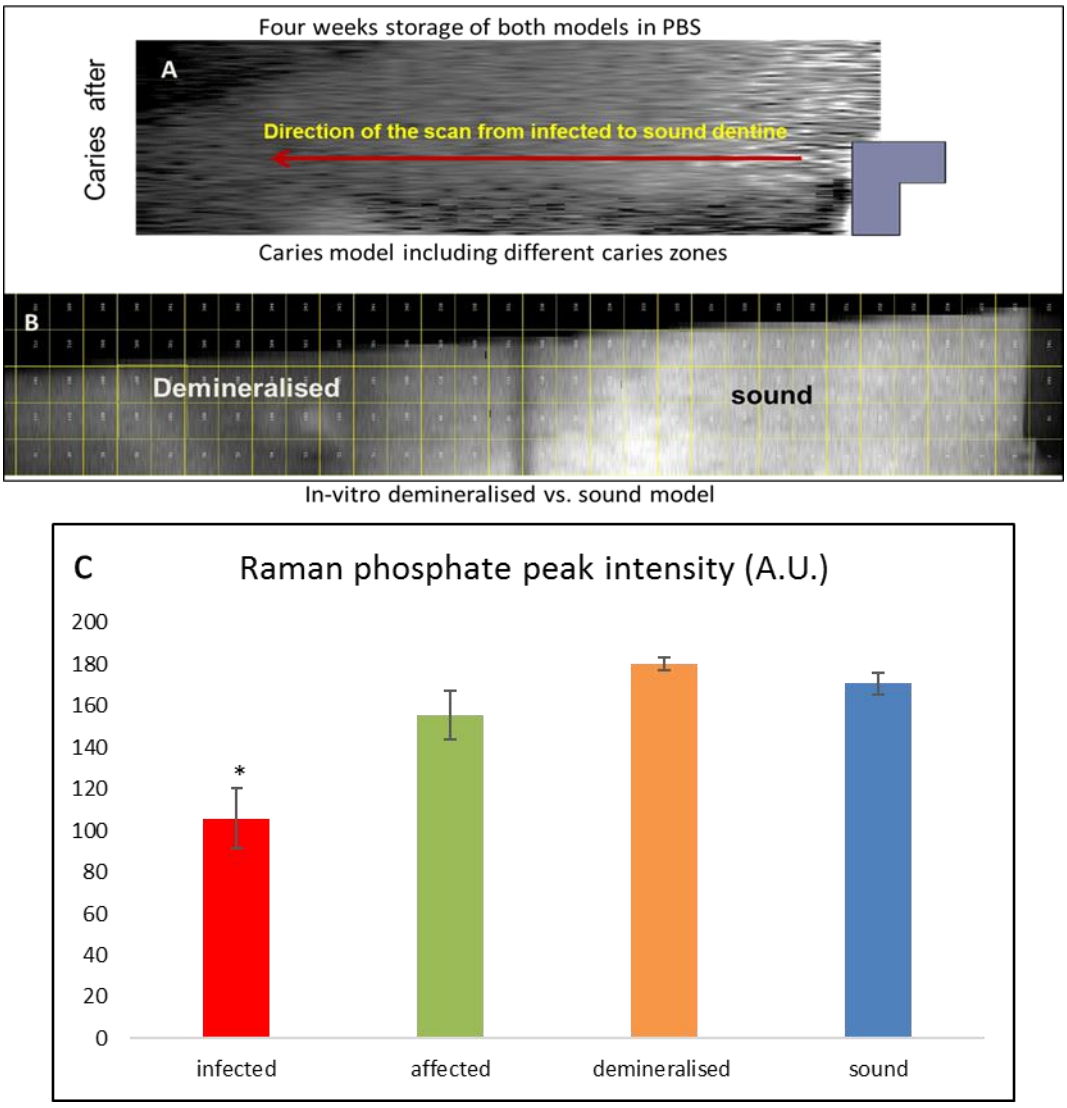

Figure 2-10. (A, B) Representative grey-scale images are showing the direction of the Raman scan on the cross-section surface of both carious model and the demineralised model after PBS storage. (C) Histogram is showing the difference in the calculated average Raman phosphate peak intensity of different dentine substrates after storage. Error bars represent the standard error of means. Results reported the least phosphate peak intensity was related to infected tissues compared to all other groups (p=0.001) and marked by (*) in the graph. No difference was noticed in the phosphate peak between the demineralised sample and sound dentine after storage (p=0.39), and with the affected dentine (p=0.81).

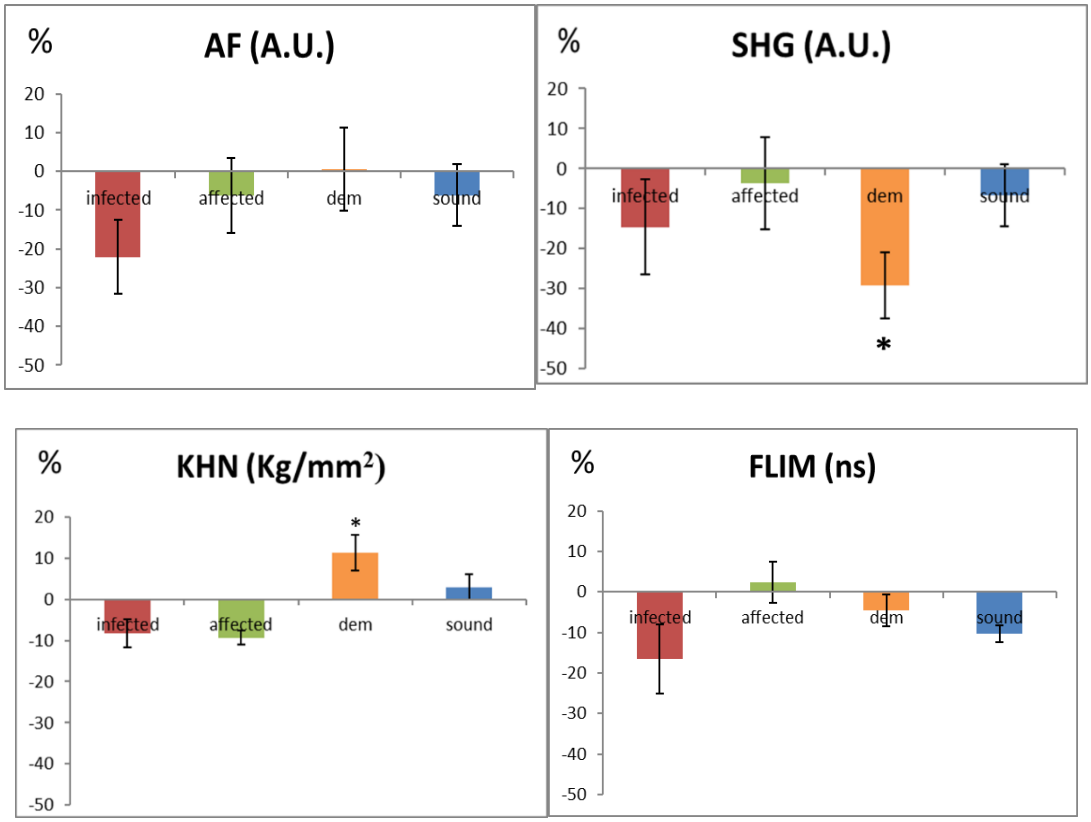

Figure 2-11. Percentage changes of mean intensity values of each optical characterisation technique with different substrates were calculated and plotted in bar graphs for effective comparison following dentine storage in PBS. Infected and affected dentine values were reduced in all measured techniques, but they were not significant from the sound dentine control group. A significant decrease in SHG intensity of the demineralised group compared to the sound dentine (0.01), associated with a significant increase in the demineralised KHN compared to the infected and affected tissues (p=0.005, 0.003 respectively).

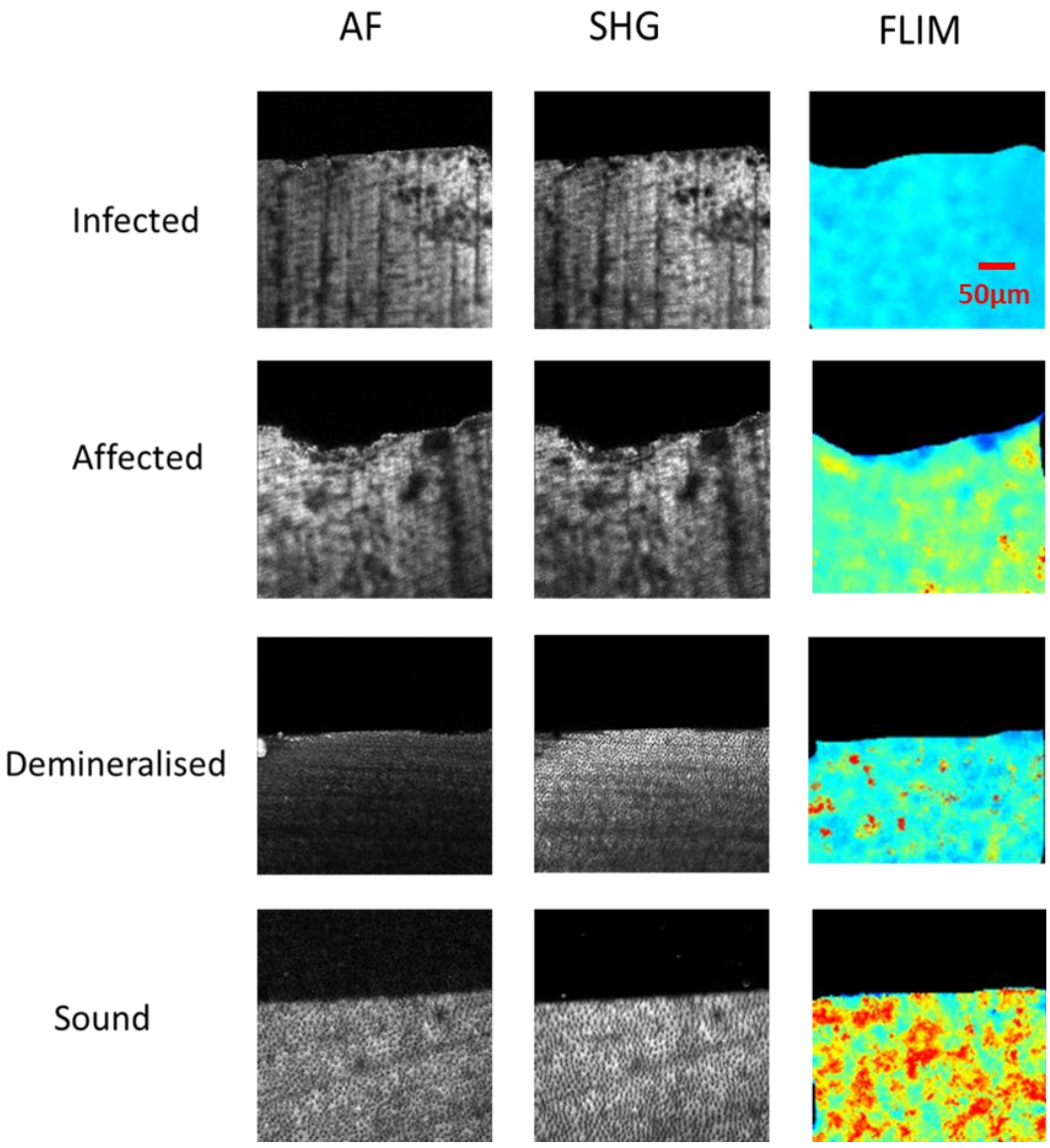

Figure 2-12. Representative images of autofluorescence (AF), Second harmonic generation (SHG), and fluorescence life time imaging (FLIM) were shown for each dentine substrate after storage. Infected and affected dentine intensity images were brighter than other groups, which was associated with the blue-green FLIM images indicating short life time for these tissues. SHG intensity image was brighter than AF in the demineralised group with more greenish lifetime image indicating no change in the lifetime after storage. Sound dentine is showing the green-red lifetime image as before the storage image.

2.4. Discussion

This study used a multi-modal approach to characterise a variety of encountered dentine substrates in dental clinical procedures (sound, demineralised, caries-infected and affected dentine). This approach compared optical and chemical

properties of the non-excavated carious dentine containing different histological tissues to those measured in the artificially demineralised dentine model, correlated with their hardness values. Furthermore, these techniques provided baseline control data for future experiments following storage with different dental materials. They are simple, reliable and non-invasive assessment methods and have been tested and applied in an earlier study to distinguish the carious zones using Raman spectroscopy correlated with their hardness and fluorescence behaviour (Almahdy et al., 2012). Partially demineralised/etched dentine surface using the phosphoric acid gel etching is one of the substrates involved in dental bonding mechanisms. Therefore, it is important to understand their properties using the same multimodal approach to predict the interactions of these substrates with the applied restorative materials in the following chapter.

Microhardness testing was used in this study as a direct *in-vitro* translational value that reflects relatively the mineral content of dentine and then facilitate differentiation of the carious zones (Banerjee et al., 2010a, Banerjee, 2013).

Since there are wide variations in the morphology and the micro-structure of natural carious dentine histological layers and the artificially demineralised dentine, their interaction with the illuminating incident light may also be different. In addition, their biochemical response when interacting with different restorative materials will also vary. The characteristics of dentine substrate influence directly the bond strength of the dentine/adhesive interface. However, a simple demineralisation protocol used in the current study has provided a simple model with partial loss of minerals and intact collagen matrix.

Differences between natural and artificial dentine lesions were explained by the difference in remnant mineral content in the deep and superficial part of the lesion. The etched/demineralised dentine contains more mineral in the deep layer of the cavity that serve as seed crystals for future tissue remineralisation. In contrast, the natural CAD contains more mineral crystals in the superficial layer of the lesion. These differences play a key role in how these tissues interact with different restorative materials and in their optical properties (Wang and Yao, 2010). In addition, the integrity of collagen fibre is another key factor for the dentine tissue healing and repair when comparing acid-etched and natural caries dentine.

2.4.1 Characterisation of sound, demineralised and carious (infected and affected) dentine before storage

Based on the results of this study before PBS storage, analysis of AF and SHG intensities revealed significant differences between the examined substrates compared to sound controls (Fig.2-8), which partially rejects the first null hypothesis of this study. Similar changes in fluorescence intensity have been reported (Stoller et al., 2002). Results showed that the highest AF intensity was related to the infected dentine followed by the affected dentine, while the lower intensity was noticed in demineralised tissues, which was not significantly different from the sound dentine average intensity. Part of the results concur well with the results of a previous study; that the natural AF intensity of the dentine might help in objective quantification of carious zones both in clinic and laboratory, which further has been correlated with the tissue hardness of each substrate (Banerjee et al., 2010a, Almahdy et al., 2012).

The AF intensity of dentine is stronger than that of enamel. This is believed to be due to tryptophan and hydroxypyridinium in dentine collagen protein composition, together with a higher organic content compared to enamel (Hoerman and Mancewicz, 1964, König, 2000). It was also previously suggested that the dentine AF originates from several endogenous fluorophores. Consistent with this suggestion, collagen cross-linking can be a reliable indicator of the dentine microstructure state (Tanzer, 1973). This was based on the similar excitation and fluorescence characteristic of the cross-linked collagen and dentine AF (Rivera and Yamauchi, 1993). However, both are unlikely to have any relevance since their excitation wavelengths (350-400nm) lie outside the range covered in this study (Foreman, 1980). Moreover, microstructural change in dentine due to surface treatment (etching) or pathological action (caries) play a role in the degree of tissue destruction and their effect on associated optical properties.

Enhanced intensity associated with the infected dentine may be explained by complete matrix degradation and release of porphyrins which is one of the major cariogenic bacterial by-products during the caries process. CAD is also influenced by the acidic media which induces structural changes followed by defibrillation of unprotected collagen fibrils due to matrix metalloproteinase

enzymes (MMPs) release. This explains the high AF signals in this layer but to a lesser extent than the infected tissues (Kleter et al., 1998a, de Carvalho et al., 2009, Lee, 2015). Using UV excitation, investigations of teeth indicated that the origin of light emission was from the organic component embedded in the inorganic calcium apatite matrix (Lee, 2015). It was also reported that fluorescence in human teeth may be organic in nature, possibly proteins, as well as the inorganic matrix (Horsley and Barrow, 1967). In agreement with these assumptions, the results of this study showed the insignificant difference in AF intensity of the artificially demineralised dentine compared to the sound dentine (Fig.2-9). This may indicate the independent direct relation between AF intensities and the mineral content of dentine. On the other hand, laser fluctuation, cannot be ruled out, despite their calibration and the laser power measurements (Gallagher et al., 2003). This additionally may validate that the proposed demineralisation protocol by etching did not affect the cross-linking of the collagen in that substrate, which makes it a proper model to test the potential remineralisation effect of different applied materials. In contrast, SHG showed the reverse data, with an increase in its intensity in the demineralised dentine, while the lowest intensity was related to infected tissues.

It was previously found that the dentine structure generates an intense SHG signal compared to enamel and cementum, due to a strong correlation between collagen and SHG signals (Kim et al., 2000, Chen et al., 2007). This coincides with the results of the present study, as infected tissues revealed the lowest SHG signals due to organic dentine matrix degeneration. However, the demineralised group, following the removal of the superficial mineral leaving an exposed collagen fibril to laser light, yielded the highest SHG intensity signals.

FLIM imaging was used in limited studies to investigate dental tissues, as it requires a high repetition rate pulse laser with an excitation wavelength that must be well-matched with the absorption wavelength of tested sample (Matsumoto et al., 1999, McConnell et al., 2007). This could be achieved by using the ultrafast Ti-Sapphire laser with the two-photon microscopy (Curtis and Watson, 2014). Sensitivity and specificity are widely used measures in quantification of the diagnostic ability of proposed testing techniques. A previous study has confirmed significant specificity and sensitivity of AF intensity measurement combined with

FLIM to effectively distinguish between carious dentine zones. Enhanced AF in infected tissues was accompanied with the shortest lifetime which agrees with the result of previous study (Lin et al., 2011). Short lifetime has been mentioned in an earlier study and was attributed to changes in both chemical and physical properties of dentine (Webb et al., 2002). Lifetime can be influenced by the fluorophore environment including polarity, ion concentration, temperature and pH. Hence, it is used as a parameter for biological sensors. The dentine substrates showed a gradual increase in FLIM from CID to sound dentine. This could be explained by possible pH differences between substrates. Lowest hardness values were in the infected tissues group and it gradually increased towards the sound dentine group. However, loss of fluorescence in demineralised tissues indicates that dentine fluorescence is not only generated due to collagen but to the interplay of calcium phosphate crystals with collagen (Panayotov et al., 2013).

2.4.2 Characterisation of sound, demineralised and carious (infected and affected) dentine after storage

To compare the obtained results before and after storage from same samples, percentage change % was calculated. These data will be further used as a control when comparing the effect of different restorative materials interaction with investigated substrates. With regards to infected tissues, they showed a decrease but not significant in their % values with all recorded parameters, which may indicate further progression of caries when stored with no material. However, reduction in AF intensity could possibly be due to the deposition of some minerals from PBS media on the dentine surface. Demineralised dentine showed a significant reduction in SHG signals as etching with phosphoric acid may activate MMP enzyme activity and continue their effects during storage. This result partially rejects the second hypothesis.

Despite these findings, hardness and Raman provided opposite results, which may indicate surface precipitation of salts in the demineralised dentine surface from PBS media which could increase their surface hardness (Goodis et al., 1991). Demineralised dentine Raman values after storage have increased to lie in between sound and caries-affected dentine values with no statistical

difference from both substrates. It seems that storage in PBS solution have an impact on optical properties of infected and demineralised dentine. Both substrates have a mineral depleted superficial zone which demonstrates possible future interaction with restorative materials in similar storage media. Unlike CAD in which their dentinal tubules are occluded by mineral crystals due to continuous deposition of minerals during caries progression. Thus, CAD showed insignificant changes after storage as with sound dentine, which partially rejects the second hypothesis.

In conclusion:

- The optical techniques used in this study offer quantitative differentiation measures between examined substrates. They can be used as an alternative, non-invasive, and objective microscopic markers, to differentiate between natural carious tissue zones and the artificially created lesion.
- The design of both the demineralisation and carious model allowed co-localisation of multiple modalities used for sample evaluation.
- These measurements provided base line data for further assessments required when the examined substrates interact and stored with different restorative materials to assess the change after storage.
- Results partially rejected the null hypotheses, as there was a non-significant difference in mineral content between natural caries and artificially demineralised dentine after storage.

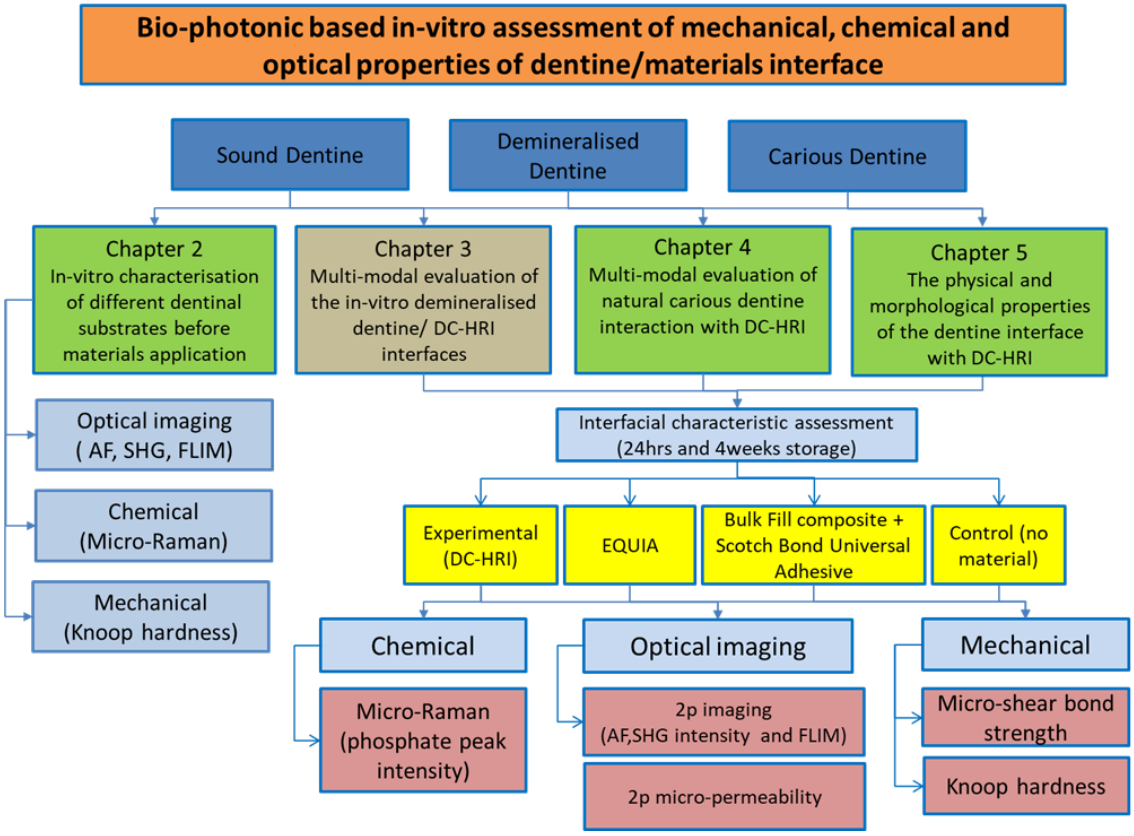

Chapter 3. *In-vitro* Demineralised Dentine Interactions with the Novel Dual-cure Hybrid Resin Ionomer (DC-HRI)

3.1 Introduction

The treatment modalities of any dental procedure are concerned about preservation of the maximum quantity of repairable dental tissues whilst providing natural function and aesthetics. The change from using dental amalgam to adhesive materials has led to the conservation of dental tissue, with no need for excessive tissue removal for restoration retention. With *in-vitro* studies, the variability in activity, size, shape, depth and structural difference between different natural lesions make this substrate difficult to standardise for testing materials and new techniques (Lenzi et al., 2015). Several samples are needed for a single test to overcome the variation between samples. Therefore, this study used a demineralised dentine model for standardisation and analytical purposes when testing the performance of a new restorative compared to the sound dentine (Marquezan et al., 2009).

Nowadays, the decrease in the number of amalgam fillings is influenced by the high demand for tooth-coloured materials and more biocompatible restorations.

The most favourable direct posterior restorations compared to amalgam are resin composites and glass-ionomer cements (GICs). Resin composites provided both aesthetic and satisfactory physical properties. GICs provide chemical adhesion to the moist tooth structure with an anti-cariogenic activity due to fluoride ion release (Frencken, 2017). However, low fracture strength, toughness and wear indicate the poor mechanical properties of glass-ionomers and limit their extensive use in dentistry as a definitive restorative material in stress-bearing areas (Lohbauer, 2009). They have been subjected to various improvements and developments. Resin-modified glass-ionomer cements (RMGICs) were one of these developments patented in the late 1980s (Antonucci et al., 1988). They were initially considered an alternative to amalgam, combining the benefits of a glass-ionomer with those of a resin composite. As such, RMGICs have been reported to demonstrate an increased elastic modulus, compressive strength, and lower solubility than conventional glass-ionomer luting agents, as well as biocompatibility and fluoride release (Hatibovic-Kofman and Koch, 1991).

More recently, a high viscosity dual-cure hybrid resin/glass-ionomer (DC-HRI) restorative material has been introduced to meet the clinical requirements for the conservative deep caries management. The organic matrix consists of a novel multifunctional, phosphoric acid-modified methacrylate, which generates self-adhesion without the need for separate adhesive step. The unique dual-cure initiator system allows for efficient polymerisation with high mechanical properties and dimensional stability (Zidan et al., 2015). It is provided in a capsulated form which minimises hand mixing errors and void incorporation. It allows adequate working time (±3-5 mins) and can be manipulated before polymerisation of the material starts. It is still unknown if this material has any bio-interactive effect when bonded to both sound and demineralised dentine. This will be investigated in this study compared to other control materials.

Remineralisation is a natural repair process that occurs to counterbalance the demineralisation of teeth caused by acidic attack. It requires the presence of calcium and phosphate ions on the surface of the pre-existing crystals in enamel or dentine. Therefore, recrystallization and formation of the newly acid resistant minerals occurs, especially if the fluoride exists to be included in the new crystals formation.

Glass-ionomer cements have been studied extensively for their potential re-mineralising effects on carious dental tissues (Miyauchi, 1976, ten Cate, 1995, Martinez-Ramirez et al., 2006). This makes it an ideal material for minimally invasive caries management (Frencken, 2017). From its composition, it was speculated that GIC may induce dentine remineralisation due to its high fluoride release which is already known to form an acid-resistant fluorapatite (Tsanidis and Koulourides, 1992). A study by a Creanor (1998) reported that RMGICs have the potential for remineralisation of artificially created dentine carious lesions compared to amalgam restorations (Chung et al., 1998). This has been shown in terms of both total mineral content and lesion body content. They were attributed the increase in the radiopacity to an increase of mineral deposition in the RMGIC group. Another study has also confirmed that RMGIC was associated with higher reduction of demineralisation adjacent to the tooth tissue under carious challenge, when compared with non-fluoride releasing composite restoration, while there was no difference found when RMGIC was compared to the fluoride containing composite (Mickenautsch and Yengopal, 2010).

A partially demineralised dentine model with an internal sound dentine control was used in this study to compare the response of both substrates when interacting with different restorative materials. It has been proven in the previous chapter that the demineralised dentine substrate differs significantly from both sound and CAD in some optical properties before any material application. Therefore, it can be assumed that the structural difference between these substrates will affect their response when they are in proximity with different restorative materials.

Several techniques have been utilised to quantify changes in the mineral content of different *in-vitro* dentine caries models following their interaction with dental restorative materials. In this study, changes in all parameters that have been already assessed in the previous chapter were re-evaluated including two-photon auto-fluorescence (AF), second harmonic generation (SHG) intensities, fluorescence life time imaging (FLIM), Knoop hardness (KHN) and Micro-Raman phosphate peak intensity in both sound and artificially demineralised dentine (ACD). These parameters would then be re-measured after storage in phosphate rich media with different restorative materials which are; the new material (DC-

HRI, 3M, USA), conventional glass-ionomer (EQUIA Fill, GC Corporation. Tokyo, Japan), and Bulk-fill composite (Filtek Bulk Fill, 3M, USA) bonded with Scotchbond Universal adhesive.

The null hypothesis of this study was that there is no difference in AF, KHN, phosphate Raman peak intensity and FLIM between sound and demineralised dentine after 4 weeks' storage with materials in phosphate buffer saline (PBS). There is no difference between the experimental material and other tested materials on either sound or demineralised dentine.

3.2 Materials and methods

Ten extracted sound molar human teeth were collected using an ethics protocol reviewed and approved by NHS Health Research Authority (16/SW/0220). The teeth were cleaned using ultrasonic cleaner and refrigerated in deionised water at 4 °C and were used within one-month post-extraction. Roots were sectioned just below the cemento-enamel junction to create a horizontal reference. Each tooth was mesio-distally sectioned into two 2 mm thick flat dentine slices. Specimens were distributed randomly into four groups, including five dentine slices in each group. These were then polished using 1200-grit carborundum paper under running water for 30 secs.

The materials used in this study are summarised in Table 3-1.

Table 3-1. List of materials used in the study.

Material	Product & Manufacturer	Material composition	LOT Number
Hybrid RMGI analogue	DC-HRI, 3M dental products, USA	Powder: surface modified glass powder, oxide glass chemicals, calcium hydroxide. Liquid: mono, di, tri-glycerin-dimethacrylate phosphoric acid ester, tri-ethylene glycol dimethacrylate, substituted dimethacrylate	609854
GIC	EQUIA Fil, GC, Tokyo, Japan	Powder: fluoro-alumino-silicate glass, polyacrylic acid powder Liquid: polyacrylic acid, Polybasic carboxylic acid	1509100
Resin Composite	Filtek Bulk Fill, 3M dental products, USA	The resin-based matrix contains ERGP-DMA, diurethane-DMA and 1,12-dodecane-DMA. The fillers are a combination of zirconia/silica cluster fillers 76.6% by weight and ytterbium trifluoride filler.	N840823
Self-etch adhesive	Scotchbond™ Universal, 3M, USA	MDP phosphate monomer, Dimethacrylate resins, HEMA, Vitrebond Copolymer, filler, ethanol, water initiators, silane	455500
Etchant	Scotchbond™ Universal, 3M, USA	37% phosphoric acid by weight	455500

3.2.1 Assessment of dentine changes after storage with materials

Following the baseline dentine assessment before material application, as described in the previous chapter, demineralised samples with internal sound controls were rinsed with the deionised water and ultra-sonicated for 5 minutes to ensure removal of the surface debris. Different materials were then prepared and applied as per the manufacturer's instructions to cover the previously characterised surface. For DC-HRI (3M, dental products USA), RotoMix™ Capsule Mixing Device (3M, USA) was used for 10 seconds then the material was adapted using a plastic instrument against the dentine surface Then, the restoration was light cured for 10 secs using a Deep Cure-S LED curing light (3M, USA) with the light intensity 1470 mW/cm^2 (-10%/+20%). For EQUIA Fill group (GC Corporation. Tokyo, Japan), material capsule was shaken, activated, then mixed using the same RotoMix™ mixing device for 10 seconds (+/- 4,000 RPM), and was applied as per the manufacturer's instructions on the dentine surface. Filtek Bulk Fill resin composite was applied following bonding with the Universal Scotchbond adhesive (3M, USA) as per manufacturer's recommendations. All samples were then incubated at 37°C temperature for 4 weeks in separate glass vials containing 7.0 ml of phosphate buffered saline (PBS) solution with 7.4 pH (Oxoid Limited, Hampshire, UK) and the storage solutions were replaced every 3 days.

- Optical assessment

Following four weeks storage, samples were sectioned at the previously marked reference landmark using a hard tissue microtome (Isomet 1000, Buehler, Lake Bluff, IL, USA) equipped with a slow-speed (330 Rpm), water-cooled diamond wafering blade (XL 12205, Benetec Limited, London, UK) to expose the interface for further evaluations. They were polished using 1200 grit Si Ca paper for 30 secs, and then sonicated for 3 minutes. Samples were imaged immediately using the in-house manufactured two-photon fluorescence microscope with the same settings as previously described in chapter 2 (section 2.2.3) for a consistent comparison. Twelve points were imaged on the cross-sectioned surface, within 50 µm from the dentine/material interface based on a previously recorded reference point (Fig.3-1). Using the same setting in the previous imaging setup,

AF and SHG intensities (256 x 256 pixels) and FLIM were reimaged as shown in the schematic diagram (Fig. 3-1B). The obtained data were analysed using Image J software (ImageJ, Wayne Rasband, NIH, USA) to measure the fluorescence and SHG average intensity. Using TRI2 FLIM analysis software (courtesy of Paul Barber, Grey Cancer Institute, Oxford), the fluorescence decay curves were fitted using a bi-exponential model and the average lifetime was calculated for each image and averaged for each tissue layer in each experimental group and further displayed as bar graph. The percentage change was then calculated using the before and after values of average intensity and lifetime using the following equation:

$$((Xa - Xb) / Xb) \times 100\%$$

Where Xa is the value after storage, Xb is the initial value before storage.

- Knoop hardness number (KHN)

Following the optical evaluation, tissue hardness was re-measured following the previous measured distance from the reference point. This was within 50 µm from the dentine restoration interface edge.

- Raman Spectroscopy

A similar analytical protocol was used to calculate the percentage change of the mineral phosphate peak intensity between baseline and storage values using the following equation:

$$((Xa - Xb) / Xb) \times 100\%$$

Where Xa is the value after storage, Xb is the initial value before storage.

3.2.2 Statistical analysis

The previous values (before materials application) were compared with post-storage by calculating the percentage change in both sound and demineralised dentine tissue in all material groups. The percentage change values were then used to compare different materials in each technique separately with both sound and demineralised dentine using a multiple regression test. If overall significance was found, then further Post-Hoc analysis was performed to find out which

particular group or material was significant. All the p values (level of significance) were adjusted for multiple comparisons.

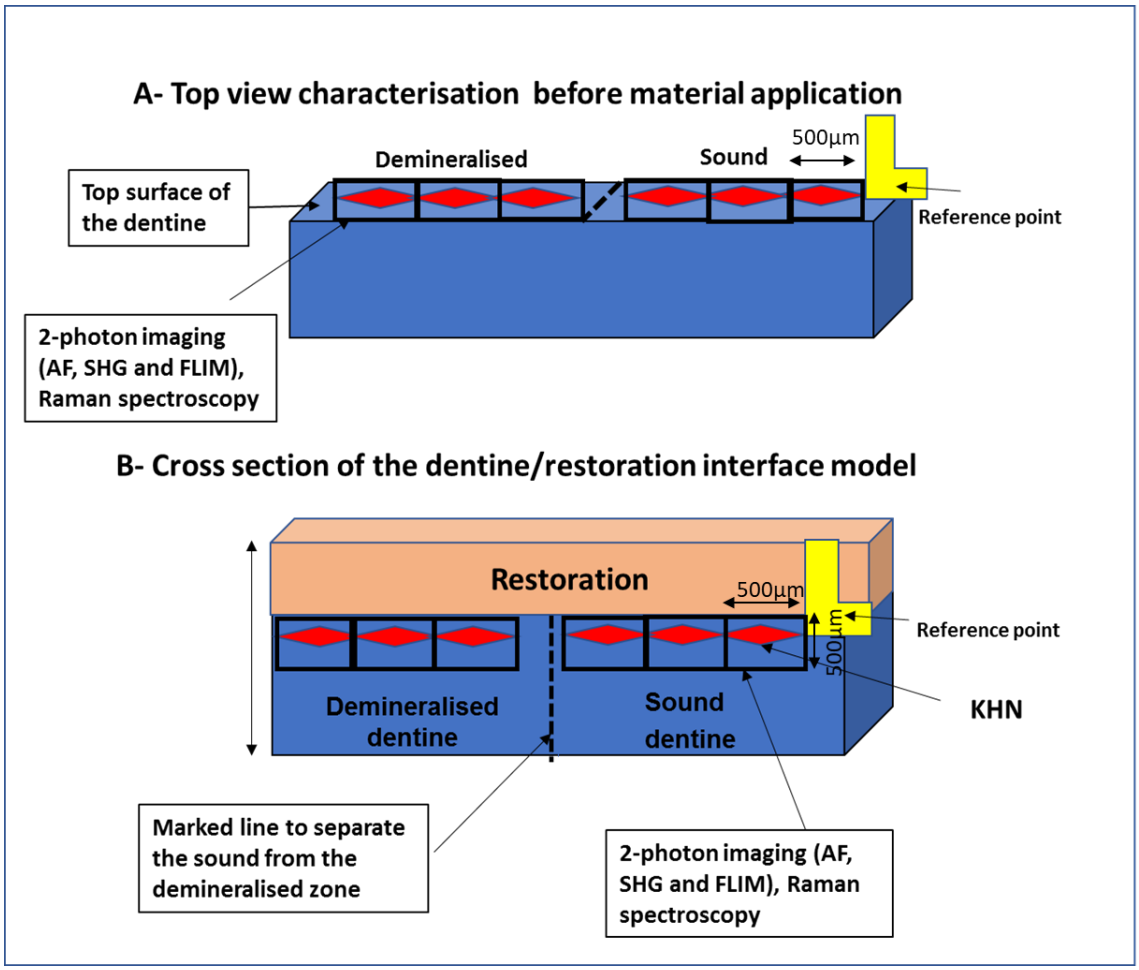

Figure 3-1. Schematic diagram showing the model used in the study (A) Sample before storage with the marked reference point and top surface characterisation using two-photon, Raman spectroscopy and Knoop hardness number (KHN) as described in chapter 2 (section 2.2.3). (B) cross-section view through the dentine/restoration interface, showed the position of the corresponding recorded points of the AF and SHG intensities, FLIM and Raman phosphate peaks intensities (black squares) and Knoop hardness points (red diamonds) based on a previously recorded reference point (yellow). Marked line using a sharp blade is well delineated between sound and demineralised dentine.

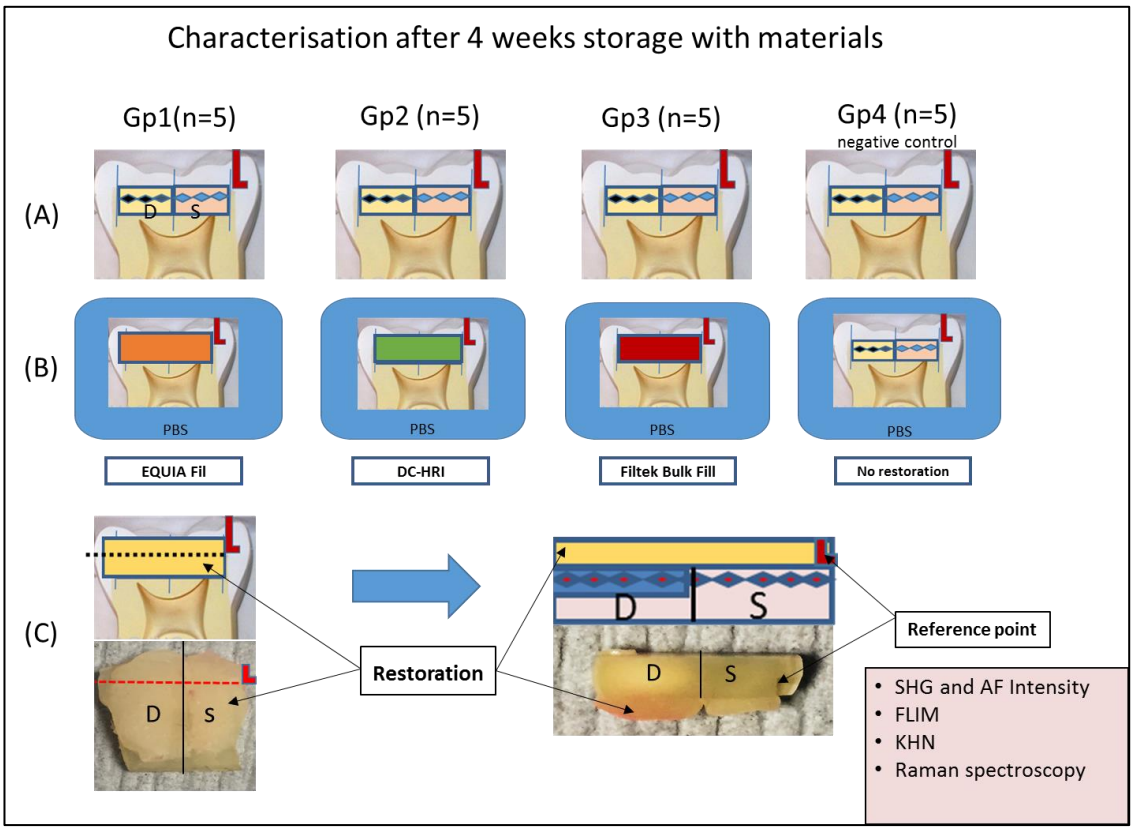

Figure 3-2. Diagram showing the setup and sample distribution for four interfacial dentine group evaluation. Letters (S, D) represents sound and demineralised dentine respectively. (A) Five random demineralised models were selected as tested samples for each group before restorations were applied and characterisation undertaken. (B) Samples were then restored with the three tested materials and one negative control group without restoration. Samples were incubated at 37°C temperature in phosphate buffer solution (PBS) solution. (C) After storage, samples were sectioned based on the previously marked reference point and re-evaluation of auto-fluorescence (AF) and second harmonic generation (SHG) intensity, fluorescence life time (FLIM), Raman mineral peaks intensity and Knoop hardness number (KHN) was done to calculate the percentage change. Further statistical analysis of the obtained percentage changes was performed.

3.3 Results:

3.3.1 Characterisation after material storage

- Optical assessment

Representative images of AF, SHG and FLIM of both sound and demineralised dentine before and after restoration are shown in Fig. 3-3 (A, B).

They were divided into four different groups: (a) DC-HRI, (b) EQUIA Fill, (c) Filtek Bulk Fill, (d) negative control (no material). All materials results were compared to the experimental material and then against the control group. Qualitative image analysis of AF and SHG showed minimal changes which were prominent in the sound EQUIA Fill group. FLIM imaging of sound dentine showed a red colour, while it was blue in the demineralised dentine. No changes were noticed in the FLIM images of the sound group after storage with materials except the Filtek Bulk Fill group as the redness was decreased that could reflect a shorter lifetime (Fig. 3-3A). However, changes in the FLIM images of the demineralised group were noticed after storage with EQUIA Fill and DC-HRI groups from blue to red, compared to the blue baseline and control images which may indicate longer lifetime (Fig. 3-3B)

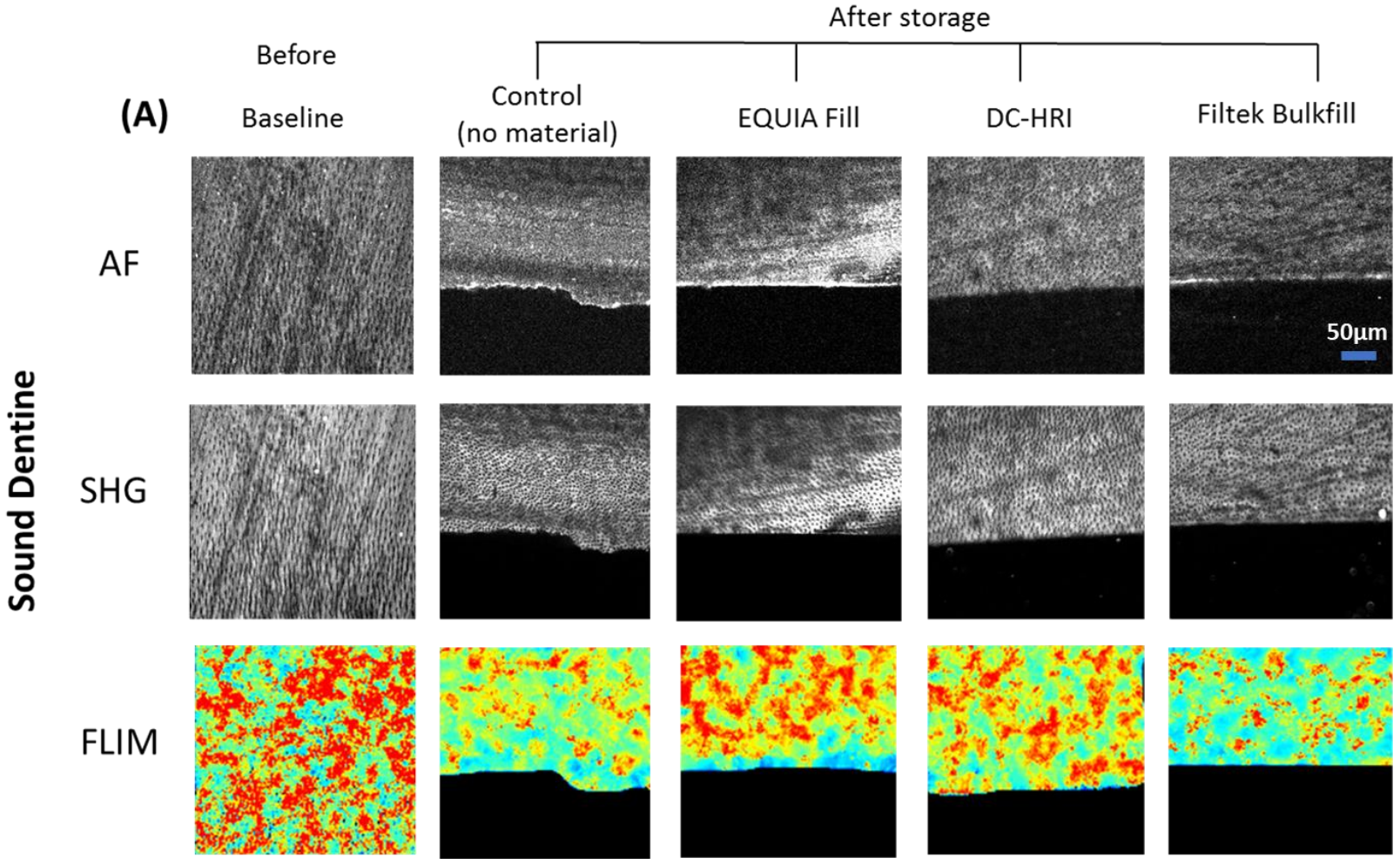
(A)
Before
After storage
Baseline
Control
(no material)
EQUIA Fill
DC-HRI
Filtek Bulkfill
AF
SHG
FLIM
Sound Dentine
50µm

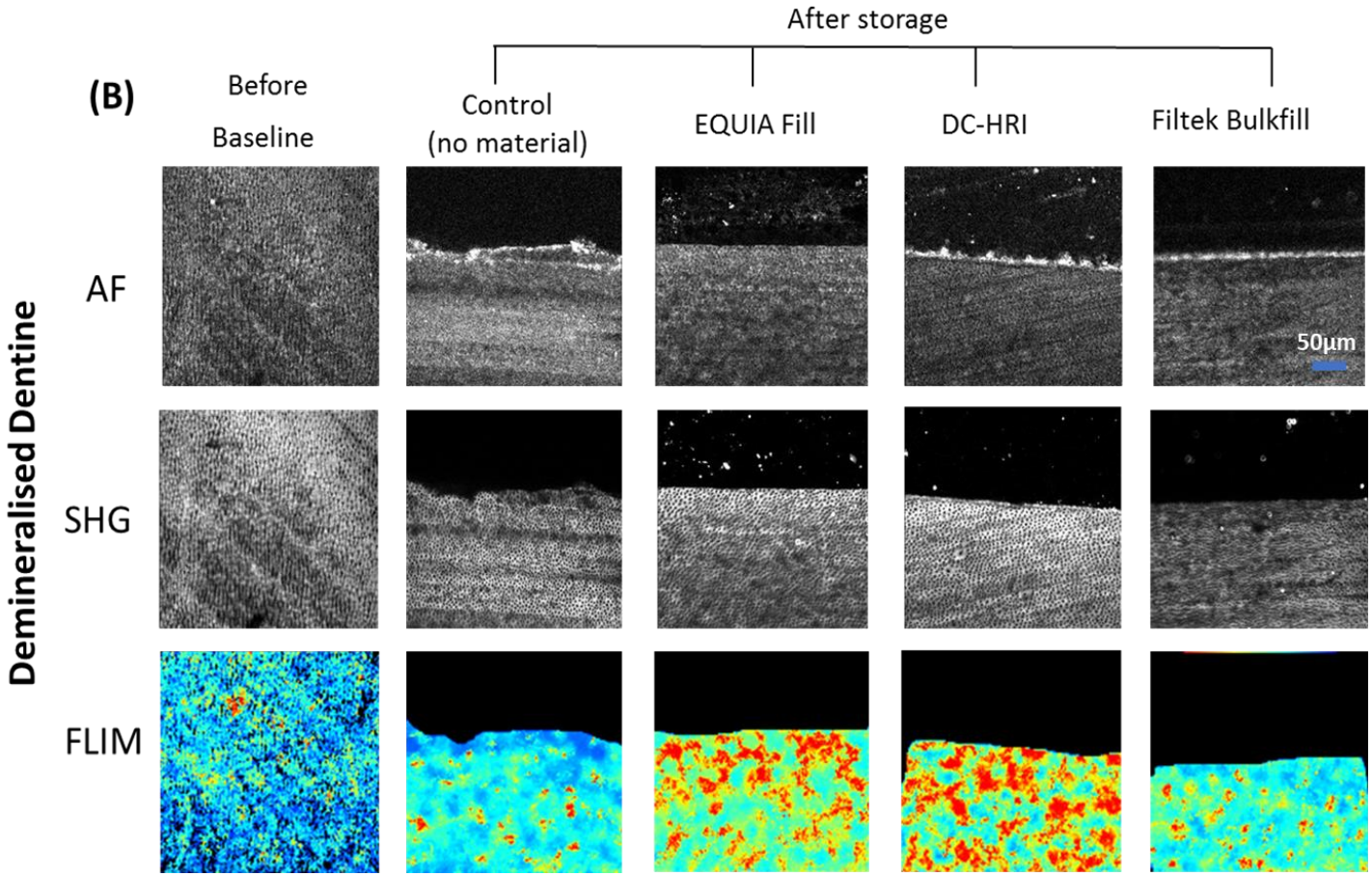

Figure 3-3. Representative two-photon and FLIM images are showing sound and demineralised dentine groups. (A) Set of sound and (B) demineralised dentine images at the baseline (before material application), and after storage with different materials were presented. Qualitative

Cont. (Fig. 3-3) evaluation of autofluorescence and second harmonic generation images showed minimal changes between groups, especially in sound EQUIA Fill group, while measuring their intensity quantitatively showed some significant variations. However, FLIM images evaluation showed the difference between the experimental groups compared to the baseline and to the control group as well. It is well noticed that FLIM images remained red in EQUIA and DC-HRI in the sound groups but not with the Filtek Bulk Fill group. In addition, FLIM images became redder in the demineralised group after storage with EQUIA and DC-HRI groups. The reddish colour may indicate longer lifetime which may represent similar properties to the sound dentine. However, bluish-green colour indicated shorter lifetime and may indicates dentine degradation.

- Autofluorescence (AF) intensity

  Multiple linear regression statistical analysis and percentage change calculations between initial and storage values were performed for each group and each technique separately.

- In the sound dentine group, results showed a comparable insignificant decrease in fluorescence intensity of all materials, with a significant reduction in Bulk Fill group (B+), (-34.3% ±7), (p= 0.001) compared to both sound DC-HRI (D+) and no material control (C+) groups.
- In the demineralised dentine groups, a comparable increase in the fluorescence intensity was noted in both DC-HRI (D-) and EQUIA Fill (E-) groups (17.3% ±9.2, 23.2% ±17.2 respectively), while no change was found in the control (C-) group. Filtek Bulk Fill (B-) group was significantly lower than other groups (-28.7% ±8.7), (p= 0.03).

  These changes among all four groups were shown in Fig. 3-4. There is a significant difference between sound and demineralised groups (p=0.023).

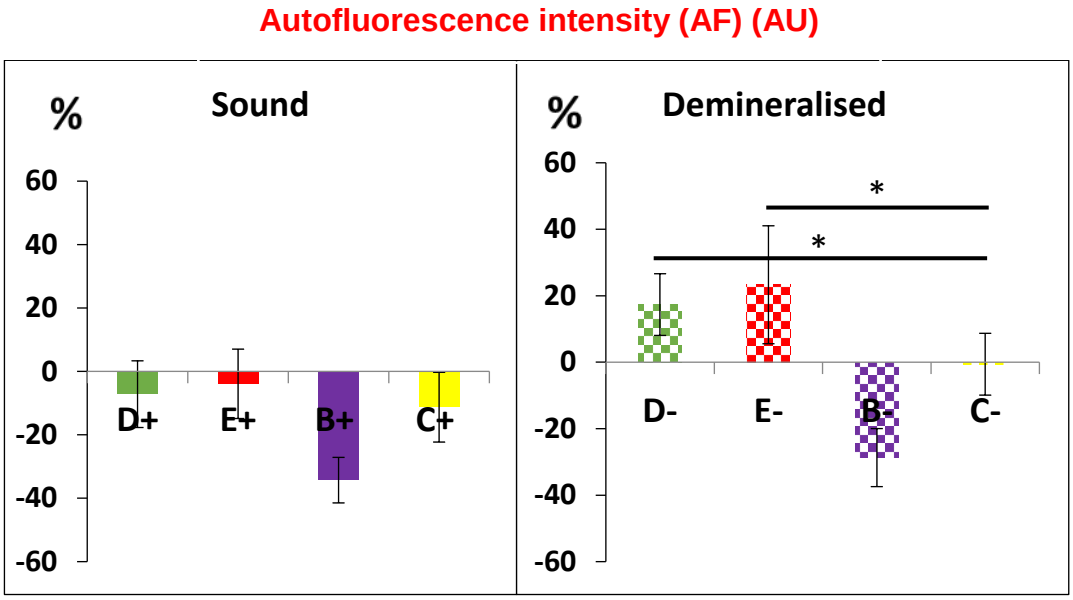

Figure 3-4. Percentage change (%) of autofluorescence (AF) intensity in sound and demineralised dentine showed a significant decrease in Filtek Bulk Fill group intensity (B+, B-). There were no significant changes in intensities of the other groups with the sound dentine. However, the demineralised group showed a significant increase in intensity of the DC-HRI (D-) and EQUIA (E-) groups with no change in the control group (C-). Abbreviations used stands for different materials groups; (D+) DC-HRI sound dentine, (E+) EQUIA sound dentine, (B+) Bulk Fill sound dentine, (C+) control sound dentine, (-) referred for the demineralised dentine groups of the corresponding materials. Error bars represent the standard errors of means.

Second harmonic generation intensity (SHG)

SHG intensity showed a significant reduction in experimental group DC-HRI (D+, D-), (-20.8% ±8.8), ($p < 0.05$) compared to other groups and to the control as shown in Fig. 3-5. Demineralised groups showed a comparable decrease in intensity in both DC-HRI (D-) and control (C-) groups (-20.5% ±6.2, -29.2% ±10 respectively) which was significant from other tested materials ($p=0.04$, 0.011 respectively). Both sound and demineralised Bulk Fill groups (B+, B-), sound E+ showed an increase in intensity (21.09% ±12.9, 15.9% ±9.2, 16.7% ± 13 respectively), compared to D+, D- ($p < 0.05$), with no change in EQUIA demineralised group (E-) (1.3% ±16) which is shown in Fig.3-5. There is no significant difference between sound and demineralised groups ($p=0.074$).

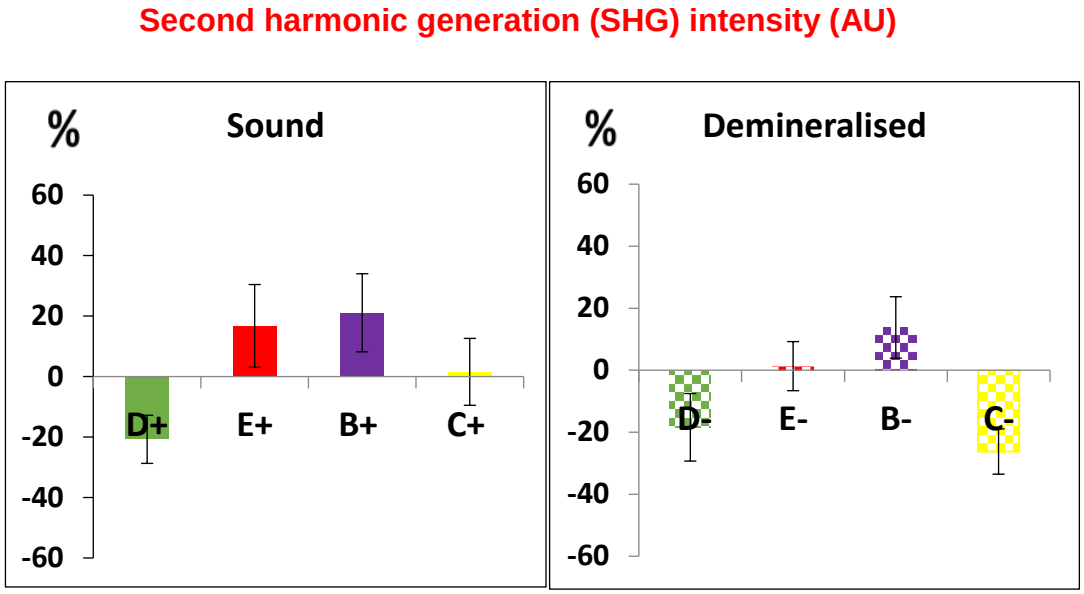

Figure 3-5. Percentage change of SHG intensity showed an increase in Bulk Fill group with both sound and demineralised dentine (B+, B-) and sound EQUIA (E+). Decrease in intensity of both sound and demineralised experimental group (D+, D-) but was comparable to the control group (C+, C-). No change was noticed in demineralised EQUIA group (E-). Error bars represent standard errors of means.

- Fluorescence lifetime (FLIM)

Sound dentine results showed a significant decrease in lifetime in the control (C+) group (-15.18% ±1.8), compared to D+ (-3.31% ± 1.7) (p= 0.0001). On the other hand, the demineralised dentine showed a significant increase in EQUIA Fill (E-) group compared to all other groups (16.48% ±2.9), (p= 0.001) which is shown in Fig.3-6. There was a significant difference between sound and demineralised groups in EQUIA Fill group only (p=0.002).

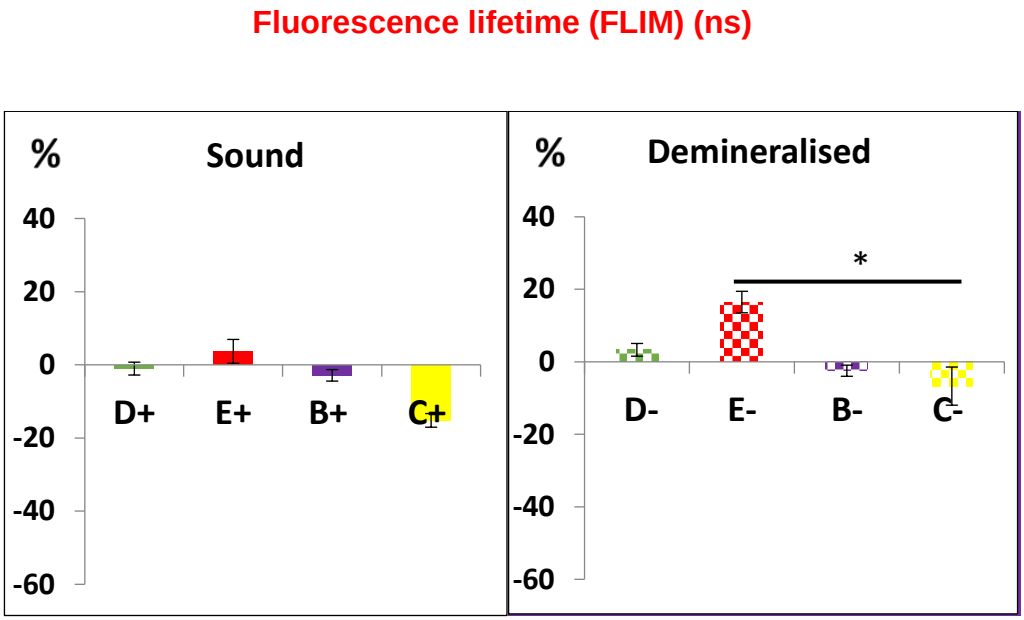

Figure 3-6. Percentage change of sound dentine FLIM showed no significant changes in lifetime between the materials but significant decrease was noticed in the control group. Demineralised dentine showed significant increase in EQUIA group only. Error bars represent standard errors of means.

- Dentine tissue hardness (KHN)

Percentage change of the dentine hardness before and after materials storage was also calculated and averaged for each group. The demineralised dentine was significantly getting harder when stored with DC-HRI and EQUIA Fill (41.11% ±5.6, 48.6% ±8.1 respectively), ($p= 0.001$, $p=0.002$) compared to other demineralised groups. The average value of Knoop hardness number was increased from (26.2 to 36.4) within the D- group. In the EQUIA group this increase was greater from (27.15 to 39.4). Non-significant increase was noticed regarding sound dentine groups. These changes are displayed in Fig. 3-7. There is a significant difference between the sound and demineralised group ($p<0.001$).

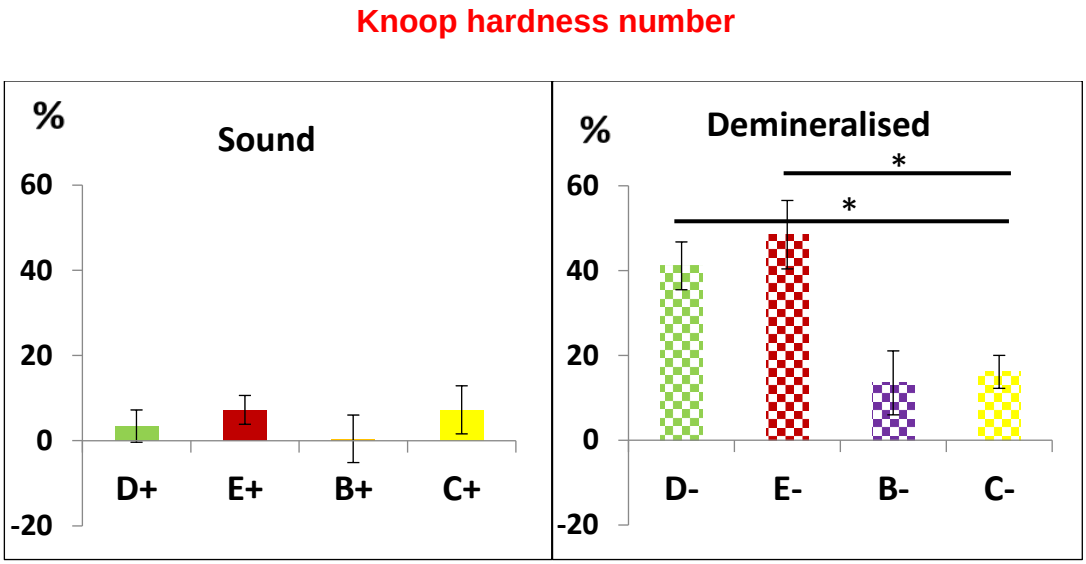

Figure 3-7. Percentage change of KHN showed no changes in sound dentine groups, with significant increase in demineralised experimental and EQUIA groups. Error bars represent standard errors of means.

- Raman spectroscopy

Raman analysis and percentage changes of Raman mineral peak intensity were calculated and presented in Fig. 3-8. In the sound dentine group, the percentage change in the C+ group mineral intensity has significantly decreased (-12% ± 1.8), (p=0.01). On the other hand, the demineralised groups showed significant increase in intensity of both D- and E- groups (13% ±7.3, 22.8% ±6.8), when compared with the control group (-3% ±4.4), (p=0.021). The difference was also significant when comparing sound and demineralised DC-HRI and EQUIA groups separately. However, this difference wasn't significant when comparing demineralised D- and E- (p=0.07). There is a significant difference between sound and demineralised groups (p=0.006).

Based on the previous analysis, results indicate comparable changes in optical properties and mineral intensity of the demineralised dentine adjacent to D- and E- groups.

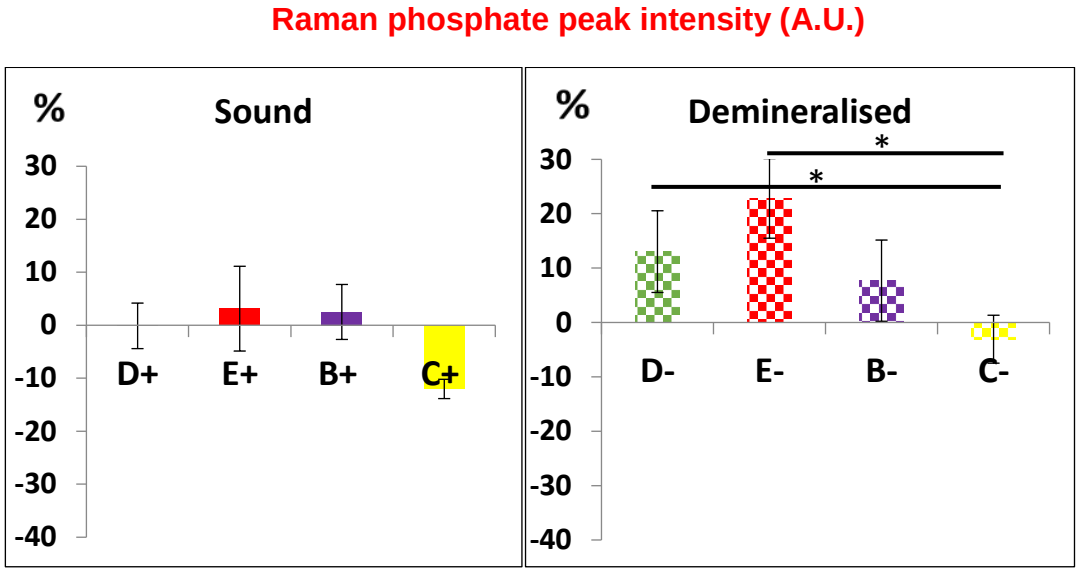

Figure 3-8. Percentage change of Raman intensity showed significant increase in demineralised EQUIA and DC-HRI groups compared to the control group, while no change was observed in any of the sound groups.

3.4 Discussion:

3.4.1 Sample preparation

Based on the minimally invasive dentistry approach (MID), CAD remineralisation has been studied extensively using different *in-vitro* models. It has been simulated by partial demineralisation of sound dentine using pH cycling or short duration etching by phosphoric acids (Klont and Ten Cate, 1991) or total demineralisation (Arends and Ten Bosch, 1992). Most of the simulated caries models have an intact collagen matrix which is capable of re-mineralising. However, artificial carious models have shortcomings as they do not model the effect of pulp response, dead tracts, secondary dentine and crystalline growth within the dentine tubules (Watson et al., 2014). As compared to the acid-etched/ demineralised matrices of normal dentine, the bio-altered natural caries-affected dentine would exhibit a complex, non-uniform composition and structure which have a direct effect on the quality, strength, and the durability of the adhesive/dentine interface.

In this study, the created demineralised dentine model was compared to the internal sound dentine control within the same sample, to monitor the changes in

optical, chemical and mechanical properties of these models, as a result of interaction with the applied restorative materials.

Despite the differences between the natural and artificial caries, an earlier study compared the Ca/P ratio of the carious model produced by either “biological bacterial” or the “chemical gel” methods using energy dispersive x-ray analysis (EDX). They stated that both substrates were similar in Ca/P ratio compared to the natural caries (Pacheco et al., 2013). In addition, the non-significant differences in values of hardness (KHN), lifetime (FLIM) and Raman phosphate peak intensity were reported in the previous chapter (section 2.3.2) between the natural CAD and the demineralised dentine groups. A significant difference when comparing the Raman shift of the collagen type I between artificial bacterial and chemical caries simulation methods but not compared to the natural CAD has been reported (Pacheco et al., 2013). Wang et al. study used micro-Raman spectroscopy to determine the degree of dentine demineralisation as a function of spatial position. This has been determined from the ratios of the relative integrated intensities associated with mineral phosphate peak at (961 cm^{-1} P-O symmetric stretch) and collagen peaks (1454 cm^{-1}, CH_2 deformation), based on the calculated mineral content at different positions directly after acid exposure (Wang and Yao, 2010).

Okamoto et al. reported a degradation in dental collagen following acid etching using 30% and higher concentrations of phosphoric acid (PA) for 1 min. Their results indicate that phosphoric acid induces a conformational change in dentine collagen (denaturation or perturbation) similar to that observed with HCl (Okamoto et al., 1991). Conversely, Gwinnett used SEM and ESEM to examine the demineralised dentine in wet, dry state and concluded that the micro-morphological change of the collagen was minimal (Gwinnett and Kanca 3rd, 1992). Wider ranges of demineralised dentine depth following acid etching were reported in earlier studies ranging between 10-2000 μm (Van der Veen and Ten Bosch, 1996, Tay and Pashley, 2008, Bertassoni et al., 2011). In the previous chapter, the collagen reference was identified by recording SHG intensity values which were significantly higher in the demineralised dentine than those of sound dentine before material applications. This increase in intensity may be attributed to the exposure of collagen fibrils following the removal of the smear layer and

opening of the dentine tubules by acid etching. However, in the current study, these intensities were either increased or decreased indicating the change in collagen status following storage and interaction with the different restorative materials.

Demineralisation of dentine leads to reduction of its mechanical properties by removing mineral ions from the tooth apatite which can be re-constituted by restoring the inorganic matrix (Xu et al., 2011). Dentine remineralisation is a complicated process as it involves minerals, collagen and non-collagenous proteins (NCPs). A number of studies agreed that dentine remineralisation occurs through the growth of residual crystals within the demineralised structures (Kawasaki et al., 1999, Xu et al., 2011, Qi et al., 2012). In addition, the presence of non-collagenous proteins that adhere to the collagen matrix, are involved in the regulation of both inhibition and acceleration of the remineralisation (Linde, 1989).The remineralisation occurs when the mineral is reabsorbed by the damaged surface. It has been shown that dentine, even in the absence of cells, is able to participate actively in tissue reparative processes (Smith et al., 2012). Thus, the demineralised dentine can be re-incorporated by minerals which may act as a constant site for further nucleation. This can be induced by local supersaturation of Ca and P in the surrounding media and due to the presence of the non-specific tissue alkaline phosphatase. Furthermore, dentine provides both structural and chemical frameworks, acting as a scaffold for mineral deposition at specific sites to render a stronger and durable adhesion to dental tissues although the severe conditions in the oral environment (Toledano et al., 2015b).

Stream Line^{TM} scanning confocal Raman spectroscopy was utilised in the present study to assess the potential increase or decrease in phosphate content within the demineralised dentine model as a result of interaction with the tested materials (Milly et al., 2014). This can be performed by quantitative chemical analysis and calculation of the percentage change in phosphate mineral peak intensity of interfacial dentine adjacent to variant of tested materials (Tsuda and Arends, 1997, Tramini et al., 2000). Similar increases in Raman phosphate peak was previously reported in other studies indicate biological mineralisation in

cartilage and in teeth as a sign for HA formation (Sauer et al., 1994, Parker et al., 2014).

This study compared the micro-indentation hardness to the optical macroscopic appearance of the demineralised dentine against the internal sound control. As reported in the earlier study, and along with the results of our study, the Knoop hardness number can be used as a confirmative test of remineralisation correlated with optical changes in dentine following mineral deposition (Sajini et al., 2013).

3.4.2 Effect of tested materials on the dentine substrates

Several *in-vitro* studies have investigated the capability of remineralisation of the artificially demineralised dentine adjacent to glass-ionomer cement (Ten Cate, 1994, Ngo et al., 2006), resin modified glass ionomer (Creanor et al., 1998) and calcium silicate cements (Tay et al., 2007, Watson et al., 2014, Atmeh et al., 2015). In general, the mineral deposition precipitation is mainly driven by local factors such as pH, the presence of seed crystals in the collagen matrix and the surface area available for crystal growth (Yang et al., 2011). Previous studies confirmed the mineral transfer and apatite formation in different dentine substrates with variable mechanisms when they interact with GIC (Lee et al., 2008, Ngo et al., 2011). In contrast, other studies didn't show any dentine remineralisation with GIC; claiming that the acidic media generated from the acid-base reaction would be less favourable for apatite formation (Watson et al., 2014), or that a completely demineralised dentine substrate is unlikely to remineralise as it lacks crystal seeds for apatite growth, despite their well-adaptation to dentine (Kim et al., 2010a).

In this study, dentine interactions with the experimental restorative material DC-HRI, EQUIA and Bulk Fill resin composite bonded with Scotchbond Universal adhesive were examined using multi-modal non-invasive optical, chemical and mechanical approaches to test their potential ability to re-mineralize the partially demineralised dentine model. For EQUIA with the demineralised dentine group (E-), results showed a favourable increase in the percentage change of their AF, FLIM, KHN, and Raman with no change in SHG after storage, as compared to the minimal but not significant increase in the sound control substrate. The increase in these parameters may indicate a remineralisation of the adjacent

demineralised dentine substrate as presented. The explanation for the basic mechanisms behind the changes in each parameter were described earlier in the discussion of the previous chapter (Chapter 2, section 2.4). Moreover, results partially reject the first null hypothesis as they showed a statistically significant difference between the sound and demineralised dentine results in all parameters except SHG. This result agrees well with the study suggested that the ion exchange can occur in the presence of the partially demineralised carious dentine (Ngo et al., 2006). Demineralisation of the inorganic dentine component happens due to the cement's PAA and tartaric acids etching effect (Sennou et al., 1999). Therefore, this triggers the ionic flow of elements from the glass including fluoride, strontium, aluminium and residual hydroxyapatite attached to collagen of the partially demineralised dentine, which in turn neutralise the acidity and induce the mineralisation thus enhancing the fluorescence intensity and FLIM. Chemical bonding and continuous fluoride release are the most favourable properties of GIC (Asmussen and Peutzfeldt, 2002). With the presence of phosphate ions in the storage media combined with the release of calcium and phosphate from the tooth, fluoroapatites are believed to be formed to re-mineralise the "hypo mineralised"/ etched dentine (Tsanidis and Koulourides, 1992, ten Cate, 1995).

In an earlier study, to assess the degree of demineralisation in dentine, the Raman phosphate peak (PO_4^{-3} *v1*) has been detected at the exact position on the Raman spectrum (959 cm^{-1}), this peak directly reflects the mineralisation of the tissue (Almahdy et al., 2012). Therefore, the significant increase in Raman PO_4^{3-} peak may indicate the HA formations (Parker et al., 2014), as noticed in the current study in both GIC and DC-HRI/demineralised dentine groups. In agreement with the present results, an earlier study has confirmed the remineralisation effect of the conventional GIC together with Biodentine when bonded to the partially demineralised dentine using the same assessment methods (Sajini. S et al., 2016). On the other hand, no such remineralisation was observed adjacent to GIC in a totally mineral-depleted dentine as the GIC requires pre-existing nucleation sites (Atmeh et. al 2014).

The experimental dual-cure hybrid resin/glass ionomer (DC-HRI) restorative material was introduced by 3M as a novel RMGIC derivative that may replace the other existing commercial conventional GICs, RMGICs, and composite

restorations in treating the deep carious lesions. This material aimed to simplify the restorative clinical steps by the self-adhesion and improved mechanical properties. Their chemical composition resembles the commercial self-adhesive Universal resin cements (RelyX^{TM} Unicem, 3M), but with a higher viscosity and bulk-fill application approach to be used as a permanent posterior restoration in a high stress bearing area. Based on the results obtained from this study, DC-HRI behaves in a comparable way to its control group; the conventional highly viscous GIC (EQUIA Fill), in their biological response, when they interact with the demineralised dentine, but differs from the Bulk Fill composite group bonded with the Scotchbond Universal adhesive. Significant increase in mineral content using Raman phosphate peak and Knoop hardness (KHN), as well as the increase in AF optical values of the demineralised dentine group were also noticed with this group. These results may reflect the tissue repair of this demineralised tissue when stored with DC-HRI in a phosphate rich media, while no changes were noticed in the FLIM results. SHG intensity was reduced in both sound and demineralised dentine which was significant compared to the other groups. Such a result might be referred to the proximity of their mechanism of action to the glass ionomer materials. The initial acidity of the mixed material during the first minute was very low pH <2, which may induce changes in the collagen microstructure that result in the reduction in the SHG intensity of the dentine adjacent to this material. However, no such change was noticed in the SHG of the EQUIA demineralised group. Although a significant increase in the mineral content was detected within demineralised tissues beneath DC-HRI and EQUIA groups, comparing the results of both restorations interestingly revealed statistically insignificant but higher percentage change with GIC than DC-HRI.

DC-HRI contains a methacrylate ester of phosphoric acid (PAE), which induces a complex ionic exchange initiated by interaction of PAE functional groups and mineral apatite of the tooth, as well as interaction with the basic filler glass (Hikita et al., 2007). Many of the self-etch primers contain PAE in their composition. This ester simultaneously demineralises and infiltrates both the smear layer and the underlying dentine providing micromechanical retention. This interaction might be encouraged by the phosphate present in the storage media. In the current study, there is a difference in viscosity and pH between PAE in DC-HRI, HEMA in

Scotchbond adhesive and PAA in GIC. PAE has the highest acidity due to the phosphoric acid functional group which can ionise in the presence of water and further react with the HA mineral in dentine to form a complex structure (Fukegawa et al., 2006).Therefore, the improved optical properties showed signs of tissue repair of the demineralised dentine adjacent to DC-HRI was mainly confirmed by KHN and Raman values. Despite these optical properties changes do not confirm an absolute repair has been undertaken in the examined substrate, a previous study has reported a clear relation between the mineralisation and dentine auto-fluorescence properties. Such result supports our findings, when the hydrated cement was stored in PBS (Tay et al., 2007). Another study found a direct correlation between the natural fluorescence lifetime and the change in the mineral content of the tooth (Banerjee et al., 2010a). It has been confirmed also in earlier findings that the longer fluorescence lifetime was associated with a higher mineral content within sound dentine (McConnell et al., 2007, Lin et al., 2011). In the current study, the FLIM percentage increased only with EQUIA demineralised group as shown in Fig. 3-6, while no significant changes were noticed in the other groups. This result may confirm the ability of EQUIA to repair the partially demineralised dentine more effectively than DC-HRI, which correlates well with the results of the mineral change evaluation using Raman and KHN.

Among functional monomers contained in self-etch adhesives, the monomer 10-methacryloyloxydecyl dihydrogen phosphate (10-MDP) was found to adhere to the hydroxyapatite in the tooth more intensively (Yoshida et al., 2004). However, the enzymatic degradation, mediated by the activity of matrix metalloproteinases (MMPs), which is possibly happening in the Bulk Fill group as it showed a decrease in AF of both sound and demineralised dentine substrates. The further demineralisation may be proceed due to incomplete impregnation of the exposed collagen space and imperfect resin monomer infiltration to the full depth of the demineralised layer, with no any reparative action of the applied adhesive (Hashimoto et al., 2011). However, minimal but not significant increases in SHG, KHN and Raman was reported with the demineralised group. This may be attributed to the change in collagen crosslinking when they were locally infiltrated

by the adhesive, which may alter the mechanical properties as noticed by the increase in hardness and change in scattering property of the substrate.

3.5 Conclusions:

This study has introduced multimodal non-invasive optical approaches to assess the potential action of a new restorative material, designed for treating the deep carious lesion, to induce apatite formation or further demineralisation on a simple partially demineralised dentine model.

- The created demineralised model was characterised with an internal sound dentine control that facilitated the future comparison with the demineralised substrate.
- Optical characterisation was further correlated with mechanical (KHN) and chemical (Raman) evaluation methods indicating a direct relation between the change in mineral content and their effect of optical properties of the dentine substrate.
- Remineralisation of the demineralised model was achieved with the glass-ionomer (EQUIA Fill) and DC-HRI groups following storage in the phosphate rich media.

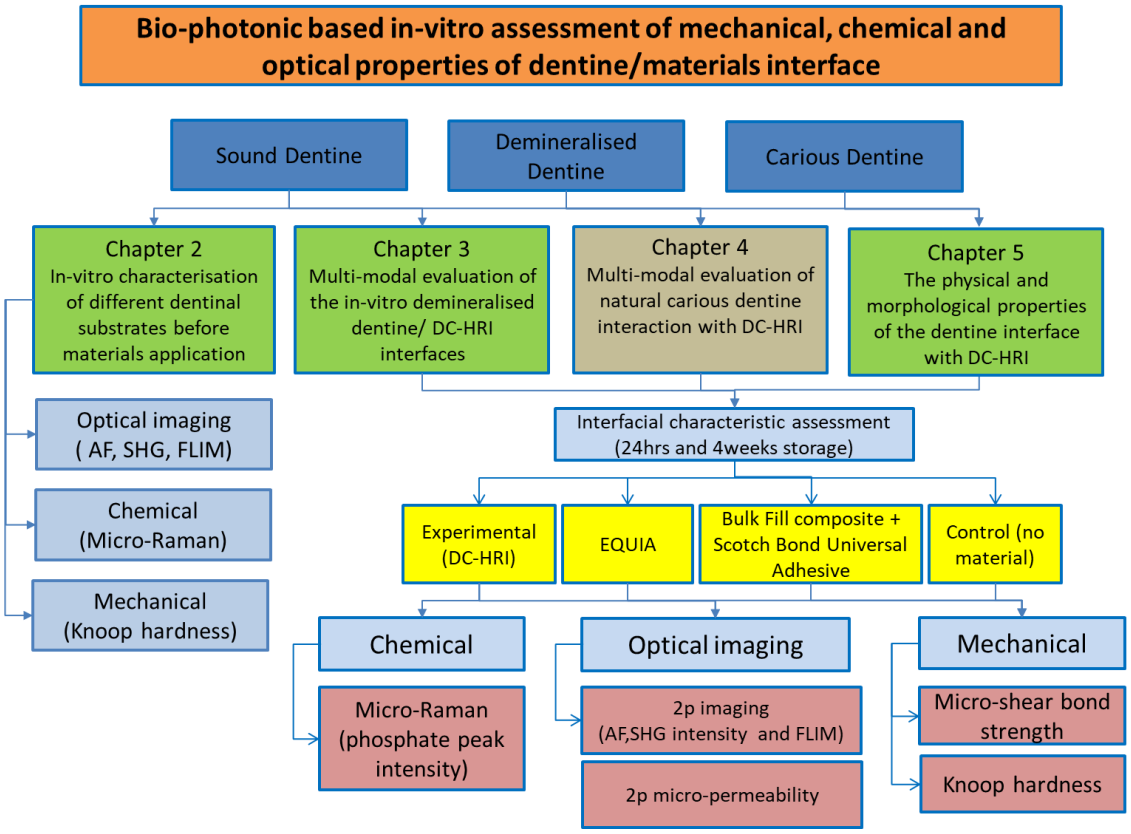

Chapter 4. Stain-free optical evaluation of carious dentine interaction with the novel DC-HRI restoration

4.1 Introduction

Minimally invasive carious tissue removal preserves the potentially repairable, caries-affected dentine (CAD), which is left intentionally in proximity to the pulp to avoid its exposure (Schwendicke et al., 2016). Selective tissue removal / atraumatic restorative treatment (ART) are the recommended techniques to control and avoid excessive tissue removal in managing deep carious lesions (Frencken et al., 1994, Mertz-Fairhurst et al., 1998a, Maltz et al., 2002, Ricketts et al., 2013). The sealed bacteria are supposed to be inactivated due to deprivation from carbohydrates (Griffin et al., 2008).

Therefore, when such treatments are performed, it is expected to find a combination of sound dentine at the periphery and of completely or partially demineralised dentine, overlying the pulpal aspect of the lesion. The mineral

distribution of the CAD is highly variable and the depth of the lesion can extend hundreds of microns below the excavated surface (Garchitorena Ferreira, 2016). The annual failure rate for teeth with selective carious tissue removal was reported to mimic those with complete caries excavation (Schwendicke et al., 2013). The radiographic observation of the carious tissue retained following selective carious tissue removal showed an increased radiodensity at 6-7 months follow up period (Maltz et al., 2002, Alves et al., 2010).

Clinically, it is difficult to locate the exact caries excavation endpoint, due to the non-selective nature of the traditional carious tissue excavation techniques. Therefore, chemo-mechanical caries removal system such as Carisolv ™ (Rubicon Lifesciences, Sweden) provides some self-limiting characteristic to the excavation endpoint to prevent excessive caries tissue removal (Banerjee et al., 2000).

Studies have investigated the effect of different caries excavation methods on the surface texture of the residual tissue following excavation. Varied patterns of dentine texture were obtained and a lower Vicker's hardness was reported with the Carisolv treated group, compared to rotary bur excavation (Mollica et al., 2012). Despite the reliability of the use of Carisolv as a selective caries excavation technique (Kathuria et al., 2013), there is no definitive procedure has confirmed the exact tissue type left in the cavity along the interface (de Almeida Neves et al., 2011). In addition, it is not predictable how Carisolv will affect the dentine substrate properties, and in turn the nature of bonding to the applied restorative material (Jepsen et al., 1999, Burrow et al., 2003). Therefore, in this study, the intact carious lesion was examined against different restorative materials, without any operative intervention or caries excavation. Stain-free microscopic evaluation was used for carious tissue zones characterisation and to study the effect of selected restorative materials on the optical, chemical and mechanical properties of these carious zones.

Remineralisation of the remaining carious tissue is a prerequisite to enhance the mechanical integrity of the tooth-restoration complex (TRC) and to avoid further pulp irritation (Bertassoni et al., 2009). The residual carious tissue would be favourable for remineralisation using bio-interactive materials such as calcium hydroxide (Conrado, 2004), mineral trioxide aggregate MTA, and Biodentine™

(Kim et al., 2016) or ion-releasing materials such as glass ionomer cements (GICs) (Ngo et al., 2006).The hermetic seal of the restoration is essential for successful conservative treatment, within comprehensive planning based on minimal intervention principles (Bjørndal et al., 2010, Schwendicke et al., 2013). However, full dentine tissue recovery is a complex process which requires the reconstruction of the lost organic collagen and inorganic apatite, as a result of acid attacks during the caries process. When the full recovery of dentine is achieved, improvement of mechanical properties of the remineralised dentine can be noticed, which indicates intrafibrillar remineralisation (Shibata et al., 2008). Conventional remineralisation of the carious dentine often requires solutions with calcium and phosphate ions in various fluoride concentrations. Some studies showed that the presence of seed crystals in the deeper caries sites can act as a nucleation site for calcium and phosphate epitaxial growth (Ten Cate, 2001, Deyhle et al., 2011, Bertassoni et al., 2011). It has been established that this type of remineralisation does not occur spontaneously, but rather through the growth of apatite crystals in the partially demineralised dentine. However, other studies showed that the apatite depleted surface can be re-mineralised in the absence of seed crystals by “bottom up”, non-classical bio-remineralisation approaches (Kim et al., 2010a, Cölfen, 2010). Both partially or totally demineralised dentine have been successfully remineralised using this strategy (Dai et al., 2011). Deposition of calcium and phosphate ions from the restoration or the surrounding media into the demineralised dentine result in net mineral gain (Cochrane et al., 2010).

A range of studies have investigated the role of GICs in remineralising natural carious dental tissues (van Amerongen, 1996, Hatibovic-Kofman et al., 1997, Kuhn et al., 2014). The material of choice of ART is the high-viscosity GICs because of its desirable handling, adhesive, anti-cariogenic and physical properties (Mickenautsch et al., 2009). The adhesive properties of GICs facilitated their use on tooth surfaces that have had only minimal preparation (Sidhu and Nicholson, 2016). However, their reduced mechanical properties have limited their use (Sidhu et al., 1997). Clinical trials have reported the chemical ionic exchange between the cement and the demineralised dentine (Ngo et al., 2006), as well as successful indirect pulp capping (Hashem et al., 2015). This could be related to the sustained release of fluoride ions from the cement and

rechargeability which is responsible for the anti-cariogenic activity (Forsten, 1998). Other ions were also reported to be included in the ion exchange such as aluminium, strontium. Theoretically, the concentration of mineral ions at the site of precipitation should exceed supersaturation to hydroxyapatite, hence remineralisation occurs. Precipitation reaction happens at slow rate compared to mass transfer of ions. Little data are available to confirm this assumption (Ten Cate, 2008).

As mentioned in the previous chapter, recent development in dental biomaterials research has introduced DC-HRI; a self-adhesive, dual-cure resin-modified glass-ionomer restorative material, aiming to restore the deep carious lesion, combining the improved handling, self-adhesion and better mechanical properties compared with the conventional GICs. Additionally, they were designed to achieve this adhesion without priming or pre-treatment of the tooth. Despite the promising results of DC-HRI interactions with the demineralised dentine model, it is yet unknown how these materials react with natural carious tooth tissues. Remineralisation of hard dental tissues adjacent to RMGIC restorations has been reported (ten Cate, 1995, Yengopal and Mickenautsch, 2011). Therefore, the aim of this study was to examine the possible mineralisation or caries arresting effect of this material when bonded to natural carious dentine tissues, compared to the commercial conventional high viscous glass ionomer restorative material and Bulk-fill resin composite restoration.

Advanced optical imaging techniques such as two-photon fluorescence microscopy, lifetime imaging and second harmonic generation imaging were used in this study to assess the changes in the carious dentine tissue fluorescence behaviours and optical properties adjacent to different coronal restorative materials. Moreover, Raman spectroscopy has been used for the assessment of mineral content change (as mentioned in Chapter 2, section 2.1). It was used to monitor the phosphate mineral peak change in carious tissues following the storage with materials. The Raman mineral peak intensity analysis used in this study has been reported in the literature for monitoring the mineralisation effect of different materials on cartilage and on dental tissues as well (Sauer et al., 1994, Milly et al., 2014).

Promising results in mineral evaluation have been achieved when tetracycline was used with caries-affected dentine (Watson et al., 2014) and with completely artificial demineralised dentine (Atmeh et al., 2015) using different remineralising agents. Further to the positive results with the partially demineralised dentine model formerly in this thesis (chapter 3). Sealing both infected and affected dentine with the restorative materials may influence mineral precipitation and ionic exchange with these substrates, and therefore mineralisation or caries inhibition may follow especially when they stored in a phosphate rich media such as phosphate buffered saline (PBS) solution (Tay and Pashley, 2008, Atmeh et al., 2015). Differentiation between the carious tissue zones was performed earlier based on their Knoop hardness values (KHN), (chapter 2). The same characterised carious samples were then used in this study to assess the changes in their optical, chemical and mechanical properties following storage in PBS with different restorative materials. Using these multimodal approaches may provide a valuable evidence in tissue repair or further demineralisation at the interface following storage. The null hypothesis of this study that there is no difference between the carious zones and materials groups in all examined properties.

4.2 Materials and methods

4.2.1 Sample preparation

This study was divided into two stages. The first part was to characterise the carious lesion using two-photon microscopy and KHN before the restorative materials were applied. The second part was to examine the effect of the applied restorative materials on the optical, chemical and mechanical properties of the carious tissue zones including infected, affected and sound dentine after four weeks' storage in PBS.

In chapter 2, section (2.2.1), fifteen extracted carious human molar teeth were used for these characterisations. Samples were sectioned into two halves through deep carious lesions extending halfway through the dentine with no pulp exposure. Each carious sample had been characterised based on a previously marked reference point, to ensure the future recording of the same points after storage with the chosen dental materials. In this study, the same samples were

used and were divided into groups according to the applied materials as shown in Table 4-1. Five carious halves were allocated to each material group; 5 halves bonded with the restorations and the other corresponding 5 halves were stored with no material as a negative control. All samples were restored and incubated in PBS (Oxoid Limited, Hampshire, UK) for four weeks. The storage solutions were replaced every 3 days.

Table 4-1. Table shows the experimental groups according to restorative material used

	DC+	DC-	EQ+	EQ-	BF+	BF-
Sample#	5 halves	5 halves	5 halves	5 halves	5 halves	5 halves
Storage media	PBS	PBS	PBS	PBS	PBS	PBS
Storage time	4 weeks	4 weeks	4 weeks	4 weeks	4 weeks	4 weeks

Where DC+ carious dentine with DC-HRI, DC- carious dentine with no material, EQ+ carious dentine with EQUIA, EQ- carious dentine with no material, BF+ carious dentine with Bulk Fill, BF- carious dentine with no material.

Following caries characterisation using two-photon imaging and microhardness testing, samples were rinsed with deionised water and sonicated in a water bath for 3 minutes to remove any surface debris. After that, each material was prepared and dispensed as per manufacturer's instructions and was applied using a plastic instrument to one half of a carious tooth, leaving the other half to act as a negative control with no restoration. Future localisations of the previously examined points were enabled by leaving the reference mark exposed (see Fig. 4-1). DC-HRI was an encapsulated form which was activated for 2 seconds using the Aplicap™ capsule activator (3M, USA) supplied from the company. It was mixed using the RotoMix™ Capsule Mixing Device (3M, USA) for 10 seconds. A further ten seconds light curing using Elipar™ Deep Cure-S LED curing light (3M, USA) was applied with 1200 mW/cm² intensity. Likewise, EQUIA Fill (GC, Tokyo, Japan) capsules were mixed and applied with no curing and were left to set for 30 mins in a damp environment at 37°C temperature. Bulk Fill Filtek™ resin composite was used with Scotchbond™ Universal Adhesive (3M, USA). Scotchbond™ Universal adhesive was applied in a self-etch mode and cured as

per the manufacturer's instruction. Resin composite Bulk Fill was added, and light cured for 40 seconds. The reference point was left exposed as a future mark for cutting after storage.

4.2.2 Characterisation of carious dentine after 4 weeks storage with materials

Following storage, samples were rinsed with deionised water. The previously imaged points in each sample were precisely located and marked for cutting based on the reference angle. Then, the sample was sectioned using a hard tissue microtome (Isomet 1000, Buehler, Lake Bluff, IL, USA) equipped with slow-speed water-cooled diamond wafering blade (Benetec Limited, London, UK) (300 Rpm). After sectioning, all specimens were rinsed with deionised water and cleaned in ultrasonic bath for 3 minutes to remove any surface debris. All samples were then finished with wet 1200-grit carborundum paper for 30 secs, and samples were sonicated for 5 minutes to become ready for imaging.

- **Two-photon microscope imaging (AF, SHG intensities, spectrum and FLIM imaging) and their analysis**

A two-photon microscope was adjusted using the same setting and the laser power as those used in previous chapters (2 and 3), to evaluate the changes in dentine carious zones and sound tissues properties adjacent to the tested materials interface (Fig. 4-1). Data were obtained using a 20x 0.75 NA air objective lens, 854 nm excitation wavelength and 550 ± 20 nm, 427 nm emission filter for imaging to allow reliable comparisons (McConnell et al., 2007, Banerjee et al., 2010a). Autofluorescence (AF), second harmonic generation (SHG) intensity and fluorescence lifetime (FLIM) were recorded and analysed. All recorded data after storage were analysed the same way as before storage, for a reliable comparison. AF and SHG intensity images were analysed and their intensity was measured for each carious zone in each experimental group, using Image J analysis software (ImageJ, Wayne Rasband, NIH, USA) as shown in Fig. 4-2. Likewise, FLIM images were analysed and the average lifetime was calculated using TRI2 FLIM analysis software (courtesy of Paul Barber, Grey Cancer Institute, Oxford). A bi-exponential model was used to fit the fluorescence decay curves for each point and then averaged for each tissue zone (caries-infected, -affected and sound dentine tissue). Then the percentage change in

intensity and lifetime were calculated for each point measurement using the following equation:

$$((Xa - Xb) / Xb) \times 100\%$$

Where Xa refers to after storage, Xb before storage which have been recorded in the chapter 2.

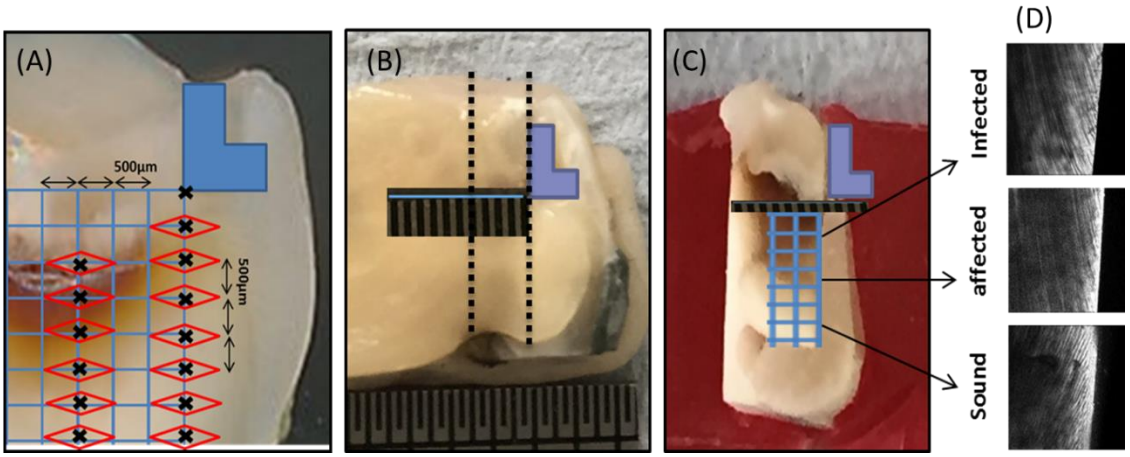

Figure 4-1. Experimental design for the sample preparation (A) previously recorded points including the carious zones and the sound controls points before storage. (B) Sectioning of the sample through the dentine/ restoration interface that was positioned at the carious line. An additional cut was applied through the sound internal control dentine/ materials interface points that was selected away from the caries line and based on the reference angle.

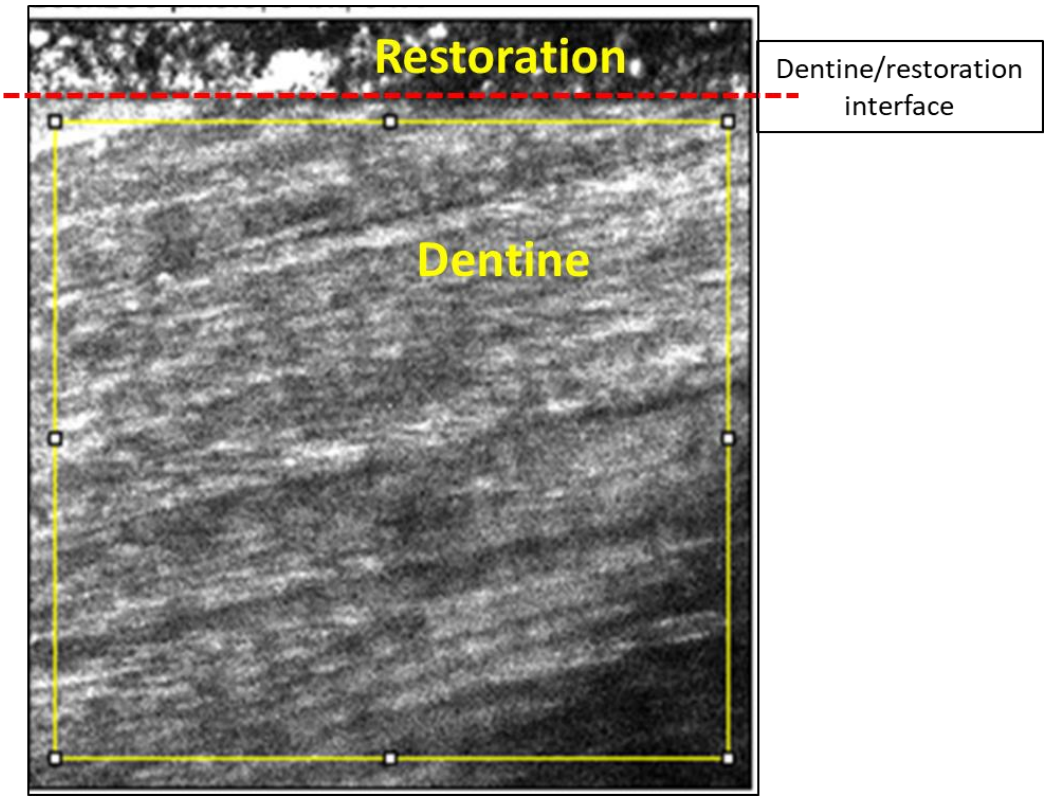

Figure 4-2. Representative AF image showing how to select the dentine for intensity measurement using Image J software excluding the restoration from the analysis.

- **Knoop microhardness measurement (KHN)**

Following the two-photon and lifetime imaging recording, samples were re-evaluated using 40x 0.65 NA objective and recorded using a Struers Duramin microhardness tester (Struers Ltd., Denmark). The same setting and applied forces used before storage were readjusted. The hardness number was calculated using the manufacturer's software. Percentage change was calculated for each point using the same equation applied with the two-photon results for adequate comparison. After that, these measurements were allocated to the previously recorded points at the different carious zones. Samples were rinsed and ultra-sonicated for 3 minutes for the next imaging technique.

- **Raman spectroscopy and analysis**

Following two-photon and hardness evaluations of the interfacial dentine, Raman spectroscopy was used to quantify the mineral change in the different dentine tissue zones after storage with the applied materials. A Renishaw in Via Raman

microscope (Renishaw Plc, Wotton-under-Edge, UK) in StreamLine™ scanning mode was used with the scanning parameters specified in (Chapter 2, Methods 2.2.1). Calibration of the spectra was done before every use by taking a spectrum for reference silicon samples. Prior to Raman measurements, each sample was focused, and the dental interface was positioned parallel to the horizontal line of a crosshair pointer and a montage image was created using the charge-coupled device (CCD) camera. Using a 20x 0.40 NA air objective, this interface was scanned using a 785 diode laser (100 mW laser power), and to obtain the Raman signal, a 600 lines/mm diffraction grating was used and centred between 849 cm-1 and 1603 cm-1, with 2 seconds CCD exposure time. As this method was used to detect the change in mineral peaks, samples were positioned to acquire the signals along the interface with inter-spectrum distance of 2.7 μm in (Y) axis (covering the previously recorded caries zones by two-photon and hardness based on the reference point) and 50 μm from the materials toward the dentine in X axis. In-house curve-fitting software was used to fit the acquired Raman spectra. Then, using the Raman software, grey scale images and phosphate peak intensity depth profiles were generated at 959 cm^{-1} ($PO4^{-3}$ v1). A Gaussian function was used to fit the spectra a first order polynomial option in the analysis software. To measure and analyse the Raman intensity peak, a Tiff image of the peak height was moved into Image J software. An area of 500μm X 500μm was then selected starting from the reference point at the dentine / material junction and along the Y axis (excluding any material in the selected area). Each average peak intensity value of a selected area was allocated to the previously recorded intensity and hardness values of different caries zones (Fig. 4-3), and then were statistically analysed.

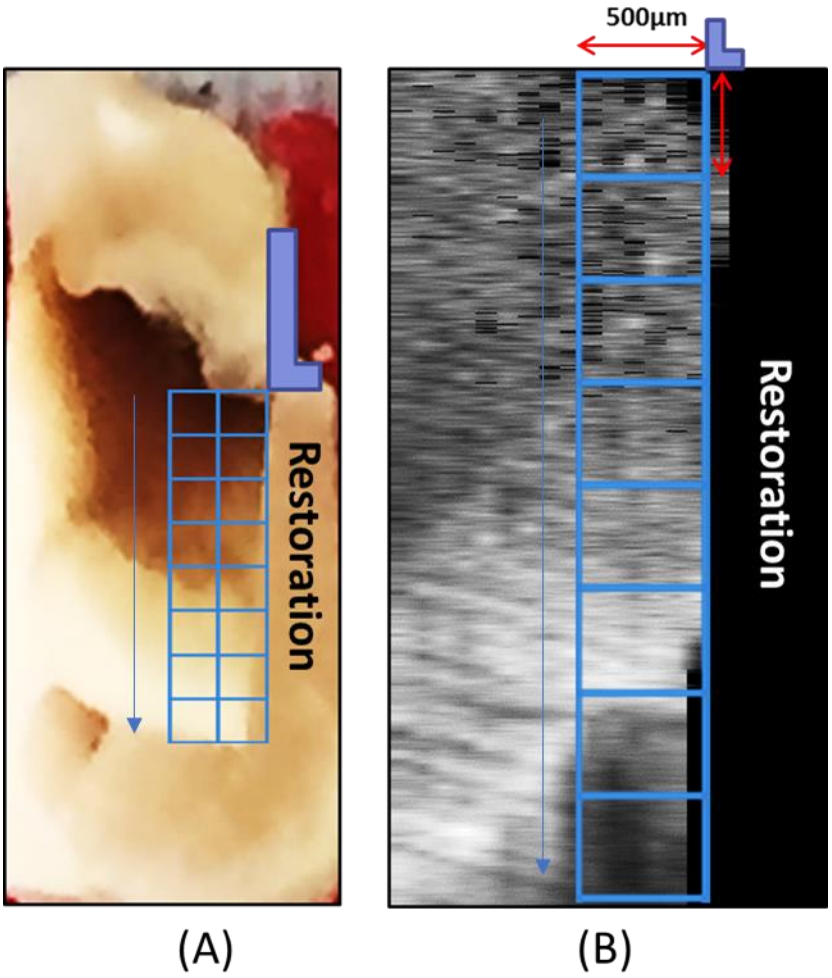

Figure 4-3. Sample preparation for Raman imaging showing (A) Representative clinical macrograph that show the selected area for Raman imaging including the different carious zones (infected, affected and sound dentine). (B) Montage image after Raman mineral peaks analysis.

4.2.3 Statistical Analysis

Multiple linear regression models were used to compare the effect of different applied materials and different tissue types on the intensity, lifetime and hardness number using the percentage change values and Raman peak intensity values after storage. All the analyses were carried out using Stata version 12.0 (StataCorp LP, Texas, USA).

4.3. Results

4.3.1 Carious zones characterisation using the two-photon microscopy

The carious zones were initially verified in chapter 2 using the laboratory “gold standard” KHN. Representative images of AF intensity and lifetime of different caries zones were presented in Fig. 4-4. AF intensity results indicated a

significant increase in intensity values from sound to infected dentine. On the other hand, FLIM decreases from sound to infected tissues, which is transferred from blue to more yellow/reddish toward sound tissues.

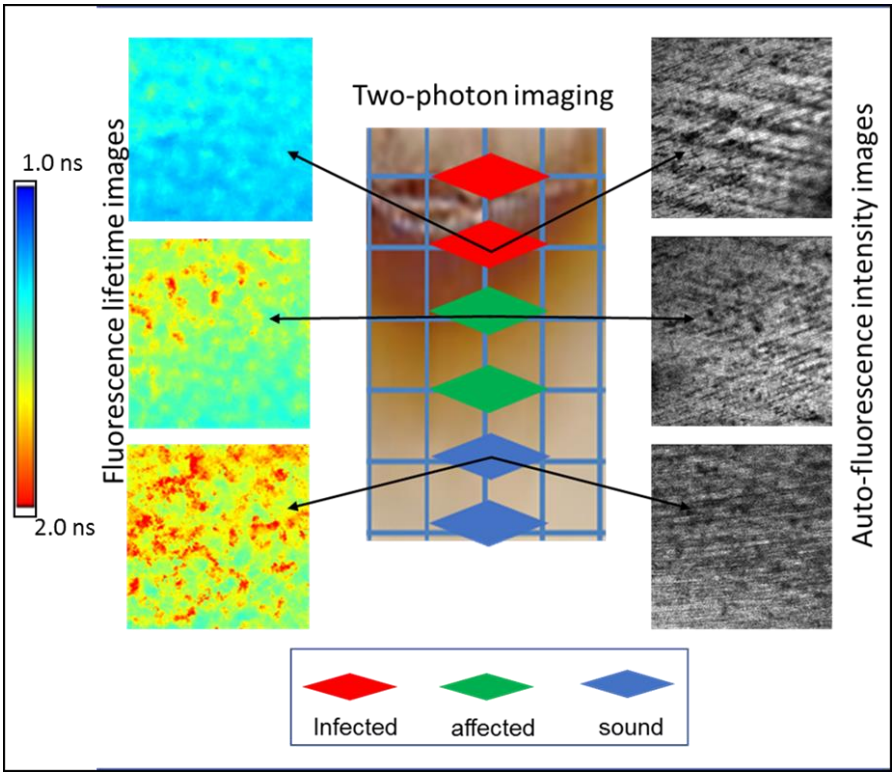

Figure 4-4. Representative AF, FLIM images of different caries tissue zones before materials application are showing the increase in redness from infected layer toward the sound dentine which become redder in colour. The AF image was brighter in the infected tissue than the other zones.

Following the storage with materials and re-evaluation of the same properties, calculations of the percentage changes for each technique and statistical analysis showed the following results:

A. Autofluorescence intensity AF (AU):

The comparison of the average percentage change in AF intensity of different materials/dentine interface, against the control (no material) of each dentine layer were presented in Fig.4-5

Caries-infected dentine (CID)

A significant increase in the percentage change of AF intensity in both DC-HRI (24%±16) and EQUIA (28%±17.5) groups compared to the control (-29%±7) group (p=0.047, 0.029 respectively). Bulk Fill intensity (-36%±13) showed a non-significant difference from the control group (p=0.9).

Caries-affected dentine (CAD)

Significant increase in %change was noticed in both DC-HRI (25.5%±18.7) and EQUIA (22%±10.4) from the control group (-20.5%±10.7), (p=0.047, 0.024 respectively). Bulk Fill group (-28%±5.8) group showed a non-significant difference from control group (p=0.9).

Sound dentine

No significant changes were noticed between all groups.

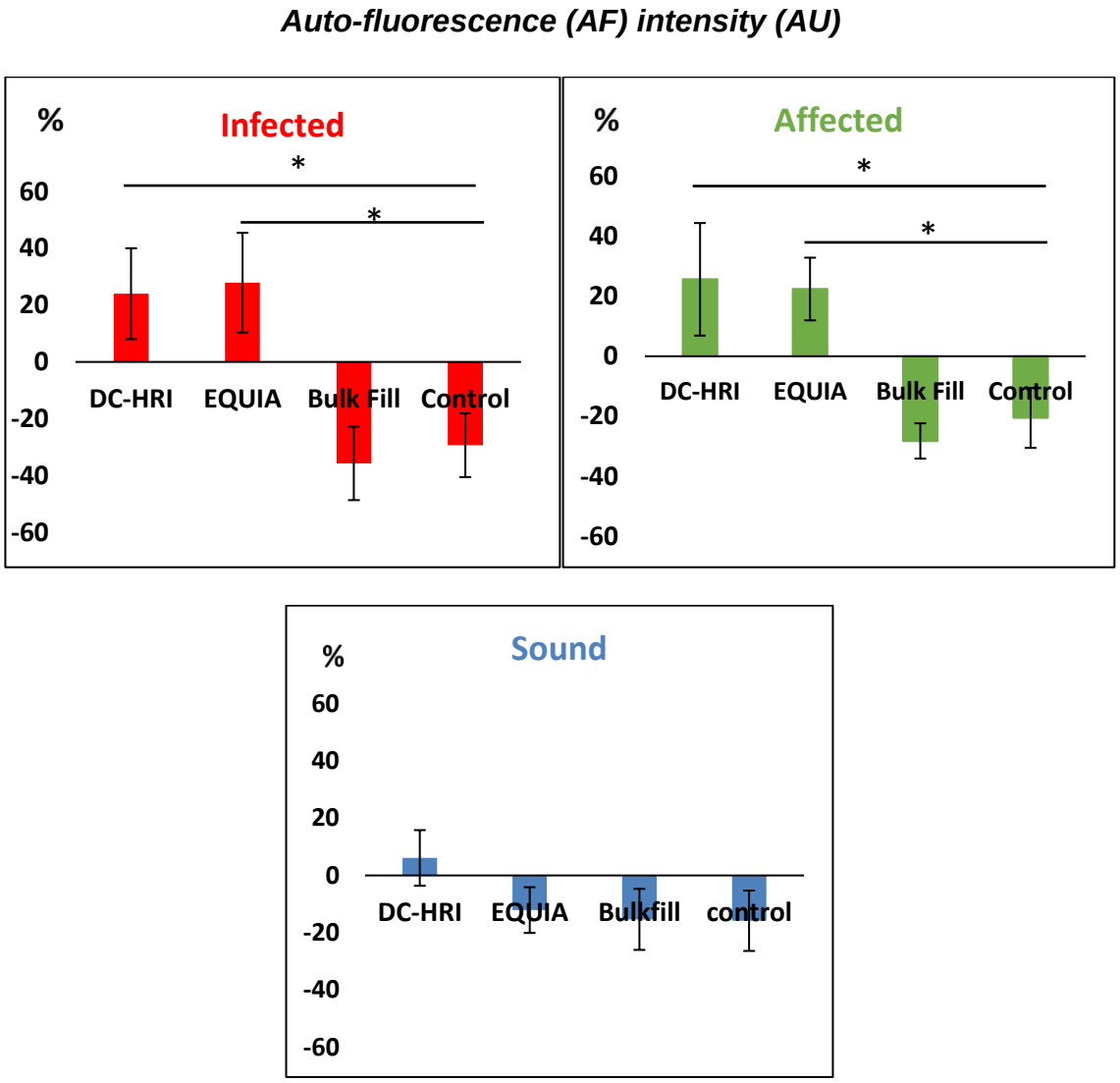

Figure 4-5. Graphs are showing the changes in AF intensity in the different carious zones (infected, affected and sound dentine). Significant increase in AF intensity was noticed in both infected and affected zones when bonded with DC-HRI and EQUIA against the control group as indicated using (*), with a decrease in Bulk Fill and control groups. However, a non-significant change was noticed with the sound dentine in all materials groups.

B. Fluorescence life time imaging FLIM (ns):

Caries-infected dentine

Generalised increase in the fluorescence lifetime of all materials groups was observed but this increase wasn't significant (Fig. 4-6) between materials and control groups (p=0.86).

Caries-affected and sound dentine

There were no significant changes noticed in both layers when bonded to all materials groups (p= 0.7).

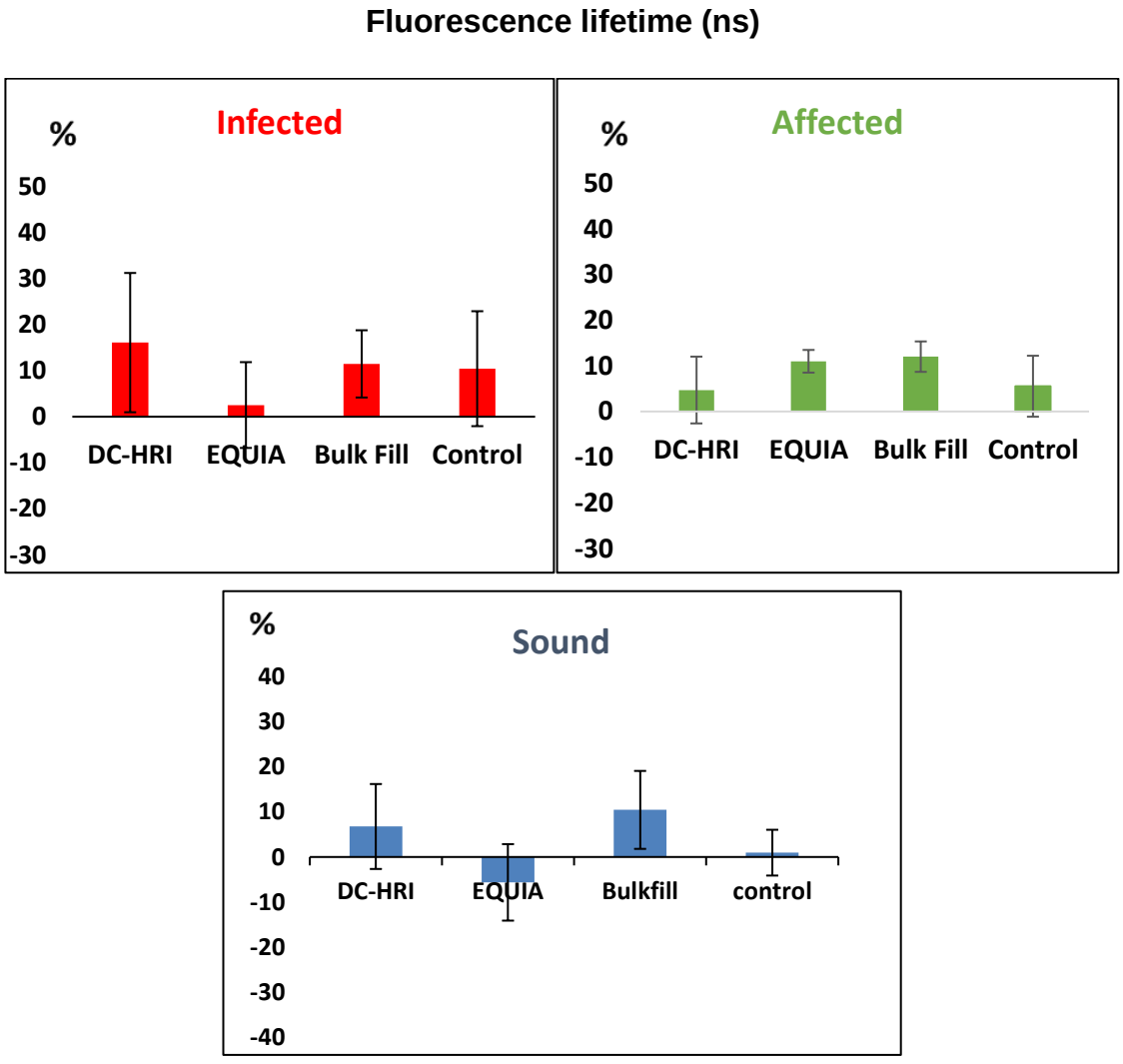

Figure 4-6. Graphs are showing the changes in FLIM in different carious zones (caries infected, affected and sound dentine). A non-significant increase in the lifetime was noticed among all dentine tissues when bonded to all materials group.

C. Second harmonic generation SHG (AU):

- General increase in the intensity of the infected dentine among all material's groups except the Bulk Fill group although these changes were not significant from each other (p=0.29).
- No significant difference between materials groups when bonded to affected and sound dentine (p=0.4).

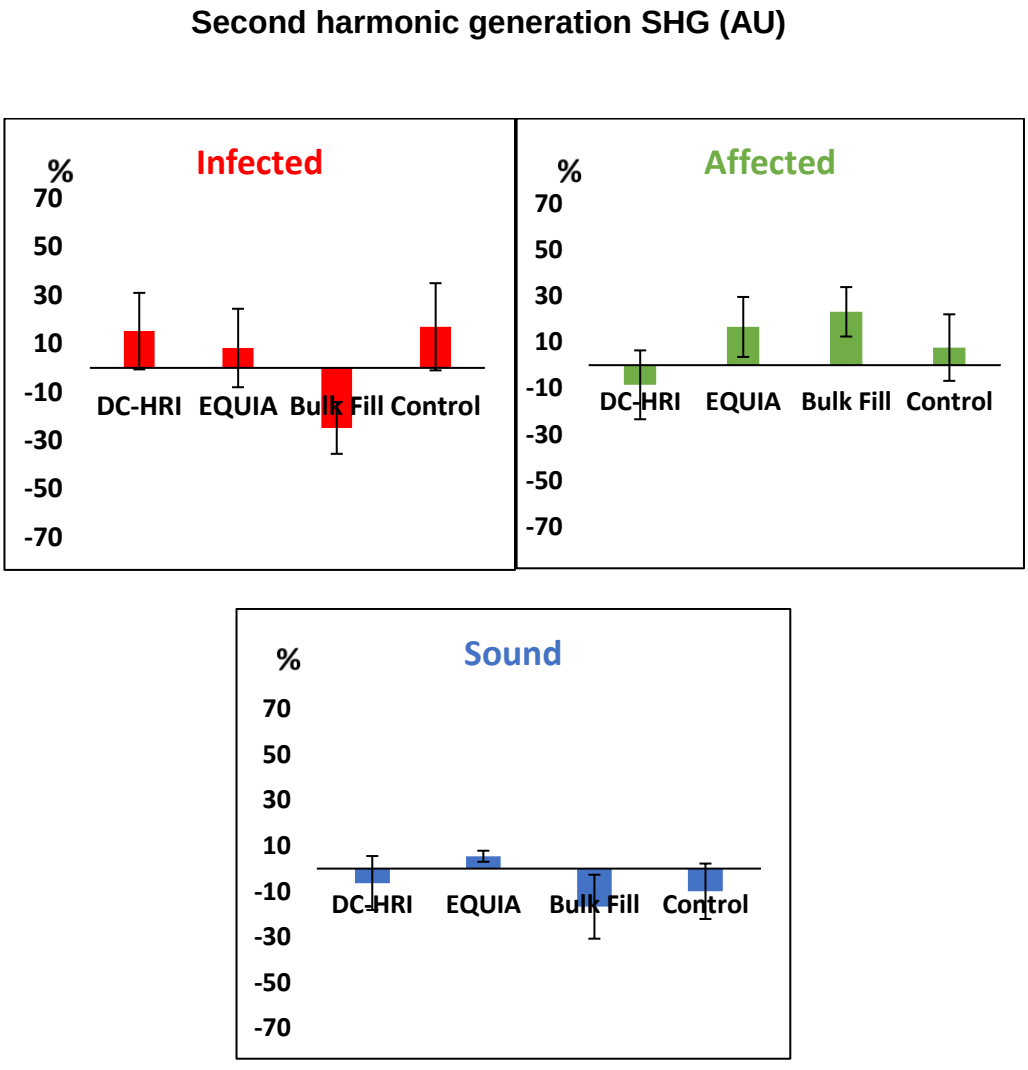

Figure 4-7. Graphs showing that there was no significant effect from different materials groups on the SHG intensity in all carious dentine layers.

4.3.2 Microhardness measurements

- Results showed a significant increase in the hardness of the infected dentine when bonded to DC-HRI and EQUIA (12.6±7, 17.7±4.6), (p=0.007, 0.001 respectively) compared to the control group (-11.14±2).
- No significant changes were noticed between the materials groups bonded to CAD (p=0.5).
- The sound dentine substrate showed a comparable decrease in the hardness in all materials groups with no significant differences from controls (Fig. 4-8).

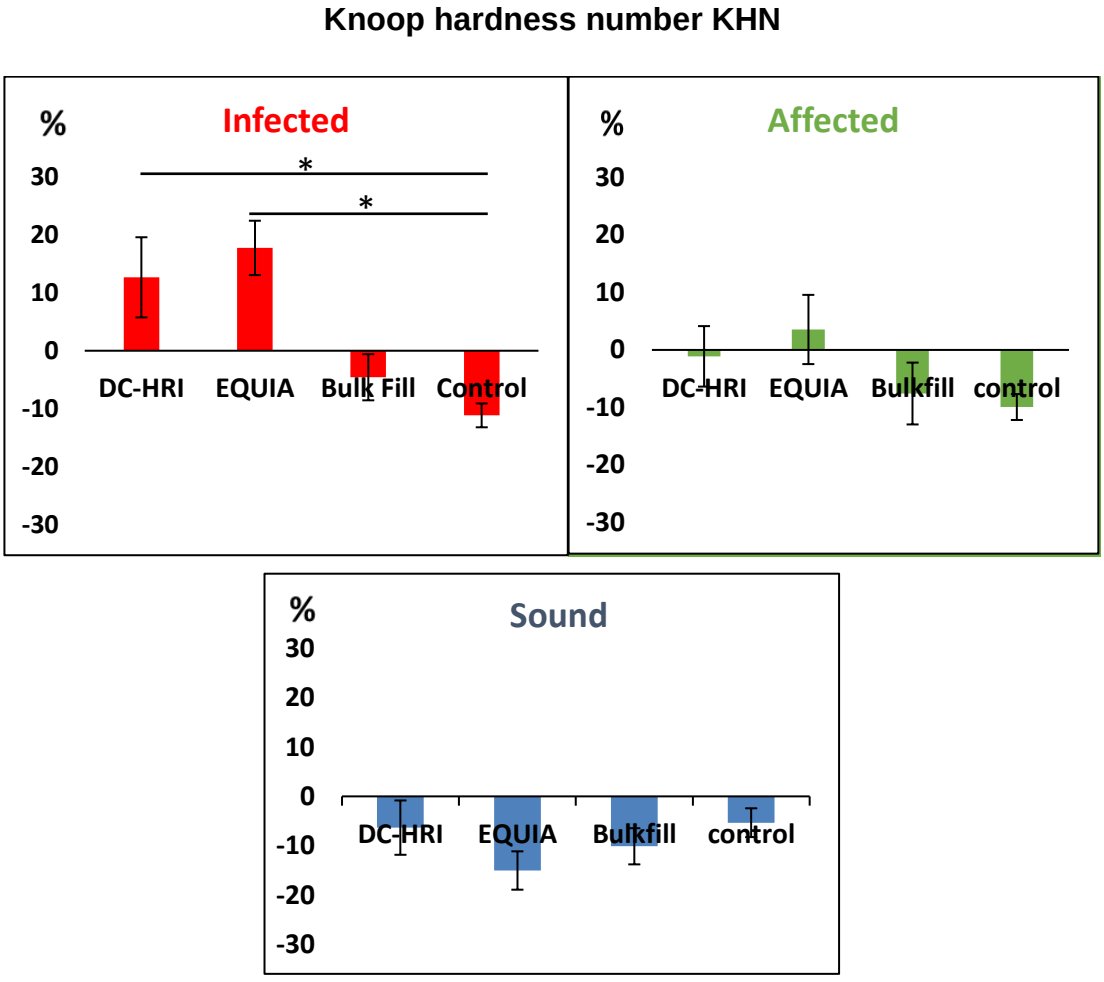

Figure 4-8. Representative graphs showed the percentage changes in the hardness of carious zones after storage with different restorative materials. The significant increase in hardness was only noticed in the caries infected dentine when bonded to DC-HRI and EQUIA. No significant changes were observed with the caries affected dentine substrate. However, decrease in hardness was noticed among all materials groups when bonded to the sound dentine. (*) denotes significant difference from control group. Error bars in al graphs represent standard error of means.

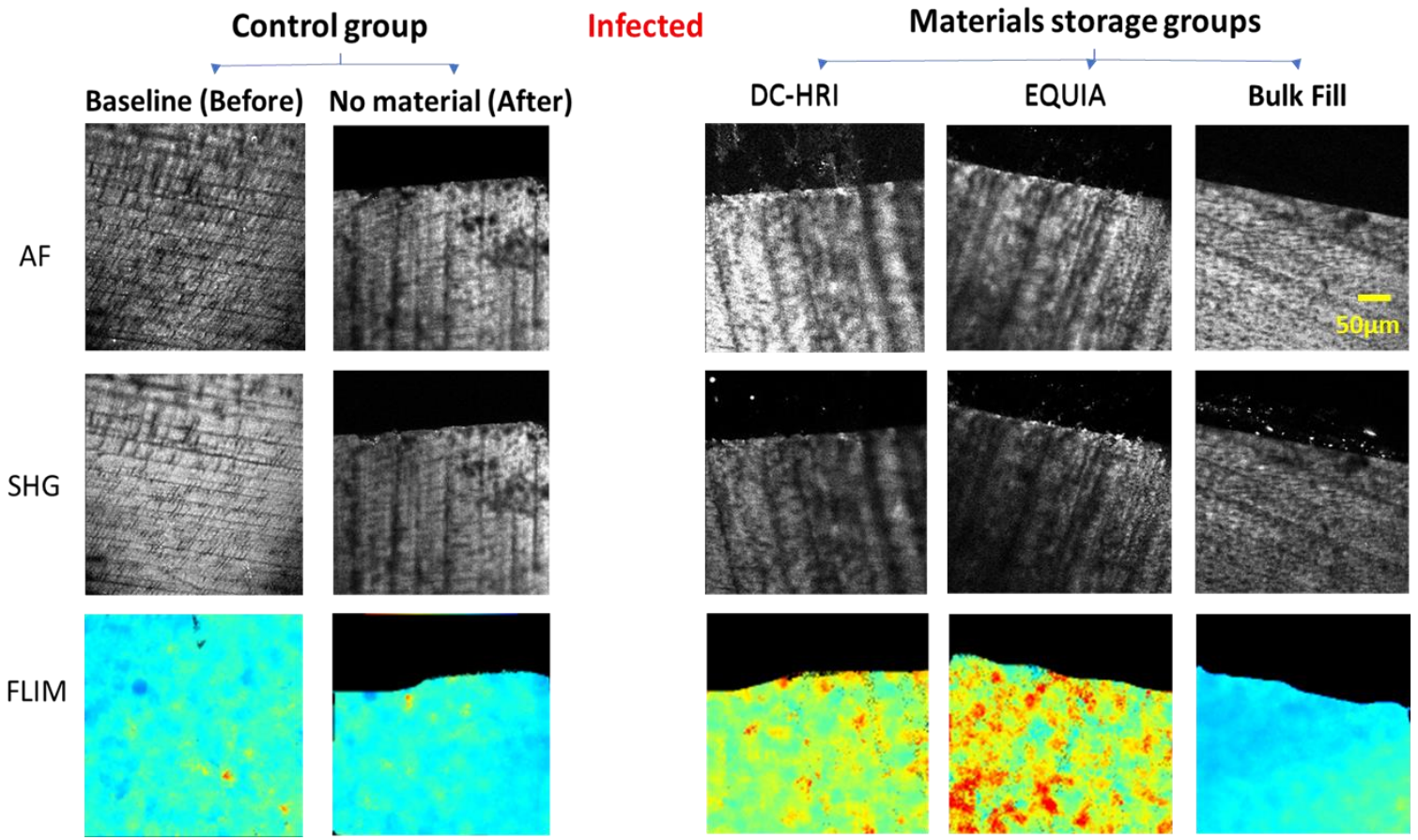

Figure 4-9. Representative two-photon imaging of the interface between caries-infected dentine/ DC-HRI, GIC and Bulk Fill composite. The figure compares baseline auto-fluorescence, second harmonic generation intensities and lifetime images for the caries-infected dentine before materials application with the after-storage images for each group (control, no material), (After storage material groups).

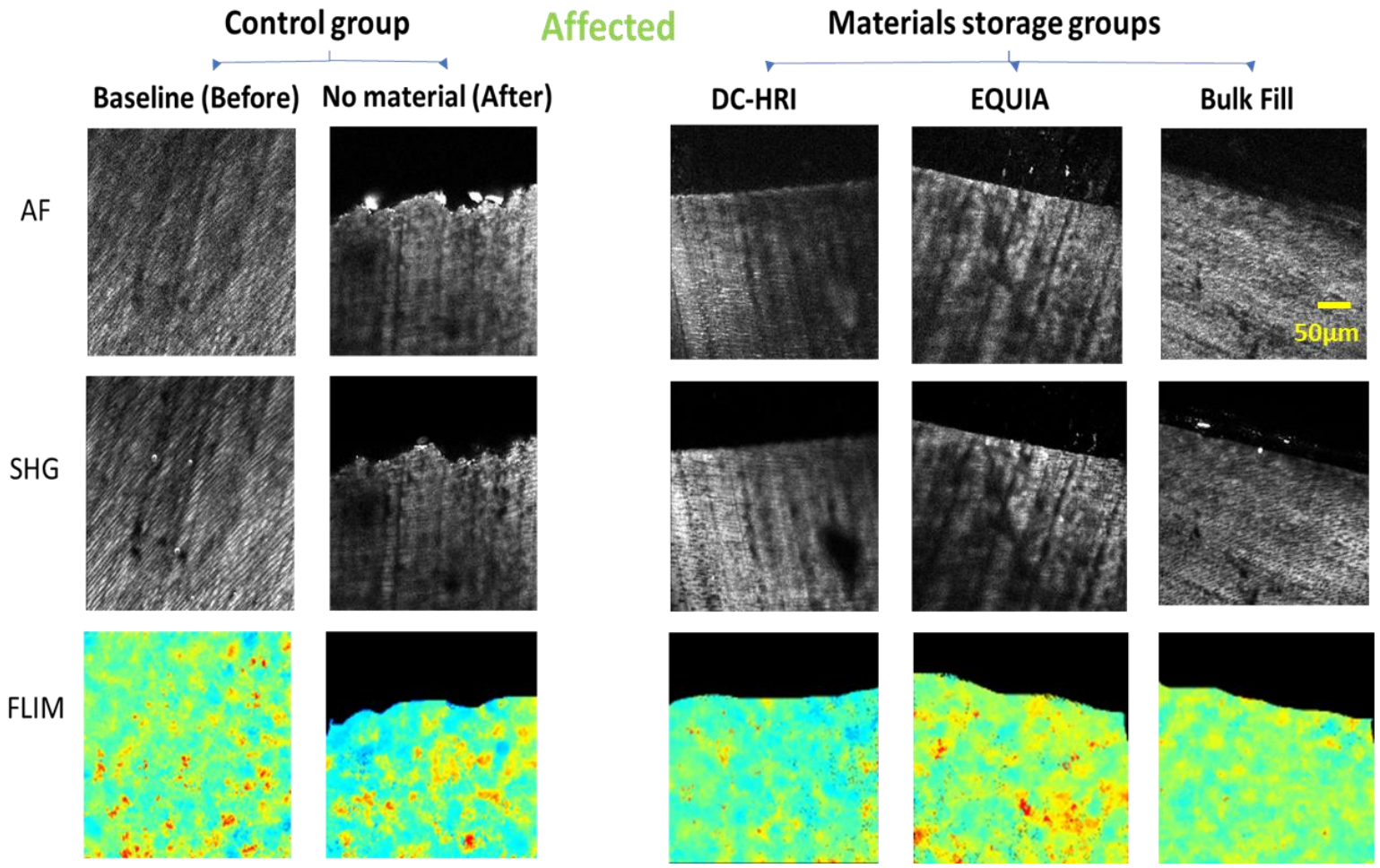

Figure 4-10. Representative Two-photon imaging of the interface between caries-affected dentine/ DC-HRI, GIC and Bulk Fill composite. The figure compares baseline auto-fluorescence, second harmonic generation intensities and lifetime images for the caries-affected dentine before materials application with the after-storage images for each group (Control (no material), (after storage group).

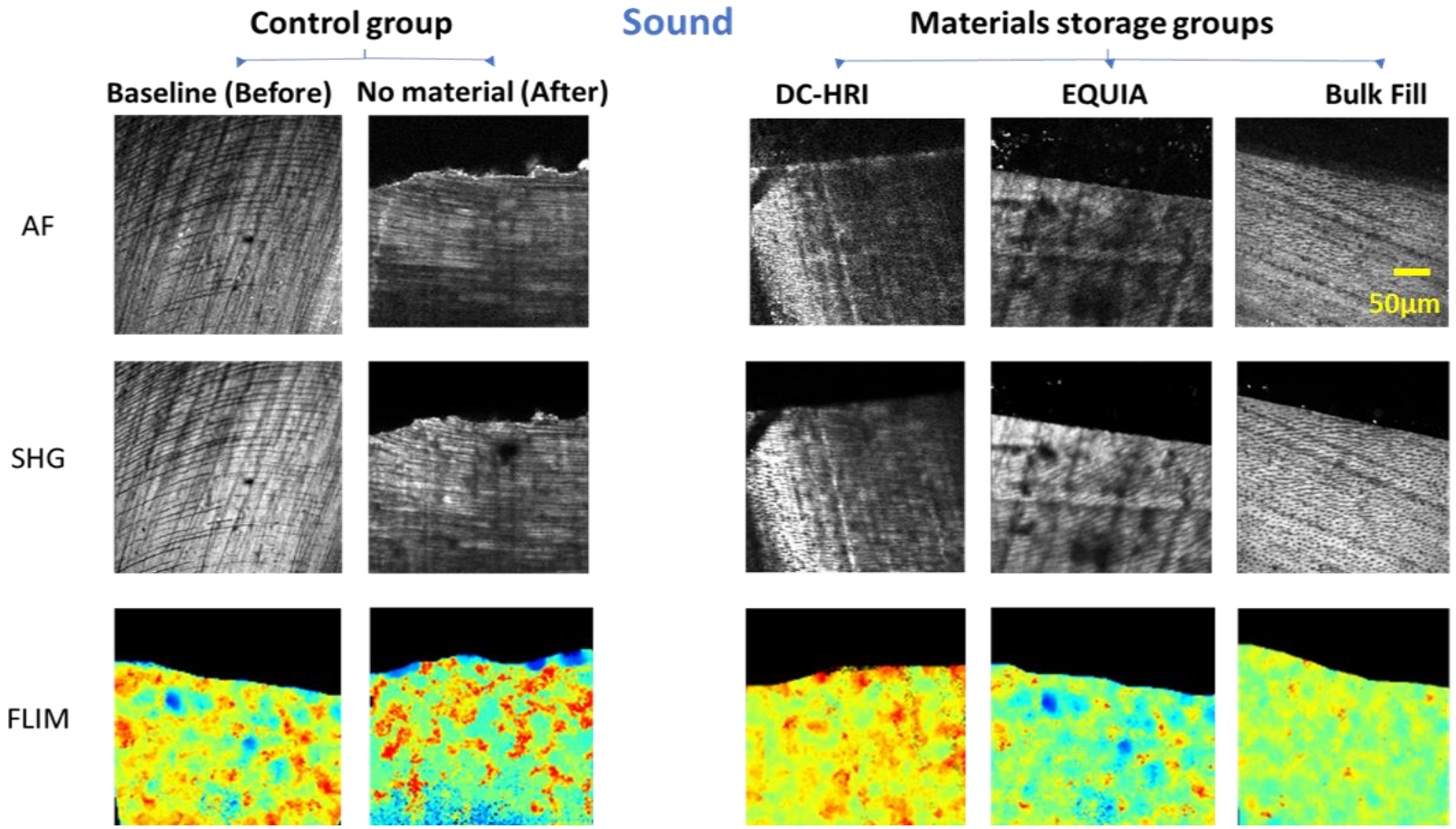

Figure 4-11. Representative Two-photon imaging of the interface between sound dentine/ DC-HRI, EQUIA and Bulk Fill composite. The figure compares baseline auto-fluorescence, second harmonic generation intensities and lifetime images for the sound dentine before materials application with the after-storage images for each group (Control (no material), (after storage group).

4.3.3 Raman Spectroscopy

Caries-infected dentine:

The EQUIA group revealed the highest intensity values among all other substrates (133 AU± 12), (p=0.001). Then, DC-HRI and Bulk Fill groups presented similar values (105 AU± 6, 105 AU± 12) which were higher than the control group (70 AU± 6) (p=0.05).

Caries-affected dentine:

DC-HRI and EQUIA reported higher intensity values (170.5 AU± 9.6, 180 AU± 9 respectively) compared to the control group (135.2 AU± 7) (p=0.025, 0.003). significant differences between the material groups were observed (p=0.001).

Sound dentine:

DC-HRI and EQUIA groups recorded the highest intensity values (189.4 AU± 20, 194 AU±23 respectively) compared to the other groups. Bulk Fill showed a comparable value (160 AU± 5.4) to the control group (153 AU± 8.4).

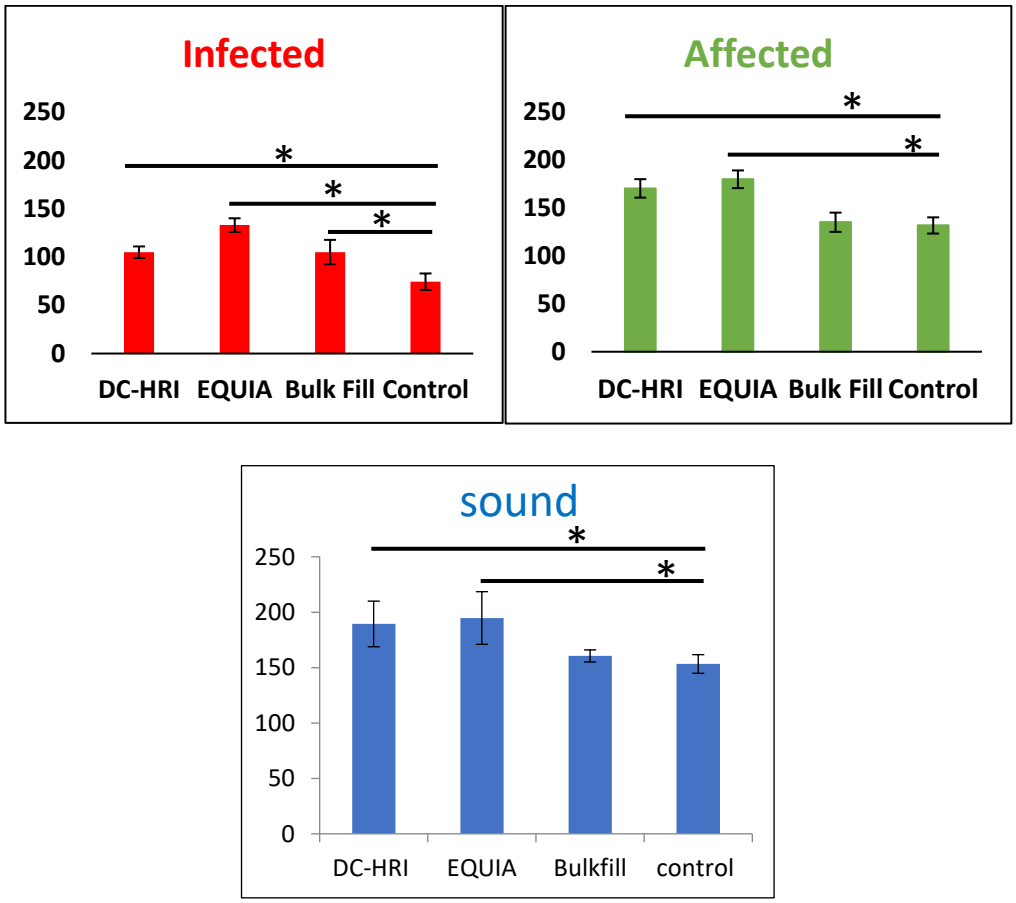

Figure 4-12. Graphs showed Raman intensity values of different dentine carious zones. DC-HRI and EQUIA recorded the highest intensity among all substrates, while Bulk Fill showed comparable intensity values to the control groups (*) denotes significance from control group.

4.4. Discussion

In the current study, the interaction of the experimental restorative material DC-HRI with non-excavated carious dentine layers has been compared to that of a restorative GIC (EQUIA Fill, GC, Japan) and a resin composite material (Filtek Bulk Fill, 3M, USA). The carious lesion zones have been characterised and differentiated from each other in chapter 2, using advanced optical imaging techniques together with mechanical and quantitative chemical Raman spectroscopy analysis.

Clinically, the suggested protocol for carious tissue interfacial assessment helps in understanding the behaviour of the new restorative material when applied in deep carious cavities. Minimal invasive dentistry (MID) aims to preserve the partially demineralised CAD, providing an adequate seal of the lesion to arrest or rejuvenate these tissues following their interaction with the tested restorative materials. In addition, it should ideally provide a mineral supply and anti-bacterial properties as well as chemical or mechanical bonding to the remaining dentine (Banerjee, 2013).

GICs have been the material of choice for MID, thus they have been used as a control material in this study to compare their effect to those obtained with the experimental material. In addition, the Bulk Fill resin composite is usually used as a posterior permanent filling material in deep cavities, bonded with Scotchbond adhesive, aiming to provide an adequate seal of the lesion and so was also used as a comparative material. The experimental material combines the properties of GICs and resin-based materials, providing a hybrid self-adhesive material with improved mechanical properties and wear resistance.

The unexcavated carious lesion model has been previously introduced and tested in an earlier study, to delineate between the carious tissue zones and their interaction with bio-interactive cements: Biodentine™ and GICs. Autofluorescence intensity and lifetime imaging techniques were used for these assessments, which were followed by the Raman spectroscopy and KHN evaluations. The results of that study confirmed the sensitivity and specificity of the tested techniques in determining the carious zones with a significant correlation between them. In addition, the bioactivity of both cements was verified by assessing the repair of the partially demineralised carious tissues (Sajini, S. 2016). Following a similar protocol in the current study, carious tissue characterisation of all samples was successfully achieved in the first experiment (chapter 2). The examined points were re-located based on a previously marked reference point, to re-evaluate the carious zone properties following interaction and storage with the applied restorative materials, using the same setup used in chapter 2. The techniques used in this study enabled quantitative evaluation of the samples with minimal sample preparation and stain-free imaging.

Moreover, samples in this study were stored in PBS. Earlier studies have confirmed the dentine ion uptake from the adjacent restoration when surrounded by phosphate-rich solution. Han et al. (2011) showed that both Biodentine and MTA have influenced the calcium uptake in the adjacent root canal dentine when stored in PBS solution (Han and Okiji, 2011). Several studies have reported the capability of MTA to form an apatite layer when in contact with phosphate-containing physiological fluids (Reyes-Carmona et al., 2009, Gandolfi et al., 2010, Han et al., 2010, Han et al., 2015). The dentine ion uptake was more prominent for Biodentine than MTA at 30 and 90 days (Goldberg et al., 2009). Further study has reported that the Biodentine is able to interact with dentine forming a mineralised interfacial zone, with dentinal tubule tags formation, in the presence of PBS (Atmeh et al., 2012, Han and Okiji, 2013). Such processes could be mediated by the formation of calcium- (or strontium in case of the GIC) containing minerals such as hydroxyapatite, in the presence of calcium (from the hydrated cement) and phosphate (from the PBS) under high pH conditions (Watson et al, 2014).

The design of the present study allowed a precise comparison to be made between baseline and 30 days storage data because samples were examined at the same location as measured before storage.

- **Caries-infected dentine (bacterially contaminated)**

The results of this study showed an increase in AF intensity of the infected dentine when bonded to EQUIA and DC-HRI materials, while a reduction in the intensity was observed when bonded to the Bulk Fill composite, which partially rejects the null hypothesis. This increase in intensity may signify changes in the dentine microstructure as it was associated with an increase in both Raman and KHN values. On the other hand, SHG intensity has not been influenced when bonded to any of tested materials.

As previously mentioned, the AF intensity is mainly influenced by changes in the dentine microstructure. Optical changes have been correlated to the change in the mineral content of the dentine in earlier study (Sajini, S. 2016). Results of the study presented in chapter 2 have shown an enhanced AF intensity associated with the infected dentine before the materials application, but this was associated with a reduction in KHN, indicating low mineral content compared to the sound dentine. Improvement of the AF intensity of CID was possibly attributed to the accumulation of porphyrin “cariogenic bacterial by-products” due to the dentine collagen breakdown during the caries process. As reported earlier in the review chapter (1.6.1), AF intensity can be originated from either organic or inorganic changes in the dentine structure. Foreman (1980) identified two fluorophores extracted from normal dentine and found that they are bonded initially to the organic constituent with possible secondary bonding to calcium (Foreman, 1980). However, an earlier study suggested that the dentine fluorescence may originate from inorganic complex with some organic components (Armstrong, 1963).

In the CID, the dentine microstructure has shown a complete degeneration of the collagen matrix and loss of minerals that can play as a nucleation site for further remineralisation. Previous studies have suggested that GICs can re-mineralise tooth tissues through epitaxial growth of the remaining crystals, when nucleation site pre-exist (Kim et al., 2010b, Atmeh et al., 2015). The fact that carious lesion can be arrested by a good cavity sealing is also very well documented in the literature (Corralo and Maltz, 2013, Chibinski et al., 2016).

When the AF intensity of the infected tissue improves after sealing with either EQUIA or DC-HRI, the only explanation for such outcome is related to mineral

changes as the collagenous part is completely degenerated and can't be restored at this substrate. Ionic interaction with the existing minerals remained following the dentine degeneration by the caries process is possibly suggested. Hence, an active interaction between both DC-HRI and EQUIA and the infected dentine tissue may follow. This interaction was expressed further as a significant increase in KHN and Raman mineral peak intensity % change values of both DC-HRI and EQUIA groups. The reported increase in the phosphate mineral peaks and regain the tissue hardness confirmed the mineral gain from adjacent materials. However, no ultrastructural evidence of mineral deposition or crystal formation could be detected in this experiment (Kim et al., 2010a).

Mertz-Fairhurst et al. showed that after a 10 years of complete sealing of soft, wet and demineralised dentine in the floor of the cavity, the carious lesion did not progress further or jeopardise the restoration above it (Mertz-Fairhurst et al., 1998b). This finding may indicate that microstructural changes in the infected dentine could occur when its properly sealed and hence the associated optical properties can be influenced.

An *in-vivo* study on partial caries removal in permanent teeth showed signs of carious dentine remineralisation following 60 days of sealing. These signs include dentine reorganization with intertubular dentine thickening and the formation of a dense collagen network, as well as reduction of the bacterial count following the sealing with GIC, calcium hydroxide cement or wax (Corralo and Maltz, 2013, Kuhn et al., 2014). Some authors believe that fluorine uptake from the GIC plays a role in the repair and the remineralisation of the carious lesion (Ferracane et al., 2010).

In contrast, some authors claim that the healing of the infected tissues was irrespective of the sealing material used, but was mainly influenced by the effective sealing of these tissues (Marchi et al., 2008, Corralo and Maltz, 2013, Kidd and Fejerskov, 2013).They provided evidence that dentine reorganization and mineral changes were irrelevant to the material placed in contact with the carious tissue, suggesting that the arresting of the carious lesion is a host-driven process, not a material-induced process. They claimed that the sealing of the cavity by any material isolates the bacteria from the oral environment and active biofilm, which in turn enables the regeneration from the dentine-pulp

(Schwendicke et al., 2015). Cavity sealing changes the environment of the lesion through stimulation of tubular sclerosis and reduces permeability of the dentine and amount of the viable bacterial in the lesion (Paddick et al., 2005).

These claims contradict present results as there was a significant difference between the materials groups, indicating the influence of the material interaction with this substrate. Such results reinforce the bioactive potential effect of DC-HRI and EQUIA materials in repairing or hardening of the infected dentine layer compared to the Bulk Fill composite group, despite the decrease in AF in Bulk Fill group which may reflect inhibition of caries process progression due to the adhesive mechanical interlocking between collagen fibrils.

GICs materials are known with their anti-cariogenic properties due to the sustained fluoride release and recharging ability from the surrounding media. It has been suggested that the GIC ionic uptake occurs as a result of an equilibrium-driven diffusion of aluminium, strontium and fluorine ions into the dentine matrix, which was depleted of Ca^{2+} ions (Ngo et al., 2006) . Therefore, our findings of the infected tissues interaction with GIC and the experimental materials agrees with this suggestion.

One can assume a similar increase in the FLIM results as AF increases, when the infected tissues interact with EQUIA and DC-HRI. However, the results showed non-significant difference between the FLIM data. This outcome may attributed to the quenching effect of the low pH induced by the high bacterial amount within the infected tissues. Such results have been reported in an earlier study by Gannot et al (2004). The decrease in pH values leads to a reduction in the fluorescence lifetime as observed in caries characterisation studies (Gannot et al., 2004). However, compared to the FLIM data before material application in chapter 2, infected tissues exhibited a shorter lifetime. FLIM data increased following the interaction with the tested materials, which may reflect a sign of improvement of these tissue after storage although this increase was not significantly different from the control group.

On the other hand, the significant decrease in AF intensity and hardness of the control group may be explained by the absence of the cross-striated banding pattern of collagen fibres due to the denaturation of collagen molecules.

Regardless of the mineral deposition by EQUAI and DC-HRI in the infected tissues, the characteristic of collagen fibres was not restored. Thus, no changes were observed in the SHG intensity of any materials groups.

The main difference between the present study and earlier studies is that the natural caries model evaluated in this study has included the infected dentine layer with no operative intervention. A clinical study has examined a similar model of deep caries sealing (including CID) in the primary teeth. Following 60 days of caries sealing, their results showed better dentine reorganization, substantial reduction in the number of bacteria, compact intertubular dentine and narrowing of dentine tubules when compared to the baseline data (Chibinski et al., 2016). However, similar results were also reported in previous studies when infected dentine was completely excavated (Massara et al., 2002, Wambier et al., 2007). Drastic reduction of bacterial count has been reported in the literature when a carious cavity is sealed irrespective of the materials used for sealing (Maltz et al., 2012, Corralo and Maltz, 2013). Quantitative bacterial count measurement lies beyond the scope of the present study. Current results based on the assessment of optical, mechanical and chemical changes in the dentine substrate properties, may also support the reduction in the bacterial counts. It can be assumed that both synergetic actions of the applied materials together with the proper sealing and decrease of the bacterial activity have positively influenced the properties of the infected dentine.

- **Caries-affected dentine**

CAD substrate differs in morphology and composition from the CID. A conventional remineralisation strategy relies on the epitaxial growth of the pre-existing apatite crystallites (Dai et al., 2011) which is regulated by the presence of non-collagenous proteins. The caries process is believed to induce the expression of organic matrix non-collagenous proteins. Therefore, CAD provided a suitable scaffold for a potential tissue healing due to presence of the residual minerals and the non-collagenous protein. Studies have shown the regulatory role of these proteins in dentine remineralisation as they are the key for the crystallites stability (Chen et al., 2015). Collagen scaffold maintains their banding pattern as in sound dentine, promoting crystal growth and remineralisation of the

organic matrix. (Ohgushi and Fusayama, 1975, Nakornchai et al., 2004). Based on the results of the present study, bonding of CAD to EQUIA and DC-HRI has resulted in a significant enhancement in AF intensity together with an increase in the Raman phosphate mineral peak intensity, compared with other materials groups. Such results may reflect the tissue repair of this partially demineralised substrate because of interaction with such materials. One can expect an improvement in the other examined properties, as the AF and Raman are quantitative measures when tissue remineralisations take place. However, no significant changes were noticed in FLIM and SHG intensity between materials groups which partially accept the null hypothesis. AF and Raman findings are comparable to optical results obtained with the same materials interaction with the *in-vitro* demineralised dentine model (chapter 3).

When samples bond to GICs, the release of fluoride and calcium/strontium ions due to acid/base chemical reaction of the GIC cement during setting provides GIC with the high potential for remineralisation of carious tissues (Ngo et al. 2006). Furthermore, an ion-rich layer may be involved in subsequent remineralisation of remaining apatite crystals within the CID tissue (Sennou et al., 1999).

In theory, phosphate-based monomers should be able to bind to collagen, such as those found in adhesive materials. Scotchbond adhesive incorporates a phosphoric acid monomer, 10-MDP, which has a potential for chemical bonding to the calcium ions (Yoshida et al., 2004) and induce nucleation and growth of apatite crystal (Hayakawa et al., 2004). However, there is no evidence on the contribution of raw methacrylate phosphate ester monomers biomimetic mineralization of type I collagen. It is documented that phosphate esters (as those found in DC-HRI) with a negative charge, bind to the collagen gap zones with a positive charge to form a negatively charged surface which promotes mineralisation by establishing local ion supersaturation (Hartgerink et al., 2001). This interaction may simulate the interaction of the phosphoric acid ester monomer of the new experimental materials with the dentine collagen, especially when they stored in a phosphate containing media. Similar reactions were explained in an earlier study stating that “when the phosphorylated collagen was

incubated in the simulated dentinal fluid (SDF) solution, the phosphate groups from the monomers initiated the mineral nucleation by attracting positively charged calcium ions in SDF" (Nurrohman et al., 2015). Therefore, calcium and phosphate will be consumed spontaneously and grow around the nuclei of the collagen fibres when they incubated in SDF.

- **Sound dentine**

Based on current results, the interaction of the tested materials with sound dentine has resulted in non-significant changes in their optical, chemical or mechanical properties examined, which indicates a minimal effect of the tested materials on the fluorescence and mechanical properties of the sound dentine. However, another study reported a degradation of the sound dentine when they interact with the calcium silicate cements due to their caustic effect and high alkalinity which indicate their adverse effect on the integrity of the dentine collagen matrix (Leiendecker et al., 2012).

In conclusion:

- The combined techniques have provided an effective protocol to study the changes in optical, chemical and mechanical properties of caries zones and sound dentine, following the interaction with range of highly viscous restorative materials.
- Results have confirmed the potential bioactive action of both DC-HRI and EQUIA when bonded to CID and CAD.
- Results confirmed the significant increase in AF and mineral intensity when interacting with these materials compared to the control with no materials. Such a finding may be due to the collagen structural changes when attached to apatites, which is associated with the improvement in the mechanical behaviour of these substrates.
- Simple precipitation of minerals within tubules is most likely insufficient. Instead, intrafibrillar mineralisation and restoration of intertubular and peritubular dentine seem far more important.
- Further analyses are required to evaluate the source of the observed mineral gains. Moreover, analytic systems which allow repeated measurements (e.g., wavelength-independent microradiography, μCT) could be advantageous.

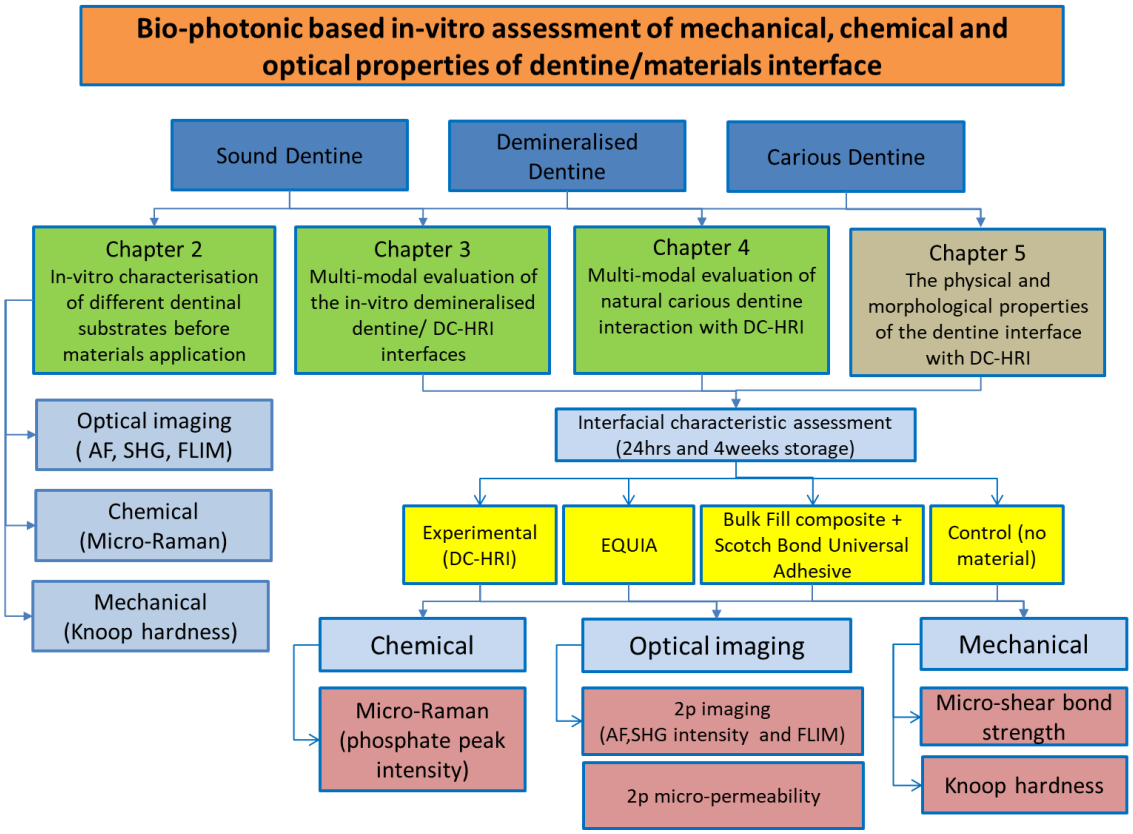

Chapter 5. The physical and morphological characteristics of the dentine interface with a novel dual cure hybrid resin ionomer (DC-HRI)

5.1 Introduction

Resin-based dental restorative materials are in continuous progression in their chemical composition, in order to overcome their inherent polymerization shrinkage, optimise the bond to dentine and to simplify their application procedures. In addition, there is an increasing interest in self-adhesive restorations since there is a reduced need for pre-treating the tooth surface to attain adhesion, as well as the operator benefits of single step application.

As mentioned earlier, glass-ionomer cements (GICs) have unique properties that make them useful as restorative and adhesive materials; their ability to adhere to moist tooth structure and base metals, anticariogenic properties and low toxicity. However, RMGICs were introduced to offset the downsides of GICs such as poor aesthetics, early reduced mechanical properties, early moisture sensitivity, lack of toughness and wear resistance and their elongated setting time. In addition,

they aimed to maintain their clinical advantage of adhesion to tooth structure, fluoride release and aesthetics.

As discussed in previous chapters, recent innovations have introduced an experimental self-adhesive restoration, RMGI bulk-fill derivative that is convenient to place and adapt, with one-step application. Based on the performed optical and chemical evaluation results, this material as well as GICs have shown some potential of reactivity when bonded to both carious and partially demineralised dentine substrates.

Mechanical testing has been used to evaluate and predict dental material performance and longevity. However, it has been difficult correlating laboratory tests with clinical performance and despite the plethora of *in-vitro* tests that have been performed, there are no truly predictive tests of long-term clinical performance (Green and Banerjee, 2011, Dennison and Sarrett, 2012).

To some extent, one can predict aspects of the longevity of a restoration by assessing its adhesive ability and this can be evaluated by bond strength testing (Sirisha et al., 2014). Several testing methodologies have been used to assess the interfacial bond strength between dentine and different restorative materials (Yang et al., 2006, Armstrong et al., 2010, Bonifácio et al., 2012, Ilie et al., 2014, Stefaneli Marques et al., 2018). It can be measured using either macro- or micro-tests, depending on the area of the tested interface. A micro-shear test was used in the study proposed by (Shimada et al., 2002) allowing simpler specimen preparation, with a reduced risk of sample damage during thin stick preparation as is the case for the micro-tensile testing. However, the methodology itself can be challenging when using relatively viscous materials during sample preparation.

The durability of the bonded restoration could also be affected by the nature of the dentine substrate: whether it is sound, demineralised or carious (Nakajima et al., 2011, Costa et al., 2017). A number of studies have confirmed the lower bond strength to CAD compared to sound dentine, though some of these bond strength values were found to be clinically acceptable (Ceballos et al., 2003, Rocha et al., 2014, Ekambaram et al., 2015, Follak et al., 2018a). However, some studies

found that bonding to CAD did not jeopardize the bond strength in comparison to sound dentine (Alves et al., 2013, Suzuki et al., 2013). For this reason, to overcome the variation in the results between studies, creation of CAD artificially in a standardized laboratory model might represent an important contribution to *in-vitro* studies.

Several models of artificial carious lesion formation have been used to improve the understanding of caries pathogenesis, preventive treatment, caries removal, and the adhesive efficacy of restorative materials (Joves et al., 2013). These methods can be chemical (pH cycling and acidified gel) or microbiological (bacterial) methods (Marquezan et al., 2009, Yu et al., 2017). They have aided the assessment of adhesion properties to dentine (Garcia-Godoy et al., 2010) or the physical and mechanical properties of human dentine (Gopalakrishna, 2009). However, acid etching using 37% phosphoric acid (PA) has been used frequently as a method to facilitate bonding to both enamel and dentine, yielding a simple demineralised model, with partial removal of mineral from inter-tubular and peritubular dentine and exposing collagen fibres (Perdigão and Lopes, 2001). It can be used as a standardised method for testing a new material. Thus, the choice of dentine demineralisation depends on what the aim of the investigation is.

Clinical problems such as micro-leakage and fluid influx can be prevented by effective sealing and intimate bonding at the tooth-restoration interface (Carvalho et al., 2012). This can be evaluated by different laboratory methods including nanoleakage, micro-leakage and micro-permeability. A direct reflective technique using two-photon fluorescent label assisted micro-permeability assessment was used in this study.

Aims:

1- Evaluate and compare the interfacial properties of a new experimental dual cure hybrid resin-ionomer DC-HRI (3M) material with dentine, to those achieved with conventional GICs, EQUIA Fill (GC) and Filtek™ Bulk Fill composite bonded with Scotchbond™ Universal adhesive (3M).

2- Examine the effect of bonding to different dentine substrates; sound, demineralised and natural caries-affected (CAD) dentine on the bond strength results.

3- Assess the change in the bond strength values following storage.

These could help predict the adhesion performance and short-term deterioration of the new restorative material. These evaluations and assessments were carried out using micro-shear bond strength testing (μSBS) and the two-photon excitation microscopy for morphological evaluation.

The null hypotheses were that:

(1) There is no difference in the bond strength between the substrates (sound, demineralised, CAD).

(2) There is no difference between the tested materials in bond strength to these respective dentine substrates.

(3) Aging of the dentine/restorations interface has no influence on their bond strength.

(4) There is no difference in morphology of these respective interfaces.

5.2 Materials and Methods

5.2.1 Micro-shear bond strength test (μSBS)

- Sample selection and preparation

A total of 90 teeth were utilised in the micro-shear bond strength evaluation, with 270 flat dentine slices**.** Sixty extracted sound human molar teeth and thirty carious teeth were collected using ethics approved by NHS Health Research Authority (Reference 16/SW/0220) and refrigerated in deionised water within one-month post-extraction. The roots of all teeth were sectioned transversely below the cemento-enamel junction using a slow-speed (300 rpm) water-cooled diamond wafering blade XL 12205, (Benetec Ltd, London, UK). Each tooth was sliced mesio-distally to obtain 2mm-thick dentine slabs which were distributed randomly into three major groups; sound, demineralised and carious dentine groups (n=30 each group). Teeth selected for the carious bond test group, contained a coronal "moderate" carious dentine lesion, surrounded by healthy dentine, limited to the occlusal surface and extending halfway from the enamel-dentine junction to the pulp chamber. The selection of these samples was judged after sectioning through the lesions. All dentine slabs were polished using 600-grit silicon carbide (SiC) paper for 60 seconds (Tedesco et al*.*, 2013), to standardise the smear layer and then sonicated for 3 minutes. To localise the CAD, random selected points using the Knoop hardness test was measured with hardness number range from 25-40 as shown in Fig. 5-1. The dentine surface was covered by an adhesive yellow vinyl tape (1231-8767, Fisher scientific, Laboratory equipment supplier in Loughborough, England) having an exposed window of CAD (1.6-mm in diameter). Each group was further subdivided based on the material used; DC-HRI, EQUIA Fill and Filtek Bulk Fill composite with Scotchbond Universal Adhesive (n=10). Micro-shear groups and number of samples are summarised in Table 5-1.

Table 5-1. Number of samples tested for micro-shear bond strength in each group

	Sound dentine **24h** incubation in PBS at 37˚C	Sound dentine **4W** incubation in PBS at 37˚C	PAE (37%)dentine (1min) **24h** incubation in PBS at 37˚C	PAE (37%)dentine (1min) **4W** incubation in PBS at 37˚C	CAD **24h** incubation in PBS at 37˚C	CAD **4w** incubation in PBS at 37˚C
DC-HRI	5	5	5	5	5	5
EQUIA Fil	5	5	5	5	5	5
Filtek Bulk Fill	5	5	5	5	5	5

PAE phosphoric acid etched dentine, CAD Caries affected dentine, PBS Phosphate buffered saline

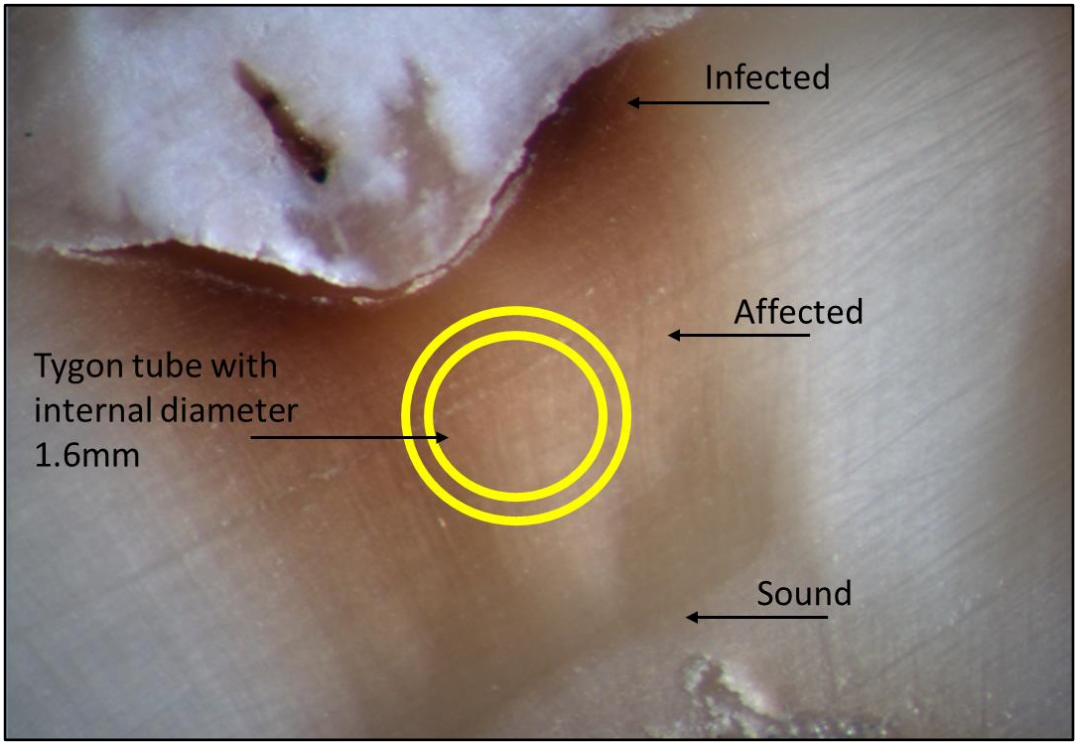

Figure 5-1. Representative sample for caries-affected dentine used in this study that previously was characterised by Knoop hardness test.

- Simple partial demineralised dentine model (phosphoric-acid etched dentine)

For the partially demineralised dentine group (n=30), dentine slabs were subjected to acid etching using 37% phosphoric acid gel for 60 seconds to create the partially demineralised dentine lesion (Gopalakrishna, 2009, Cao et al., 2013). Samples were then cleaned in an ultrasonic bath for 3 minutes.

- Bonding procedures and micro-shear bond test

Tygon tubing (Saint-Gobain, USA) with a 2-mm length and 1.6-mm internal diameter was placed over a pre-adjusted adhesive tape with a 1.6-mm width exposed window on the flat dentine surface and filled with the different materials as per the manufacturers' instructions (Fig. 5-2 a, b). All groups (n=10) were stored in phosphate buffered saline (PBS) at 37°C for 24 hours or 4 weeks before testing. The tubes were removed using a sharp scalpel (Swan-Morton, Sheffield, England) and any pre-test failures (PTFs) were recorded but not included in the statistics. Instead, percentage of failure was calculated and displayed in Fig. 5-4. The samples were fixed to the micro-shear test device using cyano-acrylate cement (Zapit, Dental Ventures of America, USA). The device was attached to a SMAC LAL300 linear actuator (SMAC Europe Ltd, Crawley, UK). The shear force was applied at a crosshead speed of 1 mm/min until failure occurred using orthodontic stainless-steel wire (0.2-mm in diameter) looped around the material cylinders (Fig.5-2, C). The micro-shear bond strength (t) in MPa was calculated using the equation:

$$t=F/(\pi R^2)$$

Where *F* was the applied load at failure and *R* was the radius of the material's cylinder.

- De-bonded failure mode evaluation

After de-bonding, the mode of failure was determined using a stereomicroscope (Kyowa Optical Co. Ltd., Tokyo, Japan) with x20 magnification. It was categorised into adhesive, cohesive and mixed failures (Armstrong et al., 2010). Representative samples (n=10) were selected randomly from each group and examined using a scanning electron microscope (SEM) (Hitachi S3500, Japan). Prior to the SEM evaluation, samples were air dried and gold sputter-coated at 45 mA current for 2 mins (Emitech K550, Kent,England). The samples were examined under a high vacuum with 10 KV at different magnifications (x30, x700).

Figure 5-2. Steps of micro-shear samples preparation and examination: **(a)** adjust the polyvinyl tubes on the flat dentine surface. **(b)** fill the tube with the tested materials as per manufacturer's instructions, then gentle removal of the tube following storage and directly before the test was performed. **(c)** fix the dentine sample on the metal jig and run the micro-shear test until failure occurs.

5.2.2. Sample preparation for two-photon microscopic interfacial evaluation

Roots were sectioned at the cemento-enamel junction level to expose the pulp chamber. Cervical cavities were prepared with dimensions 4x4x7mm using carbide flat end fissure and diamond burs in the buccal and lingual surface of a further fifteen sound molar teeth (Atmeh et al., 2012). Pulp tissue was gently extirpated from the pulp space. Then, samples were distributed into two groups for evaluation:

- **Morphological interface group (n=6)**

All tested materials were labelled with 0.025 mg of fluorescein powder (F6377 Sigma-Aldrich, Dorest UK) to evaluate the labelled materials' interaction with the dentine. The cervical cavities were then restored according to the manufacturers' instructions, one day before the test was conducted. Bucco-lingual sectioning was then performed to expose the dentine/restoration interface. Sequential polishing of the exposed surface using 1200, 2000, and 2500 SiC papers followed. Samples were sonicated with deionised water for 3 mins between grits and for 5 mins after final polishing.

- **Micro-permeability group (n=9)**

In this group, all the buccal cavities were previously etched using 37% phosphoric acid etchant gel for 1 min, to act as demineralised dentine model similar to those used in the micro-shear testing, while the lingual cavities were restored following the manufacturer's instructions (self-etch mode). The tested materials were labelled using 0.025mg of fluorescein powder and incubated in humid

environment for 24hr in PBS at 37˚C. On the day of imaging, teeth were inverted and mounted upside down in a water-filled container to keep the dentine wet, to a level not reaching the top surface of the exposed pulp chamber (Sidhu and Watson, 1998a). An aqueous 0.25% solution of rhodamine-B (R6626-Sigma-Aldrich, Dorset, UK) was injected into the pulp space using an endodontic syringe until the level of the dye was well above the level of the restoration and left for 3 hours before the specimens were sectioned. Dye solution was injected periodically while it was being taken by the dentine tubules or by the restorative material. After being stained, all samples were removed from the wet medium and the dye was thoroughly rinsed by water from the pulp chamber. The teeth were then sectioned longitudinally through the restorations, with a slow-speed diamond saw running under water (Benetec Limited, London, UK) (Fig.5-3 a, b). Each half was gradually polished using 1200, 2000, and 2500 grit SiC papers for 30 seconds each and ultra-sonicated with deionised water in ultrasonic bath cleaner for 3 mins in between and 5 mins after final polishing to remove the loose debris from the sectioning and polishing process. Samples were transferred for two-photon imaging for qualitative evaluation of their interfacial morphology.

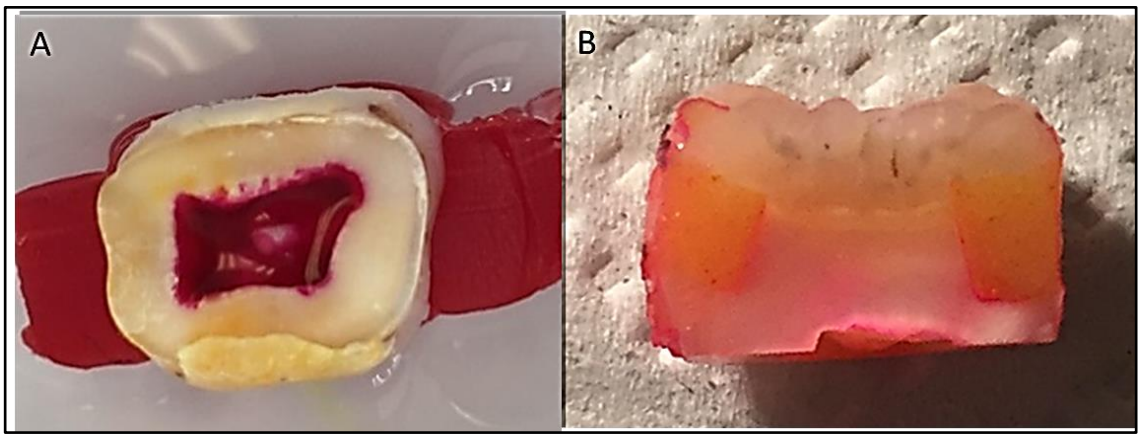

Figure 5-3. Micro-permeability sample preparation; following cavity restoration with fluorescein labelled restorations for 24hrs before imaging. (A) injection of an aqueous solution of rhodamine B into a cleaned pulp chamber of up-side down mounted restored teeth, it was left for 3 hours before sectioning. (B) Bucco-lingual sectioning through the dentine material interface and polished with serial SiC papers (1200, 2000, and 2500) and ultra-sonicate for 3 mins in between and 5mins after final polishing.

- **Pilot study (n=4)**

In this group, eight cavities were prepared on four teeth including mesial and distal cavities in each tooth. Mesial cavities were restored by DC-HRI and distal cavities were filled by the light cured resin modified glass ionomer cement (Fuji II LC, GC Corp., Tokyo, Japan) according to manufacturers' instructions to compare the micro-permeability of these materials. The tested materials were labelled as mentioned in the previous section.

5.2.2.1 Two-photon imaging

An in-house built two-photon fluorescence microscope with a Nikon inverted fluorescence microscope base (Eclipse Ti, Nikon, UK) was used for permeability evaluation. It had a repetition rate of 80 MHz and pulse width 140 fs with tuneable wavelength (between 680-1080nm) Ti: Sapphire pulse laser (Chameleon vision2, Coherent UK Ltd, Ely, UK). The infrared two-photon signals were detected using a photomultiplier tube (PMT) (HPM-100-40, Becker & Hickl, Germany), using a 40x 1.4 NA oil immersion objective lens (Nikon UK Limited, Kingston Upon Thames, UK), with cover slide glass 20x22cm. 854 nm excitation, 510 ±42 nm emission filters for fluorescence, 1020 nm excitation, 510 ±42 nm emission for second harmonic generation (SHG) and 790 nm excitation, 650 ±40 nm emission were used for rhodamine-B uptake evaluation. The obtained images were analysed and montaged using ImageJ software (ImageJ, Wayne Rasband, NIH, USA).

5.2.3 Statistical analyses

A linear model (regression model) was used to test the effect of materials, substrates and time on bond strength. The model was used to find out the significant predictors of strength. The p values given for the linear combinations were not adjusted for multiple comparisons. The normality of the outcome was checked using histogram, boxplot and Shapiro Wilk's test. Since the outcome was not normal, the values were log transformed and the transformed data were used for the analyses. The initial model included the main effect of material, substrate, time and the interaction terms between material and substrate, material and time, substrate and time. Only significant interaction terms were included in the final model along with the main effects. Further post hoc analyses were then carried out to find out which combination was significant. The

significance was assumed at 5% level. All the analysis was carried out using Stata version 12.0 for windows (Statacorp LP, USA). Failure modes and pre-test failures (PTFs) of different substrates were presented using percentages (Fig. 5-4, 5) and were not included in statistical analysis.

5.3 Results

5.3.1 Micro-shear bond strength test

The results of the μSBS of all experimental groups and standard errors of means are summarized in (Fig.5 a, b). The pre-test failures (PTFs) percentages are presented in parentheses within the figures.

- **Time effect:** When considering the interaction between time vs. material type and time vs. substrate, the interaction effects generally were not statistically significant, (p=0.89 and 0.78 respectively) except those labelled with ^ in the graphs that indicated significance when storing EQUIA (Fig.5-4 B) in the demineralised group (p<0.05), and DC-HRI and Bulk Fill (Fig. 5-4 A) in the caries group (p=0.001).

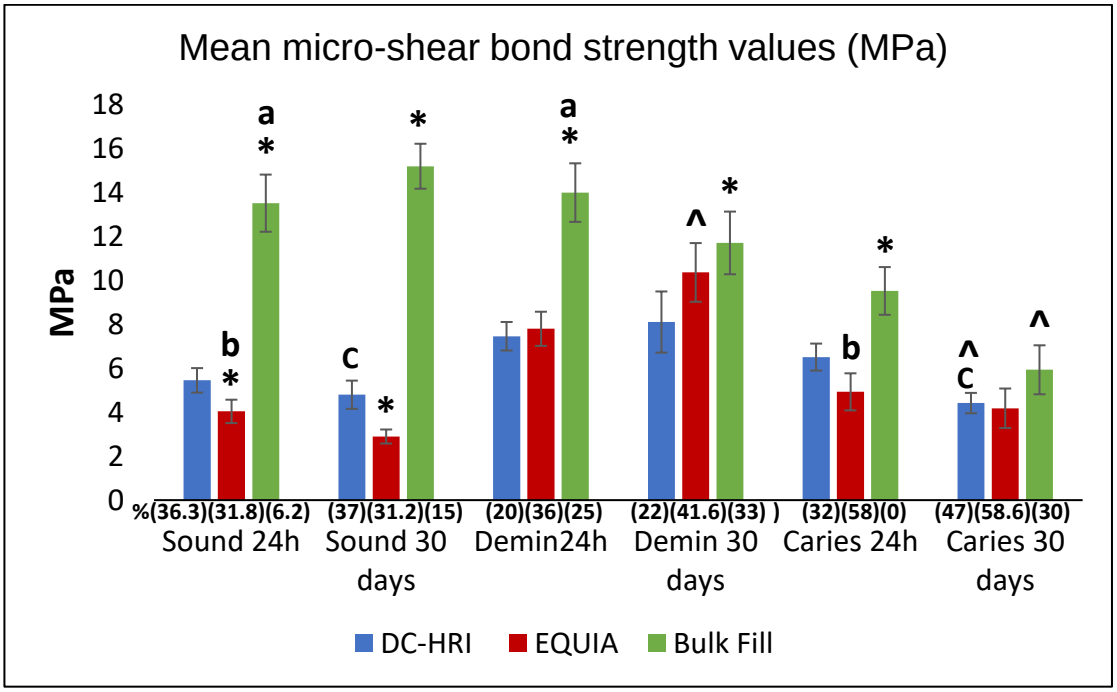

Figure 5-4. Mean micro-shear bond strength values (MPa) before and after aging the materials (DC-HRI, EQUIA Fill, Filtek Bulk Fill) with different dentinal substrates. Error bars depict standard errors of means, * Indicates a statistically significant difference (p<0.0001) from DC-HRI in identical testing conditions. ^ Indicates a statistically significant effect of storage time within each substrate. Similar letters indicate no

significant difference between sound and caries storage groups. % represents percentage of pre-test failures (PTFs) in parentheses. Graph is showing the difference in the mean bond strength of different material groups with different substrates at different storage time.

- **Substrate effect:** The analyses showed that the mean bond strength for each material differed significantly between the substrates regardless the storage timing as shown in Fig. 5-4. The interaction between materials and substrates was statistically significant ($p<0.001$) and hence this term was included along with the main effects of materials, substrates and time in the analysis model. A significant increase in the bond strength of both the demineralised DC-HRI and EQUIA groups was found when compared to the sound and carious groups. No significant difference was found between sound and demineralised resin composite (Filtek Bulk Fill) groups ($p=0.24$) but it was significant with the carious group ($p<0.006$).

- **Material effect:** DC-HRI in the carious group recorded a significantly higher bond strength compared to EQUIA within the same group ($p<0.001$). When considering different materials in the same sound group, a significant increase of the bond strength of the sound DC-HRI was found compared to the EQUIA values in the same group ($p<0.006$). Filtek Bulk Fill recorded the significant highest bond strength values among the other groups.

5.3.1.1 De-bond failure mode evaluation

Assessment of mode of failure showed the predominance of failures was adhesive in nature between the material and the substrate, followed by mixed failure and a few cohesively within the materials, as shown in Fig. 5-5. This result might not reflect the true interfacial bond strength. Representative SEM images in different failure modes are also presented (Fig. 5-6). Compared to the sound group, the percentage of pre-test failure (PTFs) of DC-HRI was decreased with the demineralised group while recording the same as or higher with the carious group. In contrast, PTFs of EQUIA were increased with the demineralised group and even more with the caries group. Filtek Bulk Fill resin composite also showed an increase in PTFs % with the demineralised group but the sound and carious groups recorded similar PTFs.

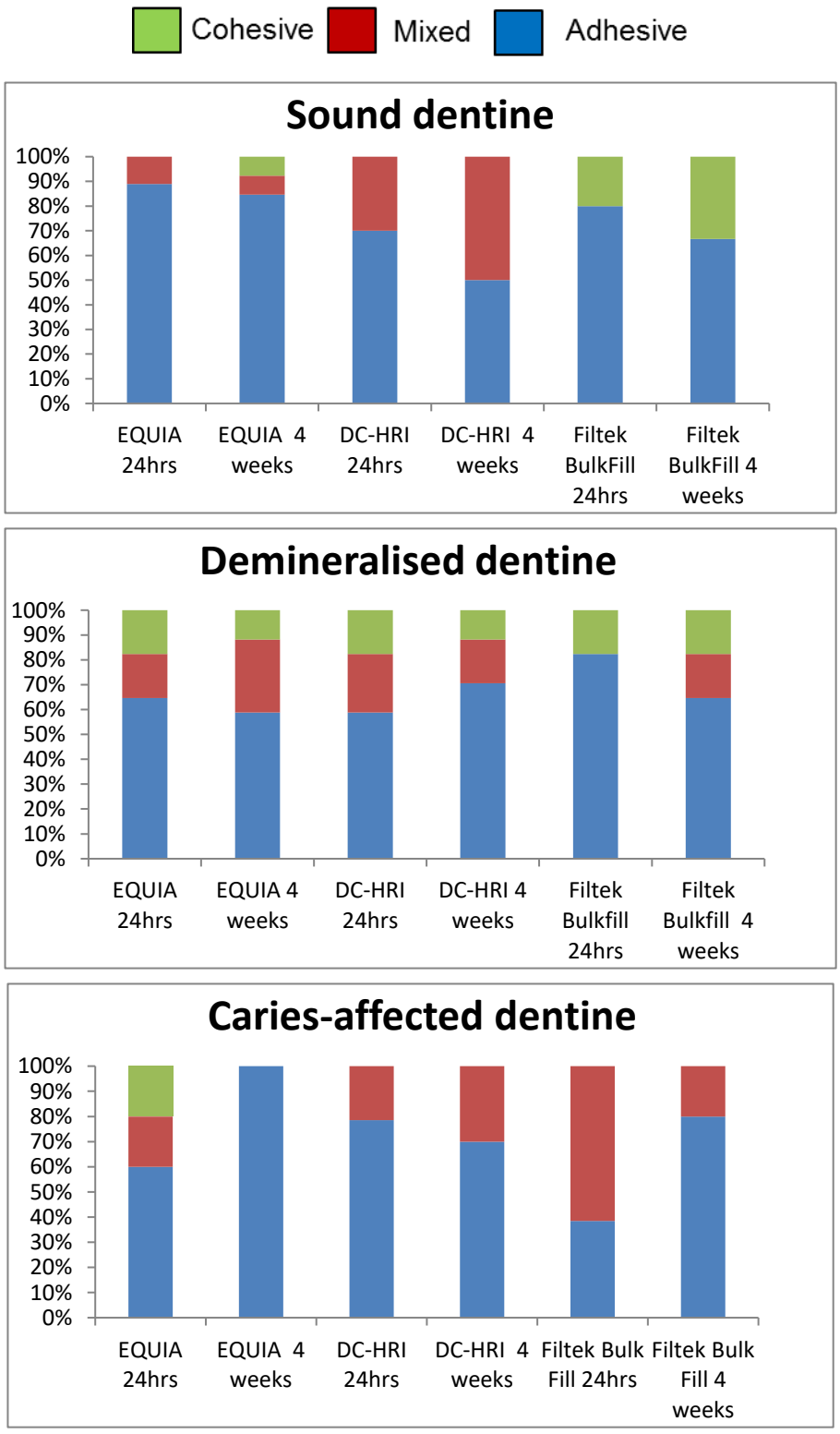

Figure 5-5. Graphs showing the mode of failures of tested materials with different dentine substrates in different storage timing. The majority of failures were adhesive in nature, followed by mixed and cohesive that were minimal. A similar pattern of failure

was noticed between DC-HRI and EQUIA within the demineralised group. In both sound and carious groups, DC-HRI materials showed a similar figure of failure.

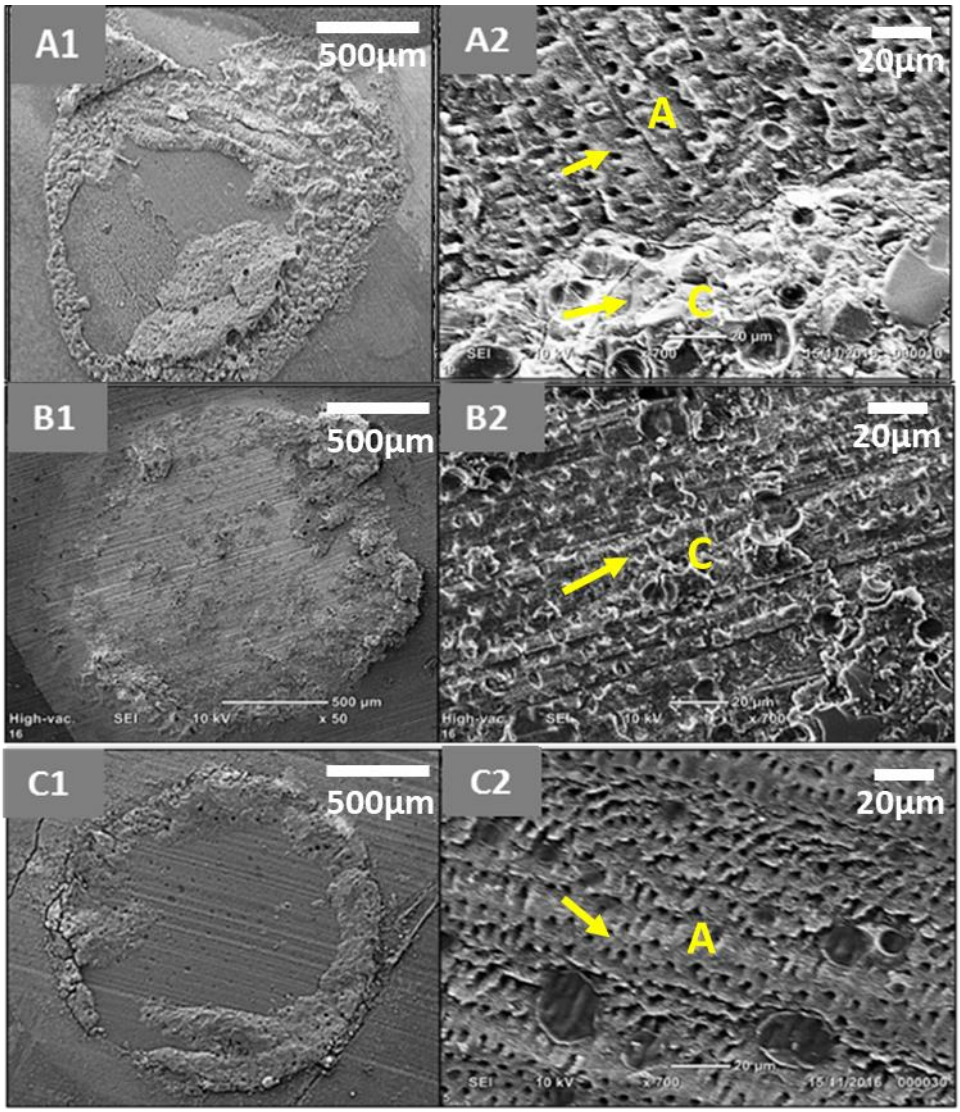

Figure 5-6. Representative SEM micrographs showed different patterns of DC-HRI failure with different substrates. Mixed failure of the demineralised dentine storage group showed a combination of empty (A) and blocked tubules (C) (A1, 2). Cohesive failure of demineralised dentine within the material with dentinal tubules blocked with the material (B1, 2). Adhesive failure of 24hrs sound dentine showed the empty opening of the dentine tubules (C 1, 2).

5.3.2 Two-photon interface evaluation

5.3.2.1 Morphological interface group of single-labelled materials

Representative images of the fluorescein labelled DC-HRI dentine interface showed the distribution of the fluorescein within the adjacent dentine substrate and into the lateral dentine tubules branches as indicated by the red arrows (Fig.5-7). In addition to the difference noticed in the interfacial layer thickness when bonded to sound and demineralised dentine substrates, sound dentine showed a 6-10 µm ± 2.3 wide hybrid interfacial layer, while the demineralised dentine showed a 21 µm ± 3 wide as labelled by yellow dash lines in Fig.5-7 a, b.

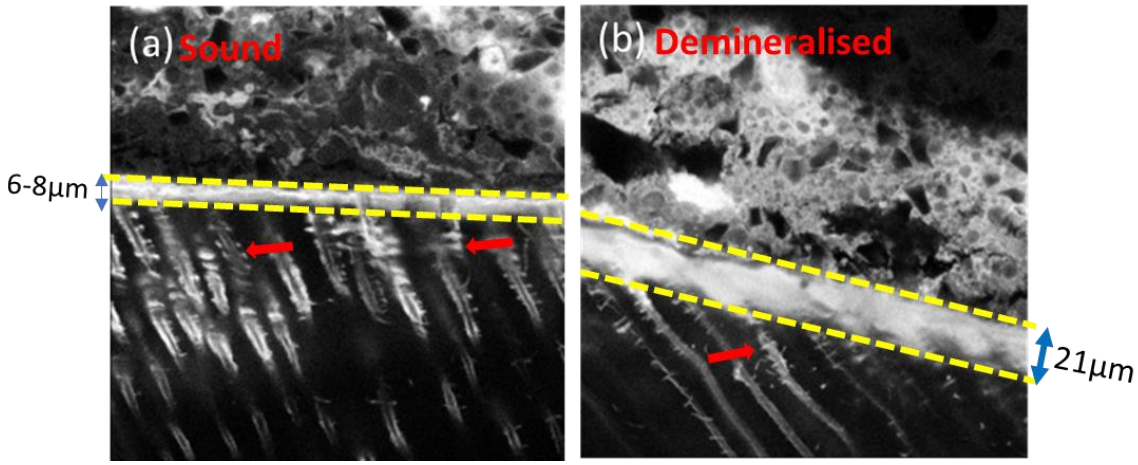

Figure 5-7. Representative two-photon fluorescence images of fluorescein labelled DC-HRI material bonded to sound and demineralised/etched dentine. (a) thin interfacial layer (6-8 µm), with a lateral diffusion of fluorescein dye into the lateral tubules, labelled by red arrows, which indicates the initial acidity of the material, and may reflect changes in the peritubular and inter-tubular dentine. (b) Thicker interfacial layer (21 µm) due to the pre-etching of the dentine surface using 37% phosphoric acid gel for 60 seconds to create the simple artificial caries affected dentine (CAD) model. Both sound and demineralised dentine hybrid interfacial layers are indicated by the yellow dashed lines.

5.3.2.2 Double-labelled micro-permeability

Representative two-photon interfacial images of double labelled micro-permeability samples are displayed in Fig. 5-8,9,10 for both sound and demineralised dentine of all the material groups. The green channel represents the fluorescein labelled materials to show their distribution into the dentine tubules. The red channel reflects the rhodamine-B diffusion through the interface,

whilst the blue channel records the second harmonic generation signals which reflect the collagen state of the dentine.

Representative two-photon images of the experimental material DC-HRI (Fig.5-8) revealed a thin bright band along the interface that was hybridised in both etched and non-etched dentine with a thicker interfacial layer in the etched group as shown in Fig.5-8. a1, e1. The two-photon qualitative analysis of the DC-HRI group showed the permeability of the interface and dye uptake by the material resulting in an appearance of an absorption layer (Fig.5-8 b1, f1). It also showed a good adaptation to dentine with no voids or gaps noticed either in sound or demineralised dentine groups. Diffusion of the fluorescein dye from the material into the lateral dentine tubules was noticed (Fig.5-8 a1, e1). Rhodamine-B can be noted permeating from the pulp and diffusing into the restoration above the interface with minimal mixing with fluorescein in the sound dentine group (Fig.5-8. d1). However, the demineralised dentine group showed diffuse mixing of both dyes below the interface pointed by the black arrows (Fig.5-8 h1).

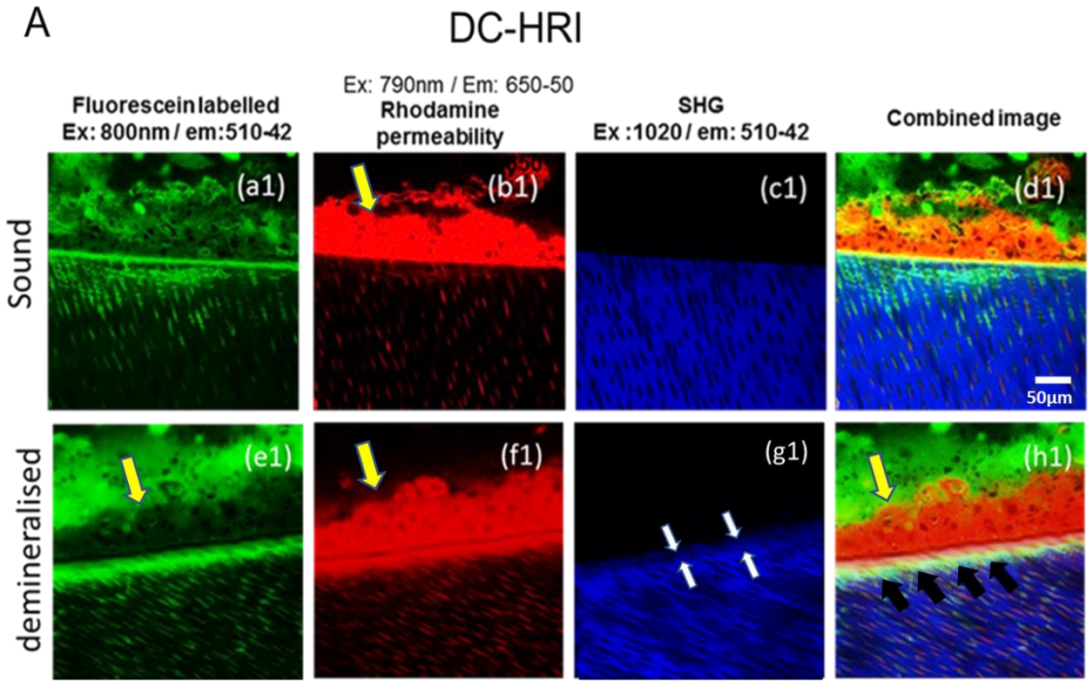

Figure 5-8. Representative 2-Photon micrographs of DC-HRI/ dentine interface with both sound and etched dentine. Column a, e (green) shows the fluorescein-labelled material and intrinsic dentine autofluorescence, column b, f (red) represent the rhodamine-B dyed pulpal fluid, column c, g (blue) show intrinsic fluorescence images of dentinal collagen as a reference called second harmonic generation (SHG). Column d, h (combined) show

Cont. (Fig.5-8): a composite image of the three channels. These channels showed fluorescein diffused below the dentine/material interface and into the lateral dentine tubules (a1, e1), together with the permeation of rhodamine-B through the interface into the restoration above the interface (b1, f1), with the minimal mixing of the dyes at the sound dentine interface (d1), and a diffuse mixing of the dyes was noticed in the demineralised dentine below the interface (black arrow h1).This mixing may indicate that the acidity of the material affected the inter-tubular and peri-tubular dentine structure. However, a clear hollow space just above the interface was also noticed in both sound and etched groups (a1, e1), which has been filled by the rhodamine dye as labelled by the yellow arrow in (b1, f1, e1, h1). No mixing of rhodamine and fluorescein at this space was found as presented in (d1, h1), this band was only characteristic to the DC-HRI group only. SHG channels showed an intact collagen in the sound group (c1), with a minimal change in the superficial dentine layer (labelled by white arrows in g1) duo to etching of dentine in this group.

The EQUIA group showed a gap at the interface in the sound dentine group (Fig.5-9 a3, d3, yellow arrows). A diffusion of rhodamine dye in the gap and a minor absorption of rhodamine-B into the EQUIA was noticed (Fig.5-9 b3). Rhodamine-B penetrated from the pulp through the dentine tubules into the interfacial layer, thus characterizing the interface with the presence of multiple cement projections (Fig.5-9 b3, f3). In the sound dentine group, no mixing of fluorescein and rhodamine-B was noticed (Fig.5-9 d3). However, mixing of dyes was observed in the demineralised dentine group just below the interface, presented as a yellow layer (Fig.5-9 h3, white arrows) (Sidhu and Watson, 1998a, Atmeh et al., 2012).

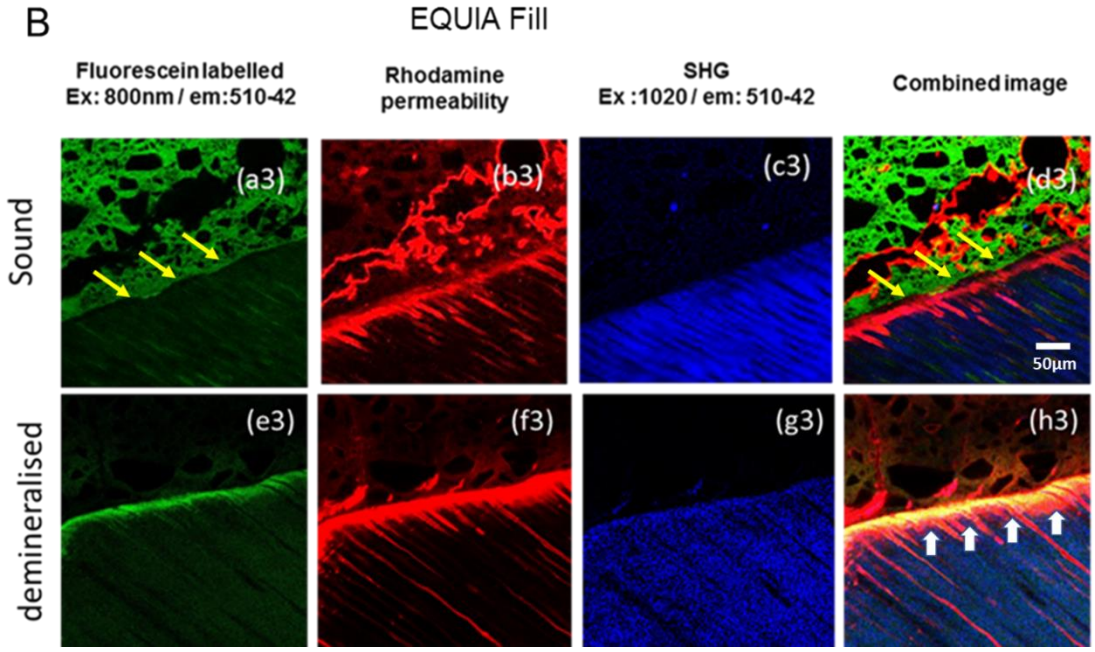

Figure 5-9. The EQUIA group did not show the fluorescein diffusion into the sound dentine group (a3), with minimal penetration of the dye in the demineralised group (e3). Gap was noticed in the sound dentine group at the interface as labelled by yellow arrows (a3, d3). Rhodamine-B labelled multiple cement projections were clearly noticed in both groups (d3, h3), with a partial seepage into the cement matrix (d3, h3). Both dyes were clearly mixed at and below the interface in the demineralised dentine group (white arrows, h3).

Filtek Bulk Fill resin composite group bonded with the Scotchbond Universal adhesive showed multiple spherical voids along the interface, a thin hybrid layer and concentration of rhodamine-B dye at the hybrid layer in the sound dentine group (Fig. 5-10 A3, d3), with thicker and well-defined resin tags in the etched group (Fig.5-10 h3, white arrows). No lateral seepage of rhodamine-B or fluorescein was noticed with this material. Second harmonic generation (SHG) was used as a reference to detect changes in the dentine collagen. It showed a lighter colour in the superficial dentine layer in both groups with a thicker demineralised dentine noticed in the etched group (Fig.5-10 g3, as labelled by yellow arrows). Scotchbond Universal adhesive did not provide adequate tubule sealing allowing interfacial leakage of pulp fluid.

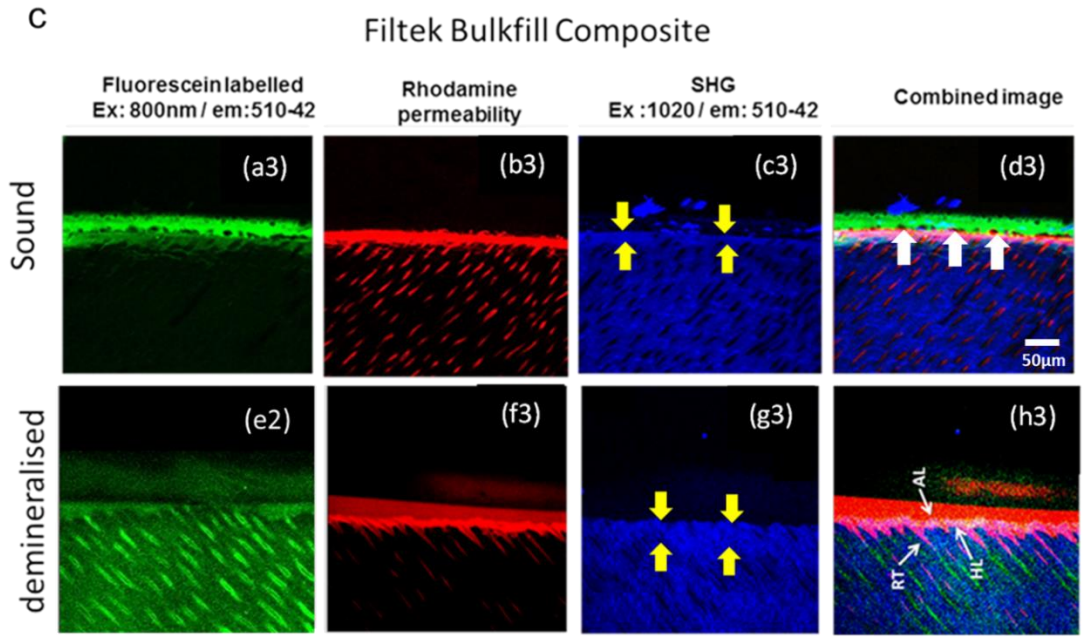

Figure 5-10. Filtek Bulk Fill group displayed a fluorescent labelled adhesive layer in sound dentine with short resin tags obtained in the sound dentine (a3). Spherical voids were also noticed at the junction between the fluorescein labelled adhesive and rhodamine-B dye diffused from the pulp at the interface (d3, white arrows). However, in the demineralised/etched dentine, the scalloped appearance of well-defined resin tags was presented with mixing of dyes at the interface but no diffusion into the composite structure (h3). SHG images of both groups reflect alteration in the superficial layer of the collagen image due to etching with variable thickness of this layer (c3, g3, yellow arrows).

5.3.2.3 Pilot study

Two-photon micro-permeability qualitative evaluations showed that DC-HRI behaves in a similar way to Fuji II with a diffuse absorption of rhodamine dye by Fuji II (Fig. 5-11 a). However, DC-HRI showed a more localised layer of rhodamine dye in the area just above the interface but not totally diffused in the restoration matrix (Fig. 5-11 b).

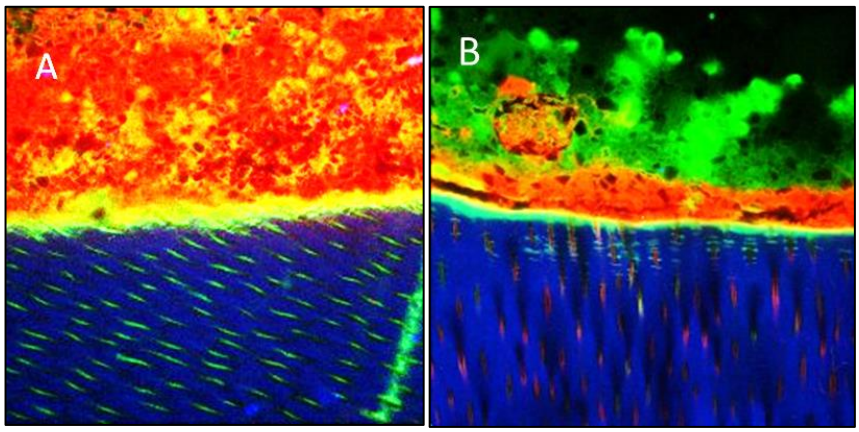

Figure 5- 11. Representative 2-photon micro-permeability micrographs of (A) Fuji II LC RMGI which showed complete absorption of rhodamine-B dye through the material bulk, with thin hybrid layer formation. (B) DC-HRI showed the absorption layer confined to the area of the material adjacent to the interface with a thin interfacial zone and lateral infiltration of fluorescein dye released from the labelled material.

5.4. Discussion

Bonding to dentine substrates, whether sound or carious, is less reliable and more complex than enamel bonding due to the complicated structure of the dentine (Swift, 2002). The ultimate goal for dentine adhesion is to obtain an effective and durable interfacial bond with an adequate seal to dentine (Swift et al., 1995). Several studies have been conducted to examine the bond strength to the sound dentine which does not necessarily represent the most common dentine type encountered during clinical restorative procedures. The expected substrate in the clinical situation is caries-affected dentine following the removal of caries-infected dentine.

Since there is no data about the experimental self-adhesive DC-HRI (3M, USA) materials, this study has assessed its interfacial properties with different dentine substrates in comparison to other commercial self-adhesive bulk-fill restorative materials such as conventional glass-ionomer EQUIA Fill, (GC, Japan) and Filtek Bulk Fill bonded with Scotchbond Universal adhesive (3M, USA). The manufacturer claims that DC-HRI bonding does not require pretreatment of the dentine, as it is a self-adhesive bulk-fill hybrid restoration.

It is unknown how the experimental material adheres to tooth substrate. Theoretically, from its composition, as previously mentioned with RelyX™, it can

be assumed that the phosphoric acid ester monomer (PAE) reacts with calcium in the tooth hydroxyapatite (HAp) via substitution of $PO4^{3-}$- and OH--groups and/or by decalcification of HAp, resulting in the formation of diverse solid products (Fukegawa et al., 2006). Hence, a micromechanical bond could be initiated and followed by chemical adhesion. Their initial reaction is mainly depending on the free radical methacrylate polymerisation which was either activated by chemical or photochemical routes to initiate the cross-linking polymerisation. An acid-base reaction further proceeds, and the pH rises from 2-4 in the first hour, which is neutralised gradually to reach pH 7 within 24-48h due to the release of water and alkaline filler that raises pH level and buffering components of the smear layer. Following neutralisation, the material transforms from the hydrophilic state into the hydrophobic state which minimises water absorption, further swelling and should reduce the material deterioration due to hydrolysis.

This study investigated the performance of the experimental material DC-HRI with natural caries or artificially demineralised dentine compared to the sound dentine, by measuring the micro-shear bond strength. The sealing ability of the tested materials was also evaluated with sound and etched/demineralised dentine using fluorescent labelled two-photon microscopy. In previous studies, these tests have been performed on natural lesions after *in-vitro* removal of the caries-infected dentine (Nakajima et al., 2005, Wei et al., 2008, Joves et al., 2013). It has been reported that there is a significant difference in bond strength values between hand and Carisolv caries excavation. Laser caries excavation also showed a difference in bond strength outcomes from bur and chemomechanical caries removal (Banerjee et al., 2010b, Yildiz et al., 2013). In this study, natural caries-affected dentine (CAD) was selected and characterised without any mechanical debridement or intervention to exclude operative factors that might contribute to the final result.

The natural CAD substrate presents a variation in lesion depth, mineral and organic content which makes its use as a standardized substrate for laboratory research difficult (Marquezan et al., 2009). Therefore, creation of a demineralised dentine model was undertaken for standardisation and comparative purposes. This study implemented the acid gel etching method using 37% phosphoric acid

etching for 60 seconds which provides a partially demineralised substrate with an intact organic matrix similar to that found in natural caries-affected dentine (Kuboki et al., 1977, Cao et al., 2013).This protocol demonstrated a direct demineralisation effect and simple method compared to the prolonged sample emersion in EDTA (Garcia-Godoy et al., 2010), acetate or lactic acid which necessitate immersion of the samples for a few days or weeks.The present study compared natural caries, a partially demineralised (by etching) dentine surface with sound dentine substrates and their influence on the obtained bond strength values. All samples were stored in physiologic phosphate buffered saline (PBS), which may closely mimic intraoral conditions and influence the materials ionic exchange with the tooth structure (Colon et al., 2010).

5.4.1 Micro-shear bond strength test:

Unlike the micro-tensile test that creates micro-cracks during specimen preparation, the micro-shear test is simpler and less stressful to the sample itself (Roeder et al., 2011). It could be a viable test when evaluating brittle materials, having a low modulus of elasticity, such as GICs (Bonifácio et al., 2012). The great variability in bonding protocols and testing conditions makes it difficult to compare results from one research laboratory to another. Bonifacio et al compared the adhesion of GICs to sound dentine with micro-shear or micro-tensile bond strength tests, reporting that both tests resulted in different material rankings and failure patterns (Bonifácio et al., 2012). The micro-shear bond test measures more accurately the strength in the adhesive interface (Tedesco et al., 2013).

In the current study, a looped orthodontic wire was used for micro-shear testing instead of the blade as mentioned by Shimida et al. (2002). Barga et al. claimed a lower bond strength was obtained when using a chisel as a loading device (Braga et al., 2010). Specimens were tested after 30 days, a time after which the hybrid restoration would have completed its polymerization chemically, rendering the bonding region more resistant physically to micro-shear forces. However, the mechanism of Scotchbond Universal adhesives bonding to dentine differs from those with GIC and RMGIC and their polymerization should have been completed immediately after curing.

Results from both bond strength and morphologic two-photon microscopy evaluations suggest that the characteristics of the substrate directly impact the bonds formed. All tested materials exhibited higher bond strength to the demineralised dentine group compared to both sound and natural caries-affected dentine. Thus, the first null hypothesis was rejected, as the substrate type has significantly influenced the bond strength results of the three materials groups. Such result agrees with the findings of previous work reported a higher bond strength of RMGIC to the demineralised dentine (Zhao et al., 2017). However, this result contradicts the findings of Alves et al, which showed that GIC bond strength to primary teeth wasn't affected by the type of the substrate whether sound or CAD (Alves et al., 2013). This might be attributed to the difference in microstructural and chemical structure between primary and permanent teeth which result in different bond strength outcomes.

A further study also reported that RMGIC showed a lower tensile bond strength when bonded to the carious permanent teeth (Choi et al., 2006). Direct comparisons between these studies are difficult to be applied, as the type of tests and substrates were different from those used in the present study.

Differences in morphology and physical structure of dentine substrates are key factors contributing to the variability of the formed bonded interfaces. Previous studies have reported that bonding to the natural caries-affected dentine (CAD) provides lower bond strength than that to normal dentine regardless of the type of adhesives used (Nakajima et al., 2000, Rocha et al., 2014, Follak et al., 2018b). The present finding of the current study agrees with the previous investigations that showed a significant reduction in the bond strength of the Bulk Fill resin composite group, using Scotchbond Universal adhesive (SBU), when bonded to the natural CAD as shown in Fig.5-4, A. This can be explained by improper diffusion of the Scotchbond Universal adhesive into acid-resistant minerals (whitlockite) blocked dentinal tubules of CAD substrate (Nakajima et al., 2000, Erhardt et al., 2008, Scholtanus et al., 2010).

The processes of demineralisation and remineralisation in caries-affected dentine promotes the formation of β-tricalcium phosphate (βTCP) within dentine tubules which is less soluble than hydroxyapatite and impermeable to water (Müller et al., 2017). Caries-affected dentine typically exhibits a higher degree of porosity,

which is commonly associated with a partial lack of mineral around and within the collagen fibrils, with lower mechanical properties and higher water content than the sound dentine (Palma-Dibb et al., 2003). The hypomineralised and porous caries-affected dentine substrate may allow for a deeper penetration of the cement and thus a thicker hybrid layer formed (Wang et al., 2007). The unprotected hypomineralised collagen may become a site for the non-bacterial self-degradation of collagen due to the activation of endogenous enzymes, matrix metalloproteinases and cathepsins (Nascimento et al., 2011). However, this unprotected collagen layer should be preserved for potential remineralisation (Wang and Spencer, 2003, Osorio et al., 2011). Although previous studies reported a thicker hybrid layer when resin composite was bonded to natural CAD, the self-etch adhesive promotes a thinner hybrid layer compared to the etch and rinse system, but thicker than those obtained with the sound dentine (Nakajima et al., 1995, Yoshiyama et al., 2002, Say et al., 2006). However, thickening of the hybrid layer does not necessarily reflect better bond formation.

Studies have examined etched CAD using light microscopy, which showed a deeper, non-uniform, non-encapsulated collagen with a poor resin infiltration that facilitated dentine/resin bond degradation (Fruits et al., 1996, Palma-Dibb et al., 2003). The variation in morphology and chemical composition of caries-affected dentine structure would be one of the possible reasons for their lower bond strength results (Nakajima et al., 2000). Arrias et al (2004), reported that increasing etching time to 45 instead of 15 seconds using 35% phosphoric acid leads to better bond strength values of Single Bond Universal (3M, St. Paul, MN, USA) to caries-affected dentine. This can be explained by further removal of minerals from the blocked dentine tubules facilitating the infiltration of adhesive resin into the CAD surface (Arrais et al., 2004). In contrast to Scotchbond Universal Adhesive, DC-HRI and EQUIA groups reported opposite results when bonded to the CAD; a higher immediate (24hrs) bond strength to the natural CAD compared to that with the sound dentine group was observed. Therefore, the second null hypothesis was rejected as the materials differ in their bond strengths to different dentine substrates. The higher porosity of inter-tubular dentine in CAD, however, may permit deeper etching of the inter-tubular dentine, and the adhesiveness to this area probably improves the μTBS values (Alves et al.,

2013). In addition, better ionic diffusion and interaction may anticipated between DC-HRI and EQUIA due to their bioactive nature with the tooth, compared to the composite group. Thereby, the phosphoric acid from DC-HRI and carboxylic groups of polyalkenoic acid from EQUIA generate ionic bonds with hydroxyapatite, ensuring a second means of retention.

With regards to the sound dentine group, higher bond strength values of DC-HRI when compared to EQUIA have been reported. The organic matrix of DC-HRI, consisting of multifunctional monomer of DC-HRI, a mono, di and tri methacrylated phosphoric ester that reacts chemically with the hydroxyapatite, promoting a strong bond to the dentine substrate. The higher acidity of the phosphoric acid monomer in DC-HRI may demineralise and infiltrate the dentine deeper than the poly acrylic acid (PAA) in EQUIA. Additionally, multifunctional phosphoric acid methacrylate is proposed to be capable of demineralising and infiltrating the tooth surface simultaneously. Previous studies have reported that GIC shear bond strength to dentine lies in the range 1–3 MPa (Berry and Powers, 1994, Burke and Lynch, 1994), while the bond strength of RMGICs to dentine have been noted as higher than that of GICs. The better bonding performance of RMGICs compared to conventional GICs could be due to their dual mechanism of adhesion (Almuammar et al., 2001).

Moreover, a comparable increase in the bond strength of DC-HRI and EQUIA in the demineralised dentine group was noticed, compared to both the sound and caries dentine groups. Acid demineralised dentine promotes a protein-rich collagen exposure by removal of the smear layer and dentine plugs, which in turn changes the surface free energy of the dentine and enhances its wettability (Gopalakrishna, 2009, Hamama et al., 2014). Additional micro-mechanical infiltration may occur following etching (Imbery et al., 2013). It has previously been reported that dentine pre-etching (demineralised dentine model in this study) improves the surface wettability and the ion-exchange between the PAA carboxyl group in the GIC and hydroxyapatite from the tooth, which dislocated calcium and phosphate ions from the latter (Korkmaz et al., 2010, El-Askary and Nassif, 2011, Inoue et al., 2012). However, it is still controversial whether to etch the dentine or not before GIC application. When GIC is bonded to hydrated substrates, ionization of the PAA acidic monomers will be more efficient. This

ionization is followed by acid–base neutralization reactions involving the tooth and the basic filler (Ferracane et al., 2011).

Results of the present study revealed higher bond strength of Bulk Fill resin composite compared to both DC-HRI and EQUIA. This result is in accordance with previous studies which concluded that GICs as well as RMGICs have lower shear bond strengths when compared with resin composite adhesive systems (Fruits et al., 1996, Nicholson, 1998). A few factors may contribute to this finding. First, the dual-cured DC-HRI exhibits a high viscosity and limited penetration ability. Second, self-adhesive restorations need to be applied with some pressure to ensure the adaptation of the material to the dentine surface. Third, the design of micro-shear testing necessitates that materials cylinders be adjusted well to the tooth. Light-curing of these specimens might result in some polymerisation stress, causing resin contraction away from the surface and thus reduce their bond strength values. Moreover, DC-HRI should be capable of demineralising and infiltrating the tooth structure. however, only inconsistent areas of etching (De Munck et al., 2004) and almost no distinct demineralisation (Lin et al., 2010) or hybrid layer formation (Al-Assaf et al., 2007) have been noticed with these materials. Consequently, chemical rather than micromechanical bonding is responsible for the dental adhesion of the resin components of DC-HRI.

The lower bond strength of GICs may be attributed to their brittleness, initial sensitivity to moisture contamination and sensitivity to dehydration. Moisture leads the material to be chalky and porous, resulting in a loss of surface hardness (Cook, 1990).

Higher mean shear bond strength of resin composite in permanent teeth as compared to compomers and RMGICs was also reported (Prabhakar et al., 2003). Scotchbond Universal adhesive provided a higher bond strength due to both micro-mechanical and chemical adhesion to the dentine. The basic mechanism of Scotchbond adhesion to dentine is by replacement of minerals extracted by acid-etching with resin monomers, which generates micro-mechanical adhesion. In addition to the presence of 10-MDP in their composition, which bonds chemically to the hydroxyapatite in dentine and enamel, favoring the bond to dental tissue and reducing the degradation of the bond overtime (Yoshida et al., 2004). Yoshida et. al showed that these chemical interactions provided a

stable MDP-Ca salt deposition along with nano-layering which may explain the higher bond strength to the dentine (Yoshida et al., 2012). Moreover, the presence of HEMA in its composition generates an ionic bond between the carboxylic group of the polyalkenoic acid monomer and the HA of the tooth (Harashima and Hirasawa, 1990)

DC-HRI exhibited a higher or equivalent bond strength compared to EQUIA when bonded to different dentine substrates. This could be explained by their superior mechanical properties achieved by the higher cross-linkage between the carbon double bonds of their methacrylate monomer. In addition, their initial moisture tolerance and hydrophilicity facilitates the good adaptation to the hydrophilic tooth surface.

It is believed that the excellent initial GIC adhesion properties refer to its ion exchange with the underlying dentine. This involves the transfer of strontium, aluminium, and fluorine ions, as a result of an ion concentration gradient between GIC and dentine, which is further followed by dentine demineralisation and release of Ca^{2+} ions caused by polyalkenoic acid (Ngo et al., 2006). Based on the previous explanation, EQUIA showed a progression in bond strength values following storage due to complete maturation after ion exchanges (Ngo et al., 1997). Likewise, an initial polymerisation of DC-HRI by light-curing or by the chemical reaction of the initiator system, has started the setting reaction of the material. This reaction is further followed by a chemical reaction of the phosphoric acid functional group and ionic exchange with the tooth apatite. Simultaneously, a neutralisation reaction takes place to increase the pH level.

Storage negatively influenced the bond strength of both Bulk Fill and DC-HRI with CAD substrate, as it reduced significantly when compared to the immediate bond strength (24hrs) data. On the other hand, storage improved the bond strength of EQUIA with the demineralised/etched group as shown in Fig.5-4. This result partially rejects the third hypothesis in this study confirming a significant effect of storage on some of the tested materials. It was expected from similar studies of bonding to CAD that the bond will decrease overtime for several reasons. One of the leading causes is activation of an endogenous proteolytic enzymes (MMPs) that leads to hydrolytic degradation of the bond at the interface and compromises the longevity of the bonded restoration (Mazzoni et al., 2006, Longhi et al., 2014).

Durability studies on bonding to caries-affected dentine are still limited and their results are controversial, since some authors had reported reduction in the bond strength, while others did not (Omar et al., 2007, Erhardt et al., 2008, Komori et al., 2009). These studies have evaluated the bond strength longevity of different resin adhesives to CAD in different time exposures and varied storage media. However, they did not provide insight into what potential differences in caries-affected dentine structure may affect the bonding longevity. Nakajima et al. (2006) had also reported a significant decrease in the micro-tensile dentine bond strength of the 2-steps self-etch (Clearfil SE Bond, Kuraray) following one-month storage with hydrostatic pulp pressure to normal dentine but didn't affect the CAD results (Nakajima et al., 2006). Recently, a dentine biomodification concept has been employed to achieve a more stabilized and durable adhesive interface (Bedran-Russo et al., 2014).This can be achieved by using several natural and synthetic agents, acting as MMP inhibitor and collagen cross-linker which bio-modify and enhance the mechanical properties of the dentine substrate. These bio-modifiers can be whether pre-treat the dentine surface or by their addition to the primers, their results were promising and has preserved the resin-dentine bond following 6 months storage (Singh et al., 2017).

Another factor that should be considered when analysing the bond strength data is the percentage of pre-test failures (PTFs) that were reported earlier in the results section (Fig. 5-4 A, B). The highest percentage of PTFs generally was in the caries storage group of all materials, which correlates well with the low bond strength values obtained with this substrate. Nevertheless, the immediate carious Bulk Fill group showed a reduction in bond strength results but with no PTFs noticed in that group. Such results may indicate an immediate micromechanical interaction with the porous inter-tubular dentine in the carious substrates (Huang et al., 2011). In contrast, PTFs reduced with the demineralised group which confirms the high bond strength of this group. PTFs can be greatly affected by the technique of Tygon tube removal which is critical and not easily performed, as some level of stress can be induced at the interface yielding a high number of failures. The issue about inclusion or exclusion of PTFs is still controversial in the literature as they are not treated in the same statistical manner by different research groups (Scherrer et al., 2010). Including PTFs as a zero value would

prevent over-estimating the quality of the bond to the material. However, exclusion of PTFs might be indicated when a high incidence exists (Saad et al., 2017). In the present study, the PTFs cylinders were excluded and not recorded in the statistical analysis as their percentage was high, with the possibility of these failures owing to external stress during mould removal, thereby compromising the bond strength. Although the flowability of the materials is favourable with micro-shear test to easily fill the Tygon tube, all materials used in this study were highly viscous. This factor might also influence the PTFs during specimen preparations (Andrade et al., 2010).

With regards to the fracture analysis, results showed a predominance of adhesive/mixed failures in all groups with few cohesive failures which belonged to the Bulk Fill groups. These results compare well with Schneider et al. (2000) who found that the better the bond between dentine and resin composite, the higher the resulting percentage of cohesive failure within each sample (Schneider et al., 2000). Conversely, GIC and DC-HRI tend to exhibit more adhesive failures. These results agree with Chung et al., (2009), who reported that failures in conventional GICs were adhesive along the dentine interface, indicating a weak bond between material and dentine (Chen et al., 2009). Some researchers have claimed that cohesive fracture in the substrate reflects high bond strength (Scherrer et al., 2010). However, others claimed that there is no relationship between the bond strength and fracture type (Almuammar et al., 2001) There are several factors affecting the mode of failure results including sample preparation, load force, crosshead speed and the type of test used.

5.4.2 Micro-permeability and two-photon imaging

The term “micro-permeability” was explained as a simple evaluation method to screen the restorations’ interfacial integrity and the sealing ability, to determine how their adhesion to dentine substrates will affect the restoration’s marginal adaptation (Griffiths et al., 1999). This technique allows for sample evaluation that contain two fluorophores with different target labels, thus permitting each target to be observed separately, or at the same time (Sidhu and Watson, 1998b, Toledano et al., 2017). This evaluation was aided by using an aqueous solution of rhodamine B, in conjunction with fluorescein powder to label the restorations to be examined further by the two-photon microscopy. The use of fluorescent

dyes with microscopy is a powerful investigative technique. An aqueous solution of rhodamine-B was injected into the pulp chamber, resulting in the seepage of fluorescent tracer around resin tags to lateral branches of the dentine tubules or at the base of the hybrid layer. Maintaining a constant dye reservoir for 3 hrs is fundamental to ensure a complete seepage of the dye through the dentinal tubules to all possible routes of the restoration interface (Sidhu and Watson, 1998a). Therefore, this method reveals the micro-porosity and pathways for fluid permeability.

In the present study, the interfacial properties of the dentine underneath the new restoration DC-HRI was compared to EQUIA and Bulk Fill resin composite with Scotchbond Universal adhesive. The micro-permeability test was performed on both sound and demineralised/etched dentine. Two-photon confocal microscopy allowed imaging of the subsurface layer of the dentine/restoration interface with minimal sample preparation. The only sample preparation required is to section the specimen vertically to permit microscopic observation of the interface. Routine SEM examination is not possible without dehydration of the sample, which in turn interferes with capturing the dynamic tooth/restoration relationship.

DC-HRI groups revealed a good adaptation with no gaps or voids noticed and a fluorescein dye-infiltrated band just below the interface was observed with minimal mixing with rhodamine-B in the sound group. There was no evidence of any resin tags formed with the sound dentine (Fig.5-8 a1, d1). However, in the demineralised dentine, mixing of the dyes was noticed with the pooling of rhodamine-B at the interface and to the bulk of the material, indicating some deficiencies in the inter-tubular and peritubular dentine with minimal resin tag formation (Fig.5-8 d1, h1). This may be attributed to the very low initial pH of the new material which may affect the peritubular and inter-tubular dentine integrity at this stage, followed by quick neutralisation after curing. Moreover, the high viscosity of the restorative material may interfere with the complete infiltration of the material into the full length of the demineralised dentine zone.

Previous studies have shown a unique resin-rich, interfacial zone with dentine bonded with certain RMGICs (Watson et al, 1994, Pereira et al., 1997). The

restorative version of RMGIC produces what is called the “absorption layer”, an amorphous, non-particulate zone at the dentine interface. It was indicated that the formation of this layer was attributed to swelling of the HEMA component of the resin matrix via water sorption within the maturing RMGIC when placed in the deep moist dentine (Sidhu and Watson, 1998b). However, it was absent from enamel and from the finished surface of RMGIC when exposed to water (Tay et al., 2004).

Second harmonic generation images (SHG) showed a change in intensity only in the demineralised groups due to the acid-etching effect in the superficial dentine layer (Fig. 5-8 g1, 5-9 g2, 5-10 c3, g3).

A rhodamine-labelled cement interfacial layer was noticed when evaluating EQUIA at the interface, with less dye uptake into material in the etched group. This may result due to the demineralising effect of PAA and tartaric acids on the inorganic dentine structure component (Sennou et al., 1999). Moreover, a thicker interfacial hybrid layer was obtained. Based on the result of this study, the DC-HRI group showed a complete diffusion of rhodamine-B through the hybrid layer and the interface into the bulk of the material, indicating the permeability of the interface and absorption of the fluid through the interface. This might lead to an instability of the interface in the long term (Shafiei et al., 2015). On the other hand, etching of the dentine and the removal of the smear layer, in the demineralised group, may influence the interface integrity as showed in Fig. 5-10 (d1, h1).

Examining the interfacial sealing over time will not be accurate as the dyes used in this study are easy to permeate and might create false readings with long time storage (Paulo et al., 2006). The etched group has a characteristic feature of funnelling of the tubular orifices and well defined lateral tubules which also contributed to rhodamine-B seepage around the main tags and the rest of the interface.

In the EQUIA group, the pattern of dye infiltration through the hybrid layer and cement matrix was different from the experimental group. Two-photon images demonstrated the lack of intimate interaction within the hydroxyapatite-coated collagen, accompanied with a highly stained area within the hybrid layer with permeability into the cement matrix. It has been reported earlier that if there is a

gap at the dentine/ material interface, the dye is likely to pool at this space and fill the gap not leaving sufficient dye to leak into the bulk of the restorative material (Sidhu and Watson, 1998a).

The Bulk Fill resin composite group showed voids in the hybrid layer with dye staining of the adhesive layer but not penetrating the composite, which indicated the partial sealing ability of the self-etch adhesive.

5.4.3 Pilot study

In the current study, a pilot study involved micro-permeability samples prepared and filled by flowable resin modified glass ionomer (Fuji II LC, GC-Japan) to compare the sealing ability of this cement with the new high viscous restorative hybrid material (DC-HRI) when bonded to sound dentine as shown (Fig.5-11). Two-photon micro-permeability evaluations have shown that DC-HRI behaves in a similar way to Fuji II LC with the observation of the absorption layer within the material as documented in an earlier study by Sidhu et al., (1998), that was strongly labelled by rhodamine-B dye (Fig.5-11 A, red colour). This layer has not been found when examining the interface with EQUIA Fill. However, rhodamine-B dye uptake in DC-HRI samples was more localised to the area of restoration adjacent to dentine but not to the whole matrix as noticed in Fuji II LC. This indicated a more permeable system of Fuji II LC compared to the new material that has a higher filler content. The absorption layer is critical for the interfacial adaptation of resin cement. It possibly acts as a stress relief layer to compensate for the polymerisation shrinkage of the restoration (Sidhu et al., 2002). A reason behind the difference in their permeability may be related to their chemical compositional differences as Fuji II LC contains HEMA which is a hydrophilic monomer that facilitates water permeability. However, DC-HRI contains TEGDMA which comprises small hydrophilic monomers, that was added to improve the viscosity of the restorative material for a better handling in the clinic. Therefore, in Fuji II LC, water can diffuse from the underlying moist dentine into the HEMA filled hydrophilic matrix to form the diffuse absorption layer as seen in Fig. 5-11 (red label). It can be assumed also that diffusion of both water and HEMA may also occur into empty air voids that are close to the RMGIC/dentine interfaces. On the other hand, such water diffusion was limited to the area adjacent to the interface but not the whole material matrix. This may be

attributed to the higher density of the experimental material compared to the less viscous Fuji II. Formation of this layer is effective for the stress compensation that was generated during the setting, and to prevent further fracture at the dentine/material interface.

Further investigation is needed to confirm the clinical effectiveness of DC-HRI. The success and stability of a restoration can be influenced by many factors such as wear rate, solubility and water sorption which have to be considered.

In conclusion,

- The experimental material may perform better than a conventional GICs with sound dentine and performed comparably to it with artificially demineralised or carious dentine.
- None of the tested materials provided proper sealing to the dentine tubules. However, sealing was better with the demineralised dentine compared to the sound.
- Despite there being several limitations of Bulk Fill resin composite with Scotch bond adhesive, it still demonstrates predominance in bond strength and optical behaviours. However, the experimental material facilitates the dental procedure, reduced the application sensitivity and time possibly providing combined advantages of both composite and GICs.

Chapter 6. General discussion and future work

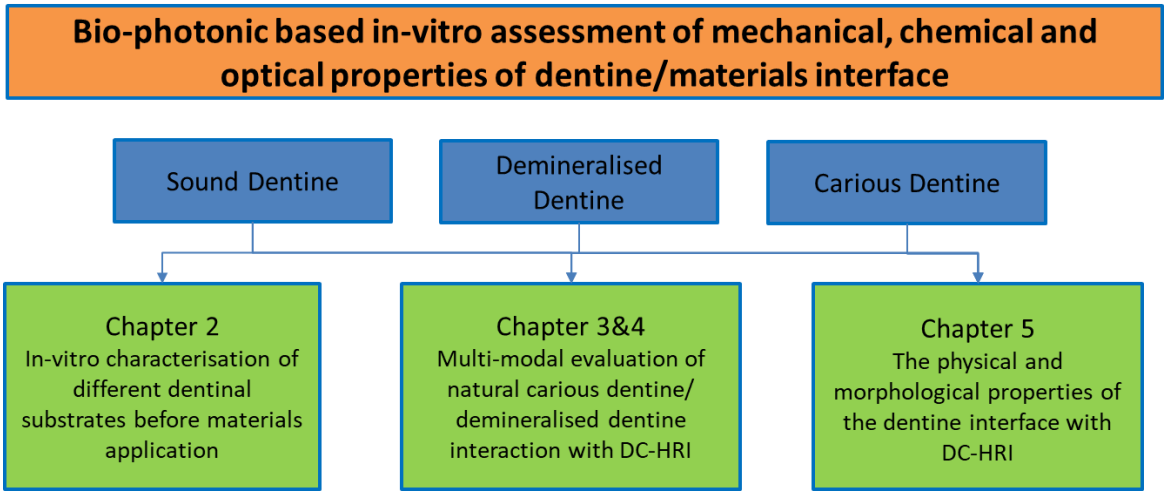

6.1 General discussion

Despite many controversies about its suitability as a real alternative to amalgam, resin composite has turned out to be the material of choice as a relatively durable, restorative aesthetic material, for posterior teeth. However, its use requires an intermediate bonding agent / adhesive to provide retention. As another alternative restorative material, glass-ionomer cements (GICs) are self-adhering materials that can bond directly to the tooth structure without an intermediate adhesive layer. However, a preconditioning step by polyacrylic acid is recommended, resulting in a two-step approach (Peumans et al., 2014). The clinical success of GICs as non-stress bearing restorations and the atraumatic restorative treatment is derived from the two-fold bonding mechanism which combines micro-mechanical interlocking and chemical interaction (Mickenautsch and Yengopal, 2012). GICs are widely used in restorative dentistry for their long-term fluoride release and ease of use, as well as their biocompatibility with pulp tissues. However, some drawbacks such as low flexural strength, prolonged setting time, early moisture sensitivity, dehydration, and poor aesthetics exist. Nevertheless, a new high-viscosity glass-ionomer cement has been showing promising clinical performance in posterior permanent restorations (Gurgan et al., 2017), which was used as a control material in the studies presented in this dissertation.

Consequently, hybrid versions of the material were introduced. Among these, resin-modified glass-ionomer cements (RMGICs) were developed with better physical properties, early resistance to water contaminations, ease of placement and better aesthetics but could not be used for comparison in the current studies, as all the currently available RMGICs have low viscosity and not indicated as a posterior restorative material. With the improvement of the chemistry and nanotechnology in this field, a novel dual-cure hybrid resin glass-ionomer restorative material with modified functional monomer including phosphoric acid ester was introduced by 3M company. It is claimed to have a self-adhesive, bulk-fill properties which minimise the restoration placement time in deep cavities and reduce the technique sensitivity and variability between operators as no bonding step is required.

Although most of the literature related to the performance of dental materials refers to sound dentine as a standard substrate, clinicians are daily challenged by the presence of caries-affected dentine rather than the sound dentine substrate. In the same way, manufacturers base their new materials on the adhesion to sound dentine which does not represent the clinically relevant substrate. The minimally invasive approach advocates complete removal of the infected dentine and preservation of the CAD on the pulpal cavity floor. Handleman et al. indicated that the residual bacteria became dormant and much less active when sealed properly by a resin sealant (Jensen and Handelman, 1980). Studies relied on relatively old materials rather than contemporary hydrophilic adhesive formulations. However, the residual bacteria in CID can be embedded by adhesive resins and become inactive. Therefore, it might be possible to leave even CID without progression of the caries process if it was sealed properly (Mertz-Fairhurst et al., 1998, Maltz et al., 2002, Ricketts et al., 2006, Schwendicke et al., 2013, Imparato et al., 2017).

Accordingly, in the present study, various human dentine substrates were used including sound, demineralised, CID and CAD. This wide range of substrates provides a profound understanding of the introduced experimental materials' interaction with dentine in comparison to control materials.

Chapter 6

Methods used in biomedical research require high spatial resolution to delineate the diseased from normal tissues, high sensitivity to monitor changes in the microenvironment, and high precision to objectively recognise those changes. For the study of the interaction of restorative materials with dental tissues, different optical, non-invasive imaging techniques have been widely used. These techniques rely on the generated photons as a result of interaction between an illuminating light and the matter within different substrates. These optical techniques provide valuable information about the substrate, if minimal or no alternation caused to the samples. In this study, an in-house built two-photon imaging microscope was utilised all through different experiments generating fluorescence, SHG and lifetime data that help in studying the interaction of different dentine substrates with the applied restorative materials. Additionally, these optical investigations of the interfaces were confirmed by Knoop hardness recording, coupled with Raman spectral analysis, for monitoring mineral phosphate peak spectral changes if demineralisation or remineralisation occurs. Moreover, the adhesion strength of the examined restorative dental materials to various dentine substrates were tested and measured using the micro-shear bond strength, and the sealing ability was assessed by micro-permeability study.

Dentine fluorescence properties were investigated using the in-house built two-photon imaging microscope, coupled with monitoring the change in their mineral contents using micro-Raman spectroscopy and the Knoop hardness number before and following the storage with materials in phosphate buffered saline solution. Prior to materials placement, various dentinal substrates were examined to compare their optical intensities and lifetimes (AF, SHG and FLIM), along with their mechanical properties (Knoop hardness) and their mineral content (using Raman spectroscopy). These substrates include caries infected, affected, partially demineralised (phosphoric acid-etched) and sound dentine. The obtained data have shown significant differences in most of the optical properties between the substrates due to the variation in their either mineral contents or collagen configurations prior to any application of restorative materials.

CID recorded the highest fluorescence intensity among other substrates (Fig.2-8), while SHG was the least. Despite the controversial debate about the

fluorescence nature of dental tissues, it was previously suggested that the dentine AF originates from several endogenous fluorophores (Collin and Julian, 2004). The organic component within human dentine is believed to be the source of its fluorescence behaviour (Van der Veen and Ten Bosch, 1996, Banerjee and Boyde, 1998, McConnell et al., 2007). In previous studies, variation of dentine AF was observed throughout the caries process (Bjørndal and Mjör, 2001, Slimani et al., 2014). In order to understand the underlying phenomena, various hypotheses were suggested (Buchalla et al., 2004) such as alteration of the collagen fibres due to acidic degeneration, non-centrosymmetric structure with fluorescence properties and/or accumulation of specific bacterial by-products with specific endogenous porphyrin (Maillard reaction products). CID is a superficial necrotic zone of vastly demineralized substrate, characterised by degenerated collagen fibrils that lost their cross-linking. They are characterised by their brownish discolouration of crosslinked proteins and advanced glycation end-products (AGEs). AGEs are likely to bind to dentine collagen fibres modifying their intrinsic optical properties (Kleter et al., 1998b).

A study by Buchalla et al., (2004) also linked porphyrin to the auto-fluorescence signal of the root dentine caries compared to the sound dentine. They found that the fluorescence emission bands of the carious root were shifted to longer wavelengths (red-shifted bands) between 600-700nm. The strongest band for the excitation wavelength was at 405nm which is equivalent to the band of porphyrin compounds. Further studies observed that one of either the organic or inorganic components of healthy dentine that generates green fluorescence partially disappears during the caries process; hence, the red fluorescence appears (Terrer et al., 2009, Salehi et al., 2013). Other studies aimed to examine the role of Streptococcus mutans in the generation of the fluorescence detected in carious lesions. They observed that dentine lesions induced by S. mutans exhibited an increase in red and green fluorescence spectral regions, with a stronger signal in the red region (Lennon et al., 2006, Shigetani et al., 2008). As this substrate has a complete degeneration of collagen structure, it showed a very strong AF intensity associated with a lower SHG signal and a shorter lifetime (Lin et al., 2011).

Additionally, when a photon is absorbed by a fluorescent molecule, electron transition from ground state to excited state and relaxation of the excited molecule then follow, resulting in the emission of photon of reduced energy and with a longer wavelength, termed “fluorescence”. The time required by the molecule to relax before emission is called “fluorescence lifetime” and is influenced by the interaction with the environment (Wang et al., 2018). It is difficult to quantify changes in the microenvironment based on the AF and SHG intensities only, hence, lifetime data was recorded as an additional biological marker, which is not affected by laser fluctuations, wavelengths, fluorophore concentration or quenching (Becker, 2012, Pliss et al., 2015). In an earlier study, short lifetime was reported in carious tissues and was referred to changes in both chemical and physical properties of dentine (Webb et al., 2002). Lifetime can be influenced by the fluorophore environment including polarity, ion concentration, temperature and pH. So, it can be used as a parameter or biological sensor.

Conversely, caries-affected dentine contains mixed reactionary dentine, formed in the response to stimuli like caries, showing some alterations in the cross-linking of its collagen fibrils. Based on the collagen biochemistry of infected and affected dentine, a study by Kuboki et al., (1977) found that there was no difference in the pattern of amino acid composition of collagen fibres between these layers and the sound dentine. However, the intermolecular cross links of collagen fibres were observed to be less in the affected dentine, but these changes seem to be reversible. In contrast, caries-infected dentine cross links and the precursors was remarkably reduced. In addition, the hexitollysines (protein-saccharide, bacterial by-product) were noticed and several peaks of unknown materials appeared. Hence, these changes indicate irreversible destruction of cross-linkage in the caries-infected dentine (Kuboki et al., 1977).

Results of the current study showed a high AF intensity in the caries-affected dentine group but to a lesser extent than the infected dentine. This may indicate the influence of the acidic media in the affected dentine, which induces structural changes, followed by defibrillation of unprotected collagen fibrils due to matrix metalloproteinase enzymes (MMPs) release (Kleter et al., 1998, Carvalho et al., 2009, Lee et al., 2015). Accordingly, the obtained results were in agreement with

the data of a previous study which showed the increase in the AF intensity, shorter lifetime and decrease of SHG signals (Lin et al., 2011).
It has been previously demonstrated that an intense SHG signals can be generated from the sound dentine structure compared to enamel. This was attributed to a strong correlation between collagen and SHG signals (Kim, Eichler et al. 2000, Chen et al. 2007). Therefore, the complete collagen degeneration that happens in the infected dentine and the mild alteration in the affected dentine tissues lead to reduction in SHG signals.

On the other hand, when dentine samples were demineralised by acid-etching, a simple model with partial loss of minerals and intact collagen matrix was obtained. Complete loss of peritubular dentine, demineralisation of intertubular dentine and then increase the number of exposed dentine tubules have been resulted, with potential changes in the collagen configuration and morphological dentine surface area (Zafar and Ahmed, 2015). These changes in demineralised dentine have resulted in the reduction of AF intensity compared to infected and affected dentine but not significantly different from the sound dentine. However, a significant increase in SHG intensity was also observed due to collagen exposure. Lifetime was decreased, and this could be attributed to the low pH of the demineralisation protocol.

Moreover, fluorescence and lifetime data were supported by the Knoop hardness values recorded for the same samples. Knoop hardness number (KHN) indicates the mechanical properties of the dentine substrate and indirectly reflect their mineral content. Therefore, results of infected and affected dentine that indicate increase in AF intensity, reduction in SHG and shorter lifetime, have also shown a reduction in KHN which was attributed to reduction of their mineral content compared to sound dentine. Mineral contents were also confirmed by the variation in phosphate peak intensity recorded by micro-Raman spectroscopy imaging.

Dental caries is a dynamic disease process, which is developed by the imbalance between the demineralisation and remineralisation in dental hard tissues (Featherstone, 2000). From a biological point of view, apatite growth and recrystallisation have been classified into classical and non-classical approaches. Remineralisation can be obtained by classical approach including epitaxial

growth of residual inorganic crystals in the lesion (Kawasaki et al., 1999) and reformation of inorganic mineral-like structure (Cao et al., 2015). Alternatively, an *in-vitro* biomimetic remineralisation approach refers to the "bottom up" remineralisation. This approach doesn't rely on the pre-existence of seed crystallites and may be considered as a feasible method for remineralisation of partially or totally demineralised dentine. Biomineralisation of dentine dictates the presence of intact collagen matrix that can act as a template for mineral deposition together with existence of non-collagenous protein (NCPs) such as dentine matrix protein (DMP1) and dentine phosphoprotein (DPP) (George and Veis, 2008).

Regarding the dentine models used in this work, infected dentine exhibited a degenerated collagen matrix, hence no remineralisation is expected to be seen when interact with any of the applied materials. In contrast, caries-affected dentine and the partially demineralised dentine models have an intact collagen structure which makes them liable to be remineralised if they interact with bioactive materials.

Based on the composition of the introduced dual-cure self-adhesive experimental material DC-HRI, it is claimed that the new acidic adhesive monomer existed in its formulation (phosphoric acid ester of methacrylate) is responsible for the self-adhesion. It also contains double carbon bonds, which makes it capable for a high degree of cross-linking. In addition, the presence of silanated and alkaline fillers make them responsible for neutralisation and buffering process during setting. DC-HRI combines the self-adhesiveness, the anti-cariogenic properties of glass ionomers and the high mechanical strength of the composite bulk-fill restorations. Thereby, they are anticipated to interact with dentine substrates in a similar way to these materials.

Several *in-vitro* studies demonstrated the liability of remineralisation of the artificially demineralised dentine adjacent to glass-ionomer cement (Ten Cate, 1994, Ngo et al., 2006), RMGIC (Creanor et al., 1998) and calcium silicate cements (Tay et al., 2007, Watson et al., 2014, Atmeh et al., 2015). Previous studies have shown the mineral transfer and apatite formation of different dentinal substrates with variable mechanisms when they interact with GIC (Lee et al., 2008, Ngo et al., 2011). Conversely, Watson et al., (2014) reported inability of the

acidic media generated by GIC acid-base reaction to remineralise the demineralised dentine. Moreover, the completely depleted demineralised dentine is unlikely to have any remineralisation due to the lack of crystal seeds in their surface (Kim et al., 2010a).

The results presented in this study showed a favourable increase in the demineralised dentine properties. These changes are presented by an increase in the percentage change of AF intensity and lifetimes. In addition, regaining of the KHN was also noticed, associated with increase in Raman peak intensity, while no change was noticed in SHG after storage with the DC-HRI and EQUIA groups (Fig. 3-6,7,8,9). However, with the carious dentine substrate, the only significant changes were noticed in the caries-infected dentine presented by increase in AF and KHN when interact with DC-HRI and EQUIA. Caries-affected dentine only showed an increase in AF intensity of DC-HRI and EQUIA with no significant changes in other properties when comparing the effect of different materials on this substrate. Both carious substrates showed a significant increase in the mineral peak when compared to the control group, which complement the increase in their fluorescence intensity. However, the interaction of materials with the sound dentine substrate resulted in non-significant changes in their fluorescence intensity, lifetime or Raman phosphate peak intensity.

For the partially demineralised dentine, the organic matrix within these samples was not affected so we can presume any optical changes after sealing with the restorative materials are due to remineralisation of the underlying dentine. Previous studies have proved that GICs can re-mineralise tooth tissues through epitaxial growth of the remaining crystals, when nucleation site pre-exist (Kim et al., 2010b, Atmeh et al., 2015). The possible explanation for such results including that the acidic etching effect of the monomers exists in either DC-HRI or EQUIA can cause a demineralisation of the inorganic dentine contents (Sennou et al., 1999). Therefore, this process triggers the ionic flow of elements from the glass including fluoride, strontium, aluminium and residual hydroxyapatite attached to collagen of the partially demineralised dentine, which in turn neutralise the acidity and induce the mineralisation thus enhancing the fluorescence intensity and FLIM. Moreover, when polyacrylic acid modifies the smear layer, it has numerous carbonyl ions that form hydrogen bonds, which

promote substrate wettability (Pereira et al., 2017). In addition, the presence of phosphate ions within the alkaline PBS storage media favoured these ionic interactions. A previous study performed in our laboratory demonstrated the remineralisation effect of the conventional GIC together with Biodentine™ when bonded to the partially demineralised dentine using the same assessment methods. Han et al. (2011) showed an increase in calcium uptake in the root canal dentine adjacent to Biodentine™ and MTA when they stored in PBS (Han and Okiji, 2011).

Regarding the increase in AF and KHN of the infected dentine group, this indicates an improvement in the ultrastructural properties of this tissue. This was presented by an increase in the mechanical properties like hardness following sealing with materials. These changes may be attributed to precipitation of ions either from storage media or from a GICs with none of the physiological remineralisation, accompanied by Ca^{+2} and PO_4^{-3} diffusion from the underlying dentine as a result of acidic demineralisation. This ion exchange is responsible for the initial bond between the restoration and the dentine surface.

In order to determine the real efficacy and durability of polymeric dental materials, a thorough clinical testing is necessary. However, clinical testing is expensive and impractical as it requires long time to evaluate the effect and success rates. Alternatively, reliable laboratory tests can serve as screening tools to examine the new dental materials and the improvement to the existing materials. Micro-shear bond strength has been claimed to be a reliable test, due to the homogenous stress distribution in the bonding surface of specimens. Stress concentration is reduced due to small sample dimensions thus the failure pattern shifts to adhesive instead of cohesive failure and this will decrease the errors. It could be a feasible test when evaluating brittle materials, having a low modulus of elasticity, such as GICs (Bonifácio et al., 2012). The micro-shear bond test measures more accurately the strength in the adhesive interface (Tedesco et al., 2013).

Bond strength and morphologic two-photon microscopic evaluations results of our study showed that the characteristics of the substrate directly impact the bonds formed. All examined materials have shown significant higher bond strength values, when bonded to the partially demineralised substrate compared

to the sound and carious dentine. Differences in morphology and physical structure of dentine substrates are key factors, which directly influence the formed bonded interfaces. As previously mentioned, partially demineralised dentine has an intact collagen matrix with partial loss of the superficial mineral content. Although the collagen matrix has no direct effect in the bonding mechanism, the minerals that are attached to these collagen fibrils can encourage the ionic exchange between the restoration and dentine. Thus, the resulting bond interface may be enhanced. Dentine acid-etching promotes a protein rich collagen exposure by removal of the smear layer and dentine plugs, thereby changes the surface free energy of the dentine and enhances the dentine wettability (Gopalakrishna, 2009, Hamama et al., 2014). It also provides additional micro-mechanical retention (Imbery et al., 2013), along with ion-exchange between the PAA carboxyl group in the GIC, calcium and phosphate from the tooth, which improve the bond strength (Korkmaz et al., 2010, El-Askary and Nassif, 2011, Inoue et al., 2012).

Moreover, the type of the material used has also influenced the bond strength values. This was demonstrated by the high bond strength of the Filtek Bulk Fill resin composite group compared to other materials' groups regardless the type of the substrate. This was supported by other studies showing that Scotchbond Universal adhesive has provided higher bond strength due to both micro-mechanical and chemical adhesion to the dentine. In addition, the presence of 10-MDP in their composition encourages the bonding to the tooth and reduces the bond degradations overtime (Yoshida et al., 2004).

DC-HRI reported higher or equivalent bond strength compared to EQUIA when bonded to different dentine substrates. This can be explained by its superior mechanical properties achieved by the higher cross-linkage between the carbon double bonds of their methacrylate monomer. Additionally, its initial moisture tolerance and hydrophilicity facilitates the good adaptation to the hydrophilic tooth surface. The organic matrix of DC-HRI exhibited a multifunctional phosphoric acid methacrylate which is capable of simultaneously demineralising and infiltrating the dentine surface together with forming an ionic bond with the hydroxyapatite, providing a second means of retention.

The low bond strength of DC-HRI compared to the resin composite group (Filtek Bulk Fill, 3M, USA) may be attributed to the high viscosity of the material and limited penetration ability which requires some pressure during application. In addition, light curing of this material may generate polymerisation stress, contraction of the material and reduction of the bond strength. Likewise, GIC showed low bond strength values due to brittleness, initial sensitivity to moisture contamination and sensitivity to dehydration. Moisture leads the material to be chalky and porous, resulting in a loss of surface hardness (Cook, 1990).

Another factor has influenced the bond strength values is the storage time. An increase in bond strength was noticed after storing GICs when they were bonded to the demineralised dentine. This result was attributed to the maturation process of GIC after ion exchange (Ngo et al., 1997). In contrast, bond strength was decreased when DC-HRI and Bulk Fill were stored and bonded to the CAD. Such findings may be explained by the activation of an endogenous proteolytic enzyme; matrix metalloproteinase (MMPs) that leads to hydrolytic degradation of the bond at the interface and compromises the longevity of the bonded restoration (Inoue et al., 2005, Mazzoni et al., 2006, Longhi et al., 2014). In the literature, results of bonding durability to CAD are still limited and controversial. Some studies reported a decrease in bond strength of different resin adhesives bonded to CAD in different time exposures (Omar et al., 2007, Komori et al., 2009). Other studies reported non-significant changes in bond strength results to CAD following storage (Omar et al., 2007, Erhardt et al., 2008). The possible explanations of such results might be due to the great variability of natural CAD substrate as well as other non-consistent factors between laboratories and different storage media. All of which can affect the final outcome of the study.

One cannot exclude the role of recording pre-test failures of the samples (PTFs) in the interpretation of the bond strength data. In the current study, findings reported the highest PTFs in the CAD storage group, which correlates well with the low bond strength values recorded with this substrate. However, PTFs reduced with the demineralised group which confirms the high bond strength of this group. Nevertheless, PTFs may also be affected by the way of Tygon tube removal which is critical and not easily performed as stress can be induced at the interface yielding a high number of failures and is related to the pressure applied

to the tube. The issue about inclusion or exclusion of PTFs is still controversial in the literature as they are not treated in the same statistical manner by different research groups (Scherrer et al., 2010). The current studies excluded PTFs readings in the statistical analysis as their numbers were high in the caries group and would greatly affect the final result, despite being helpful in understanding and confirming some bond strength data (Saad et al., 2017). If PTFs were included in statistics, it is very likely that the normal distribution of data is lost especially with a high number of failures. It should be also noted that PTFs are usually associated with relatively low bond strength values measured for those samples that didn't fail prior testing.

Results showed generalised adhesive failures in DCHRI and EQUIA Fill groups, whereas cohesive failure in Bulk Fill resin composite group. Although some researchers have claimed a higher bond strength results in more cohesive failure (Scherrer et al., 2010), others claimed that there is no relationship between the bond strength and fracture type (Almuammar et al., 2001). There are lots of factors affecting the mode of failure results including; sample preparation, load force, crosshead speed and the type of test used.

Further assessment of the sealing ability of different dental materials was assessed using the two-photon microscope and revealed the variation in the sealing ability between the materials groups. DC-HRI groups revealed a good adaptation with no gaps or voids noticed. Absorption layer was a characteristic feature noticed in the area adjacent to interface with DC-HRI which was strongly labelled by rhodamine-B dye and wasn't found when examining the interface with EQUIA Fill or Bulk Fill composite. It possibly acts as a stress relief layer to compensate for the polymerisation shrinkage of the restoration (Sidhu et al., 2002).

Few interfacial gaps were noticed at EQUIA/dentine interface which decreased when bonded to the demineralised dentine. The Bulk Fill resin composite group showed voids at the interface (water tree/osmotic blistering) when Scotch bond adhesive was applied in a self-etch mode, that was disappeared when applied on the demineralised/etched dentine surface. None of the tested materials has provided an adequate sealing to the dentine. However, sealing was better with the demineralised dentine compared to the sound dentine group.

In conclusion, the experimental material DC-HRI demonstrated good adhesive properties and potential bioactivity when applied to the partially demineralised dentine or infected dentine, which was comparable to the conventional GICs. This activity is mediated by the phosphate ions in the storage media. The clinical decision on which material to choose should be influenced by other clinical factors. Moreover, the introduced *in-vitro* caries model allowed the evaluation of changes happen across the carious lesion which could be used in different experimental settings. Using two-photon microscopy to achieve fluorescence intensity and lifetime data is a promising less invasive microscopic technique that introduces additional microscopic parameters to investigate dental tissues and to identify/monitor remineralisation within these tissues.

6.5 Suggestions for future work

- **In-situ measurement of pH change during materials setting using FLIM imaging**

As reported earlier, the two-photon FLIM imaging can be used as a reliable biologic marker for imaging dental tissues. Likewise, it is very sensitive to pH change and it provides an indication about the ultrastructural changes of the surrounding environment. Dental materials can set by different setting mechanisms. Whether the material sets by self-curing, dual-curing or light curing, it undergoes changing in their pH during the setting process until neutralization occurs. Examining the setting chemistry of dental materials using high resolution in-situ pH measurements can be beneficial. Initially, a series of dye-dosed (LysoSensor Yellow/Blue DND-160 pH indicator dye) TRIS buffer solutions is prepared ranging from pH2 – pH7.5 to create a pH standard curve versus FLIM imaging. The material then labeled with the same pH indicator dye. This can be used in exploring the pH changes during DC-HRI setting compared to both self-cure/light cure GICs and light cure RMGIC controls. Performing this study can provides valuable accurate information about the acidity of the material when clinically applied in managing deep carious lesions. This study is currently being carried out by one of the postdocs in our department.

- ***In-vitro*** **evaluation of different caries excavation methods and their effect on chemical properties and morphology of DC-HRI/dentine interaction**

Intact carious dentine model was used in this thesis without any caries excavation to examine the effect of the applied materials on all carious zones. However, a more clinically related model has to be created using any mean of caries excavation approaches to perform cavities. Carisolv gel, rotary burs, polymer burs or laser excavation can be used to excavate deep carious lesions with no pulp exposure, and then cavities are subdivided randomly and restored with different coronal restorative materials including Biodentine, DC-HRI, GIC and RMGICs with a control (no material) group. This protocol is aiming to compare the effect of these materials on the interfacial chemical and morphological properties of the dentine substrate left following different caries excavation techniques to those before materials application. *In-vitro* evaluation using

transverse micoradiography (TMR), for mineral density and mineral profile detection, and nonohardness, for tissue hardness assessment, can be performed before and following 3- and 6-months storage in PBS solution. The mean mineral density values at different depths up to 150 µm will be calculated as well as nanohardness measurements on the cross-section view of dentine. These evaluations might be assisted by SEM evaluation following fracture of the dentine/ materials interface on representative samples of different materials and control groups.

- **Monitoring Demineralization and Subsequent Remineralization at dentine/materials interface using optical coherence tomography (OCT).**

In this thesis, simple demineralisation model was used, exhibited partial mineral loss and intact collagen fibres. However, for a better comparison with the natural caries-affected dentine, laboratory methods for artificial caries creation must be applied such as pH-cycling or bacterial methods which highly recommended methods are to mimic CAD. Bacterial methods were criticised for their time-consuming protocol and more softening of the dentine surface. Therefore, pH cycling is performed on half surface of the natural dentine slices, while covering the other half as an internal control. Following pH cycling method, the demineralised depth of the dentine substrate is measured using OCT and Raman imaging compared to the sound control. Understanding the depth and chemical profile of the demineralised dentine is important for improving reliability and durability of the restorative materials. Both quantitative and qualitative evaluation can be obtained. The applied imaging techniques are non-invasive which can help in detection of the lesion depth and subsequent remineralisation if occurs. Dentine slices are then distributed randomly into two restoration groups (Biodentine and DC-HRI) with a control group with no material to be stored in PBS. The materials/dentine interface then is exposed to image and measure if remineralisation occurs.

- **Nanomechanical properties of Novel DC-HRI materials and depth of cure evaluations**

To determine by nanoindentation the hardness and elastic modulus of DC-HRI compared with bulk-fill and conventional nano-hybrid resin composites. In addition, comparative evaluation of the depth of cure of these materials to evaluate their degree of conversion using Fourier Transform Infrared (FTIR) spectroscopy method. For the nanoindentation test, disc specimens (15 mm × 2 mm) are prepared from each material using the metallic mold. Specimens are irradiated in the mold at top and bottom surfaces using a Deep Cure-S LED curing light (3M, USA) with the light intensity 1470 mW/cm^2 (-10%/+20%). Specimens are then mounted in 3 cm diameter phenolic ring forms and embedded in a self-curing polystyrene resin and stored in distilled water at 37 °C for 7 days. Nanoindentations (n=30) are then applied using the load (10 mN). For the depth of cure measurements, other set of specimens are prepared. Depth of cure is determined according to "ISO 4049; Depth of Cure" method, and FTIR spectroscopy method is used to estimate the degree of conversion of the bulk fill composites, conventional nano-hybrid composites and DC-HRI.

Appendix

Ethical approval

Health Research Authority

Prof Tim Watson
Professor of Biomaterials & Restorative Dentistry
King's College London Dental Institute
Biomaterials Research Group
Floor 17 Guy's Tower
King's College London
SE1 9RT

Email:
hra.approval@nhs.net

19 January 2017

Dear Prof Watson

Letter of HRA Approval

Study title:	**Improving Caries and Toothwear Management Techniques**
IRAS project ID:	**157705**
Protocol number:	**N/A**
REC reference:	**16/SW/0220**
Sponsor	**King's College London**

I am pleased to confirm that **HRA Approval** has been given for the above referenced study, on the basis described in the application form, protocol, supporting documentation and any clarifications noted in this letter.

Participation of NHS Organisations in England

The sponsor should now provide a copy of this letter to all participating NHS organisations in England.

Appendix B provides important information for sponsors and participating NHS organisations in England for arranging and confirming capacity and capability. **Please read *Appendix B* carefully**, in particular the following sections:

- *Participating NHS organisations in England* – this clarifies the types of participating organisations in the study and whether or not all organisations will be undertaking the same activities
- *Confirmation of capacity and capability* - this confirms whether or not each type of participating NHS organisation in England is expected to give formal confirmation of capacity and capability. Where formal confirmation is not expected, the section also provides details on the time limit given to participating organisations to opt out of the study, or request additional time, before their participation is assumed.
- *Allocation of responsibilities and rights are agreed and documented (4.1 of HRA assessment criteria)* - this provides detail on the form of agreement to be used in the study to confirm capacity and capability, where applicable.

Further information on funding, HR processes, and compliance with HRA criteria and standards is also provided.

It is critical that you involve both the research management function (e.g. R&D office) supporting each organisation and the local research team (where there is one) in setting up your study. Contact details and further information about working with the research management function for each organisation can be accessed from www.hra.nhs.uk/hra-approval.

Appendices

The HRA Approval letter contains the following appendices:

- A – List of documents reviewed during HRA assessment
- B – Summary of HRA assessment

After HRA Approval

The document *"After Ethical Review – guidance for sponsors and investigators"*, issued with your REC favourable opinion, gives detailed guidance on reporting expectations for studies, including:

- Registration of research
- Notifying amendments
- Notifying the end of the study

The HRA website also provides guidance on these topics, and is updated in the light of changes in reporting expectations or procedures.

In addition to the guidance in the above, please note the following:

- HRA Approval applies for the duration of your REC favourable opinion, unless otherwise notified in writing by the HRA.
- Substantial amendments should be submitted directly to the Research Ethics Committee, as detailed in the *After Ethical Review* document. Non-substantial

amendments should be submitted for review by the HRA using the form provided on the HRA website, and emailed to hra.amendments@nhs.net.

- The HRA will categorise amendments (substantial and non-substantial) and issue confirmation of continued HRA Approval. Further details can be found on the HRA website.

Scope

HRA Approval provides an approval for research involving patients or staff in NHS organisations in England.

If your study involves NHS organisations in other countries in the UK, please contact the relevant national coordinating functions for support and advice. Further information can be found at http://www.hra.nhs.uk/resources/applying-for-reviews/nhs-hsc-rd-review/.

If there are participating non-NHS organisations, local agreement should be obtained in accordance with the procedures of the local participating non-NHS organisation.

User Feedback

The Health Research Authority is continually striving to provide a high quality service to all applicants and sponsors. You are invited to give your view of the service you have received and the application procedure. If you wish to make your views known please email the HRA at hra.approval@nhs.net. Additionally, one of our staff would be happy to call and discuss your experience of HRA Approval.

HRA Training

We are pleased to welcome researchers and research management staff at our training days – see details at http://www.hra.nhs.uk/hra-training/

Your IRAS project ID is **157705**. Please quote this on all correspondence.

Yours sincerely

Rekha Keshvara

Assessor

Email: hra.approval@nhs.net

Copy to: *Mr Keith Brennan*

Ms Jen Boston, Guy's and St Thomas' NHS Foundation Trust

Appendix A - List of Documents

The final document set assessed and approved by HRA Approval is listed below.

Document	*Version*	*Date*
Covering letter on headed paper [Covering letter]	1	23 June 2016
IRAS Application Form [IRAS_Form_14072016]		14 July 2016
IRAS Checklist XML [Checklist_14072016]		14 July 2016
Participant consent form [Perticipant Consent Form]	1	23 June 2016
Participant information sheet (PIS) [Information Sheet]	1	23 June 2016
Research protocol or project proposal [Research Protocol]	1	23 June 2016
Summary CV for Chief Investigator (CI) [Tim Watson Summary CV]	1	23 June 2016
Summary, synopsis or diagram (flowchart) of protocol in non technical language [Summary Flowchart]	1	

Appendix B - Summary of HRA Assessment

This appendix provides assurance to you, the sponsor and the NHS in England that the study, as reviewed for HRA Approval, is compliant with relevant standards. It also provides information and clarification, where appropriate, to participating NHS organisations in England to assist in assessing and arranging capacity and capability.

For information on how the sponsor should be working with participating NHS organisations in

England, please refer to the, *participating NHS organisations*, *capacity and capability* and *Allocation of responsibilities and rights are agreed and documented (4.1 of HRA assessment criteria)* sections in this appendix.

The following person is the sponsor contact for the purpose of addressing participating organisation questions relating to the study:

Keith Brennan
Email: keith.brennan@kcl.ac.uk
Tel: 02078486960

HRA assessment criteria

Section	HRA Assessment Criteria	Compliant with Standards	Comments

1.1	IRAS application completed correctly	Yes	No comments
2.1	Participant information/consent documents and consent process	Yes	No comments
3.1	Protocol assessment	Yes	No comments
4.1	Allocation of responsibilities and rights are agreed and documented	Yes	Statement of activities & schedule of events or any other study agreement is not expected for this study as the single NHS site participating in this study is also the co-sponsor of the study.
4.2	Insurance/indemnity arrangements assessed	Yes	Where applicable, independent contractors (e.g. General Practitioners) should ensure that the professional indemnity provided by their medical
Section	**HRA Assessment Criteria**	**Compliant with Standards**	**Comments**
			defence organisation covers the activities expected of them for this research study
4.3	Financial arrangements assessed	Yes	No application for external funding has been made.
5.1	Compliance with the Data Protection Act and data security issues assessed	Yes	No comments
5.2	CTIMPS – Arrangements for compliance with the Clinical Trials Regulations assessed	Not Applicable	No comments
5.3	Compliance with any applicable laws or regulations	Yes	Human Tissue Act is applicable.

6.1	NHS Research Ethics Committee favourable opinion received for applicable studies	Yes	No comments
6.2	CTIMPS – Clinical Trials Authorisation (CTA) letter received	Not Applicable	No comments
6.3	Devices – MHRA notice of no objection received	Not Applicable	No comments
6.4	Other regulatory approvals and authorisations received	Not Applicable	No comments

Participating NHS Organisations in England

This provides detail on the types of participating NHS organisations in the study and a statement as to whether the activities at all organisations are the same or different.

There is only one NHS organisation taking part in the study, there is therefore one type of participating organisation undertaking the research activity as detailed in the study protocol.

If this study is subsequently extended to other NHS organisation(s) in England, an amendment should be submitted to the HRA, with a Statement of Activities and Schedule of Events for the newly participating NHS organisation(s) in England.

The Chief Investigator or sponsor should share relevant study documents with participating NHS organisations in England in order to put arrangements in place to deliver the study. The documents should be sent to both the local study team, where applicable, and the office providing the research management function at the participating organisation. For NIHR CRN Portfolio studies, the Local LCRN contact should also be copied into this correspondence. For further guidance on working with participating NHS organisations please see the HRA website.

If chief investigators, sponsors or principal investigators are asked to complete site level forms for participating NHS organisations in England which are not provided in IRAS or on the HRA website, the chief investigator, sponsor or principal investigator should notify the HRA immediately at hra.approval@nhs.net. The HRA will work with these organisations to achieve a consistent approach to information provision.

Confirmation of Capacity and Capability

This describes whether formal confirmation of capacity and capability is expected from participating NHS organisations in England.

This is a single site study co-sponsored by the site. The R&D office will confirm to the CI when the study can start.

Principal Investigator Suitability

This confirms whether the sponsor position on whether a PI, LC or neither should be in place is correct for each type of participating NHS organisation in England and the minimum expectations for education, training and experience that PIs should meet (where applicable).
A Principal Investigator is expected to be in place at the NHS organisation. GCP training is not a generic training expectation, in line with the HRA statement on training expectations.

HR Good Practice Resource Pack Expectations

This confirms the HR Good Practice Resource Pack expectations for the study and the pre-engagement checks that should and should not be undertaken
Honorary research contracts and letters of access will not be expected for this study as it is limited to using fully anonymised extracted samples that will be carried as part of routine care.

Other Information to Aid Study Set-up

This details any other information that may be helpful to sponsors and participating NHS organisations in England to aid study set-up.
☐ The applicant has indicated that they do not intend to apply for inclusion on the NIHR CRN Portfolio.

Appendix C- Test of Normality

Before storage:

Tests of Normality

		Kolmogorov-Smirnov			Shapiro-Wilk		
	Group	Statistic	Df	Sig.	Statistic	df	Sig.
AF	Infected	.102	53	.200*	.973	53	.261
	Affected	.114	53	.083	.973	53	.270
	Demin	.115	53	.076	.895	53	.067
	Sound	.113	53	.089	.976	53	.375

*. This is a lower bound of the true significance.

Tests of Normality

		Kolmogorov-Smirnov			Shapiro-Wilk		
	Group	Statistic	Df	Sig.	Statistic	df	Sig.
SHG	Infected	.081	53	.200*	.960	53	.075
	Affected	.105	53	.200*	.966	53	.136
	Demin	.165	53	.200*	.959	53	.062
	Sound	.096	53	.200*	.964	53	.063

*. This is a lower bound of the true significance.

Tests of Normality

		Kolmogorov-Smirnov			Shapiro-Wilk		
	Group	Statistic	Df	Sig.	Statistic	df	Sig.
FLIM	Infected	.120	53	. .200*	.934	53	.066
	Affected	.074	53	.200*	.981	53	.569
	Demin	.095	53	.200*	.955	53	.062
	Sound	.059	53	.200*	.991	53	.951

*. This is a lower bound of the true significance.

Tests of Normality

		Kolmogorov-Smirnov			Shapiro-Wilk		
	Group	Statistic	Df	Sig.	Statistic	df	Sig.
KHN	Infected	.124	53	.073	.936	53	.061
	Affected	.103	53	.200*	.962	53	.095
	Demin	.068	53	.200*	.989	53	.900
	Sound	.077	53	.200*	.975	53	.319

*. This is a lower bound of the true significance.

After Storage:

Tests of Normality

		Kolmogorov-Smirnov			Shapiro-Wilk		
	group	Statistic	Df	Sig.	Statistic	df	Sig.
AF	Infected	.123	22	.200*	.948	22	.282
	Affected	.111	22	.200*	.961	22	.500
	Demin	.122	22	.200*	.986	22	.276
	Sound	.151	22	.200*	.897	22	.115

Tests of Normality

		Kolmogorov-Smirnov			Shapiro-Wilk		
	group	Statistic	Df	Sig.	Statistic	df	Sig.
SHG	Infected	.168	22	.105	.922	22	.085
	Affected	.122	22	.200*	.933	22	.138
	Demin	.194	22	.200*	.946	22	.224
	Sound	.121	22	.200*	.931	22	.126

Tests of Normality

		Kolmogorov-Smirnov			Shapiro-Wilk		
	group	Statistic	df	Sig.	Statistic	df	Sig.
KHN	Infected	.168	22	.200*	.900	22	.062
	Affected	.103	22	.200*	.963	22	.554
	Demin	.116	22	.200*	.965	22	.607
	Sound	.125	22	.200*	.961	22	.510

Tests of Normality

		Kolmogorov-Smirnov			Shapiro-Wilk		
group	Statistic	df	Sig.	Statistic	df	Sig.	
FLIM	Infected	.115	22	.200*	.950	22	.315
	Affected	.181	22	.200*	.894	22	.071
	Demin	.138	22	.200*	.956	22	.409
	Sound	.190	22	.068	.882	22	.061

*. This is a lower bound of the true significance.

Tests of Normality

		Kolmogorov-Smirnov			Shapiro-Wilk		
	group	Statistic	df	Sig.	Statistic	df	Sig.
RAMAN	Infected	.142	17	.200*	.940	17	.351
	Affected	.198	17	.076	.935	17	.263
	Demin	.210	17	.200*	.837	17	.065
	Sound	.176	17	.170	.897	17	.068

References

Abogazalah, N., Eckert, G.J. and Ando, M., 2017. In vitro performance of near infrared light transillumination at 780-nm and digital radiography for detection of non-cavitated approximal caries. *Journal of dentistry*, *63*, pp.44-50.

Aguilar-Mendoza, J. A., Rosales-Leal, J. I., Rodríguez-Valverde, M. A. & Cabrerizo-Vílchez, M. A. 2008. Effect Of Acid Etching On Dentin Wettability And Roughness: Self-Etching Primers Versus Phosphoric Acid. *Journal Of Biomedical Materials Research Part B: Applied Biomaterials,* 84**,** 277-285.

Akkus, A., Karasik, D. & Roperto, R. 2017. Correlation Between Micro-Hardness And Mineral Content In Healthy Human Enamel. *Journal Of Clinical And Experimental Dentistry,* 9**,** E569.

Angker, L., Nockolds, C., Swain, M.V. And Kilpatrick, N., 2004. Correlating The Mechanical Properties To The Mineral Content Of Carious Dentine—A Comparative Study Using An Ultra-Micro Indentation System (Umis) And Sem-Bse Signals. *Archives Of Oral Biology*, *49*(5), Pp.369-378.

Al-Assaf, K., Chakmakchi, M., Palaghias, G., Karanika-Kouma, A. & Eliades, G. 2007. Interfacial Characteristics Of Adhesive Luting Resins And Composites With Dentine. *Dental Materials,* 23**,** 829-839.

Alfano, R., Lam, W., Zarrabi, H., Alfano, M. & Cordero, J. 1984. Human Teeth With And Without Caries Studied By Laser Scattering, Fluorescence, And Absorption Spectroscopy. *Ieee Journal Of Quantum Electronics,* 20**,** 1512-1516.

Almahdy, A., Downey, F., Sauro, S., Cook, R., Sherriff, M., Richards, D., Watson, T., Banerjee, A. & Festy, F. 2012. Microbiochemical Analysis Of Carious Dentine Using Raman And Fluorescence Spectroscopy. *Caries Research,* 46**,** 432-440.

Almuammar, M., Schulman, A. & Salama, F. 2001. Shear Bond Strength Of Six Restorative Materials. *Journal Of Clinical Pediatric Dentistry,* 25**,** 221-225.

Alves, F., Lenzi, T., Reis, A., Loguercio, A., Carvalho, T. & Raggio, D. 2013. Bonding Of Simplified Adhesive Systems To Caries-Affected Dentin Of Primary Teeth. *J Adhes Dent,* 15**,** 439-45.

References

Amaechi, B., Higham, S. & Edgar, W. 1998. Factors Affecting The Development Of Carious Lesions In Bovine Teeth In Vitro. *Archives Of Oral Biology,* 43**,** 619-628.

An, A. & Salama, F. 2001. Shear Bond Strength Of Six Restorative Materials. *Journal Of Clinical Pediatric Dentistry,* 25**,** 221-225.

Andrade, A.M.D., Moura, S.K., Reis, A., Loguercio, A.D., Garcia, E.J. And Grande, R.H.M., 2010. Evaluating Resin-Enamel Bonds By Microshear And Microtensile Bond Strength Tests: Effects Of Composite Resin. *Journal Of Applied Oral Science*, *18*(6), Pp.591-598

Alves, L. S., Fontanella, V., Damo, A. C., De Oliveira, E. F. & Maltz, M. 2010. Qualitative And Quantitative Radiographic Assessment Of Sealed Carious Dentin: A 10-Year Prospective Study. *Oral Surgery, Oral Medicine, Oral Pathology, Oral Radiology And Endodontics,* 109**,** 135-141.

Andrade, A. M. D., Moura, S. K., Reis, A., Loguercio, A. D., Garcia, E. J. & Grande, R. H. M. 2010. Evaluating Resin-Enamel Bonds By Microshear And Microtensile Bond Strength Tests: Effects Of Composite Resin. *Journal Of Applied Oral Science,* 18**,** 591-598.

Anseth, K., Newman, S. & Bowman, C. 1995. Polymeric Dental Composites: Properties And Reaction Behavior Of Multimethacrylate Dental Restorations. *Biopolymers Ii.* Springer.

Antonucci, J., Mckinney, J. & Stansbury, J. 1988. Resin-Modified Glass-Ionomer Dental Cements Field Of The Invention. *Us Patent Application,* 7160856**,** 175-179.

Arends, J. & Ten Bosch, J. 1992. Demineralization And Remineralization Evaluation Techniques. *Journal Of Dental Research,* 71.

Armstrong, S., Geraldeli, S., Maia, R., Raposo, L. H. A., Soares, C. J. & Yamagawa, J. 2010. Adhesion To Tooth Structure: A Critical Review Of “Micro” Bond Strength Test Methods. *Dental Materials,* 26**,** E50-E62.

Armstrong, W. 1963. Fluorescence Characteristics Of Sound And Carious Human Dentine Preparations. *Archives Of Oral Biology,* 8**,** 79-90.

Armstrong, S., Breschi, L., Özcan, M., Pfefferkorn, F., Ferrari, M. and Van Meerbeek, B., 2017. Academy of Dental Materials guidance on in vitro testing of dental composite bonding effectiveness to dentin/enamel using

micro-tensile bond strength (μTBS) approach. *Dental Materials*, *33*(2), pp.133-143.

Arrais, C. A. G., Giannini, M., Nakajima, M. & Tagami, J. 2004. Effects Of Additional And Extended Acid Etching On Bonding To Caries-Affected Dentine. *European Journal Of Oral Sciences,* 112**,** 458-464.

Asmussen, E. & Peutzfeldt, A. 2002. Long-Term Fluoride Release From A Glass Ionomer Cement, A Compomer, And From Experimental Resin Composites. *Acta Odontologica Scandinavica,* 60**,** 93-97.

Atmeh, A., Chong, E., Richard, G., Boyde, A., Festy, F. & Watson, T. 2015. Calcium Silicate Cement-Induced Remineralisation Of Totally Demineralised Dentine In Comparison With Glass Ionomer Cement: Tetracycline Labelling And Two-Photon Fluorescence Microscopy. *Journal Of Microscopy,* 257**,** 151-160.

Atmeh, A., Chong, E., Richard, G., Festy, F. & Watson, T. 2012. Dentin-Cement Interfacial Interaction: Calcium Silicates And Polyalkenoates. *Journal Of Dental Research,* 91**,** 454-459.

Ayar, M. K., Yildirim, T. & Yesilyurt, C. 2016. Nanoleakage Within Adhesive-Dentin Interfaces Made With Simplified Ethanol-Wet Bonding. *Journal Of Adhesion Science And Technology,* 30**,** 2511-2521.

Bader, J.D., Shugars, D.A. and Bonito, A.J., 2001. Systematic reviews of selected dental caries diagnostic and management methods. *Journal of dental education*, *65*(10), pp.960-968.

Baldwin, G. C. 2012. *An Introduction To Nonlinear Optics*, Springer Science & Business Media.

Balooch, M., Habelitz, S., Kinney, J., Marshall, S. & Marshall, G. 2008. Mechanical Properties Of Mineralized Collagen Fibrils As Influenced By Demineralization. *Journal Of Structural Biology,* 162**,** 404-410.

Banerjee, A. & Doméjean, S. 2013. The Contemporary Approach To Tooth Preservation: Minimum Intervention (Mi) Caries Management In General Practice. *Primary Dental Journal,* 2**,** 30-37.

Banerjee, A., Kidd, E. & Watson, T. 2000. In Vitro Evaluation Of Five Alternative Methods Of Carious Dentine Excavation. *Caries Research,* 34**,** 144-150.

References

Banerjee, A. 1999. *Applications Of Scanning Microscopy In The Assessment Of Dentine Caries And Methods For Its Removal.* King's College London (University Of London).

Banerjee, A. 2013. Minimal Intervention Dentistry: Part 7. Minimally Invasive Operative Caries Management: Rationale And Techniques. *British Dental Journal,* 214**,** 107.

Banerjee, A. & Boyde, A. 1998. Autofluorescence And Mineral Content Of Carious Dentine: Scanning Optical And Backscattered Electron Microscopic Studies. *Caries Research,* 32**,** 219-226.

Banerjee, A., Cook, R., Kellow, S., Shah, K., Festy, F., Sherriff, M. & Watson, T. 2010a. A Confocal Micro-Endoscopic Investigation Of The Relationship Between The Microhardness Of Carious Dentine And Its Autofluorescence. *European Journal Of Oral Sciences,* 118**,** 75-79.

Banerjee, A. & Doméjean, S. 2013. The Contemporary Approach To Tooth Preservation: Minimum Intervention (Mi) Caries Management In General Practice. *Primary Dental Journal,* 2**,** 30-37.

Banerjee, A., Hajatdoost-Sani, M., Farrell, S. & Thompson, I. 2010b. A Clinical Evaluation And Comparison Of Bioactive Glass And Sodium Bicarbonate Air-Polishing Powders. *Journal Of Dentistry,* 38**,** 475-479.

Banerjee, A. & Watson, T. F. 2015. *Pickard's Guide To Minimally Invasive Operative Dentistry*, Oup Oxford.

Banerjee, A. 2013. Minimal Intervention Dentistry: Part 7. Minimally Invasive Operative Caries Management: Rationale And Techniques. *British Dental Journal,* 214**,** 107.

Banerjee, A. & Boyde, A. 1998. Autofluorescence And Mineral Content Of Carious Dentine: Scanning Optical And Backscattered Electron Microscopic Studies. *Caries Research,* 32**,** 219-226.

Banerjee, A., Kellow, S., Mannocci, F., Cook, R. & Watson, T. 2010b. An In Vitro Evaluation Of Microtensile Bond Strengths Of Two Adhesive Bonding Agents To Residual Dentine After Caries Removal Using Three Excavation Techniques. *Journal Of Dentistry,* 38**,** 480-489.

Banerjee, A., Watson, T. & Kidd, E. 2000. Conservative Dentistry: Dentine Caries Excavation: A Review Of Current Clinical Techniques. *British Dental Journal,* 188**,** 476.

Barkmeier, W. & Cooley, R. 1992. Laboratory Evaluation Of Adhesive Systems. *Operative Dentistry***,** 50-61.

Barkmeier, W., Shaffer, S. & Gwinnett, A. 1986. Effects Of 15 Vs 60 Second Enamel Acid Conditioning On Adhesion And Morphology. *Operative Dentistry,* 11**,** 111-116.

Bayne, S. 2007. Dental Restorations For Oral Rehabilitation–Testing Of Laboratory Properties Versus Clinical Performance For Clinical Decision Making. *Journal Of Oral Rehabilitation,* 34**,** 921-932.

Becker, W., Bergmann, A., Haustein, E., Petrasek, Z., Schwille, P., Biskup, C., Kelbauskas, L., Benndorf, K., Klöcker, N. & Anhut, T. 2006. Fluorescence Lifetime Images And Correlation Spectra Obtained By Multidimensional Time-Correlated Single Photon Counting. *Microscopy Research And Technique,* 69**,** 186-195.

Beech, D. 1973. Improvement In The Adhesion Of Polyacrylate Cements To Human Dentine. *British Dental Journal,* 135**,** 442-445.

Bellahcène, A., Castronovo, V., Ogbureke, K. U., Fisher, L. W. & Fedarko, N. S. 2008. Small Integrin-Binding Ligand N-Linked Glycoproteins (Siblings): Multifunctional Proteins In Cancer. *Nature Reviews Cancer,* 8**,** 212.

Benedict, H. 1928. Note On Fluorescence Of Teeth In Ultraviolet Rays. *Science,* 67**,** 442.

Berezin, M. Y. & Achilefu, S. 2010. Fluorescence Lifetime Measurements And Biological Imaging. *Chemical Reviews,* 110**,** 2641-2684.

Bergenholtz, G. 2000. Evidence For Bacterial Causation Of Adverse Pulpal Responses In Resin-Based Dental Restorations. *Critical Reviews In Oral Biology & Medicine,* 11**,** 467-480.

Berry, E. A., 3rd & Powers, J. M. 1994. Bond Strength Of Glass Ionome

Bedran-Russo, A. K., Pauli, G. F., Chen, S.-N., Mcalpine, J., Castellan, C. S., Phansalkar, R. S., Aguiar, T. R., Vidal, C. M., Napotilano, J. G. & Nam, J.-W. 2014. Dentin Biomodification: Strategies, Renewable Resources And Clinical Applications. *Dental Materials,* 30**,** 62-76.

Berg, J. H. & Croll, T. P. 2015. Glass Ionomer Restorative Cement Systems: An Update. *Pediatric Dentistry,* 37**,** 116-124.

Berry, E. A., 3rd & Powers, J. M. 1994. Bond Strength Of Glass Ionomers To Coronal And Radicular Dentin. *Oper Dent,* 19**,** 122-6.

References

Bertassoni, L. E., Habelitz, S., Kinney, J., Marshall, S. J. & Marshall Jr, G. W. 2009. Biomechanical Perspective On The Remineralization Of Dentin. *Caries Research,* 43**,** 70-77.

Bertassoni, L. E., Habelitz, S., Marshall, S. J. & Marshall, G. W. 2011. Mechanical Recovery Of Dentin Following Remineralization In Vitro—An Indentation Study. *Journal Of Biomechanics,* 44**,** 176-181.

Berzins, D. W., Abey, S., Costache, M., Wilkie, C. A. & Roberts, H. 2010. Resin-Modified Glass-Ionomer Setting Reaction Competition. *Journal Of Dental Research,* 89**,** 82-86.

Billington, R., Williams, J. & Pearson, G. 2006. Ion Processes In Glass Ionomer Cements. *Journal Of Dentistry,* 34**,** 544-555.

Blue, C., Giuffre, A., Mergelsberg, S., Han, N., De Yoreo, J. & Dove, P. 2017. Chemical And Physical Controls On The Transformation Of Amorphous Calcium Carbonate Into Crystalline Caco 3 Polymorphs. *Geochimica Et Cosmochimica Acta,* 196**,** 179-196.

Bohren, C. F. & Huffman, D. R. 2008. *Absorption And Scattering Of Light By Small Particles*, John Wiley & Sons.

Bowen, W. H. 2013. Rodent Model In Caries Research. *Odontology,* 101**,** 9-14.

Bjørndal, L. & Mjör, I. A. 2001. Pulp-Dentin Biology In Restorative Dentistry. Part 4: Dental Caries--Characteristics Of Lesions And Pulpal Reactions. *Quintessence International,* 32.

Bjørndal, L., Reit, C., Bruun, G., Markvart, M., Kjældgaard, M., Näsman, P., Thordrup, M., Dige, I., Nyvad, B. & Fransson, H. 2010. Treatment Of Deep Caries Lesions In Adults: Randomized Clinical Trials Comparing Stepwise Vs. Direct Complete Excavation, And Direct Pulp Capping Vs. Partial Pulpotomy. *European Journal Of Oral Sciences,* 118**,** 290-297.

Bonifácio, C. C., Shimaoka, A. M., De Andrade, A. P., Raggio, D. P., Van Amerongen, W. E. & De Carvalho, R. C. R. 2012. Micro-Mechanical Bond Strength Tests For The Assessment Of The Adhesion Of Gic To Dentine. *Acta Odontologica Scandinavica,* 70**,** 555-563.

Braga, R. R., Meira, J. B., Boaro, L. C. & Xavier, T. A. 2010. Adhesion To Tooth Structure: A Critical Review Of “Macro” Test Methods. *Dental Materials,* 26**,** E38-E49.

Brockbank, K. G., Maclellan, W. R., Xie, J., Hamm-Alvarez, S. F., Chen, Z. Z. & Schenke-Layland, K. 2008. Quantitative Second Harmonic Generation Imaging Of Cartilage Damage. *Cell Tissue Bank,* 9**,** 299-307.

Buchalla, W., Lennon, A. & Attin, T. 2004. Fluorescence Spectroscopy Of Dental Calculus. *Journal Of Periodontal Research,* 39**,** 327-332.

Bucuta S., Ilie N., Light transmittance and micro-mechanical properties of bulk fill vs. conventional resin based composites, Clin. Oral Investig. 18:1991-2000 (2014).

Buonocore, M. G. 1955. A Simple Method Of Increasing The Adhesion Of Acrylic Filling Materials To Enamel Surfaces. *Journal Of Dental Research,* 34**,** 849-853.

Burke, F. & Lynch, E. 1994. Glass Polyalkenoate Bond Strength To Dentine After Chemomechanical Caries Removal. *Journal Of Dentistry,* 22**,** 283-291.

Burrow, M., Bokas, J., Tanumiharja, M. & Tyas, M. 2003. Microtensile Bond Strengths To Caries-Affected Dentine Treated With Carisolv. *Australian Dental Journal,* 48**,** 110-114.

Butler, D. L., Grood, E. S., Noyes, F. R., Zernicke, R. F. & Brackett, K. 1984. Effects Of Structure And Strain Measurement Technique On The Material Properties Of Young Human Tendons And Fascia. *Journal Of Biomechanics,* 17**,** 579-596.

Buzalaf, M. A. R., Hannas, A. R., Magalhães, A. C., Rios, D., Honório, H. M. & Delbem, A. C. B. 2010. Ph-Cycling Models For In Vitro Evaluation Of The Efficacy Of Fluoridated Dentifrices For Caries Control: Strengths And Limitations. *Journal Of Applied Oral Science,* 18**,** 316-334.

Camilleri, J. 2011. Characterization And Hydration Kinetics Of Tricalcium Silicate Cement For Use As A Dental Biomaterial. *Dental Materials,* 27**,** 836-844.

Cao, Y., Mei, M. L., Xu, J., Lo, E. C., Li, Q. & Chu, C. H. 2013. Biomimetic Mineralisation Of Phosphorylated Dentine By Cpp-Acp. *Journal Of Dentistry,* 41**,** 818-825.

Carvalho, R. M., Manso, A. P., Geraldeli, S., Tay, F. R. & Pashley, D. H. 2012. Durability Of Bonds And Clinical Success Of Adhesive Restorations. *Dental Materials,* 28**,** 72-86.

Ceballos, L., Camejo, D. G., Fuentes, M. V., Osorio, R., Toledano, M., Carvalho, R. M. & Pashley, D. H. 2003. Microtensile Bond Strength Of Total-Etch

And Self-Etching Adhesives To Caries-Affected Dentine. *Journal Of Dentistry,* 31**,** 469-477.

Chai, D., Gaster, R. N., Roizenblatt, R., Juhasz, T., Brown, D. J. & Jester, J. V. 2011. Quantitative Assessment Of Uva-Riboflavin Corneal Cross-Linking Using Nonlinear Optical Microscopy. *Investigative Ophthalmology & Visual Science,* 52**,** 4231-4238.

Chaussain-Miller, C., Fioretti, F., Goldberg, M. & Menashi, S. 2006. The Role Of Matrix Metalloproteinases (Mmps) In Human Caries. *Journal Of Dental Research,* 85**,** 22-32.

Chen, C.-C., Ho, C.-C., Chen, C.-H. D., Wang, W.-C. & Ding, S.-J. 2009. In Vitro Bioactivity And Biocompatibility Of Dicalcium Silicate Cements For Endodontic Use. *Journal Of Endodontics,* 35**,** 1554-1557.

Chen, M.-H., Chen, W.-L., Sun, Y., Fwu, P. T. & Dong, C.-Y. 2007. Multiphoton Autofluorescence And Second-Harmonic Generation Imaging Of The Tooth. *Journal Of Biomedical Optics,* 12**,** 064018.

Chen, Z., Cao, S., Wang, H., Li, Y., Kishen, A., Deng, X., Yang, X., Wang, Y., Cong, C. & Wang, H. 2015. Biomimetic Remineralization Of Demineralized Dentine Using Scaffold Of Cmc/Acp Nanocomplexes In An In Vitro Tooth Model Of Deep Caries. *Plos One,* 10**,** E0116553.

Chibinski, A. C. R., Reis, A., Kreich, E. M., Tanaka, J. L. O. & Wambier, D. S. 2013. Evaluation Of Primary Carious Dentin After Cavity Sealing In Deep Lesions: A 10-To 13-Month Follow-Up. *Pediatric Dentistry,* 35**,** 107e-112e.

Chibinski, A. C. R., Wambier, L., Reis, A. & Wambier, D. S. 2016. Clinical, Mineral And Ultrastructural Changes In Carious Dentin Of Primary Molars After Restoration. *International Dental Journal,* 66**,** 150-157.

Choi, K., Oshida, Y., Platt, J. A., Cochran, M. A., Matis, B. A. & Yi, K. 2006. Microtensile Bond Strength Of Glass Ionomer Cements To Artificially Created Carious Dentin. *Oper Dent,* 31**,** 590-7.

Clark, R. D., Smith Jr, J. G. & David-Son, E. A. 1965. Hexosamine And Acid Glycosaminoglycans In Human Teeth. *Biochimica Et Biophysica Acta,* 101**,** 267-272.

Cloitre, T., Panayotov, I. V., Tassery, H., Gergely, C., Levallois, B. & Cuisinier, F. J. 2013. Multiphoton Imaging Of The Dentine-Enamel Junction. *Journal Of Biophotonics,* 6**,** 330-337.

Chibinski, A. C. R., Wambier, L., Reis, A. & Wambier, D. S. 2016. Clinical, Mineral And Ultrastructural Changes In Carious Dentin Of Primary Molars After Restoration. *International Dental Journal,* 66**,** 150-157.

Choi, K., Oshida, Y., Platt, J. A., Cochran, M. A., Matis, B. A. & Yi, K. 2006. Microtensile Bond Strength Of Glass Ionomer Cements To Artificially Created Carious Dentin. *Oper Dent,* 31**,** 590-7.

Chung, C., Millett, D., Creanor, S., Gilmour, W. & Foye, R. 1998. Fluoride Release And Cariostatic Ability Of A Compomer And A Resin-Modified Glass Ionomer Cement Used For Orthodontic Bonding. *Journal Of Dentistry,* 26**,** 533-538.

Cochrane, N., Cai, F., Huq, N., Burrow, M. & Reynolds, E. 2010. New Approaches To Enhanced Remineralization Of Tooth Enamel. *Journal Of Dental Research,* 89**,** 1187-1197.

Coello, B., López-Álvarez, M., Rodríguez-Domínguez, M., Serra, J. & González, P. 2015. Quantitative Evaluation Of The Mineralization Level Of Dental Tissues By Raman Spectroscopy. *Biomedical Physics & Engineering Express,* 1**,** 045204.

Cölfen, H. 2010. Biomineralization: A Crystal-Clear View. *Nature Materials,* 9**,** 960.

Cominelli, A., Acconcia, G., Peronio, P., Rech, I. & Ghioni, M. 2017. Readout Architectures For High Efficiency In Time-Correlated Single Photon Counting Experiments—Analysis And Review. *Ieee Photonics Journal,* 9**,** 1-15.

Conrado, C. A. 2004. Remineralization Of Carious Dentin. I: In Vitro Microradiographic Study In Human Teeth Capped With Calcium Hydroxide. *Brazilian Dental Journal,* 15**,** 59-62.

Cook, P. 1990. Direct Bonding With Glass Ionomer Cement. *Journal Of Clinical Orthodontics: Jco,* 24**,** 509.

Corralo, D. & Maltz, M. 2013. Clinical And Ultrastructural Effects Of Different Liners/Restorative Materials On Deep Carious Dentin: A Randomized Clinical Trial. *Caries Research,* 47**,** 243-250.

Costa, A. R., Garcia-Godoy, F., Correr-Sobrinho, L., Naves, L. Z., Raposo, L. H. A., Carvalho, F. G. D., Sinhoreti, M. A. C. & Puppin-Rontani, R. M. 2017.

Influence Of Different Dentin Substrate (Caries-Affected, Caries-Infected, Sound) On Long-Term Mtbs. *Brazilian Dental Journal,* 28**,** 16-23.

Creanor, S., Awawdeh, L., Saunders, W., Foye, R. & Gilmour, W. 1998. The Effect Of A Resin-Modified Glass Ionomer Restorative Material On Artificially Demineralised Dentine Caries In Vitro. *Journal Of Dentistry,* 26**,** 527-531.

Croll, T. P., Berg, J. H. & Donly, K. J. 2015. Dental Repair Material: A Resin-Modified Glass-Ionomer Bioactive Ionic Resin-Based Composite. *Compend Contin Educ Dent,* 36**,** 60-65.

Crosignani, V., Dvornikov, A. S., Aguilar, J. S., Stringari, C., Edwards, R. A., Mantulin, W. W. & Gratton, E. 2012. Deep Tissue Fluorescence Imaging And In Vivo Biological Applications. *Journal Of Biomedical Optics,* 17**,** 116023.

Curtis, R. V. & Watson, T. F. 2014. *Dental Biomaterials: Imaging, Testing And Modelling*, Elsevier.

Dai, L., Liu, Y., Salameh, Z., Khan, S., Mao, J., Pashley, D. H. & Tay, F. R. 2011. Can Caries-Affected Dentin Be Completely Remineralized By Guided Tissue Remineralization? *Dental Hypotheses,* 2**,** 74.

Damato, F., Strang, R. & Stephen, K. 1990. Effect Of Fluoride Concentration On Remineralization Of Carious Enamel An In Vitro Ph-Cycling Study. *Caries Research,* 24**,** 174-180.

D Alpino, P. H., Pereira, J. C., Svizero, N. R., Rueggeberg, F. A., Carvalho, R. M. & Pashley, D. H. 2006. A New Technique For Assessing Hybrid Layer Interfacial Micromorphology And Integrity: Two-Photon Laser Microscopy. *Journal Of Adhesive Dentistry,* 8**,** 279.

Daculsi, G., Legeros, R., Jean, A. & Kerebel, B. 1987. Possible Physico-Chemical Processes In Human Dentin Caries. *Journal Of Dental Research,* 66**,** 1356-1359.

Dawes, C. 2003. What Is The Critical Ph And Why Does A Tooth Dissolve In Acid? *Journal-Canadian Dental Association,* 69**,** 722-725.

De Almeida Neves, A., Coutinho, E., Cardoso, M. V., Lambrechts, P. & Van Meerbeek, B. 2011. Current Concepts And Techniques For Caries Excavation And Adhesion To Residual Dentin. *Journal Of Adhesive Dentistry,* 13.

De Azevedo, C. S., Garbui, B. U., E Silva, C. M., Simionato, M. R. L., De Freitas, A. Z. & Matos, A. B. 2014. Obtaining Artificially Caries-Affected Dentin For In Vitro Studies. *The Journal Of Contemporary Dental Practice,* 15**,** 12.

De Almeida Neves, A., Coutinho, E., Cardoso, M. V., Lambrechts, P. & Van Meerbeek, B. 2011. Current Concepts And Techniques For Caries Excavation And Adhesion To Residual Dentin. *Journal Of Adhesive Dentistry,* 13.

De Carvalho, F. G., Puppin-Rontani, R. M., Soares, L. E., Santo, A. M. E., Martin, A. A. & Nociti-Junior, F. H. 2009. Mineral Distribution And Clsm Analysis Of Secondary Caries Inhibition By Fluoride/Mdpb-Containing Adhesive System After Cariogenic Challenges. *Journal Of Dentistry,* 37**,** 307-314.

De Munck, J., Mine, A., Poitevin, A., Van Ende, A., Cardoso, M. V., Van Landuyt, K. L., Peumans, M. & Van Meerbeek, B. 2012. Meta-Analytical Review Of Parameters Involved In Dentin Bonding. *Journal Of Dental Research,* 91**,** 351-357.

De Munck, J., Vargas, M., Van Landuyt, K., Hikita, K., Lambrechts, P. & Van Meerbeek, B. 2004. Bonding Of An Auto-Adhesive Luting Material To Enamel And Dentin. *Dental Materials,* 20**,** 963-971.

De Munck, J. D., Van Landuyt, K., Peumans, M., Poitevin, A., Lambrechts, P., Braem, M. & Van Meerbeek, B. 2005. A Critical Review Of The Durability Of Adhesion To Tooth Tissue: Methods And Results. *Journal Of Dental Research,* 84**,** 118-132.

De Souza Costa, C. A., Teixeira, H. M., Nascimento, A. B. L. D. & Hebling, J. 2007. Biocompatibility Of Resin-Based Dental Materials Applied As Liners In Deep Cavities Prepared In Human Teeth. *Journal Of Biomedical Materials Research Part B: Applied Biomaterials,* 81**,** 175-184.

Deb, S. & Nicholson, J. 1999. The Effect Of Strontium Oxide In Glass–Ionomer Cements. *Journal Of Materials Science: Materials In Medicine,* 10**,** 471-474.

Denk, W., Strickler, J. H. & Webb, W. W. 1990. Two-Photon Laser Scanning Fluorescence Microscopy. *Science,* 248**,** 73-76.

Dennison, J. & Sarrett, D. 2012. Prediction And Diagnosis Of Clinical Outcomes Affecting Restoration Margins. *Journal Of Oral Rehabilitation,* 39**,** 301-318.

Deyhle, H., Bunk, O. & Müller, B. 2011. Nanostructure Of Healthy And Caries-Affected Human Teeth. *Nanomedicine: Nanotechnology, Biology And Medicine,* 7**,** 694-701.

Doi, J., Itota, T., Torii, Y., Nakabo, S. And Yoshiyama, M., 2004. Micro-Tensile Bond Strength Of Self-Etching Primer Adhesive Systems To Human Coronal Carious Dentin. *Journal Of Oral Rehabilitation*, *31*(10), Pp.1023-1028.

Ekambaram, M., Yiu, C. K. Y. & Matinlinna, J. P. 2015. Bonding Of Resin Adhesives To Caries-Affected Dentin–A Systematic Review. *International Journal Of Adhesion And Adhesives,* 61**,** 23-34.

El-Askary, F. S. & Nassif, M. S. 2011. The Effect Of The Pre-Conditioning Step On The Shear Bond Strength Of Nano-Filled Resin-Modified Glass-Ionomer To Dentin. *European Journal Of Dentistry,* 5**,** 150.

El-Damanhoury, H. & Platt, J. 2014. Polymerization Shrinkage Stress Kinetics And Related Properties Of Bulk-Fill Resin Composites. *Operative Dentistry,* 39**,** 374-382.

El Feninat, F., Ellis, T., Sacher, E. & Stangel, I. 2001. A Tapping Mode Afm Study Of Collapse And Denaturation In Dentinal Collagen. *Dental Materials,* 17**,** 284-288.

El Zohairy, A. A., Saber, M. H., Abdalla, A. I. & Feilzer, A. J. 2010. Efficacy Of Microtensile Versus Microshear Bond Testing For Evaluation Of Bond Strength Of Dental Adhesive Systems To Enamel. *Dental Materials,* 26**,** 848-854.

Elbaum, R., Tal, E., Perets, A., Oron, D., Ziskind, D., Silberberg, Y. & Wagner, H. 2007. Dentin Micro-Architecture Using Harmonic Generation Microscopy. *Journal Of Dentistry,* 35**,** 150-155.

Embery, G., Hall, R., Waddington, R., Septier, D. & Goldberg, M. 2001. Proteoglycans In Dentinogenesis. *Critical Reviews In Oral Biology & Medicine,* 12**,** 331-349.

Erhardt, M. C. G., Toledano, M., Osorio, R. & Pimenta, L. A. 2008. Histomorphologic Characterization And Bond Strength Evaluation Of Caries-Affected Dentin/Resin Interfaces: Effects Of Long-Term Water Exposure. *Dental Materials,* 24**,** 786-798.

Falster, C. A., Araujo, F. B., Straffon, L. H. & Nor, J. 2002. Indirect Pulp Treatment: In Vivo Outcomes Of An Adhesive Resin System Vs Calcium Hydroxide For Protection Of The Dentin-Pulp Complex. *Pediatr Dent,* 24**,** 241-8.

Fan, Y., Sun, Z. & Moradian-Oldak, J. 2009. Controlled Remineralization Of Enamel In The Presence Of Amelogenin And Fluoride. *Biomaterials,* 30**,** 478-483.

Featherstone, J., Duncan, J. & Cutress, T. 1978. Crystallographic Changes In Human Tooth Enamel During In-Vitro Caries Simulation. *Archives Of Oral Biology,* 23**,** 405-413.

Fejerskov, O., 2004. Changing Paradigms In Concepts On Dental Caries: Consequences For Oral Health Care. *Caries Research*, *38*(3), Pp.182-191.

Ferracane, J. L., Cooper, P. R. & Smith, A. J. 2010. Can Interaction Of Materials With The Dentin-Pulp Complex Contribute To Dentin Regeneration? *Odontology,* 98**,** 2-14.

Ferracane, J. L. 2011. Resin Composite—State Of The Art. *Dental Materials,* 27**,** 29-38.

Ferracane, J. L., Cooper, P. R. & Smith, A. J. 2010. Can Interaction Of Materials With The Dentin-Pulp Complex Contribute To Dentin Regeneration? *Odontology,* 98**,** 2-14.

Ferracane, J. L., Stansbury, J. & Burke, F. J. T. 2011. Self-Adhesive Resin Cements–Chemistry, Properties And Clinical Considerations. *Journal Of Oral Rehabilitation,* 38**,** 295-314.

Ferrari, M., Goracci, C., Sadek, F. & Cardoso, P. E. C. 2002. Microtensile Bond Strength Tests: Scanning Electron Microscopy Evaluation Of Sample Integrity Before Testing. *European Journal Of Oral Sciences,* 110**,** 385-391.

Fisher, L. W. & Fedarko, N. S. 2003. Six Genes Expressed In Bones And Teeth Encode The Current Members Of The Sibling Family Of Proteins. *Connective Tissue Research,* 44**,** 33-40.

Follak, A., Miotti, L., Lenzi, T., Rocha, R. & Maxnuck Soares, F. 2018a. The Impact Of Artificially Caries-Affected Dentin On Bond Strength Of Multi-Mode Adhesives. *Journal Of Conservative Dentistry,* 21**,** 136-141.

Follak, A., Miotti, L., Lenzi, T., Rocha, R. & Soares, F. 2018b. Degradation Of Multimode Adhesive System Bond Strength To Artificial Caries-Affected Dentin Due To Water Storage. *Operative Dentistry,* 43**,** E92-E101.

Foong, J., Lee, K., Nguyen, C., Tang, G., Austin, D., Ch'ng, C., Burrow, M. & Thomas, D. 2006. Comparison Of Microshear Bond Strengths Of Four Self-Etching Bonding Systems To Enamel Using Two Test Methods. *Australian Dental Journal,* 51**,** 252-257.

Foreman, P. 1980. The Excitation And Emission Spectra Of Fluorescent Components Of Human Dentine. *Archives Of Oral Biology,* 25**,** 641-647.

Forsten, L. 1998. Fluoride Release And Uptake By Glass-Ionomers And Related Materials And Its Clinical Effect. *Biomaterials,* 19**,** 503-508.

Frank, R.M., 1966. Ultrastructure of human dentine. In *Calcified Tissues 1965* (pp. 259-272). Springer, Berlin, Heidelberg.

Frencken, J. 2017. Atraumatic Restorative Treatment And Minimal Intervention Dentistry. *British Dental Journal,* 223**,** 183.

Frencken, J. E., Songpaisan, Y., Phantumvanit, P. & Pilot, T. 1994. An Atraumatic Restorative Treatment (Art) Technique: Evaluation After One Year. *International Dental Journal,* 44**,** 460-464.

Fried, D., Glena, R. E., Featherstone, J. D. & Seka, W. 1995. Nature Of Light Scattering In Dental Enamel And Dentin At Visible And Near-Infrared Wavelengths. *Applied Optics,* 34**,** 1278-1285.

Fried, D., Staninec, M. and Darling, C.L., 2010. Near-infrared imaging of dental decay at 1310 nm. *J Laser Dent*, *18*(1), pp.8-16.

Fujimoto, N. & Adachi-Usami, E. 1988. Comparison Of Automated Perimetry And Pattern Visually Evoked Cortical Potentials In Optic Neuritis. *Documenta Ophthalmologica,* 69**,** 263-269.

Fukegawa, D., Hayakawa, S., Yoshida, Y., Suzuki, K., Osaka, A. & Van Meerbeek, B. 2006. Chemical Interaction Of Phosphoric Acid Ester With Hydroxyapatite. *Journal Of Dental Research,* 85**,** 941-944.

Fusayama, T. 1972. Differentiation Of Two Layers Of Carious Dentin By Staining. *J Dent Res,* 51**,** 866.

Fukushima, Y., Araki, T. & Yamada, M. O. 1987. Topography Of Fluorescence And Its Possible Composites In Human Teeth. *Cellular And Molecular Biology,* 33**,** 725-736.

Fumes, A. C., Silva, R. A. B. D., Longo, D. L., Rossi, A. D. & Serra, M. C. 2015. Validation Of Ph Cycling Model To Induce Artificial Carious Lesions In Bovine Dentin. *Rsbo (Online),* 12**,** 266-271.

Fusayama, T. 1972. Differentiation Of Two Layers Of Carious Dentin By Staining. *J Dent Res,* 51**,** 866.

Fusayama, T., Nakamura, M., Kurosaki, N. & Iwaku, M. 1979. Non-Pressure Adhesion Of A New Adhesive Restorative Resin. *Journal Of Dental Research,* 58**,** 1364-1370.

Fusayama, T., Okuse, K. & Hosoda, H. 1966. Relationship Between Hardness, Discoloration, And Microbial Invasion In Carious Dentin. *Journal Of Dental Research,* 45**,** 1033-1046.

Gallagher, R., Demos, S., Balooch, M., Marshall, G. & Marshall, S. 2003. Optical Spectroscopy And Imaging Of The Dentin–Enamel Junction In Human Third Molars. *Journal Of Biomedical Materials Research Part A,* 64**,** 372-377.

Gandolfi, M., Siboni, F. & Prati, C. 2012. Chemical–Physical Properties Of Theracal, A Novel Light-Curable Mta-Like Material For Pulp Capping. *International Endodontic Journal,* 45**,** 571-579.

Gandolfi, M., Taddei, P., Tinti, A. & Prati, C. 2010. Apatite-Forming Ability (Bioactivity) Of Proroot Mta. *International Endodontic Journal,* 43**,** 917-929.

Gandolfi, M. G., Siboni, F., Botero, T., Bossù, M., Riccitiello, F. & Prati, C. 2015. Calcium Silicate And Calcium Hydroxide Materials For Pulp Capping: Biointeractivity, Porosity, Solubility And Bioactivity Of Current Formulations. *Journal Of Applied Biomaterials & Functional Materials,* 13**,** 43-60.

Gannot, I., Ron, I., Hekmat, F., Chernomordik, V. & Gandjbakhche, A. 2004. Functional Optical Detection Based On Ph Dependent Fluorescence Lifetime. *Lasers In Surgery And Medicine,* 35**,** 342-348.

Garchitorena Ferreira, M. I. 2016. Bioactive Materials In Dentin Remineralization. *Odontoestomatologia,* 18**,** 11-18.

Garcia-Godoy, F., Krämer, N., Feilzer, A. J. & Frankenberger, R. 2010. Long-Term Degradation Of Enamel And Dentin Bonds: 6-Year Results In Vitro Vs. In Vivo. *Dental Materials,* 26**,** 1113-1118.

Georgakoudi, I., Jacobson, B. C., Müller, M. G., Sheets, E. E., Badizadegan, K., Carr-Locke, D. L., Crum, C. P., Boone, C. W., Dasari, R. R. & Van Dam, J. 2002. Nad (P) H And Collagen As In Vivo Quantitative Fluorescent Biomarkers Of Epithelial Precancerous Changes. *Cancer Research,* 62**,** 682-687.

George, A. and Veis, A., 2008. Phosphorylated proteins and control over apatite nucleation, crystal growth, and inhibition. *Chemical reviews*, *108*(11), pp.4670-4693.

Gerritsen, H. C., Sanders, R., Draaijer, A., Ince, C. & Levine, Y. 1997. Fluorescence Lifetime Imaging Of Oxygen In Living Cells. *Journal Of Fluorescence,* 7**,** 11-15.

Gimenez, T., Piovesan, C., Braga, M.M., Raggio, D.P., Deery, C., Ricketts, D.N., Ekstrand, K.R. and Mendes, F.M., 2015. Clinical relevance of studies on the accuracy of visual inspection for detecting caries lesions: a systematic review. *Caries research*, *49*(2), pp.91-98.

Giannini, M., Makishi, P., Ayres, A. P. A., Vermelho, P. M., Fronza, B. M., Nikaido, T. & Tagami, J. 2015. Self-Etch Adhesive Systems: A Literature Review. *Brazilian Dental Journal,* 26**,** 3-10.

Goldberg, M. and Boskey, A.L., 1996. Lipids and biomineralizations. *Progress in histochemistry and cytochemistry*, 31(2), pp.III-187.

Goldberg, M., Pradelle-Plasse, N., Tran, X. & Colon, P. 2009. *Emerging Trends In Biomaterials;* Vi-2-1 Physico-Chemical Properties.

Goldberg, M. & Takagi, M. 1993. Dentine Proteoglycans: Composition, Ultrastructure And Functions. *The Histochemical Journal,* 25**,** 781-806.

Goldberg, M., Kulkarni, A.B., Young, M. and Boskey, A., 2011. Dentin: Structure, Composition and Mineralization: The role of dentin ECM in dentin formation and mineralization. *Frontiers in bioscience (Elite edition)*, *3*, p.711.

Gopalakrishna, A. 2009. Impact Of Different Acid Etching Times On Microtensile Bond Strength To Vital Dentin, The University Of Iowa.

Goppert-Mayer, M. 1931. Elementary File With Two Quantum Fissures. *Annalen Der Physik,* 9**,** 273-294.

Goracci, C., Cury, A. H., Cantoro, A., Papacchini, F., Tay, F. R. & Ferrari, M. 2006. Microtensile Bond Strength And Interfacial Properties Of Self-

Etching And Self-Adhesive Resin Cements Used To Lute Composite Onlays Under Different Seating Forces. *Journal Of Adhesive Dentistry,* 8.

Goracci, C., Tavares, A. U., Fabianelli, A., Monticelli, F., Raffaelli, O., Cardoso, P. C., Tay, F. & Ferrari, M. 2004. The Adhesion Between Fiber Posts And Root Canal Walls: Comparison Between Microtensile And Push-Out Bond Strength Measurements. *European Journal Of Oral Sciences,* 112**,** 353-361.

Gotliv, B.-A. & Veis, A. 2007. Peritubular Dentin, A Vertebrate Apatitic Mineralized Tissue Without Collagen: Role Of A Phospholipid-Proteolipid Complex. *Calcified Tissue International,* 81**,** 191-205.

Grauw, D. 1998. Time-Gated Fluorescence Lifetime Imaging And Microvolume Spectroscopy Using Two-Photon Excitation. *Journal Of Microscopy,* 191**,** 39-51.

Green, D. J. & Banerjee, A. 2011. Contemporary Adhesive Bonding: Bridging The Gap Between Research And Clinical Practice. *Dental Update,* 38**,** 439-449.

Griffin, S. O., Oong, E., Kohn, W., Vidakovic, B., Gooch, B., Bader, J., Clarkson, J., Fontana, M., Meyer, D. & Rozier, R. 2008. The Effectiveness Of Sealants In Managing Caries Lesions. *Journal Of Dental Research,* 87**,** 169-174.

Griffiths, B.M., Watson, T.F. And Sherriff, M., 1999. The Influence Of Dentine Bonding Systems And Their Handling Characteristics On The Morphology And Micropermeability Of The Dentine Adhesive Interface. *Journal Of Dentistry*, *27*(1), Pp.63-71.

Gu, L., Kim, Y., Liu, Y., Ryou, H., Wimmer, C., Dai, L., Arola, D., Looney, S. W., Pashley, D. H. & Tay, F. 2011. Biomimetic Analogs For Collagen Biomineralization. *Journal Of Dental Research,* 90**,** 82-87.

Gruythuysen, R. 2010. Non-Restorative Cavity Treatment. Managing Rather Than Masking Caries Activity. *Nederlands Tijdschrift Voor Tandheelkunde,* 117**,** 173-180.

Gurgan, S., Kutuk, Z.B., Ergin, E., Oztas, S.S. and Cakir, F.Y., 2017. Clinical performance of a glass ionomer restorative system: a 6-year evaluation. *Clinical oral investigations*, *21*(7), pp.2335-2343.

Gupta, A., Tavane, P., Gupta, P. K., Tejolatha, B., Lakhani, A. A., Tiwari, R., Kashyap, S. & Garg, G. 2017. Evaluation Of Microleakage With Total Etch, Self Etch And Universal Adhesive Systems In Class V Restorations: An In Vitro Study. *Journal Of Clinical And Diagnostic Research: Jcdr,* 11**,** Zc53.

Gwinnett, A. & Kanca 3rd, J. 1992. Micromorphological Relationship Between Resin And Dentin In Vivo And In Vitro. *American Journal Of Dentistry,* 5**,** 19-23.

Haak, R., Wicht, M.J. and Noack, M.J., 2001. Conventional, Digital and Contrast–Enhanced Bitewing Radiographs in the Decision to Restore Approximal Carious Lesions. *Caries research*, *35*(3), pp.193-199.

Hall, A. & Girkin, J. M. 2004. A Review Of Potential New Diagnostic Modalities For Caries Lesions. *J Dent Res,* 83 Spec No C**,** C89-94.

Haefer, M., Schneider, H., Rupf, S., Busch, I., Fuchß, A., Merte, I., Jentsch, H., Haak, R. & Merte, K. 2013. Experimental And Clinical Evaluation Of A Self-Etching And An Etch-And-Rinse Adhesive System. *J Adhes Dent,* 15**,** 275-86.

Hamama, H., Burrow, M. & Yiu, C. 2014. Effect Of Dentine Conditioning On Adhesion Of Resin-Modified Glass Ionomer Adhesives. *Australian Dental Journal,* 59**,** 193-200.

Han, L., Kodama, S. & Okiji, T. 2015. Evaluation Of Calcium-Releasing And Apatite-Forming Abilities Of Fast-Setting Calcium Silicate-Based Endodontic Materials. *International Endodontic Journal,* 48**,** 124-130.

Han, L. & Okiji, T. 2011. Uptake Of Calcium And Silicon Released From Calcium Silicate–Based Endodontic Materials Into Root Canal Dentine. *International Endodontic Journal,* 44**,** 1081-1087.

Han, L. & Okiji, T. 2013. Bioactivity Evaluation Of Three Calcium Silicate-Based Endodontic Materials. *International Endodontic Journal,* 46**,** 808-814.

Han, L., Okiji, T. & Okawa, S. 2010. Morphological And Chemical Analysis Of Different Precipitates On Mineral Trioxide Aggregate Immersed In Different Fluids. *Dental Materials Journal,* 29**,** 512-517.

Hannas, A. R., Pereira, J. C., Granjeiro, J. M. & Tjäderhane, L. 2007. The Role Of Matrix Metalloproteinases In The Oral Environment. *Acta Odontologica Scandinavica,* 65**,** 1-13.

Hanson, K. M., Behne, M. J., Barry, N. P., Mauro, T. M., Gratton, E. & Clegg, R. M. 2002. Two-Photon Fluorescence Lifetime Imaging Of The Skin Stratum Corneum Ph Gradient. *Biophysical Journal,* 83**,** 1682-1690.

Harashima, I. & Hirasawa, T. 1990. Adsorption Of 2-Hydroxyethyl Methacrylate On Dentin From Aqueous Solution. *Dental Materials Journal,* 9**,** 36-46.

Hartgerink, J. D., Beniash, E. & Stupp, S. I. 2001. Self-Assembly And Mineralization Of Peptide-Amphiphile Nanofibers. *Science,* 294**,** 1684-1688.

Hashemikamangar, S. S., Pourhashemi, S. J., Nekooimehr, Z., Dehaki, M. G. & Kharazifard, M. J. 2016. Effect Of Lactic Acid On Microleakage Of Class V Low-Shrinkage Composite Restorations. *Journal Of Dentistry (Tehran, Iran),* 13**,** 223.

Hattar, S., Hatamleh, M. M., Sawair, F. & Al-Rabab'ah, M. 2015. Bond Strength Of Self-Adhesive Resin Cements To Tooth Structure. *The Saudi Dental Journal,* 27**,** 70-74.

Hashem, D., Mannocci, F., Patel, S., Manoharan, A., Brown, J., Watson, T. & Banerjee, A. 2015. Clinical And Radiographic Assessment Of The Efficacy Of Calcium Silicate Indirect Pulp Capping: A Randomized Controlled Clinical Trial. *Journal Of Dental Research,* 94**,** 562-568.

Hashimoto, M., Nagano, F., Endo, K. & Ohno, H. 2011. A Review: Biodegradation Of Resin–Dentin Bonds. *Japanese Dental Science Review,* 47**,** 5-12.

Hatibovic-Kofman, S. & Koch, G. 1991. Fluoride Release From Glass Ionomer Cement In Vivo And In Vitro. *Swed Dent J,* 15**,** 253-258.

Hatibovic-Kofman, S., Suljak, J. & Koch, G. 1997. Remineralization Of Natural Carious Lesions With A Glass Ionomer Cement. *Swedish Dental Journal,* 21**,** 11-17.

Hayakawa, T., Yoshinari, M., Sakae, T. & Nemoto, K. 2004. Calcium Phosphate Formation On The Phosphorylated Dental Bonding Agent In Electrolyte Solution. *Journal Of Oral Rehabilitation,* 31**,** 67-73.

He, S., Xue, W., Duan, Z., Sun, Q., Li, X., Gan, H., Huang, J. & Qu, J. Y. 2017. Multimodal Nonlinear Optical Microscopy Reveals Critical Role Of Kinesin-1 In Cartilage Development. *Biomed Opt Express,* 8**,** 1771-1782.

Hédoux, A., Guinet, Y. & Descamps, M. 2011. The Contribution Of Raman Spectroscopy To The Analysis Of Phase Transformations In

Pharmaceutical Compounds. *International Journal Of Pharmaceutics,* 417**,** 17-31.

Hench, L. L., Splinter, R. J., Allen, W. & Greenlee, T. 1971. Bonding Mechanisms At The Interface Of Ceramic Prosthetic Materials. *Journal Of Biomedical Materials Research Part A,* 5**,** 117-141.

Hench, L. & Ethridge, E. 1975. Biomaterials—The Interfacial Problem. *Advances In Biomedical Engineering, Volume 5.* Elsevier.

Hermanson, A. S., Bush, M. A., Miller, R. G. & Bush, P. J. 2008. Ultraviolet Illumination As An Adjunctive Aid In Dental Inspection. *Journal Of Forensic Sciences,* 53**,** 408-411.

Hewko, M. & Sowa, M. 2010. Towards Early Dental Caries Detection With Oct And Polarized Raman Spectroscopy. *Head & Neck Oncology,* 2**,** O43.

Hickel, R. & Manhart, J. 2001. Longevity Of Restorations In Posterior Teeth And Reasons For Failure. *Journal Of Adhesive Dentistry,* 3.

Hikita, K., Van Meerbeek, B., De Munck, J., Ikeda, T., Van Landuyt, K., Maida, T., Lambrechts, P. & Peumans, M. 2007. Bonding Effectiveness Of Adhesive Luting Agents To Enamel And Dentin. *Dental Materials,* 23**,** 71-80.

Hoerman, K. C. & Mancewicz, S. A. 1964. Fluorometric Demonstration Of Tryptophan In Dentin And Bone Protein. *Journal Of Dental Research,* 43**,** 276-280.

Hoshino, E., 1985. Predominant Obligate Anaerobes In Human Carious Dentin. *Journal Of Dental Research*, *64*(10), Pp.1195-1198.

Igarashi, T., Yamamoto, A. And Goto, N. (1996) 'Direct Detection Of Streptococcus Mutans In Human Dental Plaque By Polymerase Chain Reaction', *Oral Microbiology And Immunology*, 11(5), Pp. 294–298. Doi: 10.1111/J.1399-302x.1996.Tb00184.X.

Horsley, J. & Barrow, R. 1967. Absorption Spectrum Of Bromine From 6200 To 5100 Å. *Transactions Of The Faraday Society,* 63**,** 32-38.

Huang, X., Li, L., Huang, C. & Du, X. 2011. Effect Of Ethanol-Wet Bonding With Hydrophobic Adhesive On Caries-Affected Dentine. *European Journal Of Oral Sciences,* 119**,** 310-315.

Ilie, N., Schöner, C., Bücher, K. & Hickel, R. 2014. An In-Vitro Assessment Of The Shear Bond Strength Of Bulk-Fill Resin Composites To Permanent And Deciduous Teeth. *Journal Of Dentistry,* 42**,** 850-855.

Imbery, T., Namboodiri, A., Duncan, A., Amos, R., Best, A. & Moon, P. 2013. Evaluating Dentin Surface Treatments For Resin-Modified Glass Ionomer Restorative Materials. *Operative Dentistry,* 38**,** 429-438.

Inoue, G., Nikaido, T., Sadr, A. & Tagami, J. 2012. Morphological Categorization Of Acid-Base Resistant Zones With Self-Etching Primer Adhesive Systems. *Dental Materials Journal,* 31**,** 232-238.

Ismail, A. I., Tellez, M., Pitts, N. B., Ekstrand, K. R., Ricketts, D., Longbottom, C., Eggertsson, H., Deery, C., Fisher, J. & Young, D. A. 2013. Caries Management Pathways Preserve Dental Tissues And Promote Oral Health. *Community Dentistry And Oral Epidemiology,* 41.

So, I. 2003. Ts 11405: Dental Materials—Testing Of Adhesion To Tooth Structure. *Geneva, Switzerland: International Organization For Standardization Iso Central Secretariat*.

Iwami, Y., Hayashi, N., Takeshige, F. & Ebisu, S. 2008. Relationship Between The Color Of Carious Dentin With Varying Lesion Activity, And Bacterial Detection. *Journal Of Dentistry,* 36**,** 143-151.

Jang, J., Park, S. & Hwang, I. 2015. Polymerization Shrinkage And Depth Of Cure Of Bulk-Fill Resin Composites And Highly Filled Flowable Resin. *Operative Dentistry,* 40**,** 172-180.

Jardine, A. P., Da Rosa, R. A., Santini, M. F., Wagner, M., Só, M. V. R., Kuga, M. C., Pereira, J. R. & Kopper, P. M. P. 2016. The Effect Of Final Irrigation On The Penetrability Of An Epoxy Resin-Based Sealer Into Dentinal Tubules: A Confocal Microscopy Study. *Clinical Oral Investigations,* 20**,** 117-123.

Jain, A. And Bahuguna, R. (2015) 'Role Of Matrix Metalloproteinases In Dental Caries, Pulp And Periapical Inflammation: An Overview', *Journal Of Oral Biology And Craniofacial Research*, Pp. 212–218. Doi: 10.1016/J.Jobcr.2015.06.015.

Jefferies, S. 2014. Bioactive And Biomimetic Restorative Materials: A Comprehensive Review. Part Ii. *Journal Of Esthetic And Restorative Dentistry,* 26**,** 27-39.

Jepsen, S., Acil, Y., Zuch, B. & Albers, H.-K. 1999. Biochemical Analysis Of The Collagen Structure Of Residual Dentin Following Chemo-Mechanical Caries Removal (Carisolv). *Deutsche Zahnarztliche Zeitschrift,* 54**,** 120-123.

Jiang, S., Pan, H., Chen, Y., Xu, X. & Tang, R. 2015. Amorphous Calcium Phosphate Phase-Mediated Crystal Nucleation Kinetics And Pathway. *Faraday Discussions,* 179**,** 451-461.

Jin, W., Jiang, S., Pan, H. & Tang, R. 2018. Amorphous Phase Mediated Crystallization: Fundamentals Of Biomineralization. *Crystals,* 8**,** 48.

Jones, S. J., Boyde, A. & Ali, N. N. 1984. The Resorption Of Biological And Non-Biological Substrates By Cultured Avian And Mammalian Osteoclasts. *Anatomy And Embryology,* 170**,** 247-256.

Joves, G. J., Inoue, G., Nakashima, S., Sadr, A., Nikaido, T. & Tagami, J. 2013. Mineral Density, Morphology And Bond Strength Of Natural Versus Artificial Caries-Affected Dentin. *Dental Materials Journal,* 32**,** 138-143.

Kan, K., Messer, L. & Messer, H. 1997. Variability In Cytotoxicity And Fluoride Release Of Resin-Modified Glass-Ionomer Cements. *Journal Of Dental Research,* 76**,** 1502-1507.

Kao, F. J. 2004a. The Use Of Optical Parametric Oscillator For Harmonic Generation And Two-Photon Uv Fluorescence Microscopy. *Microsc Res Tech,* 63**,** 175-81.

Kao, F. J. 2004b. The Use Of Optical Parametric Oscillator For Harmonic Generation And Two-Photon Uv Fluorescence Microscopy. *Microscopy Research And Technique,* 63**,** 175-181.

Karlsson, L. 2010. Caries Detection Methods Based On Changes In Optical Properties Between Healthy And Carious Tissue. *International Journal Of Dentistry,* 2010.

Kathuria, V., Ankola, A. V., Hebbal, M. & Mocherla, M. 2013. Carisolv-An Innovative Method Of Caries Removal. *Journal Of Clinical And Diagnostic Research: Jcdr,* 7**,** 3111.

Kaur, M., Singh, H., Dhillon, J. S., Batra, M. & Saini, M. 2017. Mta Versus Biodentine: Review Of Literature With A Comparative Analysis. *Journal Of Clinical And Diagnostic Research: Jcdr,* 11**,** Zg01.

Khouw-Liu, V., Anstice, H. & Pearson, G. 1999. An In Vitro Investigation Of A Poly (Vinyl Phosphonic Acid) Based Cement With Four Conventional Glass-Ionomer Cements. Part 1: Flexural Strength And Fluoride Release. *Journal Of Dentistry,* 27**,** 351-357.

Kawasaki, K., Ruben, J., Stokroos, I., Takagi, O. & Arends, J. 1999. The Remineralization Of Edta–Treated Human Dentine. *Caries Research,* 33**,** 275-280.

Kidd, E. 2004. How 'Clean'must A Cavity Be Before Restoration? *Caries Research,* 38**,** 305-313.

Kidd, E. & Beighton, D. 1996. Prediction Of Secondary Caries Around Tooth-Colored Restorations: A Clinical And Microbiological Study. *Journal Of Dental Research,* 75**,** 1942-1946.

Kidd, E. & Fejerskov, O. 2004. What Constitutes Dental Caries? Histopathology Of Carious Enamel And Dentin Related To The Action Of Cariogenic Biofilms. *Journal Of Dental Research,* 83**,** 35-38.

Kidd, E. & Fejerskov, O. 2013. Changing Concepts In Cariology: Forty Years On. *Dental Update,* 40**,** 277-286.

Kim, B.-M., Eichler, J. & Da Silva, L. B. 1999. Frequency Doubling Of Ultrashort Laser Pulses In Biological Tissues. *Applied Optics,* 38**,** 7145-7150.

Kim, B. M., Eichler, J., Reiser, K. M., Rubenchik, A. M. & Da Silva, L. B. 2000. Collagen Structure And Nonlinear Susceptibility: Effects Of Heat, Glycation, And Enzymatic Cleavage On Second Harmonic Signal Intensity. *Lasers In Surgery And Medicine: The Official Journal Of The American Society For Laser Medicine And Surgery,* 27**,** 329-335.

Kim, J., Arola, D. D., Gu, L., Kim, Y. K., Mai, S., Liu, Y., Pashley, D. H. & Tay, F. R. 2010a. Functional Biomimetic Analogs Help Remineralize Apatite-Depleted Demineralized Resin-Infiltrated Dentin Via A Bottom–Up Approach. *Acta Biomaterialia,* 6**,** 2740-2750.

Kim, J., Song, Y.-S., Min, K.-S., Kim, S.-H., Koh, J.-T., Lee, B.-N., Chang, H.-S., Hwang, I.-N., Oh, W.-M. & Hwang, Y.-C. 2016. Evaluation Of Reparative Dentin Formation Of Proroot Mta, Biodentine And Bioaggregate Using Micro-Ct And Immunohistochemistry. *Restorative Dentistry & Endodontics,* 41**,** 29-36.

Kim, Y. K., Gu, L.-S., Bryan, T. E., Kim, J. R., Chen, L., Liu, Y., Yoon, J. C., Breschi, L., Pashley, D. H. & Tay, F. R. 2010b. Mineralisation Of Reconstituted Collagen Using Polyvinylphosphonic Acid/Polyacrylic Acid Templating Matrix Protein Analogues In The Presence Of Calcium, Phosphate And Hydroxyl Ions. *Biomaterials,* 31**,** 6618-6627.

Kinney, J. H., Nalla, R. K., Pople, J. A., Breunig, T. M. & Ritchie, R. O. 2005. Age-Related Transparent Root Dentin: Mineral Concentration, Crystallite Size, And Mechanical Properties. *Biomaterials,* 26**,** 3363-3376.

Kleter, B., Van Doorn, L.-J., Ter Schegget, J., Schrauwen, L., Van Krimpen, K., Burger, M., Ter Harmsel, B. & Quint, W. 1998a. Novel Short-Fragment Pcr Assay For Highly Sensitive Broad-Spectrum Detection Of Anogenital Human Papillomaviruses. *The American Journal Of Pathology,* 153**,** 1731-1739.

Kleter, G., Damen, J., Buijs, M. & Ten Cate, J. 1998b. Modification Of Amino Acid Residues In Carious Dentin Matrix. *Journal Of Dental Research,* 77**,** 488-495.

Klont, B. & Ten Cate, J. 1991. Susceptibility Of The Collagenous Matrix From Bovine Incisor Roots To Proteolysis After In Vitro Lesion Formation. *Caries Research,* 25**,** 46-50.

Knight, A. W. & Billinton, N. 2001. Distinguishing Gfp From Cellular Autofluorescence. *Biophotonics International,* 8**,** 42-51.

Knoop, F., Peters, C. G. & Emerson, W. B. 1939. A Sensitive Pyramidal-Diamond Tool For Indentation Measurements. *Journal Of Research Of The National Bureau Of Standards,* 23**,** 39.

Koenig, K., Hibst, R., Meyer, H., Flemming, G. & Schneckenburger, H. Laser-Induced Autofluorescence Of Carious Regions Of Human Teeth And Caries-Involved Bacteria. Dental Applications Of Lasers, 1993. International Society For Optics And Photonics, 170-181.

Koç Vural, U., Kütük, Z.B., Ergin, E., Yalçın Çakır, F. and Gürgan, S., 2017. Comparison of two different methods of detecting residual caries. *Restorative dentistry & endodontics*, *42*(1), pp.48-53.

Komori, P. C., Pashley, D. H., Tjäderhane, L., Breschi, L., Mazzoni, A., De Goes, M. F., Wang, L. & Carrilho, M. R. 2009. Effect Of 2% Chlorhexidine

Digluconate On The Bond Strength To Normal Versus Caries-Affected Dentin. *Operative Dentistry,* 34**,** 157-165.

König, K. 2000. Multiphoton Microscopy In Life Sciences. *Journal Of Microscopy,* 200**,** 83-104.

Korkmaz, Y., Ozel, E., Attar, N. & Bicer, C. O. 2010. Influence Of Different Conditioning Methods On The Shear Bond Strength Of Novel Light-Curing Nano-Ionomer Restorative To Enamel And Dentin. *Lasers In Medical Science,* 25**,** 861-866.

Koutsoukos, P. & Nancollas, G. 1981. The Kinetics Of Mineralization Of Human Dentin In Vitro. *Journal Of Dental Research,* 60**,** 1922-1928.

Kreulen, C., Soet, J. D., Weerheijm, K. & Van Amerongen, W. 1997. In Vivo Cariostatic Effect Of Resin Modified Glass Lonomer Cement And Amalgam On Dentine. *Caries Research,* 31**,** 384-389.

Kvaal, S. & Solheim, T. 1989. Fluorescence From Dentin And Cementum In Human Mandibular Second Premolars And Its Relation To Age. *Scand J Dent Res,* 97**,** 131-8.

Kreulen, C., Soet, J. D., Weerheijm, K. & Van Amerongen, W. 1997. In Vivo Cariostatic Effect Of Resin Modified Glass Lonomer Cement And Amalgam On Dentine. *Caries Research,* 31**,** 384-389.

Kuboki, Y., Ohgushi, K. & Fusayama, T. 1977. Collagen Biochemistry Of The Two Layers Of Carious Dentin. *Journal Of Dental Research,* 56**,** 1233-1237.

Kuhn, E., Chibinski, A. C. R., Reis, A. & Wambier, D. S. 2014. The Role Of Glass Ionomer Cement On The Remineralization Of Infected Dentin: An In Vivo Study. *Pediatric Dentistry,* 36**,** 118e-124e.

Lakowicz, J. R. 2004. Principles Of Fluorescence Spectroscopy, (1999). Kluwer Academic/Plenum Publishers, New York.

Lakowicz, J. R., Szmacinski, H., Nowaczyk, K. & Johnson, M. L. 1992. Fluorescence Lifetime Imaging Of Free And Protein-Bound Nadh. *Proceedings Of The National Academy Of Sciences,* 89**,** 1271-1275.

Laitala, M.L., Piipari, L., Sämpi, N., Korhonen, M., Pesonen, P., Joensuu, T. And Anttonen, V., 2017. Validity Of Digital Imaging Of Fiber-Optic Transillumination In Caries Detection On Proximal Tooth Surfaces. *International Journal Of Dentistry*, *2017*.

Lai, G., Zhu, L., Xu, X. and Kunzelmann, K.H., 2014. An in vitro comparison of fluorescence-aided caries excavation and conventional excavation by microhardness testing. *Clinical oral investigations*, *18*(2), pp.599-605.

Leaver, A., Thomas, M. & Holbrook, I. 1976. Glycoproteins Of Human Dentine. *Calcified Tissue Research,* 22**,** 347-349.

Lee, H.-S., Berg, J. H., García-Godoy, F. & Jang, K. T. 2008. Long Term Evaluation Of The Remineralization Of Interproximal Caries-Like Lesions Adjacent To Glass-Ionomer Restorations: A Micro-Ct Study. *American Journal Of Dentistry,* 21**,** 129.

Lee, Y.-K. 2015. Fluorescence Properties Of Human Teeth And Dental Calculus For Clinical Applications. *Journal Of Biomedical Optics,* 20**,** 040901.

Legeros, R. Z. & Tung, M. S. 1983. Chemical Stability Of Carbonate-And Fluoride-Containing Apatites. *Caries Research,* 17**,** 419-429.

Leiendecker, A. P., Qi, Y.-P., Sawyer, A. N., Niu, L.-N., Agee, K. A., Loushine, R. J., Weller, R. N., Pashley, D. H. & Tay, F. R. 2012. Effects Of Calcium Silicate–Based Materials On Collagen Matrix Integrity Of Mineralized Dentin. *Journal Of Endodontics,* 38**,** 829-833.

Leloup, G., D'hoore, W., Bouter, D., Degrange, M. & Vreven, J. 1998. Meta-Analytic Review Of Factors Involved In Dentin Adherence. *Journal Of Dental Research,* 77**,** 944.

Leloup, G., D'hoore, W., Bouter, D., Degrange, M. & Vreven, J. 2001. Concise Review Biomaterials & Bioengineering: Meta-Analytical Review Of Factors Involved In Dentin Adherence. *Journal Of Dental Research,* 80**,** 1605-1614.

Lenzi, T., Soares, F. & Tedesco, T. 2015a. Is It Possible To Induce Artificial Caries-Affected Dentin Using The Same Protocol To Primary And Permanent Teeth? *The Journal Of Contemporary Dental Practice,* 16**,** 638-642.

Lenzi, T. L., Prócida Raggio, D., Soares, M., Zovico, F. & De Oliveira Rocha, R. 2015b. Bonding Performance Of A Multimode Adhesive To Artificially-Induced Caries-Affected Primary Dentin. *Journal Of Adhesive Dentistry,* 17.

Lewis, S. M., Coleman, N. J., Booth, S. E. & Nicholson, J. W. 2013. Interaction Of Fluoride Complexes Derived From Glass-Ionomer Cements With Hydroxyapatite. *Ceramics-Silikáty,* 57**,** 196-200.

Li, B., Zhu, X., Ma, L., Wang, F., Liu, X., Yang, X., Zhou, J., Tan, J., Pashley, D. H. & Tay, F. R. 2016.

Selective Demineralisation Of Dentine Extrafibrillar Minerals—A Potential Method To Eliminate Water-Wet Bonding In The Etch-And-Rinse Technique. *Journal Of Dentistry,* 52**,** 55-62.

Lin, J., Shinya, A., Gomi, H. & Shinya, A. 2010. Effect Of Self-Adhesive Resin Cement And Tribochemical Treatment On Bond Strength To Zirconia. *International Journal Of Oral Science,* 2**,** 28.

Lin, P.-Y., Lyu, H.-C., Hsu, C.-Y. S., Chang, C.-S. & Kao, F.-J. 2011. Imaging Carious Dental Tissues With Multiphoton Fluorescence Lifetime Imaging Microscopy. *Biomedical Optics Express,* 2**,** 149-158.

Lin, S.-J., Lo, W., Tan, H.-Y., Chan, J.-Y., Chen, W.-L., Wang, S.-H., Sun, Y., Lin, W.-C., Chen, J.-S. & Hsu, C.-J. 2006. Prediction Of Heat-Induced Collagen Shrinkage By Use Of Second Harmonic Generation Microscopy. *Journal Of Biomedical Optics,* 11**,** 034020.

Linde, A. & Goldberg, M. 1993. Dentinogenesis. *Critical Reviews In Oral Biology & Medicine,* 4**,** 679-728.

Liu, Y., Kim, Y.-K., Dai, L., Li, N., Khan, S. O., Pashley, D. H. & Tay, F. R. 2011a. Hierarchical And Non-Hierarchical Mineralisation Of Collagen. *Biomaterials,* 32**,** 1291-1300.

Liu, Y., Mai, S., Li, N., Yiu, C. K., Mao, J., Pashley, D. H. & Tay, F. R. 2011b. Differences Between Top-Down And Bottom-Up Approaches In Mineralizing Thick, Partially Demineralized Collagen Scaffolds. *Acta Biomaterialia,* 7**,** 1742-1751.

Linde, A. 1989. Dentin Matrix Proteins: Composition And Possible Functions In Calcification. *The Anatomical Record,* 224**,** 154-166.

Loew, L. M., Campagnola, P., Lewis, A. & Wuskell, J. P. 2002. Confocal And Nonlinear Optical Imaging Of Potentiometric Dyes. *Methods Cell Biol,* 70**,** 429-52.

Lohbauer, U. 2009. Dental Glass Ionomer Cements As Permanent Filling Materials?–Properties, Limitations And Future Trends. *Materials,* 3**,** 76-96.

Lohbauer, U., Walker, J., Nikolaenko, S., Werner, J., Clare, A., Petschelt, A. & Greil, P. 2003. Reactive Fibre Reinforced Glass Ionomer Cements. *Biomaterials,* 24**,** 2901-2907.

Lovell, L. G., Berchtold, K. A., Elliott, J. E., Lu, H. & Bowman, C. N. 2001. Understanding The Kinetics And Network Formation Of Dimethacrylate Dental Resins. *Polymers For Advanced Technologies,* 12**,** 335-345.

Lutskaya, I. K., Novak, N. V. & Kavetsky, V. P. 2012. Fluorescence Of Dental Hard Tissue And Restorative Materials. *International Dentistry—African Edition,* 2**,** 1-6.

Lutz, V., Sattler, M., Gallinat, S., Wenck, H., Poertner, R. & Fischer, F. 2012. Impact Of Collagen Crosslinking On The Second Harmonic Generation Signal And The Fluorescence Lifetime Of Collagen Autofluorescence. *Skin Research And Technology,* 18**,** 168-179.

Longhi, M., Cerroni, L., Condò, S., Ariano, V. & Pasquantonio, G. 2014. The Effects Of Host Derived Metalloproteinases On Dentin Bond And The Role Of Mmps Inhibitors On Dentin Matrix Degradation. *Oral & Implantology,* 7**,** 71.

Lussi, A. *Et Al.* (2001) *Clinical Performance Of A Laser Fluorescence Device For Detection Of Occlusal Caries Lesions.*, *European Journal Of Oral Sciences*. Doi: 10.1034/J.1600-0722.2001.109001014.X.

Macdougall, M., Simmons, D., Luan, X., Nydegger, J., Feng, J. & Gu, T. T. 1997. Dentin Phosphoprotein And Dentin Sialoprotein Are Cleavage Products Expressed From A Single Transcript Coded By A Gene On Human Chromosome 4 Dentin Phosphoprotein Dna Sequence Determination. *Journal Of Biological Chemistry,* 272**,** 835-842.

Maltz, M., De Oliveira, E. F., Fontanella, V. & Bianchi, R. 2002. A Clinical, Microbiologic, And Radiographic Study Of Deep Caries Lesions After Incomplete Caries Removal. *Quintessence International,* 33.

Maltz, M., Henz, S., De Oliveira, E. & Jardim, J. 2012. Conventional Caries Removal And Sealed Caries In Permanent Teeth: A Microbiological Evaluation. *Journal Of Dentistry,* 40**,** 776-782.

Maltz, M., Jardim, J., Mestrinho, H., Yamaguti, P., Podestá, K., Moura, M. & De Paula, L. 2013. Partial Removal Of Carious Dentine: A Multicenter

Randomized Controlled Trial And 18-Month Follow-Up Results. *Caries Research,* 47**,** 103-109.

Maltz, M., Koppe, B., Jardim, J., Alves, L., De Paula, L., Yamaguti, P., Almeida, J., Moura, M. & Mestrinho, H. 2017. Partial Caries Removal In Deep Caries Lesions: A 5-Year Multicenter Randomized Controlled Trial. *Clinical Oral Investigations***,** 1-7.

Maltz, M., Oliveira, E., Fontanella, V. & Carminatti, G. 2007. Deep Caries Lesions After Incomplete Dentine Caries Removal: 40-Month Follow-Up Study. *Caries Research,* 41**,** 493-496.

Marchi, J. J., Froner, A. M., Alves, H. L., Bergmann, C. P. & Araújo, F. B. 2008. Analysis Of Primary Tooth Dentin After Indirect Pulp Capping. *Journal Of Dentistry For Children,* 75**,** 295-300.

Marquezan, M., Corrêa, F. N. P., Sanabe, M. E., Rodrigues Filho, L. E., Hebling, J., Guedes-Pinto, A. C. & Mendes, F. M. 2009. Artificial Methods Of Dentine Caries Induction: A Hardness And Morphological Comparative Study. *Archives Of Oral Biology,* 54**,** 1111-1117.

Marshall, G., Habelitz, S., Gallagher, R., Balooch, M., Balooch, G. & Marshall, S. 2001. Nanomechanical Properties Of Hydrated Carious Human Dentin. *Journal Of Dental Research,* 80**,** 1768-1771.

Marshall Jr, G. W., Inai, N., Magidi, I.-C. W., Balooch, M., Kinney, J. H., Tagami, J. & Marshall, S. J. 1997a. Dentin Demineralization: Effects Of Dentin Depth, Ph And Different Acids. *Dental Materials,* 13**,** 338-343.

Marshall Jr, G. W., Marshall, S. J., Kinney, J. H. & Balooch, M. 1997b. The Dentin Substrate: Structure And Properties Related To Bonding. *Journal Of Dentistry,* 25**,** 441-458.

Martinez-Ramirez, S., Frías, M. & Domingo, C. 2006. Micro-Raman Spectroscopy In White Portland Cement Hydration: Long-Term Study At Room Temperature. *Journal Of Raman Spectroscopy,* 37**,** 555-561.

Massara, M. D. L. D. A., Alves, J. & Brandão, P. 2002. Atraumatic Restorative Treatment: Clinical, Ultrastructural And Chemical Analysis. *Caries Research,* 36**,** 430-436.

Masters, B. R. & So, P. 2008. *Handbook Of Biomedical Nonlinear Optical Microscopy*, Oxford University Press.

Matsumoto, H., Kitamura, S. & Araki, T. 1999. Autofluorescence In Human Dentine In Relation To Age, Tooth Type And Temperature Measured By Nanosecond Time-Resolved Fluorescence Microscopy. *Archives Of Oral Biology,* 44**,** 309-318.

Matsumoto, H., Kitamura, S. & Araki, T. 2000. Applications Of Fluorescence Microscopy To Studies Of Dental Hard Tissue. *Frontiers Of Medical And Biological Engineering,* 10**,** 269-284.

Mazzoni, A., Pashley, D. H., Nishitani, Y., Breschi, L., Mannello, F., Tjäderhane, L., Toledano, M., Pashley, E. L. & Tay, F. R. 2006. Reactivation Of Inactivated Endogenous Proteolytic Activities In Phosphoric Acid-Etched Dentine By Etch-And-Rinse Adhesives. *Biomaterials,* 27**,** 4470-4476.

Mcconnell, G., Girkin, J., Ameer-Beg, S., Barber, P., Vojnovic, B., Ng, T., Banerjee, A., Watson, T. & Cook, R. 2007. Time-Correlated Single-Photon Counting Fluorescence Lifetime Confocal Imaging Of Decayed And Sound Dental Structures With A White-Light Supercontinuum Source. *Journal Of Microscopy,* 225**,** 126-136.

Mcdonough, W. G., Antonucci, J. M., He, J., Shimada, Y., Chiang, M. Y., Schumacher, G. E. & Schultheisz, C. R. 2002. A Microshear Test To Measure Bond Strengths Of Dentin–Polymer Interfaces. *Biomaterials,* 23**,** 3603-3608.

Mertz-Fairhurst, E. J., Curtis Jr, J. W., Ergle, J. W., Rueggeberg, F. A. & Adair, S. M. 1998a. Ultraconservative And Cariostatic Sealed Restorations: Results At Year 10. *The Journal Of The American Dental Association,* 129**,** 55-66.

Mertz-Fairhurst, E. J., Curtis, J. W., Ergle, J. W., Rueggeberg, F. A. & Adair, S. M. 1998b. Ultraconservative And Cariostatic Sealed Restorations: Results At Year 10. *The Journal Of The American Dental Association,* 129**,** 55-66.

Mei, M. L., Ito, L., Cao, Y., Li, Q., Lo, E. C. & Chu, C. 2013. Inhibitory Effect Of Silver Diamine Fluoride On Dentine Demineralisation And Collagen Degradation. *Journal Of Dentistry,* 41**,** 809-817.

Mickenautsch, S. & Yengopal, V. 2010. Demineralization Of Hard Tooth Tissue Adjacent To Resin-Modified Glass-Ionomers And Composite Resins: A Quantitative Systematic Review. *Journal Of Oral Science,* 52**,** 347-357.

Mickenautsch, S., Yengopal, V., Leal, S., Oliveira, L., Bezerra, A. & Bonecker, M. 2009. Absence Of Carious Lesions At Margins Of Glass-Ionomer And Amalgam Restorations: A Meta-Analysis. *European Journal Of Paediatric Dentistry,* 10**,** 41.

Milly, H., Festy, F., Watson, T. F., Thompson, I. & Banerjee, A. 2014. Enamel White Spot Lesions Can Remineralise Using Bio-Active Glass And Polyacrylic Acid-Modified Bio-Active Glass Powders. *Journal Of Dentistry,* 42**,** 158-166.

Mitra, S. 1991. Adhesion To Dentin And Physical Properties Of A Light-Cured Glass-Ionomer Liner/Base. *Journal Of Dental Research,* 70**,** 72-74.

Miyauchi, H. 1976. Physiological Recalcification Of Carious Dentin (Author's Transl). *Kokubyo Gakkai Zasshi. The Journal Of The Stomatological Society, Japan,* 43**,** 384.

Mjör, I. A. 2002. Pulp-Dentin Biology In Restorative Dentistry. Part 7: The Exposed Pulp. *Quintessence International,* 33.

Modena, K. C. D. S., Casas-Apayco, L. C., Atta, M. T., Costa, C. A. D. S., Hebling, J., Sipert, C. R., Navarro, M. F. D. L. & Santos, C. F. 2009. Cytotoxicity And Biocompatibility Of Direct And Indirect Pulp Capping Materials. *Journal Of Applied Oral Science,* 17**,** 544-554.

Mohanty, B., Dadlani, D., Mahoney, D. & Mann, A. 2013. Characterizing And Identifying Incipient Carious Lesions In Dental Enamel Using Micro-Raman Spectroscopy. *Caries Research,* 47**,** 27-33.

Monticelli, F., Osorio, R., Mazzitelli, C., Ferrari, M. & Toledano, M. 2008. Limited Decalcification/Diffusion Of Self-Adhesive Cements Into Dentin. *Journal Of Dental Research,* 87**,** 974-979.

Mollica, F. B., Torres, C. R. G., Gonçalves, S. E. D. P. & Mancini, M. N. G. 2012. Dentine Microhardness After Different Methods For Detection And Removal Of Carious Dentine Tissue. *Journal Of Applied Oral Science,* 20**,** 449-454.

Moron, B. M., Comar, L. P., Wiegand, A., Buchalla, W., Yu, H., Buzalaf, M. A. R. & Magalhães, A. C. 2013. Different Protocols To Produce Artificial Dentine Carious Lesions In Vitro And In Situ: Hardness And Mineral Content Correlation. *Caries Research,* 47**,** 162-170.

Moreira, P.L., Messora, M.R., Pereira, S.M., Almeida, S.M.D. and Cruz, A.D.D., 2011. Diagnosis of secondary caries in esthetic restorations: influence of the incidence vertical angle of the X-ray beam. *Brazilian dental journal*, *22*(2), pp.129-133.

Moshaverinia, A., Roohpour, N., Chee, W. W. & Schricker, S. R. 2011. A Review Of Powder Modifications In Conventional Glass-Ionomer Dental Cements. *Journal Of Materials Chemistry,* 21**,** 1319-1328.

Müller, C., Teixeira, G. S., Krejci, I., Bortolotto, T. & Susin, A. H. 2017. Effect Of Caries-Affected Dentin On One-Step Universal And Multi-Step Etch-And-Rinse Adhesives' Bond Strength. *Revista De Odontologia Da Unesp,* 46**,** 273-277.

Nakajima, K., Maeno, Y., Fukudome, M., Fukuda, Y., Tanaka, S., Matsuoka, S. & Sorimachi, M. 1995. Immunofluorescence Test For The Rapid Diagnosis Of Red Sea Bream Iridovirus Infection Using Monoclonal Antibody. *Fish Pathology,* 30**,** 115-119.

Nakajima, M., Hosaka, K., Yamauti, M., Foxton, R. & Tagami, J. 2006. Bonding Durability Of A Self-Etching Primer System To Normal And Caries-Affected Dentin Under Hydrostatic Pulpal Pressure In Vitro. *American Journal Of Dentistry,* 19**,** 147-150.

Nakajima, M., Kitasako, Y., Okuda, M., Foxton, R. M. & Tagami, J. 2005. Elemental Distributions And Microtensile Bond Strength Of The Adhesive Interface To Normal And Caries-Affected Dentin. *Journal Of Biomedical Materials Research Part B: Applied Biomaterials,* 72**,** 268-275.

Nakajima, M., Kunawarote, S., Prasansuttiporn, T. & Tagami, J. 2011. Bonding To Caries-Affected Dentin. *Japanese Dental Science Review,* 47**,** 102-114.

Nakajima, M., Ogata, M., Harada, N., Tagami, J. & Pashley, D. H. 2000. Bond Strengths Of Self-Etching Primer Adhesives To In Vitro-Demineralized Dentin Following Mineralizing Treatment. *Journal Of Adhesive Dentistry,* 2.

Nakornchai, S., Atsawasuwan, P., Kitamura, E., Surarit, R. & Yamauchi, M. 2004. Partial Biochemical Characterisation Of Collagen In Carious Dentin Of Human Primary Teeth. *Archives Of Oral Biology,* 49**,** 267-273.

Nanci, A. 2017. *Ten Cate's Oral Histology-E-Book: Development, Structure, And Function*, Elsevier Health Sciences.

Nascimento, F., Minciotti, C., Geraldeli, S., Carrilho, M., Pashley, D. H., Tay, F., Nader, H., Salo, T., Tjäderhane, L. & Tersariol, I. 2011. Cysteine Cathepsins In Human Carious Dentin. *Journal Of Dental Research,* 90**,** 506-511.

Neves, A. D. A., Coutinho, E., Cardoso, M. V., Jaecques, S., Lambrechts, P., Vander Sloten, J., Van Oosterwyck, H. & Van Meerbeek, B. 2008. Influence Of Notch Geometry And Interface On Stress Concentration And Distribution In Micro-Tensile Bond Strength Specimens. *Journal Of Dentistry,* 36**,** 808-815.

Ngo, H., Mount, G. & Peters, M. 1997. A Study Of Glass-Ionorner Cement And Its Interface With Enamel And Dentin Using A Low-Temperature, High-Resolution Scanning Electron Microscopic Technique. *Quintessence International,* 28.

Ngo, H. C., Mount, G., Mc Intyre, J., Tuisuva, J. & Von Doussa, R. J. 2006. Chemical Exchange Between Glass-Ionomer Restorations And Residual Carious Dentine In Permanent Molars: An In Vivo Study. *Journal Of Dentistry,* 34**,** 608-613.

Ngo, H. C., Mount, G., Mcintyre, J. & Do, L. 2011. An In Vitro Model For The Study Of Chemical Exchange Between Glass Ionomer Restorations And Partially Demineralized Dentin Using A Minimally Invasive Restorative Technique. *Journal Of Dentistry,* 39**,** S20-S26.

Nicholson, J. W. 1998. Chemistry Of Glass-Ionomer Cements: A Review. *Biomaterials,* 19**,** 485-494.

Nicholson, J. W., Czarnecka, B. & Limanowska-Shaw, H. 1999. The Long-Term Interaction Of Dental Cements With Lactic Acid Solutions. *Journal Of Materials Science: Materials In Medicine,* 10**,** 449-452.

Niu, L.-N., Zhang, W., Pashley, D. H., Breschi, L., Mao, J., Chen, J.-H. & Tay, F. R. 2014. Biomimetic Remineralization Of Dentin. *Dental Materials,* 30**,** 77-96.

Nujella, B. S., Choudary, M. T., Reddy, S. P., Kumar, M. K. & Gopal, T. 2012. Comparison Of Shear Bond Strength Of Aesthetic Restorative Materials. *Contemporary Clinical Dentistry,* 3**,** 22.

Nurrohman, H., Nakashima, S., Takagaki, T., Sadr, A., Nikaido, T., Asakawa, Y., Uo, M., Marshall, S. J. & Tagami, J. 2015. Immobilization Of Phosphate Monomers On Collagen Induces Biomimetic Mineralization. *Bio-Medical Materials And Engineering,* 25**,** 89-99.

Ogawa, K., Yamashita, Y., Ichijo, T. & Fusayama, T. 1983. The Ultrastructure And Hardness Of The Transparent Of Human Carious Dentin. *Journal Of Dental Research,* 62**,** 7-10.

Ohgushi, K. & Fusayama, T. 1975. Electron Microscopic Structure Of The Two Layers Of Carious Dentin. *Journal Of Dental Research,* 54**,** 1019-1026.

Orgel, J. P., Irving, T. C., Miller, A. & Wess, T. J. 2006. Microfibrillar Structure Of Type I Collagen In Situ. *Proceedings Of The National Academy Of Sciences,* 103**,** 9001-9005.

Okamoto, Y., Heeley, J., Dogon, I. & Shintani, H. 1991. Effects Of Phosphoric Acid And Tannic Acid On Dentine Collagen. *Journal Of Oral Rehabilitation,* 18**,** 507-512.

Omar, H., El-Badrawy, W., El-Mowafy, O., Atta, O. & Saleem, B. 2007. Microtensile Bond Strength Of Resin Composite Bonded To Caries-Affected Dentin With Three Adhesives. *Operative Dentistry,* 32**,** 24-30.

Osorio, R., Yamauti, M., Osorio, E., Ruiz-Requena, M., Pashley, D. H., Tay, F. & Toledano, M. 2011. Zinc Reduces Collagen Degradation In Demineralized Human Dentin Explants. *Journal Of Dentistry,* 39**,** 148-153.

Ozkan, G. and Guzel, K.G.U., 2017. Clinical evaluation of near-infrared light transillumination in approximal dentin caries detection. *Lasers in medical science*, *32*(6), pp.1417-1422.

Pacheco, L. F., Banzi, E. C. D. F., Rodrigues, E., Soares, L. E. S., Pascon, F. M., Correr-Sobrinho, L. & Puppin-Rontani, R. M. 2013. Molecular And Structural Evaluation Of Dentin Caries-Like Lesions Produced By Different Artificial Models. *Brazilian Dental Journal,* 24**,** 610-618.

Paddick, J., Brailsford, S., Kidd, E. & Beighton, D. 2005. Phenotypic And Genotypic Selection Of Microbiota Surviving Under Dental Restorations. *Applied And Environmental Microbiology,* 71**,** 2467-2472.

Palma-Dibb, R. G., De Castro, C. G., Ramos, R. P., Chimello, D. T. & Chinelatti, M. A. 2003. Bond Strength Of Glass-Ionomer Cements To Caries-Affected Dentin. *Journal Of Adhesive Dentistry,* 5.

Palosaari, H., Pennington, C. J., Larmas, M., Edwards, D. R., Tjäderhane, L. & Salo, T. 2003. Expression Profile Of Matrix Metalloproteinases (Mmps) And Tissue Inhibitors Of Mmps In Mature Human Odontoblasts And Pulp Tissue. *European Journal Of Oral Sciences,* 111**,** 117-127.

Panayotov, I., Terrer, E., Salehi, H., Tassery, H., Yachouh, J., Cuisinier, F. J. & Levallois, B. 2013. In Vitro Investigation Of Fluorescence Of Carious Dentin Observed With A Soprolife® Camera. *Clinical Oral Investigations,* 17**,** 757-763.

Parker, A. S., Patel, A. N., Al Botros, R., Snowden, M. E., Mckelvey, K., Unwin, P. R., Ashcroft, A. T., Carvell, M., Joiner, A. & Peruffo, M. 2014. Measurement Of The Efficacy Of Calcium Silicate For The Protection And Repair Of Dental Enamel. *Journal Of Dentistry,* 42**,** S21-S29.

Pashley, D. H. 1991. Clinical Correlations Of Dentin Structure And Function. *Journal Of Prosthetic Dentistry,* 66**,** 777-781.

Pashley, D. H. 1992. The Effects Of Acid Etching On The Pulpodentin Complex. *Operative Dentistry,* 17**,** 229-242.

Pashley, D. H. & Carvalho, R. 1997. Dentine Permeability And Dentine Adhesion. *Journal Of Dentistry,* 25**,** 355-372.

Pashley, D. H., Carvalho, R. M., Sano, H., Nakajima, M., Yoshiyama, M., Shono, Y., Fernandes, C. A. & Tay, F. 1999. The Microtensile Bond Test: A Review. *Journal Of Adhesive Dentistry,* 1.

Paula, J. S., Leite, I. C., Almeida, A. B., Ambrosano, G. M., Pereira, A. C. & Mialhe, F. L. 2012. The Influence Of Oral Health Conditions, Socioeconomic Status And Home Environment Factors On Schoolchildren's Self-Perception Of Quality Of Life. *Health And Quality Of Life Outcomes,* 10**,** 6.

Paulo, H. D., Pereira, J. C., Svizero, N. R., Rueggeberg, F. A. & Pashley, D. H. 2006. Use Of Fluorescent Compounds In Assessing Bonded Resin-Based Restorations: A Literature Review. *Journal Of Dentistry,* 34**,** 623-634.

Penel, G., Leroy, G., Rey, C. & Bres, E. 1998. Microraman Spectral Study Of The Po 4 And Co 3 Vibrational Modes In Synthetic And Biological Apatites. *Calcified Tissue International,* 63**,** 475-481.

Perdigão, J. & Lopes, M. 2001. The Effect Of Etching Time On Dentin Demineralization. *Quintessence International,* 32.

Perdigão, J., Sezinando, A. & Monteiro, P. C. 2012. Laboratory Bonding Ability Of A Multi-Purpose Dentin Adhesive. *American Journal Of Dentistry,* 25**,** 153-158.

Perdigao, J., Swift Jr, E., Denehy, G., Wefel, J. & Donly, K. 1994. In Vitro Bond Strengths And Sem Evaluation Of Dentin Bonding Systems To Different Dentin Substrates. *Journal Of Dental Research,* 73**,** 44-55.

Pereira, J. C., Segala, A. D. & Costa, C. 2000. Human Pulpal Response To Direct Pulp Capping With An Adhesive System. *American Journal Of Dentistry,* 13**,** 139-147.

Petruska, J. A. & Hodge, A. J. 1964. A Subunit Model For The Tropocollagen Macromolecule. *Proceedings Of The National Academy Of Sciences,* 51**,** 871-876.

Peumans, M., Kanumilli, P., De Munck, J., Van Landuyt, K., Lambrechts, P. & Van Meerbeek, B. 2005. Clinical Effectiveness Of Contemporary Adhesives: A Systematic Review Of Current Clinical Trials. *Dental Materials,* 21**,** 864-881.

Prabhakar, A., Raj, S. & Raju, O. 2003. Comparison Of Shear Bond Strength Of Composite, Compomer And Resin Modified Glass Ionomer In Primary And Permanent Teeth: An In Vitro Study. *Journal-Indian Society Of Pedodontics And Preventive Dentistry,* 21**,** 86.

Pretty, I.A., 2006. Caries detection and diagnosis: novel technologies. *Journal of dentistry*, *34*(10), pp.727-739.

Pinna, R. *Et Al.* (2015) 'Carious Affected Dentine: Its Behaviour In Adhesive Bonding', *Australian Dental Journal*, 60(3), Pp. 276–293. Doi: 10.1111/Adj.12309.

Pihlstrom, B. & Barnett, M. 2010. Design, Operation, And Interpretation Of Clinical Trials. *Journal Of Dental Research,* 89**,** 759-772.

Pitel, M. 2017. An Improved Glass Ionomer Restorative System: Stress-Bearing Class I And Ii Indications. *Dentistry Today,* 36**,** 130-134.

Pontes, L.R.A., Novaes, T.F., Moro, B.L.P., Braga, M.M. And Mendes, F.M., 2017. Clinical Performance Of Fluorescence-Based Methods For Detection Of Occlusal Caries Lesions In Primary Teeth. *Brazilian Oral Research*, *31*.

Pugach, M.K., Strother, J., Darling, C.L., Fried, D., Gansky, S.A., Marshall, S.J. and Marshall, G.W., 2009. Dentin caries zones: mineral, structure, and properties. *Journal of dental research*, *88*(1), pp.71-76.

Qin, C., Baba, O. & Butler, W. 2004. Post-Translational Modifications Of Sibling Proteins And Their Roles In Osteogenesis And Dentinogenesis. *Critical Reviews In Oral Biology & Medicine,* 15**,** 126-136.

Qin, C., Brunn, J., Cadena, E., Ridall, A., Tsujigiwa, H., Nagatsuka, H., Nagai, N. & Butler, W. 2002. The Expression Of Dentin Sialophosphoprotein Gene In Bone. *Journal Of Dental Research,* 81**,** 392-394.

Qi, Y.-P., Li, N., Niu, L.-N., Primus, C. M., Ling, J.-Q., Pashley, D. H. & Tay, F. R. 2012. Remineralization Of Artificial Dentinal Caries Lesions By Biomimetically Modified Mineral Trioxide Aggregate. *Acta Biomaterialia,* 8**,** 836-842.

Rahemtulla, F., Prince, C. W. & Butler, W. T. 1984. Isolation And Partial Characterization Of Proteoglycans From Rat Incisors. *Biochemical Journal,* 218**,** 877-885.

Ramakrishnaiah, R., Rehman, G. U., Basavarajappa, S., Al Khuraif, A. A., Durgesh, B., Khan, A. S. & Rehman, I. U. 2015. Applications Of Raman Spectroscopy In Dentistry: Analysis Of Tooth Structure. *Applied Spectroscopy Reviews,* 50**,** 332-350.

Rechmann, P., Rechmann, B. & Featherstone, J. 2012. Caries Detection Using Light-Based Diagnostic Tools. *Compend Contin Educ Dent,* 33**,** 582-4.

Revenko, I., Sommer, F., Minh, D. T., Garrone, R. & Franc, J. M. 1994. Atomic Force Microscopy Study Of The Collagen Fibre Structure. *Biology Of The Cell,* 80**,** 67-69.

Reyes-Carmona, J. F., Felippe, M. S. & Felippe, W. T. 2009. Biomineralization Ability And Interaction Of Mineral Trioxide Aggregate And White Portland Cement With Dentin In A Phosphate-Containing Fluid. *Journal Of Endodontics,* 35**,** 731-736.

Ricketts, D., Lamont, T., Innes, N., Kidd, E. & Clarkson, J. E. 2013. Operative Caries Management In Adults And Children. *The Cochrane Library*.

Rivera, E. & Yamauchi, M. 1993. Site Comparisons Of Dentine Collagen Cross-Links From Extracted Human Teeth. *Archives Of Oral Biology,* 38**,** 541-546.

Rocha, C., Faria-E-Silva, A. & Peixoto, A. 2014. Bond Strength Of Adhesive Luting Agents To Caries-Affected Dentin. *Operative Dentistry,* 39**,** 383-388.

Roeder, L., Pereira, P. N., Yamamoto, T., Ilie, N., Armstrong, S. & Ferracane, J. 2011. Spotlight On Bond Strength Testing—Unraveling The Complexities. *Dental Materials,* 27**,** 1197-1203.

Rosales, J., Marshall, G., Marshall, S., Watanabe, L., Toledano, M., Cabrerizo, M. & Osorio, R. 1999. Acid-Etching And Hydration Influence On Dentin Roughness And Wettability. *Journal Of Dental Research,* 78**,** 1554-1559.

Ryou, H., Romberg, E., Pashley, D. H., Tay, F. R. & Arola, D. 2012. Nanoscopic Dynamic Mechanical Properties Of Intertubular And Peritubular Dentin. *Journal Of The Mechanical Behavior Of Biomedical Materials,* 7**,** 3-16.

Saad, A., Inoue, G., Nikaido, T., Ikeda, M., Burrow, M. & Tagami, J. 2017. Microtensile Bond Strength Of Resin-Modified Glass Ionomer Cement To Sound And Artificial Caries–Affected Root Dentin With Different Conditioning. *Operative Dentistry,* 42**,** 626-635.

Saito, T., Ogawa, M., Hata, Y. & Bessho, K. 2004. Acceleration Effect Of Human Recombinant Bone Morphogenetic Protein-2 On Differentiation Of Human Pulp Cells Into Odontoblasts. *Journal Of Endodontics,* 30**,** 205-208.

Salli, K. M. & Ouwehand, A. C. 2015. The Use Of In Vitro Model Systems To Study Dental Biofilms Associated With Caries: A Short Review. *Journal Of Oral Microbiology,* 7**,** 26149.

Salz, U., Mücke, A., Zimmermann, J., Tay, F. R. & Pashley, D. H. 2006. Pka Value And Buffering Capacity Of Acidic Monomers Commonly Used In Self-Etching Primers. *Journal Of Adhesive Dentistry,* 8.

Sajini, S., Atmeh, A., Festy, F. & Watson, T. 2013. *Evaluation Of Remineralizing Potential Of Biodentine™ Using Two-Photon Fluorescence Microscopy*.

Sajini, S., 2016. *Multimodal Optical characterisation of the interface between dental cements and sound or carious dentinal substrates* (Doctoral dissertation, King's College London).

Salehi, H., Terrer, E., Panayotov, I., Levallois, B., Jacquot, B., Tassery, H. & Cuisinier, F. 2013. Functional Mapping Of Human Sound And Carious Enamel And Dentin With Raman Spectroscopy. *Journal Of Biophotonics,* 6**,** 765-774.

Sano, H., Shono, T., Sonoda, H., Takatsu, T., Ciucchi, B., Carvalho, R. & Pashley, D. H. 1994. Relationship Between Surface Area For Adhesion And Tensile Bond Strength—Evaluation Of A Micro-Tensile Bond Test. *Dental Materials,* 10**,** 236-240.

Salehi, H., Terrer, E., Panayotov, I., Levallois, B., Jacquot, B., Tassery, H. & Cuisinier, F. 2013. Functional Mapping Of Human Sound And Carious Enamel And Dentin With Raman Spectroscopy. *Journal Of Biophotonics,* 6**,** 765-774.

Sauer, G., Zunic, W., Durig, J. & Wuthier, R. 1994. Fourier Transform Raman Spectroscopy Of Synthetic And Biological Calcium Phosphates. *Calcified Tissue International,* 54**,** 414-420.

Sauro, S., Watson, T. F., Mannocci, F., Miyake, K., Huffman, B. P., Tay, F. R. & Pashley, D. H. 2009. Two-Photon Laser Confocal Microscopy Of Micropermeability Of Resin-Dentin Bonds Made With Water Or Ethanol Wet Bonding. *Journal Of Biomedical Materials Research Part B: Applied Biomaterials,* 90**,** 327-337.

Sarrett, D. C. 2005. Clinical Challenges And The Relevance Of Materials Testing For Posterior Composite Restorations. *Dental Materials,* 21**,** 9-20.

Say, E. C., Nakajima, M., Senawongse, P., Soyman, M., Özer, F., Ogata, M. & Tagami, J. 2006. Microtensile Bond Strength Of A Filled Vs Unfilled Adhesive To Dentin Using Self-Etch And Total-Etch Technique. *Journal Of Dentistry,* 34**,** 283-291.

Scherrer, S. S., Cesar, P. F. & Swain, M. V. 2010. Direct Comparison Of The Bond Strength Results Of The Different Test Methods: A Critical Literature Review. *Dental Materials,* 26**,** E78-E93.

Scholtanus, J., Purwanta, K., Dogan, N., Kleverlaan, C. J. & Felizer, A. J. 2010. Microtensile Bond Strength Of Three Simplified Adhesive Systems To Caries-Affected Dentin. *Journal Of Adhesive Dentistry,* 12.

Schwendicke, F., Eggers, K., Meyer-Lueckel, H., Dörfer, C., Kovalev, A., Gorb, S. & Paris, S. 2015. In Vitro Induction Of Residual Caries Lesions In Dentin: Comparative Mineral Loss And Nano-Hardness Analysis. *Caries Research,* 49**,** 259-265.

Schwendicke, F., Frencken, J., Bjørndal, L., Maltz, M., Manton, D., Ricketts, D., Van Landuyt, K., Banerjee, A., Campus, G. & Doméjean, S. 2016. Managing Carious Lesions: Consensus Recommendations On Carious Tissue Removal. *Advances In Dental Research,* 28**,** 58-67.

Schwendicke, F., Paris, S. & Tu, Y.-K. 2015. Effects Of Using Different Criteria For Caries Removal: A Systematic Review And Network Meta-Analysis. *Journal Of Dentistry,* 43**,** 1-15.

Schwendicke, F., Stolpe, M., Meyer-Lueckel, H., Paris, S. & Dörfer, C. 2013. Cost-Effectiveness Of One-And Two-Step Incomplete And Complete Excavations. *Journal Of Dental Research,* 92**,** 880-887.

Seah, R. K., Garland, M., Loo, J. S. & Widjaja, E. 2009. Use Of Raman Microscopy And Multivariate Data Analysis To Observe The Biomimetic Growth Of Carbonated Hydroxyapatite On Bioactive Glass. *Analytical Chemistry,* 81**,** 1442-1449.

Sennou, H., Lebugle, A. & Grégoire, G. 1999. X-Ray Photoelectron Spectroscopy Study Of The Dentin–Glass Ionomer Cement Interface. *Dental Materials,* 15**,** 229-237.

Selwitz, R.H., Ismail, A.I. And Pitts, N.B., 2007. Dental Caries. *The Lancet*, *369*(9555), Pp.51-59.

Shakibaie, F., George, R. And Walsh, L.J., 2011. Applications Of Laser Induced Fluorescence In Dentistry. *International Journal Of Dental Clinics*, *3*(3).

Shibata, Y., He, L., Kataoka, Y., Miyazaki, T. & Swain, M. 2008. Micromechanical Property Recovery Of Human Carious Dentin Achieved With Colloidal Nano-B-Tricalcium Phosphate. *Journal Of Dental Research,* 87**,** 233-237.

Shida, K., Kitasako, Y., Burrow, M. F. & Tagami, J. 2009. Micro-Shear Bond Strengths And Etching Efficacy Of A Two-Step Self-Etching Adhesive System To Fluorosed And Non-Fluorosed Enamel. *European Journal Of Oral Sciences,* 117**,** 182-186.

Shimada, Y., Kikushima, D. & Tagami, J. 2002. Micro-Shear Bond Strength Of Resin-Bonding Systems To Cervical Enamel. *American Journal Of Dentistry,* 15**,** 373-377.

Shimada, Y., Sadr, A., Sumi, Y. & Tagami, J. 2015. Application Of Optical Coherence Tomography (Oct) For Diagnosis Of Caries, Cracks, And Defects Of Restorations. *Current Oral Health Reports,* 2**,** 73-80.

Shimizu, A., Nakashima, S., Nikaido, T., Sugawara, T., Yamamoto, T. & Momoi, Y. 2013. Newly Developed Hardness Testing System,“Cariotester”: Measurement Principles And Development Of A Program For Measuring Knoop Hardness Of Carious Dentin. *Dental Materials Journal,* 32**,** 643-647.

Sidhu, S. 2011. Glass-Ionomer Cement Restorative Materials: A Sticky Subject? *Australian Dental Journal,* 56**,** 23-30.

Sidhu, S., Sherriff, M. & Watson, T. 1997. The Effects Of Maturity And Dehydration Shrinkage On Resin-Modified Glass-Ionomer Restorations. *Journal Of Dental Research,* 76**,** 1495-1501.

Sidhu, S. & Watson, T. 1998a. Interfacial Characteristics Of Resin-Modified Glass-Ionomer Materials: A Study On Fluid Permeability Using Confocal Fluorescence Microscopy. *Journal Of Dental Research,* 77**,** 1749-1759.

Sidhu, S. K. & Nicholson, J. W. 2016. A Review Of Glass-Ionomer Cements For Clinical Dentistry. *Journal Of Functional Biomaterials,* 7**,** 16.

Sidhu, S. K. & Watson, T. F. 1998b. Interfacial Characteristics Of Resin-Modified Glass-Ionomer Materials: A Study On Fluid Permeability Using Confocal Fluorescence Microscopy. *J Dent Res,* 77**,** 1749-59.

Simila, H. O., Karpukhina, N. & Hill, R. G. 2018. Bioactivity And Fluoride Release Of Strontium And Fluoride Modified Biodentine. *Dental Materials,* 34**,** E1-E7.

Singh, P., Nagpal, R. & Singh, U. P. 2017. Effect Of Dentin Biomodifiers On The Immediate And Long-Term Bond Strengths Of A Simplified Etch And Rinse Adhesive To Dentin. *Restorative Dentistry & Endodontics,* 42**,** 188-199.

Sirisha, K., Rambabu, T., Ravishankar, Y. & Ravikumar, P. 2014. Validity Of Bond Strength Tests: A Critical Review-Part Ii. *Journal Of Conservative Dentistry: Jcd,* 17**,** 420.

Slimani, A., Panayotov, I., Levallois, B., Cloitre, T., Gergely, C., Bec, N., Larroque, C., Tassery, H. & Cuisinier, F. Porphyrin Involvement In Redshift Fluorescence In Dentin Decay. Biophotonics: Photonic Solutions For Better Health Care Iv, 2014. International Society For Optics And Photonics, 91291c.

Slimani, A., Tardivo, D., Panayotov, I. V., Levallois, B., Gergely, C., Cuisinier, F., Tassery, H., Cloitre, T. & Terrer, E. 2018. Multiphoton Microscopy For Caries Detection With Icdas Classification. *Caries Research,* 52**,** 359-366.

Smith, A., Scheven, B., Takahashi, Y., Ferracane, J., Shelton, R. & Cooper, P. 2012. Dentine As A Bioactive Extracellular Matrix. *Archives Of Oral Biology,* 57**,** 109-121.

Spencer, P., Wang, Y., Katz, J. L. & Misra, A. 2005. Physicochemical Interactions At The Dentin/Adhesive Interface Using Ftir Chemical Imaging. *Journal Of Biomedical Optics,* 10**,** 031104.

Spencer, P., Wang, Y., Walker, M., Wieliczka, D. & Swafford, J. 2000. Interfacial Chemistry Of The Dentin/Adhesive Bond. *Journal Of Dental Research,* 79**,** 1458-1463.

Stefaneli Marques, J. H., Silva-Sousa, Y. T. C., Rached-Júnior, F. J. A., Macedo, L. M. D. D., Mazzi-Chaves, J. F., Camilleri, J. & Sousa-Neto, M. D. 2018. Push-Out Bond Strength Of Different Tricalcium Silicate-Based Filling Materials To Root Dentin. *Brazilian Oral Research,* 32.

Stoller, P., Reiser, K. M., Celliers, P. M. & Rubenchik, A. M. 2002. Polarization-Modulated Second Harmonic Generation In Collagen. *Biophysical Journal,* 82**,** 3330-3342.

Stookey, G. K., Jackson, R. D., Zandona, A. & Analoui, M. 1999. Dental Caries Diagnosis. *Dental Clinics Of North America,* 43**,** 665-77, Vi.

Suzuki, T. Y., Godas, A. G., Guedes, A. P., Catelan, A., Pavan, S., Briso, A. L. & Dos Santos, P. H. 2013. Microtensile Bond Strength Of Resin Cements To Caries-Affected Dentin. *Journal Of Prosthetic Dentistry,* 110**,** 47-55.

Summitt, J. B., Robbins, J. W., Hilton, T. J., Schwartz, R. S. & Dos Santos Jr, J. 2006. *Fundamentals Of Operative Dentistry: A Contemporary Approach*, Quintessence Pub.

Suppa, P., Breschi, L., Ruggeri, A., Mazzotti, G., Prati, C., Chersoni, S., Di Lenarda, R., Pashley, D. H. & Tay, F. R. 2005. Nanoleakage Within The Hybrid Layer: A Correlative Feisem/Tem Investigation. *Journal Of Biomedical Materials Research Part B: Applied Biomaterials,* 73**,** 7-14.

Swift, E. J. 2002. Dentin/Enamel Adhesives: Review Of The Literature. *Pediatric Dentistry,* 24**,** 456-461.

Swift, E. J., Perdigao, J. & Heymann, H. O. 1995. Bonding To Enamel And Dentin: A Brief History And State Of The Art, 1995. *Quintessence International-English Edition-,* 26**,** 95-95.

Sytsma, J., Vroom, J., De Grauw, C. & Gerritsen, H. 2003. Time-Gated Fluorescence Lifetime Imaging And Microvolume Spectroscopy Using Two-Photon Excitation. *Spie Milestone Series,* 175**,** 354-366.

Takamizawa, T., Barkmeier, W. W., Tsujimoto, A., Suzuki, T., Scheidel, D. D., Erickson, R. L., Latta, M. A. & Miyazaki, M. 2016. Influence Of Different Pre-Etching Times On Fatigue Strength Of Self-Etch Adhesives To Dentin. *European Journal Of Oral Sciences,* 124**,** 210-218.

Tang, G., Yip, H.-K., Cutress, T. W. & Samaranayake, L. P. 2003. Artificial Mouth Model Systems And Their Contribution To Caries Research: A Review. *Journal Of Dentistry,* 31**,** 161-171.

Tanzer, M. L. 1973. Cross-Linking Of Collagen. *Science,* 180**,** 561-566.

Tay, F., Sidhu, S., Watson, T. & Pashley, D. H. 2004. Water-Dependent Interfacial Transition Zone In Resin-Modified Glass-Ionomer Cement/Dentin Interfaces. *Journal Of Dental Research,* 83**,** 644-649.

Tay, F. R. & Pashley, D. H. 2008. Guided Tissue Remineralisation Of Partially Demineralised Human Dentine. *Biomaterials,* 29**,** 1127-1137.

Tay, F. R., Pashley, D. H., Rueggeberg, F. A., Loushine, R. J. & Weller, R. N. 2007. Calcium Phosphate Phase Transformation Produced By The Interaction Of The Portland Cement Component Of White Mineral Trioxide Aggregate With A Phosphate-Containing Fluid. *Journal Of Endodontics,* 33**,** 1347-1351.

Tedesco, T. K., Montagner, A. F., Skupien, J. A., Soares, F., Susin, A. H. & Rocha, R. D. O. 2013. Starch Tubing: An Alternative Method To Build Up Microshear Bond Test Specimens. *J Adhes Dent,* 15**,** 311-5.

Tay, F. R. & Pashley, D. H. 2001. Aggressiveness Of Contemporary Self-Etching Systems: I: Depth Of Penetration Beyond Dentin Smear Layers. *Dental Materials,* 17**,** 296-308.

Tay, F., Sidhu, S., Watson, T. & Pashley, D. H. 2004. Water-Dependent Interfacial Transition Zone In Resin-Modified Glass-Ionomer Cement/Dentin Interfaces. *Journal Of Dental Research,* 83**,** 644-649.

Ten Cate, J. 1994. In Situ Models, Physico-Chemical Aspects. *Advances In Dental Research,* 8**,** 125-133.

Ten Cate, J. 1995. Hypermineralization Of Dental Lesions Adjacent To Glass-Ionomer Cement. *Nederlands Tandartsenblad,* 50.

Ten Cate, J. 2001. Remineralization Of Caries Lesions Extending Into Dentin. *Journal Of Dental Research,* 80**,** 1407-1411.

Ten Cate, J. 2008. Remineralization Of Deep Enamel Dentine Caries Lesions. *Australian Dental Journal,* 53**,** 281-285.

Terrer, E., Koubi, S., Dionne, A., Weisrock, G., Sarraquigne, C., Mazuir, A. & Tassery, H. 2009. A New Concept In Restorative Dentistry: Light-Induced Fluorescence Evaluator For Diagnosis And Treatment. Part 1: Diagnosis And Treatment Of Initial Occlusal Caries. *J Contemp Dent Pract,* 10**,** E086-094.

Thomas, S. S., Jayanthi, J., Subhash, N., Thomas, J., Mallia, R. J. & Aparna, G. 2011. Characterization Of Dental Caries By Lif Spectroscopy With 404-Nm Excitation. *Lasers In Medical Science,* 26**,** 299-305.

Thompson, V., Craig, R. G., Curro, F. A., Green, W. S. & Ship, J. A. 2008. Treatment Of Deep Carious Lesions By Complete Excavation Or Partial Removal: A Critical Review. *J Am Dent Assoc,* 139**,** 705-12.

Tjäderhane, L., Larjava, H., Sorsa, T., Uitto, V.-J., Larmas, M. & Salo, T. 1998. The Activation And Function Of Host Matrix Metalloproteinases In Dentin Matrix Breakdown In Caries Lesions. *Journal Of Dental Research,* 77**,** 1622-1629.

Tjandrawinata, R., Irie, M., Yoshida, Y. & Suzuki, K. 2004. Effect Of Adding Spherical Silica Filler On Physico-Mechanical Properties Of Resin Modified Glass-Ionomer Cement. *Dental Materials Journal,* 23**,** 146-154.

Toledano, M., Aguilera, F. S., Osorio, E., Cabello, I., Toledano-Osorio, M. & Osorio, R. 2015a. Bond Strength And Bioactivity Of Zn-Doped Dental Adhesives Promoted By Load Cycling. *Microscopy And Microanalysis,* 21**,** 214-230.

Toledano, M., Cabello, I., Aguilera, F. S., Osorio, E., Toledano-Osorio, M. & Osorio, R. 2015b. Improved Sealing And Remineralization At The Resin-Dentin Interface After Phosphoric Acid Etching And Load Cycling. *Microscopy And Microanalysis,* 21**,** 1530-1548.

Toledano, M., Osorio, E., Aguilera, F. S., Cabello, I., Toledano-Osorio, M. & Osorio, R. 2017. Ex Vivo Detection And Characterization Of Remineralized Carious Dentin, By Nanoindentation And Single Point Raman Spectroscopy, After Amalgam Restoration. *Journal Of Raman Spectroscopy,* 48**,** 384-392.

Toledano, M., Osorio, E., Aguilera, F. S., Sauro, S., Cabello, I. & Osorio, R. 2014. In Vitro Mechanical Stimulation Promoted Remineralization At The Resin/Dentin Interface. *Journal Of The Mechanical Behavior Of Biomedical Materials,* 30**,** 61-74.

Toledano, M., Sauro, S., Cabello, I., Watson, T. & Osorio, R. 2013. A Zn-Doped Etch-And-Rinse Adhesive May Improve The Mechanical Properties And The Integrity At The Bonded-Dentin Interface. *Dent Mater,* 29**,** E142-52.

Torabinejad, M., Hong, C., Mcdonald, F. & Ford, T. P. 1995. Physical And Chemical Properties Of A New Root-End Filling Material. *Journal Of Endodontics,* 21**,** 349-353.

Tramini, P., Pélissier, B., Valcarcel, J., Bonnet, B. & Maury, L. 2000. A Raman Spectroscopic Investigation Of Dentin And Enamel Structures Modified By Lactic Acid. *Caries Research,* 34**,** 233-240.

Tsanidis, V. & Koulourides, T. 1992. An In Vitro Model For Assessment Of Fluoride Uptake From Glass-Ionomer Cements By Dentin And Its Effect On Acid Resistance. *Journal Of Dental Research,* 71**,** 7-12.

Tsuda, H. & Arends, J. 1997. Raman Spectroscopy In Dental Research: A Short Review Of Recent Studies. *Advances In Dental Research,* 11**,** 539-547.

Unemori, M., Matsuya, Y., Akashi, A., Goto, Y. & Akamine, A. 2004. Self-Etching Adhesives And Postoperative Sensitivity. *American Journal Of Dentistry,* 17**,** 191-195.

Vallittu, P.K., Boccaccini, A.R., Hupa, L. and Watts, D.C., 2018. Bioactive dental materials—Do they exist and what does bioactivity mean? *Dent Mater,* 34, 693-4.

Van Amerongen, W. E. 1996. Dental Caries Under Glass Ionomer Restorations. *Journal Of Public Health Dentistry,* 56**,** 150-154.

Van Der Rest, M. & Garrone, R. 1990. Collagens As Multidomain Proteins. *Biochimie,* 72**,** 473-484.

Van Der Rest, M. & Garrone, R. 1991. Collagen Family Of Proteins. *The Faseb Journal,* 5**,** 2814-2823.

Van Der Veen, M. & Ten Bosch, J. 1996. The Influence Of Mineral Loss On The Auto-Fluorescent Behaviour Of In Vitro Demineralised Dentine. *Caries Research,* 30**,** 93-99.

Van Meerbeek, B., De Munck, J., Yoshida, Y., Inoue, S., Vargas, M., Vijay, P., Van Landuyt, K., Lambrechts, P. & Vanherle, G. 2003. Adhesion To Enamel And Dentin: Current Status And Future Challenges. *Operative Dentistry-University Of Washington-,* 28**,** 215-235.

Van Meerbeek, B., Dhem, A., Goret-Nicaise, M., Braem, M., Lambrechts, P. & Vanherle, G. 1993. Comparative Sem And Tem Examination Of The Ultrastructure Of The Resin-Dentin Interdiffusion Zone. *Journal Of Dental Research,* 72**,** 495-501.

Van Meerbeek, B., Inokoshi, S., Braem, M., Lambrechts, P. & Vanherle, G. 1992. Morphological Aspects Of The Resin-Dentin Interdiffusion Zone With Different Dentin Adhesive Systems. *Journal Of Dental Research,* 71**,** 1530-1540.

Van Meerbeek, B., Peumans, M., Poitevin, A., Mine, A., Van Ende, A., Neves, A. & De Munck, J. 2010. Relationship Between Bond-Strength Tests And Clinical Outcomes. *Dental Materials,* 26**,** E100-E121.

Van Meerbeek, B., Van Landuyt, K., De Munck, J., Hashimoto, M., Peumans, M., Lambrechts, P., Yoshida, Y., Inoue, S. & Suzuki, K. 2005. Technique-Sensitivity Of Contemporary Adhesives. *Dental Materials Journal,* 24**,** 1-13.

Van Meerbeek, B., Yoshihara, K., Yoshida, Y., Mine, A., De Munck, J. & Van Landuyt, K. 2011. State Of The Art Of Self-Etch Adhesives. *Dental Materials,* 27**,** 17-28.

Van Noort, R., Noroozi, S., Howard, I. & Cardew, G. 1989. A Critique Of Bond Strength Measurements. *Journal Of Dentistry,* 17**,** 61-67.

Veen, M. H. & Bosch, J. J. 1995. Autofluorescence Of Bulk Sound And In Vitro Demineralized Human Root Dentin. *European Journal Of Oral Sciences,* 103**,** 375-381.

Wachsmann-Hogiu, S., Weeks, T. & Huser, T. 2009. Chemical Analysis In Vivo And In Vitro By Raman Spectroscopy—From Single Cells To Humans. *Current Opinion In Biotechnology,* 20**,** 63-73.

Walls, A. 1986. Glass Polyalkenoate (Glass-Ionomer) Cements: A Review. *Journal Of Dentistry,* 14**,** 231-246.

Wambier, D. S., Dos Santos, F. A., Guedes-Pinto, A. C., Jaeger, R. G. & Simionato, M. R. L. 2007. Ultrastructural And Microbiological Analysis Of The Dentin Layers Affected By Caries Lesions In Primary Molars Treated By Minimal Intervention. *Pediatric Dentistry,* 29**,** 228-234.

Wang, J., Chen, Y., Li, L., Sun, J., Gu, X., Xu, X., Pan, H. & Tang, R. 2013. Remineralization Of Dentin Collagen By Meta-Stabilized Amorphous Calcium Phosphate. *Crystengcomm,* 15**,** 6151-6158.

Wang, Y. & Spencer, P. 2003. Hybridization Efficiency Of The Adhesive/Dentin Interface With Wet Bonding. *Journal Of Dental Research,* 82**,** 141-145.

Wang, Y., Spencer, P. & Walker, M. P. 2007. Chemical Profile Of Adhesive/Caries-Affected Dentin Interfaces Using Raman Microspectroscopy. *Journal Of Biomedical Materials Research Part A,* 81**,** 279-286.

Wang, Y. & Yao, X. 2010. Morphological/Chemical Imaging Of Demineralized Dentin Layer In Its Natural, Wet State. *Dental Materials,* 26**,** 433-442.

Wang, Z., Zheng, Y., Zhao, D., Zhao, Z., Liu, L., Pliss, A., Zhu, F., Liu, J., Qu, J. & Luan, P. 2018. Applications Of Fluorescence Lifetime Imaging In Clinical Medicine. *Journal Of Innovative Optical Health Sciences,* 11**,** 1830001.

Watson, T. 1997. Fact And Artefact In Confocal Microscopy. *Advances In Dental Research,* 11**,** 433-441.

Watson, T. 1999. Bonding Glass-Ionomer Cements To Tooth Structure. *Advances In Glass-Ionomer Cements. Chicago: Quintessence***,** 121-135.

Watson, T. & Boyde, A. 1991. Confocal Light Microscopic Techniques For Examining Dental Operative Procedures And Dental Materials. A Status Report For The American Journal Of Dentistry. *American Journal Of Dentistry,* 4**,** 193-200.

Watson, T. F., Atmeh, A. R., Sajini, S., Cook, R. J. & Festy, F. 2014. Present And Future Of Glass-Ionomers And Calcium-Silicate Cements As Bioactive

Materials In Dentistry: Biophotonics-Based Interfacial Analyses In Health And Disease. *Dental Materials,* 30**,** 50-61.

Watson, T. F., Azzopardi, A., Etman, M., Cheng, P. C. & Sidhu, S. K. 2000. Confocal And Multi-Photon Microscopy Of Dental Hard Tissues And Biomaterials. *Am J Dent,* 13**,** 19d-24d.

White, D. 1992. The Comparative Sensitivity Of Intra-Oral, In Vitro, And Animal Models In The'profile'evaluation Of Topical Fluorides. *Journal Of Dental Research,* 71.

Webb, S., Gu, Y., Lévêque-Fort, S., Siegel, J., Cole, M., Dowling, K., Jones, R., French, P., Neil, M. & Juškaitis, R. 2002. A Wide-Field Time-Domain Fluorescence Lifetime Imaging Microscope With Optical Sectioning. *Review Of Scientific Instruments,* 73**,** 1898-1907.

Wei, S., Sadr, A., Shimada, Y. & Tagami, J. 2008. Effect Of Caries-Affected Dentin Hardness On The Hear Bond Strength Of Current Adhesives. *Journal Of Adhesive Dentistry,* 10.

Williams, K. & Everall, N. 1995. Use Of Micro Raman Spectroscopy For The Quantitative Determination Of Polyethylene Density Using Partial Least-Squares Calibration. *Journal Of Raman Spectroscopy,* 26**,** 427-433.

Wilson, A. 1974. Alumino-Silicate Polyacrylic Acid And Related Cements. *Polymer International,* 6**,** 165-179.

Wilson, A., Prosser, H. & Powis, D. 1983. Mechanism Of Adhesion Of Polyelectrolyte Cements To Hydroxyapatite. *Journal Of Dental Research,* 62**,** 590-592.

Wilson, A. D. 1990. Resin-Modified Glass-Ionomer Cements. *International Journal Of Prosthodontics,* 3.

Wilson, A. D. & Kent, B. 1971. The Glass-Ionomer Cement, A New Translucent Dental Filling Material. *Journal Of Chemical Technology And Biotechnology,* 21**,** 313-313.

Wilson, A. D. & Mclean, J. W. 1988. *Glass-Ionomer Cement*, Quintessence Pub Co.

Yamakoshi, Y., Hu, J. C., Fukae, M., Zhang, H. & Simmer, J. P. 2005. Dentin Glycoprotein: The Protein In The Middle Of The Dentin Sialophosphoprotein Chimera. *Journal Of Biological Chemistry*.

Xu, Z., Neoh, K. G., Lin, C. C. & Kishen, A. 2011. Biomimetic Deposition Of Calcium Phosphate Minerals On The Surface Of Partially Demineralized Dentine Modified With Phosphorylated Chitosan. *Journal Of Biomedical Materials Research Part B: Applied Biomaterials,* 98**,** 150-159.

Yang, B., Flaim, G. & Dickens, S. H. 2011. Remineralization Of Human Natural Caries And Artificial Caries-Like Lesions With An Experimental Whisker-Reinforced Art Composite. *Acta Biomaterialia,* 7**,** 2303-2309.

Yang, B., Ludwig, K., Adelung, R. & Kern, M. 2006. Micro-Tensile Bond Strength Of Three Luting Resins To Human Regional Dentin. *Dental Materials,* 22**,** 45-56.

Yang, H., Guo, J., Guo, J., Chen, H., Somar, M., Yue, J. & Huang, C. 2015. Nanoleakage Evaluation At Adhesive-Dentin Interfaces By Different Observation Methods. *Dental Materials Journal,* 34**,** 654-662.

Yeh, A. T., Nassif, N., Zoumi, A. & Tromberg, B. J. 2002. Selective Corneal Imaging Using Combined Second-Harmonic Generation And Two-Photon Excited Fluorescence. *Opt Lett,* 27**,** 2082-4.

Yengopal, V. & Mickenautsch, S. 2011. Caries-Preventive Effect Of Resin-Modified Glass-Ionomer Cement (Rm-Gic) Versus Composite Resin: A Quantitative Systematic Review. *European Archives Of Paediatric Dentistry,* 12**,** 5-14.

Yildirim, S., Tosun, G., Koyutürk, A. E., Şener, Y., Şengün, A., Özer, F. & Imazato, S. 2008. Microtensile And Microshear Bond Strength Of An Antibacterial Self-Etching System To Primary Tooth Dentin. *European Journal Of Dentistry,* 2**,** 11.

Yiu, C., Tay, F., King, N., Pashley, D. H., Sidhu, S., Neo, J., Toledano, M. & Wong, S. 2004. Interaction Of Glass-Ionomer Cements With Moist Dentin. *Journal Of Dental Research,* 83**,** 283-289.

Yildiz, E., Sirinkaraarslan, E., Yegin, Z., Cebe, M. & Tosun, G. 2013. Effect Of Caries Removal Techniques On The Bond Strength Of Adhesives To Caries-Affected Primary Dentin In Vitro. *Eur J Paediatr Dent,* 14**,** 209-214.

Yoshida, Y., Nagakane, K., Fukuda, R., Nakayama, Y., Okazaki, M., Shintani, H., Inoue, S., Tagawa, Y., Suzuki, K. & De Munck, J. 2004. Comparative Study On Adhesive Performance Of Functional Monomers. *Journal Of Dental Research,* 83**,** 454-458.

Yoshida, Y., Yoshihara, K., Hayakawa, S., Nagaoka, N., Okihara, T., Matsumoto, T., Minagi, S., Osaka, A., Van Landuyt, K. & Van Meerbeek, B. 2012. Hema Inhibits Interfacial Nano-Layering Of The Functional Monomer Mdp. *Journal Of Dental Research,* 91**,** 1060-1065.

Yoshiyama, M., Tay, F., Doi, J., Nishitani, Y., Yamada, T., Itou, K., Carvalho, R., Nakajima, M. & Pashley, D. 2002. Bonding Of Self-Etch And Total-Etch Adhesives To Carious Dentin. *Journal Of Dental Research,* 81**,** 556-560.

Yu, O. Y., Zhao, I. S., Mei, M. L., Lo, E. C.-M. & Chu, C.-H. 2017a. Dental Biofilm And Laboratory Microbial Culture Models For Cariology Research. *Dentistry Journal,* 5**,** 21.

Yu, O. Y., Zhao, I. S., Mei, M. L., Lo, E. C.-M. & Chu, C.-H. 2017b. A Review Of The Common Models Used In Mechanistic Studies On Demineralization-Remineralization For Cariology Research. *Dentistry Journal,* 5**,** 20.

Yu, O. Y., Zhao, I. S., Mei, M. L., Lo, E. C.-M. & Chu, C.-H. 2017. A Review Of The Common Models Used In Mechanistic Studies On Demineralization-Remineralization For Cariology Research. *Dentistry Journal,* 5**,** 20.

Zanchi, C. H., Guerra Lund, R., Perrone, L. R., Ribeiro, G. A., Del Pino, F. B., Pinto, M. B. & Demarco, F. F. 2010. Microtensile Bond Strengrth Of Two-Step Etch-And-Rinse Adhesive Systems On Sound And Artificial Caries-Affected Dentin. *American Journal Of Dentistry,* 23**,** 152.

Zhang, L., Nelson, L. Y. & Seibel, E. J. 2011. Red-Shifted Fluorescence Of Sound Dental Hard Tissue. *Journal Of Biomedical Optics,* 16**,** 071411.

Zhao, I. S., Mei, M. L., Zhou, Z. L., Burrow, M. F., Lo, E. C.-M. & Chu, C.-H. 2017. Shear Bond Strength And Remineralisation Effect Of A Casein Phosphopeptide-Amorphous Calcium Phosphate-Modified Glass Ionomer Cement On Artificial “Caries-Affected” Dentine. *International Journal Of Molecular Sciences,* 18**,** 1723.

Zidan, S., Peeran, S. W. & Ramalingam, K. 2015. Rely-X Unicem Self-Adhesive Universal Resin Cement. *Dentistry And Medical Research,* 3**,** 3.

Zipfel, W. R., Williams, R. M. & Webb, W. W. 2003. Nonlinear Magic: Multiphoton Microscopy In The Biosciences. *Nat Biotechnol,* 21**,** 1369-77.

Zorzin, J., Petschelt, A., Ebert, J. & Lohbauer, U. 2012. Ph Neutralization And Influence On Mechanical Strength In Self-Adhesive Resin Luting Agents. *Dental Materials,* 28**,** 672-679.